Deformation in the Maritimes Basin, Atlantic Canada

by

Morgan Elaine Snyder

A thesis submitted in partial fulfillment of the requirements for the degree of

Doctor of Philosophy

Department of Earth and Atmospheric Sciences

University of Alberta

Abstract

The Maritimes Basin is a sedimentary basin covering onshore and offshore Atlantic Canada with late Paleozoic strata. The basin comprises a series of partially-connected and isolated fault-bounded subbasins trending generally northeast. Two subbasins are chosen for detailed analysis: the Windsor-Kennetcook subbasin in Nova Scotia and the Bay St. George subbasin in Newfoundland. These two subbasins show complicated syndepositional and post-depositional structures. Many structures, including soft-sediment structures, folds, faults, and salt structures, crop out in the Upper Devonian to early Mississippian Horton/Anguille Group, and the Viséan Windsor/Codroy Group.

In the Windsor-Kennetcook subbasin of Nova Scotia, soft-sediment deformation structures crop out along the macrotidal Bay of Fundy. Common features such as load structures, clastic dykes, and soft-sediment folds are accompanied by more unusual structures here termed bulb structures and microbasins. Many of these soft-sediment deformation structures are documented in correlative rocks in the Bay St. George subbasin. Two structure types exist in these two subbasins: those that form by liquidization of sediment soon after deposition, and those that form later during burial. Common triggers of soft-sediment deformation structure formation in the Maritimes Basin include seismicity and overpressured conditions.

In the Bay St. George subbasin soft-sediment structure-bearing strata are overlain by an evaporite-bearing unit, the Codroy Road Formation. The Codroy Road Formation evaporites source many spectacular salt structures exposed along the coast. Remapping of key coastal outcrops led to the discovery of salt structures previously unrecognized. These structures include a primary salt weld in the northern subbasin, a secondary salt weld in the southern subbasin, and an abundance of siltstone breccia. The siltstone breccia, previously interpreted as a lithostratigraphic unit within the Codroy Road Formation, is reinterpreted as the remnants of salt-expulsion and dissolution at the surface. Offshore and in the subsurface, salt structures are imaged on bathymetric maps, aeromagnetic maps, and on seismic profiles. Salt structures offshore in Bay St. George

include: salt-cored anticlines, salt-expulsion minibasins, and salt welds. Angular unconformities and drastic sediment thickness variation across the subbasin suggest that salt was moving early in the subbasin history.

Large faults crosscut ductile structures onland and offshore in the Bay St. George subbasin. Normal and reverse faults striking NE–SW, parallel to subbasin boundaries, suggest that strike-slip deformation was the dominant tectonic style in the subbasin. The major brittle structure onshore, the Snakes Bight Fault, cuts across Anguille Group strata in the south central subbasin. In the hanging wall of the Snakes Bight Fault a thick package of Anguille Group strata is exposed at the surface. Inversion structures imaged offshore also bring older strata to the surface. Offshore, the relationship between salt movement and faulting is complicated. In the central offshore subbasin, a tectonic wedge inserted to the west cuts across suprasalt structures. Salt movement, however, could have continued during wedge insertion, as the shapes of minibasin trough surface traces, and variations in the locus of maximum accommodation through successive horizons show, that salt moved southeast northern and southern subbasin; in contrast, salt moved northwest in the central subbasin, where the tectonic wedge is present.

Later deformation is recorded by fractures. Joints, veins, and faults are commonly exposed in outcrop and in well core from the Windsor-Kennetcook subbasin. Cross-cutting and abutting relationships between fractures indicate relative timing of fractures. A Markov chain analysis, a method previously used in sedimentology, is applied here for the statistical testing of fractures. The results are used to create a history of fracturing in the subbasin that can be related to the overall Maritimes Basin history. Early fractures are related to dextral strike slip along the Minas Fault Zone in the late Paleozoic, and later fractures are related to sinistral strike-slip reactivation of the same boundary in the Mesozoic.

Preface

This thesis is the original work of M. Snyder.

Chapter 2 has been published as: Snyder, M.E., Waldron, J.W.F., 2016, Unusual soft-sediment deformation structures in the Maritimes Basin, Canada: possible seismic origin, *Sedimentary Geology* 344, 145-159. I was responsible for data collection, analysis, and manuscript preparation. J.W.F. Waldron was the supervisor and was involved with analysis and manuscript preparation.

I was responsible for data collection, interpretation, and manuscript preparation of Chapter 3 and Chapter 4. Chapters 3 and 4 are being prepared for submission to academic journals (e.g. *Atlantic Geology, Canadian Journal of Earth Sciences, Basin Research,* or *Bulletin of Canadian Petroleum Geology*) in 2019. Chapters 3 and 4 will be co-authored by J.W.F. Waldron; P.W. Durling will likely co-author Chapter 4. J.W.F. Waldron was the supervisor and was involved with analysis and editing; P.W. Durling assisted with regional correlation into the Central Maritimes Basin.

Chapter 5 has been published as: Snyder, M.E., Waldron, J.W.F., 2018, Fracture overprinting history using Markov chain analysis: Windsor-Kennetcook subbasin, Maritimes Basin, Canada, *Journal of Structural Geology* 108, 80-93. I was responsible for data collection, analysis, and manuscript composition and editing. J.W.F. Waldron was the supervisor and was involved with analysis and manuscript editing.

Acknowledgements

I'd like to thank John Waldron, supervisor extraordinaire,

Thanks to all of my examiners: Lori, Murray, Matt, and Claire.

Thanks to Triangle and PEEP who granted us the research money.

Thanks to Randy and to Paul for being as wise as they are funny.

Leprechaun Resources, to whom I am extremely grateful,

They supplied the seismic data, so my interpretation is faithful.

Thanks to Mom, Dad, and my sisters, who were just a call away,

They listened to my rambling when I had a lot to say.

To Piotr and to Marcus, is it odd to thank a pet?

I can't thank Dean enough; I am so happy that we met.

Thanks to Merilie, Natasha, Jamie, Judy, Lauren, Robyn,

Shawna, Mike, Jess, Ryan, Wenbo, Jonathan, and Martin.

And finally to one who knew I'd finish this degree,

Because of you René Gobeil, I'll have a PhD.

Table of Contents

Chapter 1. Introduction 1

1.1. Regional Geology 3

1.2. Methods 12

1.3. Thesis Layout 14

1.4. References 16

Chapter 2. Unusual soft-sediment deformation structures in the Maritimes Basin, Canada: possible seismic origin 21

2.1. Introduction 22

2.2. Regional Geology 22

2.3. Soft-sediment deformation structures 28

2.4. Discussion 53

2.5. Conclusion 59

2.6. References 60

Chapter 3. Synsedimentary and tectonic deformation of the Carboniferous Anguille and Codroy Groups, Bay St. George subbasin, southwest Newfoundland 69

3.1. Introduction 69

3.2. Regional Geology 72

3.3. Methods 82

3.4. Soft-sediment deformation structures 83

3.5. Evaporite-related and tectonic structures 99

3.6. Discussion 116

3.7. Conclusions 120

3.8. References 121

Chapter 4. Salt tectonics in a strike-slip basin: Bay St. George subbasin, Newfoundland, Canada 129

4.1. Introduction 129

4.2. Regional geology 132

4.3. Datasets 142

4.4. Stratigraphic interpretation 146

4.5. Structures 159

4.6. Discussion 166

4.7. Conclusion 175

4.8. References 176

Chapter 5. Fracture overprinting history using Markov chain analysis: Windsor-Kennetcook subbasin, Maritimes Basin, Canada 189

5.1. Introduction 189

5.2. Regional Geology 192

5.3. Economic implications 196

5.4. Data and methods 197

5.5. Presentation of joint data 202

5.6. Markov chain analysis 204

5.7. Results 209

5.8. Discussion 219

5.9. Conclusion 223

5.10. References 224

Chapter 6. Conclusions 231

6.1. Summary and Contributions 231

6.2. Chapter 2 231

6.3. Chapter 3 232

6.4. Chapter 4 233

6.5. Chapter 5 234

6.6. Future Work 234

6.7. References 236

List of Figures

Figure 1.1. Distribution of the Maritimes Basin in Atlantic Canada. 2

Figure 1.2. Stratigraphic chart of selected subbasins across the Maritimes Basin (modified from Waldron, Gibling, and Thomas 2018). 4

Figure 1.3. Geological map of the Windsor-Kennetcook subbasin in Nova Scotia after Waldron et al. (2010). 6

Figure 1.4. Bay St. George subbasin in southwest Newfoundland showing major geological units, structures, and locations (modified from Knight 1983). 7

Figure 2.1. Distribution of the Maritimes Basin in Atlantic Canada. 23

Figure 2.2. Windsor-Kennetcook subbasin in Nova Scotia 25

Figure 2.3. Microbasins at Horton Bluff 30

Figure 2.5. Photographs of exposed microbasins, numbered from Figure 2.3: 33

Figure 2.6. Schematic model for microbasin formation. 36

Figure 2.8. Intraformational breccia at Cheverie 41

Figure 2.9. Neptunian dykes 44

Figure 2.10. Sedimentary boudins 48

Figure 2.11. Bulb structures 51

Figure 2.12. Time-exploded diagram of all soft-sediment deformation structures described. 54

Figure 3.1. Map of the Maritimes Basin of Atlantic Canada. 70

Figure 3.2. Generalized stratigraphic column across the Maritimes Basin, modified from Waldron et al. (2017). 71

Figure 3.3. Bay St. George subbasin geologic map and generalized stratigraphy, modified from Knight (1983). 73

Figure 3.4. Spout Falls Formation and Ship Cove Formation contact. 76

Figure 3.5. Core photograph from.LR-98-1 showing dominantly halite and mudstone showing different breccia textures and ratios of halite to mudstone increasing with depth: 78

Figure 3.6. Soft-sediment folds at Cape Anguille. 84

Figure 3.7. Stratigraphic column measured at Cape Anguille highlighting frequency of soft-sediment structures. 86

Figure 3.8. Hinges of soft-sediment folds measured at Cape Anguille plotted on an equal area projection. 87

Figure 3.9. Poles to axial surfaces measured at Cape Anguille plotted on an equal area projection. 87

Figure 3.10. Stratigraphic column measured at Boswarlos. 88

Figure 3.11. Soft-sediment folds on Codroy Island. 89

Figure 3.12. Soft-sediment folds at Boswarlos (a) Equal area projection of axial surfaces; (b) equal area projection of fold axes; (c)(d) photographs of soft-sediment folds including a sheath fold. 90

Figure 3.13. Sedimentary boudins at Cape Anguille. 92

Figure 3.14. Clastic dykes at Cape Anguille. 94

Figure 3.15. Bulb structures at Cape Anguille. 95

Figure 3.16. 2-D seismic profiles onshore Bay St. George subbasin. 101

Figure 3.17. Stratigraphic Column and photographs of the Codroy Road Formation at Ship Cove. 103

Figure 3.18 . Photographs of (a) outcrop view siltstone breccia and (b) cut hand sample showing individual clasts. 104

Figure 3.20. New geologic map of Capelin Cove in the southern subbasin. 108

Figure 3.21. Cross section of Capelin Cove. Inset shows detailed mapping in the Codroy Road Formation. 109

Figure 3.22. Photograph of halite pseudomorphs in outcrop taken from the Woody Cape Formation. 110

Figure 3.23. Secondary salt weld at Capelin Cove. 111

Figure 3.24. Map and photos of Snakes Bight. 112

Figure 3.25. Cross section of Snakes Bight. 113

Figure 4.1. Map of the Maritimes Basin location and coverage. 130

Figure 4.2. Stratigraphic chart across subbasins within the Maritimes Basin, modified from Waldron et al. (2017). 133

Figure 4.3. Offshore wells in the Maritimes Basin. 134

Figure 4.4. Geologic map of the onshore Bay St. George subbasin of Knight (1983). 138

Figure 4.5. Geological map of onshore Bay St. George subbasin after Knight (1983) and second vertical derivative aeromagnetic map of offshore subbasin. 144

Figure 4.6. Top view of high-resolution bathymetric data showing bedrock features. 145

Figure 4.7. Geophysical data integration. 147

Figure 4.8. NNW-SSE seismic line 149

Figure 4.9. Time-structure map for horizon BA the basal Codroy Group anhydrite. Red lines represent F1 and F2. 150

Figure 4.10. NNW–SSE seismic profile. 151

Figure 4.11. NNW–SSE seismic profile. 153

Figure 4.12. Time-structure map for horizon TS, a horizon near the top of the Codroy Group evaporites. Red lines represent F1 and F2. 154

Figure 4.13. Time-structure map for horizon MC, an anhydrite horizon in the middle to upper Codroy Group 155

Figure 4.14. WSW – ENE seismic line 158

Figure 4.15. Lines W, C, and E on a map and on seismic lines showing examples of trough points migrating with decreased depth. 163

Figure 4.16. Evidence for inversion in Bay St. George. 165

Figure 4.17. Reverse faults imaged on WSW–ENE seismic profile 168

Figure 4.18. Tectonic wedge imaged on NNW–SSE seismic profile 169

Figure 4.19. Successive flattening of horizons in minibasins. 170

Figure 5.1. Map of Maritimes Basin in Atlantic Canada. 191

Figure 5.2. Windsor-Kennetcook subbasin 193

Figure 5.3. Fracture data collection methods. 199

Figure 5.4. Composite rose diagram of all fractures measured from beds with dip <30°, modes at 005°, 025°, 045°, 068°, 098°, 123°, 140°, and 163°. 203

Figure 5.5. Composite rose diagram of all measured fractures from beds with dip >30°, modes NNE-SSW and ESE-WSW. 203

Figure 5.6. Workflow for Markov Chain analysis. 205

Figure 5.7. Angular relationship between fractures. 208

Figure 5.8. (a) Photograph of circular scan-line from the Macumber Formation at Cheverie; (b) vein showing red staining in centre line; (c) rose diagram showing three types of fractures. 211

Figure 5.9. Sinistral *en echelon* veins in the Macumber Formation (left) adjacent to the Pembroke Breccia (right). Blocks of Macumber Formation show veins that do not extend into the matrix of the breccia. 212

Figure 5.10. Observed data table for Markov Chain analysis. Columns represent earlier fractures, rows represent later fractures. 214

Figure 5.11. Expected data table for Markov Chain analysis. Cell values calculated using Equation (3). 214

Figure 5.12. Standardized residuals table for Markov Chain analysis. Cell values calculated using Equation (4). 214

Figure 5.13. Resulting flow-chart from Markov Chain analysis. Top of the flow chart represents earliest fracture set. Arrows indicate sequence of fracture initiation. 216

Figure 5.14. Summary of fracture history. 218

Figure 5.15. Extract from the World Stress Map (Heidbach et al. 2008), covering Atlantic Canada. Windsor-Kennetcook subbasin is in a thrust regime having a vertical minimum compressive stress. 221

Chapter 1. Introduction

The Maritimes Basin (Fig. 1.1) is a large, deep (>12 km) basin covering a large portion of onshore and offshore Atlantic Canada with late Paleozoic strata (Roliff 1962, Keppie 1982, Gibling et al. 2008, Gibling et al. in press 2018). This basin formed during a period of transtension following the Acadian Orogeny (Calder 1998, Hibbard & Waldron 2009, Waldron et al. 2015). The Maritimes Basin is structurally complex, consisting of multiple NE and E striking subbasins separated by uplifted basement units (Boehner & Giles 1993, van de Poll et al. 1995, Gibling et al. 2008, Murphy et al. 2011, Gibling et al. in press 2018). Deformation within the Maritimes Basin was a multi-stage process including periods of folding, faulting, uplift, salt tectonism, erosion, and subsidence (Knight 1983, Hamblin & Rust 1989, Calder 1998, Waldron 2004, Wilson et al. 2006, Waldron et al. 2013). Multiple phases of subsidence and inversion has led to the deposition of many stratigraphic sequences separated by unconformities (St. Peter 1993). Because of these basement block movements, there is much lateral and vertical facies variation within and between subbasins.

The origin of the Maritimes Basin has been discussed since the mid 1900s. Belt (1968) considered three possibilities including oblique extension, strike-slip motion, and oblique shortening, but favoured the oblique extension hypothesis. Bradley (1982) suggested strike-slip motion in a modified pull-apart to explain deeper sections of the Maritimes Basin. McCutcheon and Robinson (1987) suggested a rift model where the basin formed by gravity-driven collapse of the Acadian Orogen. Martel (1987), Hyde et al. (1988), MacInnes and White (2004), Waldron et al. (2007), and Murphy et al. (2011) document strike-slip in subbasins within the Maritimes Basin, which is supported by the Hibbard and Waldron (2009) and Waldron et al. (2015) interpretation that Maritimes Basin subsidence was related to significant dextral strike-slip (~250 km) across a releasing bend in the Canadian Appalachians.

Petroleum exploration within the Maritimes Basin has focussed on Lower Carboniferous rocks as both sources and reservoirs. Mississippian potential source rocks and/or unconventional reser-

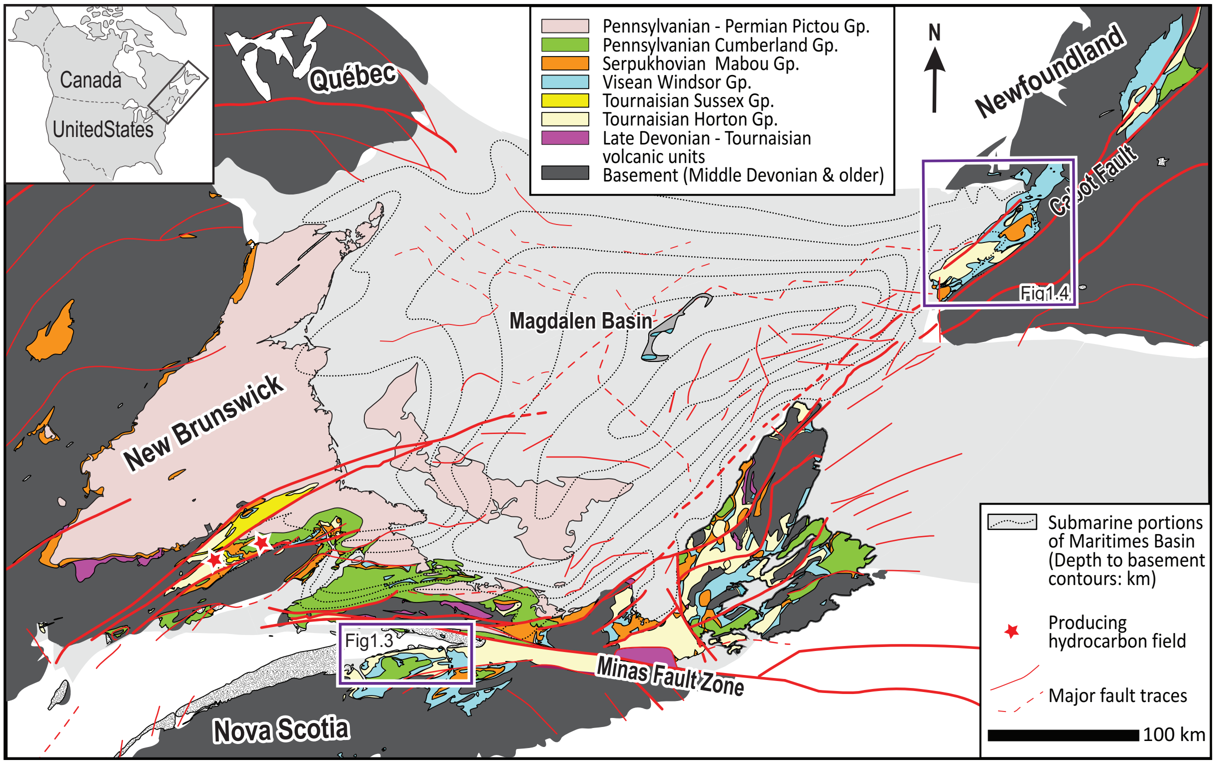

Figure 1.1. Distribution of the Maritimes Basin in Atlantic Canada.

Modified from Waldron et al. (2015). Purple boxes indicate locations of the Windsor-Kennetcook subbasin in Nova Scotia, and the Bay St. George subbasin in Newfoundland.

voirs include black organic-rich shale and carbonates of the Horton Group (Bell 1958, Bibby & Schimeld 2000, Dietrich et al. 2011). Two producing petroleum fields in the Maritimes Basin target Horton Group strata at Stoney Creek and the McCully field (Fig.1.1) in the Moncton subbasin of New Brunswick (Martel 2004, Dietrich et al. 2009). The distribution and extraction of hydrocarbons in Horton Group strata is likely to be influenced by the orientation of natural fractures, which appear numerous in outcrop.

1.1. Regional Geology

1.1.1. Stratigraphy

Stratigraphic nomenclature is variable across Atlantic Canada; a stratigraphic correlation chart (Fig. 1.2) was created by Waldron et al. (2018) and is followed below. One particular difficulty is the difference in naming of laterally equivalent units across subbasins. In Nova Scotia and southwest Newfoundland, the Horton Group and the Anguille Group are equivalent; the Windsor Group and Codroy Group are laterally approximately equivalent. Horton/Anguille Group, and Windsor/Codroy Group are the stratigraphic units of focus for this thesis in the Windsor-Kennetcook subbasin in Nova Scotia, and the Bay St. George subbasin in Newfoundland.

Horton Group/Anguille Group

The latest Devonian to Tournaisian Horton/Anguille Group overlie Proterozoic to early Paleozoic basement across the Maritimes Basin and typically consists of basal alluvial, medial lacustrine and restricted marine, and upper alluvial units (Knight 1983, Hamblin & Rust 1989, St. Peter 1993, Martel & Gibling 1996, Gibling et al. 2008, Gibling et al. in press 2018).

The Windsor-Kennetcook subbasin, or WKSB, (Fig. 1.3), is the area of definition for the Horton Group. The Horton Group is separated into two formations, the lower Horton Bluff Formation and the upper Cheverie Formation. The Horton Bluff Formation consists of a lower fining-up

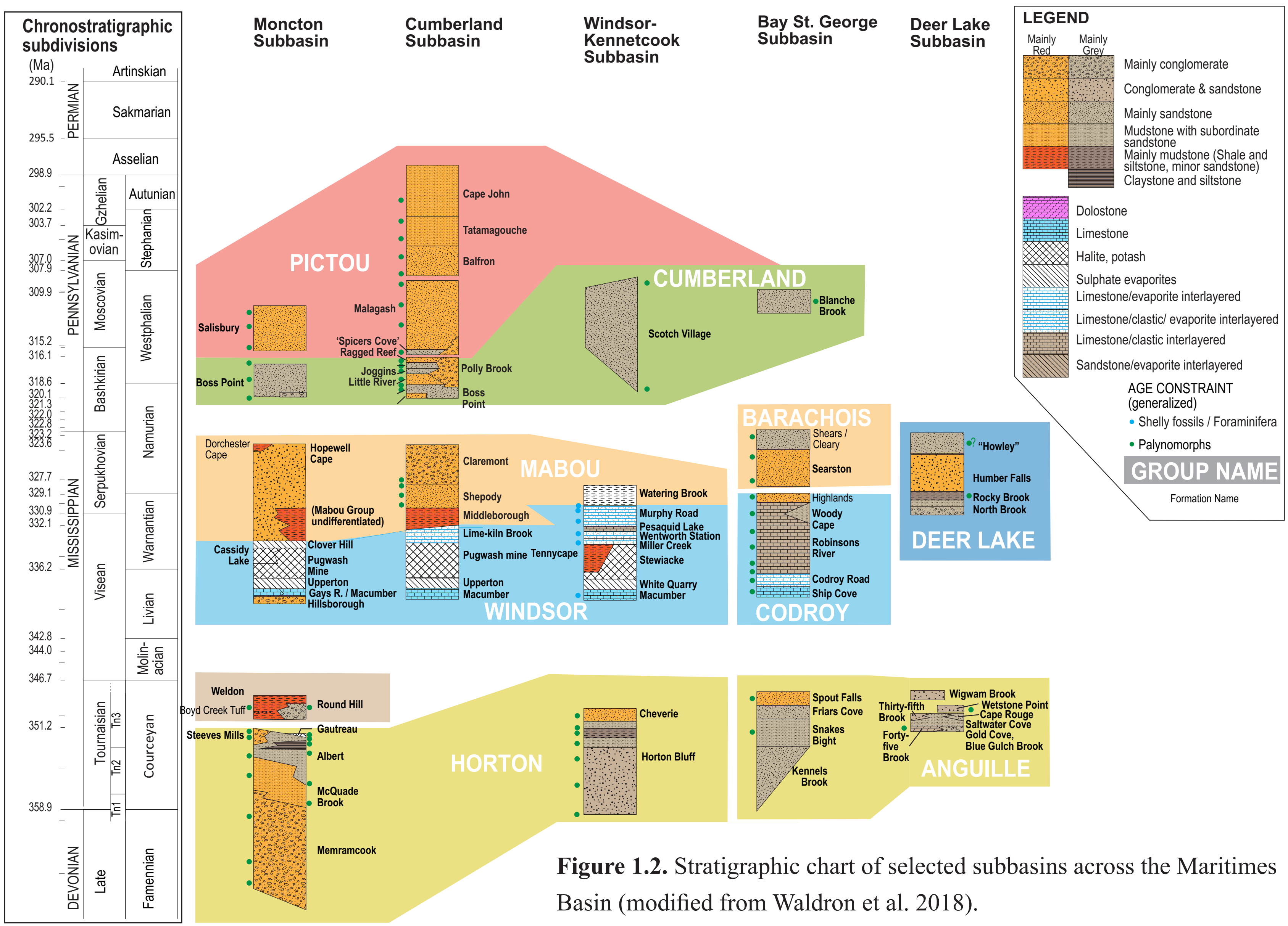

Figure 1.2. Stratigraphic chart of selected subbasins across the Maritimes Basin (modified from Waldron et al. 2018).

succession of conglomerate and sandstone; a middle unit consists of a grey, fine-grained, coarsening up shale, mudrock, siltstone and sandstone with thin carbonate and evaporite layers; and an upper arkosic sandstone (Calder 1998). Most depositional environment interpretations for the three units within the Horton Bluff Formation are: alluvial fan, lacustrine, and braided stream deposits respectively (Bell 1924, Belt 1964, Calder 1998, Gibling et al. 2008), although Wightman et al. (1993) suggests marine influence in the middle member based on the presence of agglutinated foraminifera. The Cheverie Formation consists of arkosic sandstone and fine-grained quartz-arenite, siltstone, mudstone, shale, and paleosol horizons. Sedimentary structures include planar laminae, wavy laminae, cross laminae, climbing ripples, and cross bedding. Noade (2010) divided the Cheverie Formation at the type section into three facies: channel and overbank deposits, floodplain deposits, and abandoned channel deposits.

In the Bay St. George subbasin (BSGSB), Horton Group equivalents are assigned to the Anguille Group (Fig. 1.4). Knight (1983) separated the Anguille Group into four formations: Kennels Brook, Snakes Bight, Friars Cove, and Spout Falls Formations. The Kennels Brook Formation comprises red and grey pebbly sandstone, conglomerate, slate and rare mudstone interpreted as originating in a meandering river and floodplain environment (Cote 1964, Knight 1983). The Snakes Bight Formation comprises black mudstone, siltstone and grey sandstone interpreted as being lacustrine in origin (Knight 1983). The Friars Cove Formation consists of grey sandstone, conglomerate and shale with minor carbonate and redbeds interpreted as products of a fluvial-deltaic environment (Knight 1983). The Spout Falls Formation comprises red and grey sandstone with minor siltstone and conglomerate interpreted as braided stream deposits (Knight 1983).

Windsor Group/Codroy Group

The overlying Windsor Group of Nova Scotia and the approximately equivalent Codroy Group of Newfoundland contains dominantly marine shale, limestone, and evaporite, representing the

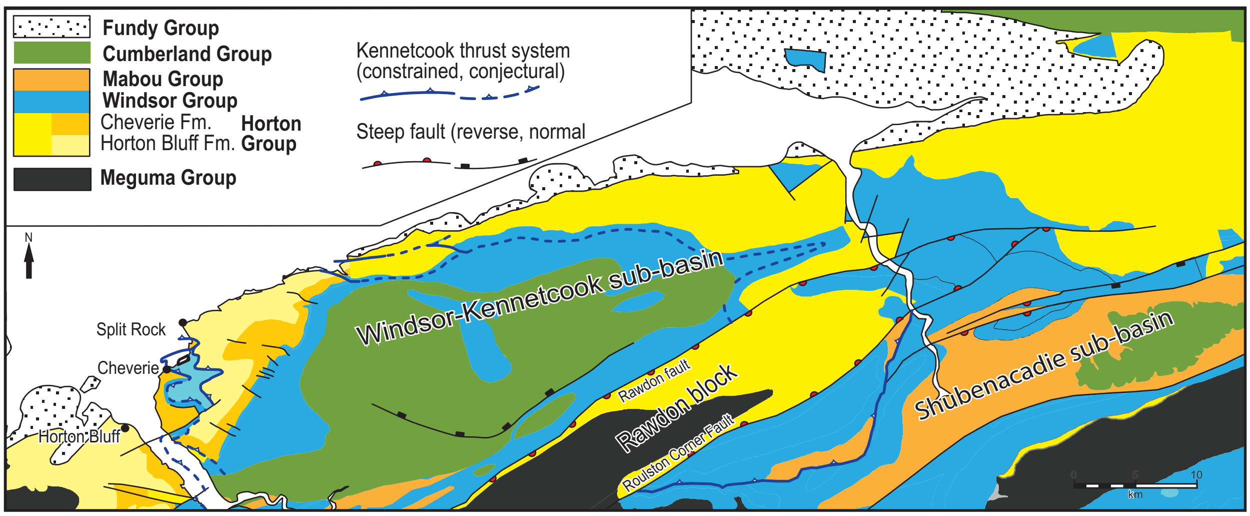

Figure 1.3. Geological map of the Windsor-Kennetcook subbasin in Nova Scotia after Waldron et al. (2010).

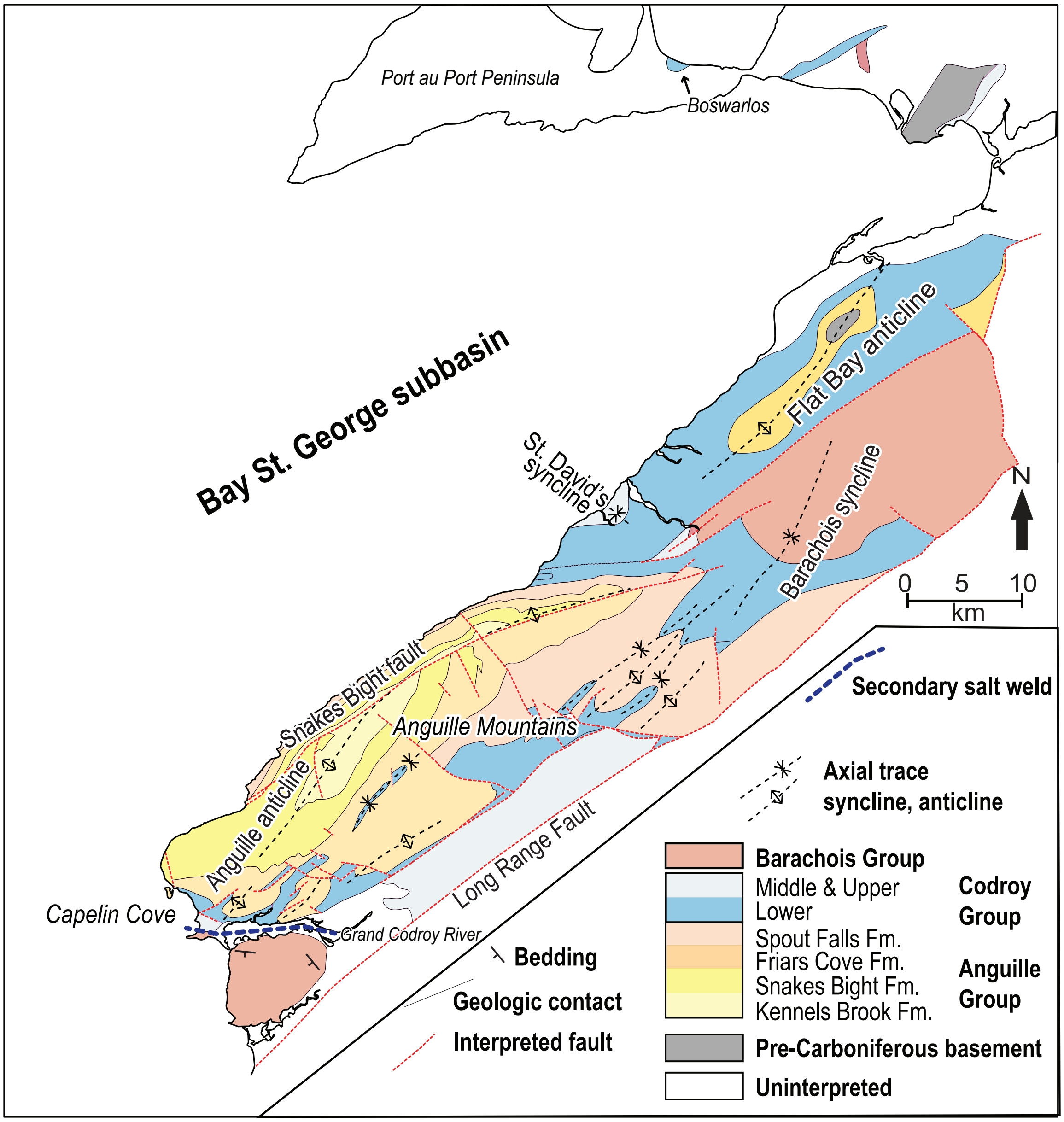

Figure 1.4. Bay St. George subbasin in southwest Newfoundland showing major geological units, structures, and locations (modified from Knight 1983).

only fully marine incursion into the Maritimes Basin in the late Paleozoic (Fig. 1.2) (Gibling et al. 2008).

The WKSB is the Windsor Group type area. In the WKSB the lowermost units, the Macumber Formation and the Pembroke Breccia, are widely exposed. The Macumber Formation is a 2–10 m thick unit of finely laminated limestone initially interpreted by Schenk (1967) to have been formed in a shallow-water environment. The Pembroke Breccia is an enigmatic unit composed of variably sized elongate clasts of weathered Macumber Formation within a grey to red carbonate-rich matrix (Bell 1924, Moore et al. 2000). The breccia could have formed by slumping of microbial mats, tectonic brecciation, or solution collapse (Lavoie et al. 1998, Johnson 1999). Waldron et al. (2007) argue that the Pembroke Breccia is associated with movement in the Windsor evaporites that originally overlay the basal carbonates but became structurally interleaved during development of the Kennetcook thrust system.

Overlying the Pembroke Breccia is a thick succession of evaporites. A lower unit consists mainly of anhydrite in the deep subsurface but has undergone partial or complete hydration to gypsum near the present weathering surface. Overlying these sulphates, a thick halite-dominated unit is present in the subsurface; halite has likely been removed by solution in the shallow subsurface (Boehner et al. 2003). In many subbasins within the Maritimes Basin, the Codroy/Windsor Group evaporites are the source of spectacular salt structures (e.g. Waldron & Rygel 2005, Wilson & White 2006, Wilson et al. 2006, Albertz et al. 2010, Craggs et al. 2013, Waldron et al. 2013, Craggs et al. 2015, Dafoe et al. 2016, Thomas & Waldron 2017). Higher units assigned to the middle and upper Windsor Group consist of alternations of marine limestone, evaporite (mainly gypsum and anhydrite), and mudstone.

In the Bay St. George subbasin (Fig. 1.4) the Codroy Group (Windsor Group equivalent) is subdivided into four formations: Ship Cove, Codroy Road, Robinsons Road, and Woody Cape Formations (Knight 1983). The Ship Cove Formation is a widespread, packstone, oolitic limestone, and sandstone unit interpreted as equivalent to the Macumber Formation in the WKSB (Schenk

1967). The Codroy Road consists of red siltstone, sandstone, and evaporite, interpreted as products of an alluvial plain to marginal marine environment (Knight 1983). The Robinsons River Formation consists of red sandstone, siltstone, and conglomerates with interbedded carbonates and evaporites, interpreted as floodplain deposits. The Woody Cape Formation consists of green and grey mudstone, siltstone, and sandstone interpreted as products of a deltaic environment.

Younger Carboniferous rocks

Younger Carboniferous rocks in the WKSB include pebbly sandstone interbedded with thick red siltstone, black shale and an upper coal-bearing sequence assigned to the Mabou Group (Fig. 1.2) (Utting & Giles 2008). These strata are interpreted as fluvial deposits (Utting & Giles 2008). These rocks are correlated with those of the Barachois Group in Newfoundland (Fig. 1.2). In the BSGSB the Searston Formation, the lowest coal-measure bearing member in the Barachois Group, crops out along the southern shore. Higher undivided units within the Barachois Group crop out in the eastern subbasin.

Pennsylvanian strata in the WKSB include sandstone and siltstone of the Cumberland and Pictou Groups. Waldron et al. (2013) determined that sedimentation of these groups was largely dependent on salt withdrawal in the Cumberland subbasin in Nova Scotia. Pennsylvanian strata in the Bay St. George subbasin consist of the sandstone-dominated Blanche Brook Formation that crops out near Stephenville Newfoundland (Fig. 1.4).

1.1.2. Structure and deformation

Maritimes Basin general

Deformation of rocks within the Maritimes Basin differ in time and magnitude throughout the basin; generally early Mississippian strata are more deformed than later Mississippian and younger strata (Martel & Gibling 1991).

Abundant faults run NE–SW, approximately parallel to the Appalachian orogen (Fig. 1.1). Hibbard and Waldron (2009) and Waldron et al. (2015) suggest that these faults were activated in the late Devonian, and were responsible for the subsidence and strike-slip motion creating the Maritimes Basin.

The Minas Fault Zone was active from the late Devonian to the late Carboniferous (Murphy et al. 2011). It consists of a network of sub-parallel faults striking approximately E–W and separating the terranes of the Appalachians; Meguma to the south and Avalon to the north (Keppie 1982, Murphy et al. 2011). The Windsor-Kennetcook subbasin is bounded to the north by the Minas Fault Zone (Fig. 1.3).

Windsor-Kennetcook subbasin

The Windsor-Kennetcook subbasin (Fig. 1.3) trends ENE–WSW on the southern shore the Bay of Fundy in Nova Scotia (Fig. 1.1). The major structures in the subbasin are the Kennetcook thrust system, small-scale fractures, including joints and veins, and folds that crop out spectacularly along the coast.

Kennetcook thrust system

South of the Minas Fault Zone in the Windsor-Kennetcook subbasin, Horton Group strata are duplicated by the Kennetcook thrust system that climbs up-section to the southeast (Waldron et al. 2010). The subbasin includes both the allochthonous hanging wall and the autochthonous footwall of the Kennetcook thrust system. The rocks in the hanging wall are intensely deformed by folds, faults, and evaporite-related structures; the footwall is less deformed but shows faults, fractures and folds in outcrop (Waldron 2005, Waldron et al. 2007, Waldron et al. 2010, Javaid 2011).

Joints and veins

In the WKSB, fractures are exposed on bedding surfaces and in surfaces perpendicular to bedding in the adjacent cliffs. Fracture types include open joints, closed joints, and veins. Fractures exposed in Kennetcook #1 and Kennetcook #2 core are dominantly open joints.

Folds

Folds are exposed in wave-cut platform and in cliffs in the WKSB from Horton Bluff to Rainy Cove (Fig. 1.3), and have been described in detail by Waldron et al. (2007). The Horton Bluff type section occurs on one limb of an open gentle syncline plunging SE. A broad, north-plunging anticline is present at Cheverie. These folds are interpreted as being in the footwall of the Kennetcook thrust system. In the interpreted hanging wall of the Kennetcook thrust system, folds are more complex along the coastal section. At Split Rock (Fig. 1.3), folds are open to tight, and upright to overturned.

Bay St. George subbasin

The Bay St. George subbasin trends northeast, covering onshore and offshore southwest Newfoundland with late Paleozoic strata (Fig. 1.4). Onshore, Anguille and Codroy Group strata commonly crop out, whereas offshore, Codroy, Barachois, and younger strata are most prevalent.

Faults

In the BSGSB major NE–SW faults include the Long Range Fault and the Snakes Bight Fault (Fig. 1.4), the main brittle onshore structural features. A number of NW–SE striking faults are mapped by Knight (1983) in the Anguille anticline area (Fig 1.4). One major NW–SE fault is the basin-bounding fault separating Carboniferous rocks from basement to the northeast (Fig. 1.4).

Folds

Folds in the BSGSB trend dominantly NE–SW, parallel to the Long Range Fault and have been described by Knight (1983). The major folds onshore include the Anguille anticline, Flat Bay anticline, St. David's syncline, and the Barachois syncline (Fig. 1.4). The Flat Bay anticline, Anguille anticline and Barachois syncline trend NE–SW and are doubly plunging, open folds. The Anguille anticline is cut by the Snakes Bight Fault (Knight 1983). Offshore BSGSB contains multiple folds observed on bathymetry and seismic sections (Fig. 1.3).

1.1.3. Research Objectives

The main objective of this research is to investigate four previously neglected aspects of deformation in the Maritimes Basin, exemplified by two subbasins within it: the Windsor-Kennetcook subbasin (Chapter 2 and 5) in Nova Scotia and the Bay St. George subbasin (Chapter 3 and 4) in western Newfoundland. In the following chapters we examine how soft-sediment deformation, salt tectonics, and conventional tectonics interact in a basin at low metamorphic grade.

Specific research objectives are to describe and interpret soft-sediment deformation structures in the Horton Group of the WKSB (Chapter 2), map and describe small and large scale salt and tectonic structures onshore in the BSGSB (Chapter 3), interpret seismic, aeromagnetic, and bathymetry data offshore BSGSB (Chapter 4), and to understand fracture overprinting history in Mississippian rocks of the WKSB (Chapter 5).

1.2. Methods

1.2.1. Field work

Twelve weeks of field work were completed between June 2011 and August 2016. Four weeks were spent in Nova Scotia in the Windsor-Kennetcook subbasin. Most of that time was spent along coastal sections from Cheverie to Selma (Fig. 1.3). Four weeks were spent in southwestern Newfoundland in the Bay St. George subbasin (Fig. 1.4). This work was performed on exposed coastal outcrops on the southwestern shore, and inland along small hiking or ATV trails. At all locations in both subbasins, GPS coordinates, structural measurements, field descriptions, and photograph numbers were recorded. Rock samples were taken for reference or thin sections. These observations were used to create new stratigraphic sections, geologic maps, and structural interpretations in these subbasins.

1.2.2. Computer programs

ArcGIS, developed by Esri, was used to make field mapping basemaps and to upload GPS waypoints for final geologic map creation.

Petrel, developed by Schlumberger, was used to upload bathymetric data, aeromagnetic maps, geological maps, and seismic data. Seismic reflections were picked using Petrel and exported to Illustrator for final interpretation.

Adobe Photoshop was used to stitch photographs, crop, or resample raster images.

Adobe Illustrator was used to produce all figures in this thesis.

Spheristat, Stereonet, and Orient were used to compile and analyse directional data including bedding, cleavage, fold hinges, axial surfaces, faults, slickenlines, joints, veins, and soft-sediment directional information.

Agisoft Photoscan was used to make vertical and horizontal orthomosaic maps from one coastal location accessed by boat.

1.3. Thesis Layout

An overview of Maritimes Basin geology is provided in Chapter 1. The body of this thesis, Chapters 2, 3, 4, and 5 is formed by four stand-alone manuscripts published or to be published in peer-reviewed journals. A summary of the contributions of this thesis and a discussion of future research is provided in Chapter 6.

1.3.1. Chapter 2

Chapter 2 describes and proposes a deformation mechanism for the formation of soft-sediment deformation structures in the Windsor-Kennetcook subbasin. This work was presented at the ATLAS symposium in Edmonton, AB, the Canadian Tectonics Group workshop in Victoria, BC in 2013, and has been published as:

Snyder, M.E., Waldron, J.W.F., 2016, Unusual soft-sediment deformation structures in the Maritimes Basin, Canada: possible seismic origin, *Sedimentary Geology* 344, 145-159.

1.3.2. Chapter 3

Chapter 3 details the description and interpretation of synsedimentary and tectonic structures that crop out onshore in Anguille and Codroy Group strata in the Bay St. George subbasin. This work has not yet been presented. A modified version of this chapter will be submitted for publication as:

Snyder, M.E., Waldron, J.W.F. Synsedimentary and tectonic deformation of the Carboniferous Anguille Group and Codroy Group, Bay St. George subbasin, southwest Newfoundland. For submission to *Atlantic Geology* or *Canadian Journal of Earth Sciences.*

1.3.3. Chapter 4

This chapter details the third research objective – to describe and interpret offshore salt and tectonic structures using seismic, bathymetry, aeromagnetic, and field data in the Bay St. George subbasin. This work was presented at the ATLAS Symposium in Edmonton, AB, and Resources for Future Generations Conference in Vancouver, BC, in 2018. A modified version of this chapter will be submitted for publication as:

Snyder, M.E., Waldron, J.W.F., Durling, P. Salt tectonics in a strike-slip basin: Bay St. George subbasin, Newfoundland. For potential submission to *Bulletin of Canadian Petroleum Geology* or *Basin Research.*

1.3.4. Chapter 5

Chapter 5 uses fractures measured in outcrop in the Windsor-Kennetcook subbasin of Nova Scotia and in well-core to distinguish a statistically valid sequence of formation. This work was presented at the Atlantic Geoscience Society Annual Conference in Wolfville, NS, the GAC-MAC Annual Conference in St. John's, NL, in 2012, and has been published as:

Snyder, M.E., Waldron, J.W.F., 2018, Fracture overprinting history using Markov chain analysis: Windsor-Kennetcook subbasin, Maritimes Basin, Canada, *Journal of Structural Geology* 108, 80-93.

1.4. References

Albertz, M., Beaumont, C., Shimeld, J. W., Ings, S. J. & Gradmann, S. 2010. An investigation of salt tectonic structural styles in the Scotian Basin, offshore Atlantic Canada: 1. Comparison of observations with geometrically simple numerical models. *Tectonics* **29**(4), TC4017.

Bell, W. A. 1924. Carboniferous formations of Northumberland Strait, Nova Scotia. *Geological Survey of Canada* **Part C**, 142-180.

Bell, W. A. 1958. *Possibilities for occurrence of petroleum reservoirs in Nova Scotia.* Province of Nova Scotia Department of Mines, Halifax.

Belt, E. S. 1964. Revision of Nova Scotia Middle Carboniferous Units. *American Journal of Science* **262**, 653-673.

Bibby, C. & Schimeld, J. 2000. *Compilation of reservoir data for sandstones of the Devonian-Permian Maritimes Basin, Eastern Canada. Geological Survey of Canada, Open File Report 3895*.

Boehner, R. C., Adams, G. C. & Giles, P. S. 2003. Karst geology in the salt-bearing Windsor Group evaporites and controls on the origin of gypsum deposits in south-central Cape Breton Island, Nova Scotia. In: *Mineral Resources Branch, Report of Activities 2002*. Nova Scotia Department of Natural Resources, Report 2003-1, 9-24.

Boehner, R. C. & Giles, P. S. 1993. Geology of the Antigonish Basin, Antigonish County, Nova Scotia. In: *Nova Scotia Department of Natural Resources, Mines and Energy Branch, Memoir* **8**.

Calder, J. H. 1998. The Carboniferous evolution of Nova Scotia. In: *Geological Society, London, Special Publications* **143**, 261-302.

Cote, P. R. 1964. Lower Carboniferous sedimentary rocks of the Horton Group in parts of Cape Breton Island, and their relation to similar strata of the Anguille Group in southwestern Newfoundland, University of Ottawa.

Craggs, S., Keighley, D., Park, A. F. & Waldron, J. W. F. 2013. Stratigraphy and salt tectonics of Missisippian-Pennsylvanian strata of the northern Cumberland Basin, Maringouin Peninsula, southeastern New Brunswick. *Atlantic Geology* **49**, 24-24.

Craggs, S., Keighley, D., Waldron, J. W. F. & Park, A. 2015. Salt tectonics in an intracontinental transform setting: Cumberland and Sackville basins, southern New Brunswick, Canada. *Basin Research*, 1-18.

Dafoe, L. T., Shaw, J., Jauer, C., Giles, P. S., Waldron, J. W. F. & Potter, D. P. 2016. New insights into the Bedrock and Quaternary Geology of St. George's Bay from a vertical integration of marine datasets, offshore western Newfoundland. *Bulletin of Canadian Petroleum Geology* **64**(1), 1.

Dietrich, J., Hannigan, P., Kezhen, H. & Giles, P. S. 2009. Petroleum resource potential of the Carboniferous Maritimes Basin, eastern Canada. *Frontiers + Innovation* **2009 CSPG CSEG CWLS Convention**, 1-3.

Dietrich, J., Lavoie, D. & Hannigan, P. 2011. Geological setting and resource potential of conventional petroleum plays in Paleozoic basins in eastern Canada. *Bulletin of Canadian Petroleum Geology* **59**(1), 54-84.

Gibling, M. R., Culshaw, N., Pascucci, V., Waldron, J. W. F. & Rygel, M. C. in press 2018. The Maritimes Basin of Atlantic Canada: Basin Creation and Destruction during the Paleozoic Assembly of Pangea. In: *Sedimentary Basins of the World* (edited by Miall, A.) **5**.

Gibling, M. R., Culshaw, N., Rygel, M. C. & Pascucci, V. 2008. Chapter 6 The Maritimes Basin of Atlantic Canada: Basin Creation and Destruction in the Collisional Zone of Pangea. In: *Sedimentary Basins of the World 5* (edited by Miall, A. D.). Elsevier, 211-244.

Hamblin, A. P. & Rust, B. R. 1989. Tectono-sedimentary analysis of alternate-polarite half-graben basin-fill successions: Late Devonian-Early Carboniferous Horton Group, Cape Breton Island, Nova Scotia. *Basin Research* **2**, 239-255.

Hibbard, J. & Waldron, J. W. F. 2009. Truncation and translation of Appalachian promontories: mid-Paleozoic strike-slip tectonics and basin initiation. *Geology* **37**, 487-490.

Javaid, K. M. 2011. Development and structure of the Kennetcook-Windsor basin, Nova Scotia, Atlantic Canada. Unpublished M.Sc. thesis, University of Alberta.

Johnson, S. K. 1999. Structural geology of the Horton and Windsor Groups, Cheverie, Nova Scotia, St. Mary's University.

Keppie, J. D. 1982. The Minas Geofracture. In: *Special Paper - Geological Association of Canada* (edited by St-Julien, P. & Beland, J.). Geological Association of Canada, Toronto, 263-280.

Knight, I. 1983. Geology of the Carboniferous Bay St. George subbasin, Western Newfoundland. *Mineral Development Division Department of Mines and Energy, Government of Newfoundland and Labrador* **Memoir 1**.

Lavoie, D., Sangster, D. F., Savard, M. M. & Fallara, F. 1998. Breccias in the lower part of the Mississippian Windsor Group and their relation to Zn-Pb mineralization; a summary. *Economic Geology* **93**(6), 734-745.

Martel, A. T. 2004. *The Horton Group Depositional Sequence and its Significance for Hydrocarbon Exploration. Report ME 2004-002 Mining Matters for Nova Scotia 2004: Opportunities for Economic Development*.

Martel, A. T. & Gibling, M. R. 1991. Wave-dominated lacustrine facies and tectonically controlled cyclicity in the Lower Carboniferous Horton Bluff Formation, Nova Scotia, Canada. In: *Lacustrine Facies Analysis* (edited by Anadon, P., Cabrera, L. & Kelts, K.). Blackwell Publising Ltd., Halifax, 223-243.

Martel, A. T. & Gibling, M. R. 1996. Stratigraphy and tectonic history of the Upper Devonian to Lower Carboniferous Horton Bluff Formation, Nova Scotia. *Atlantic Geology* **32**, 13-38.

Moore, R. G., Ferguson, S. A., Boehner, R. C. & Kennedy, C. M. 2000. Bedrock geology map of the Wolfville-Windsor area, NTS Sheet 21H/01 and part of 21A/16, Hants and Kings Counties, Nova Scotia. In: *Nova Scotia Department of Natural Resources Mineral Resource Branch Open File Map ME 2000-3, Version 2 scale 1: 50 000*.

Murphy, J. B., Waldron, J. W. F., Kontak, D. J., Pe-Piper, G. & Piper, D. J. W. 2011. Minas Fault Zone: Late Paleozoic history of an intra-continental orogenic transform fault in the Canadian Appalachians. *Journal of Structural Geology* **33**, 312-328.

Noade, J. E. 2010. Stratigraphy of the Cheverie Formation type section, Cheverie, Hants County, Nova Scotia, Dalhousie University Unpublished B.Sc. thesis.

Roliff, W. A. 1962. The Maritimes Carboniferous Basin of Eastern Canada. *Proceedings of the Geological Association of Canada* **14**, 21-41.

Schenk, P. E. 1967. The Macumber Formation of the Maritime Provinces, Canada; a Mississippian analogue to Recent strand-line carbonates of the Persian Gulf. *Journal of Sedimentary Petrology* **37**(2), 365-376.

Snyder, M. E. & Waldron, J. W. F. 2016. Unusual soft-sediment deformation structures in the Maritimes Basin, Canada; possible seismic origin. *Sedimentary Geology* **344**, 145-159.

Snyder, M. E. & Waldron, J. W. F. 2018. Fracture overprinting history using Markov chain analysis; Windsor-Kennetcook Subbasin, Maritimes Basin, Canada. *Journal of Structural Geology* **108**, 80-93.

St. Peter, C. 1993. Maritimes Basin evolution: key geologic and seismic evidence from the Moncton subbasin of New Brunswick. *Atlantic Geology* **29**, 233-270.

Thomas, A. K. & Waldron, J. W. F. 2017. Faults in the late Paleozoic Antigonish sub-basin, Nova Scotia, reinterpreted as potential salt welds. In: *Program with Abstracts - Geological Association of Canada; Mineralogical Association of Canada: Joint Annual Meeting* **40**, Kingston, Ontario, 376.

Utting, J. & Giles, P. S. 2008. Palynostratigraphy and lithostratigraphy of Carboniferous Upper Codroy Group and Barachois Group, southwestern Newfoundland. *Canadian Journal of Earth Sciences* **45**(1), 45-67.

van de Poll, H. W., Gibling, M. R. & Hyde, R. S. 1995. Upper Paleozoic Rocks. In: *Geology of the Appalachian Caledonian Orogen in Canada and Greenland* (edited by Williams, H.). Geological Survey of Canada, 449-455.

Waldron, J. W. F. 2004. Anatomy and evolution of a pull-apart basin, Stellarton, Nova Scotia. *Geological Society of America Bulletin* **116**, 109-207.

Waldron, J. W. F. 2005. Extensional fault arrays in strike-slip and transtension. *Journal of Structural Geology* **27**, 23-34.

Waldron, J. W. F., Barr, S. M., Park, A. F., White, C. E. & Hibbard, J. 2015. Late Paleozoic strike-slip faults in Maritime Canada and their role in the reconfiguration of the northern Appalachian orogen. *Tectonics* **34**(8), 1661-1684.

Waldron, J. W. F., Roselli, C. & Johnston, S. K. 2007. Transpressional structures on a Late Paleozoic intracontinental transform fault, Canadian Appalachians. In: *Tectonics of Strike-Slip Restraining and Releasing Bends* (edited by Cunningham, W. D., and Mann, P.). Geological Society, London, Special Publications 290, 367-385.

Waldron, J. W. F., Roselli, C., Utting, J. & Johnston, S. K. 2010. Kennetcook thrust system: late Paleozoic transpression near the southern margin of the Maritimes Basin, Nova Scotia. *Canadian Journal of Earth Sciences* **47**, 137-159.

Waldron, J. W. F. & Rygel, M. C. 2005. Role of evaporite withdrawal in the preservation of a unique coal-bearing succession: Pennsylvanian Joggins Formation, Nova Scotia. *Geology* **33**(5), 337-340.

Waldron, J. W. F., Rygel, M. C., Gibling, M. R. & Calder, J. H. 2013. Evaporite tectonics and the late Paleozoic stratigraphic development of the Cumberland Basin, Appalachians of Atlantic Canada. *Geological Society of America Bulletin* **125**(5-6), 945-960.

Wightman, W. G., Scott, D. B., Medioli, F. S. & Gibling, M. R. 1993. Carboniferous marsh foraminifera from coal-bearing strata at the Sydney basin, Nova Scotia: A new tool for identifying paralic coal-forming environments. *Geology* **21**, 631-634.

Wilson, P. & White, J. C. 2006. Tectonic evolution of the Moncton Basin, New Brunswick, Eastern Canada; new evidence from field and sub-surface data. *Bulletin of Canadian Petroleum Geology* **54**(4), 319-336.

Wilson, P., White, J. C. & Roulston, B. V. 2006. Structural geology of the Penobsquis salt structure: late Bashkirian inversion tectonics in the Moncton Basin, New Brunswick, eastern Canada. *Canadian Journal of Earth Sciences* **43**, 405-419.

Chapter 2. Unusual soft-sediment deformation structures in the Maritimes Basin, Canada: possible seismic origin

A version of this chapter has been published as: Snyder, M.E., Waldron, J.W.F., 2016, Unusual soft-sediment deformation structures in the Maritimes Basin, Canada: possible seismic origin, *Sedimentary Geology* 344, 145-159.

Soft-sediment deformation structures provide information on the early deformation history of sedimentary rocks. In the Mississippian Horton Group of the Windsor-Kennetcook subbasin of the Maritimes Basin in Nova Scotia, soft-sediment deformation structures include well-known features like load structures, neptunian dykes, and an intraformational breccia. More unusual features include sedimentary boudins, upward-convex bulb structures, and unique structures here termed microbasins. Microbasins are geometrically similar to minibasins associated with salt tectonics, but about three orders of magnitude smaller. These deformation structures formed when primary stratification was in a weakened state due to liquidization of sediment. Two types of structures exist: those that formed at the sediment surface and those that formed later, during burial. The triggering mechanism for soft-sediment deformation structures in the Horton Group was likely seismicity and overpressured conditions. A strong preferred orientation of soft-sediment structures oriented NW–SE is attributed to dextral strike-slip on the E–W Minas Fault Zone. Seismicity associated with movement along faults associated with the Minas Fault Zone could have induced liquidization of sediment.

2.1. Introduction

Soft-sediment deformation structures provide information on early deformation of sedimentary rocks mainly in tectonically active environments such as strike-slip systems, pull-apart basins, and sedimentary basins cut by faults (Hempton & Dewey 1983, Plint 1985, Rossetti 1999, Alsop & Marco 2011, Berra & Felletti 2011, Waldron & Gagnon 2011). Common soft-sediment deformation structures include convolute laminae, load structures, and slump deposits (Allen 1986, Obermeier 1996, Collinson 2005, Gibert et al. 2005, Kang et al. 2010, Owen & Moretti 2011), interpreted to result from liquidization of sediment. Striking soft-sediment deformation structures are present in the Mississippian Horton Group within the Windsor-Kennetcook subbasin of the Maritimes Basin in Nova Scotia (Fig. 2.1), which is known to have been tectonically active during deposition. The structures here described include common examples like load structures, neptunian dykes, and an intraformational breccia, but also structures that have been more rarely described, here termed sedimentary boudins, bulb structures, and microbasins. Dykes within Horton Group strata were described by Hesse and Reading (1978) and Martel and Gibling (1993); sedimentary boudins were described by Waldron et al. (2007). However, these authors made contrasting interpretations. No previous interpretation accounts for all soft-sediment deformation structures in the Windsor-Kennetcook subbasin. The purpose of this study is to describe and interpret the many soft-sediment deformation structures present in the well-exposed coastal outcrops on the shores of the macrotidal Bay of Fundy, and to integrate interpretations in order to attribute them to a deformation mechanism and trigger for deformation.

2.2. Regional Geology

The Upper Paleozoic Maritimes Basin is a large (400 km maximum diameter) and deep (>12 km) basin covering a large portion of onshore and offshore Atlantic Canada (Fig. 2.1) (Roliff 1962, Keppie 1982, Gibling et al. 2008, Hibbard & Waldron 2009). This basin formed in the Appalachian orogen, following Devonian (Acadian) orogenic events, during a period of trans-

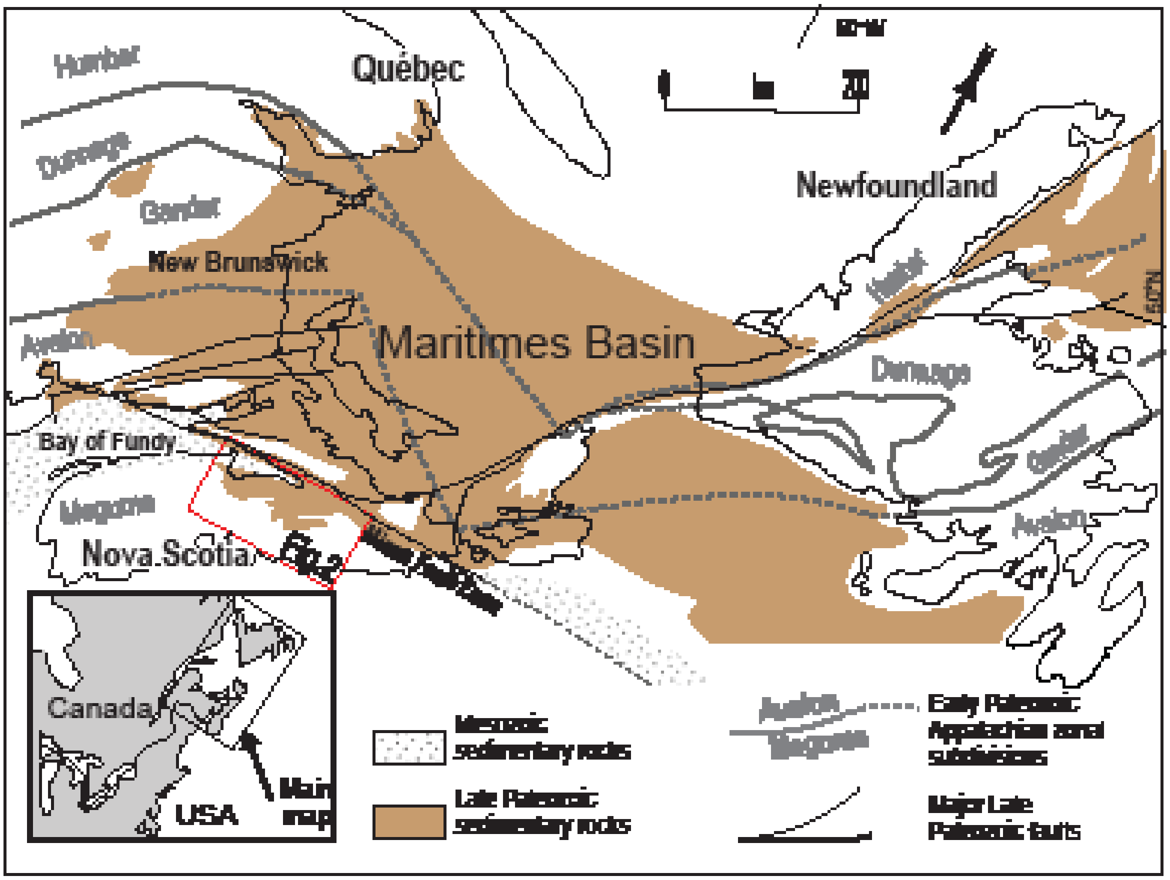

Figure 2.1. Distribution of the Maritimes Basin in Atlantic Canada.
Location of the Windsor-Kennetcook subbasin highlighted (modified from Waldron et al. 2007).

tension (Calder 1998, Hibbard & Waldron 2009, Waldron et al. 2014, Waldron et al. 2015). The Maritimes Basin is structurally complex, consisting of multiple subbasins trending generally northeast and east, and separated by uplifted basement rocks (Boehner & Giles 1993, van de Poll et al. 1995, Murphy et al. 2011, Waldron et al. 2013). Deformation of strata within the Maritimes Basin was a multi-stage process including periods of folding, faulting, uplift, salt tectonism, erosion, and subsidence (Knight 1983, Hamblin & Rust 1989, Calder 1998, Waldron 2004, Wilson et al. 2006, Waldron et al. 2013, Craggs et al. 2015, Dafoe et al. 2016). The subbasins have undergone multiple phases of subsidence and inversion, leading to the deposition of stratigraphic sequences separated by unconformities (St. Peter 1993). Because of these basement block movements, there is much lateral and vertical facies variation within and between subbasins.

The Windsor-Kennetcook subbasin is located within the Maritimes Basin (Figure 2.2). The lowest stratigraphic unit within the subbasin, and the unit of interest in this study, is the Late Devonian to Tournaisian Horton Group (Fig. 2.2) (Bell 1929). Across the Maritimes Basin, Horton Group and equivalent strata are typically interpreted as fluvial and lacustrine clastic deposits (Bell 1944, Knight 1983, Martel & Gibling 1996, Lynch et al. 1998, Park et al. 2010) with possible local marine influence suggested by Wightman et al. (1993).

Within the Windsor-Kennetcook subbasin the Horton Group is separated into two formations: the lower Horton Bluff Formation, and the upper Cheverie Formation (Bell 1929).

2.2.1. Horton Bluff Formation

Several stratigraphic schemes have been used to subdivide the Horton Bluff Formation in the Windsor-Kennetcook subbasin. Bell (1929) initially divided the formation into a basal, middle and upper member, whereas Martel and Gibling (1996) recognized four members: Harding Brook, Curry Brook, Blue Beach and Hurd Creek. Moore et al. (2000) grouped Martel and Gibling's Harding Brook Member and Curry Brook Member into a redefined lower member,

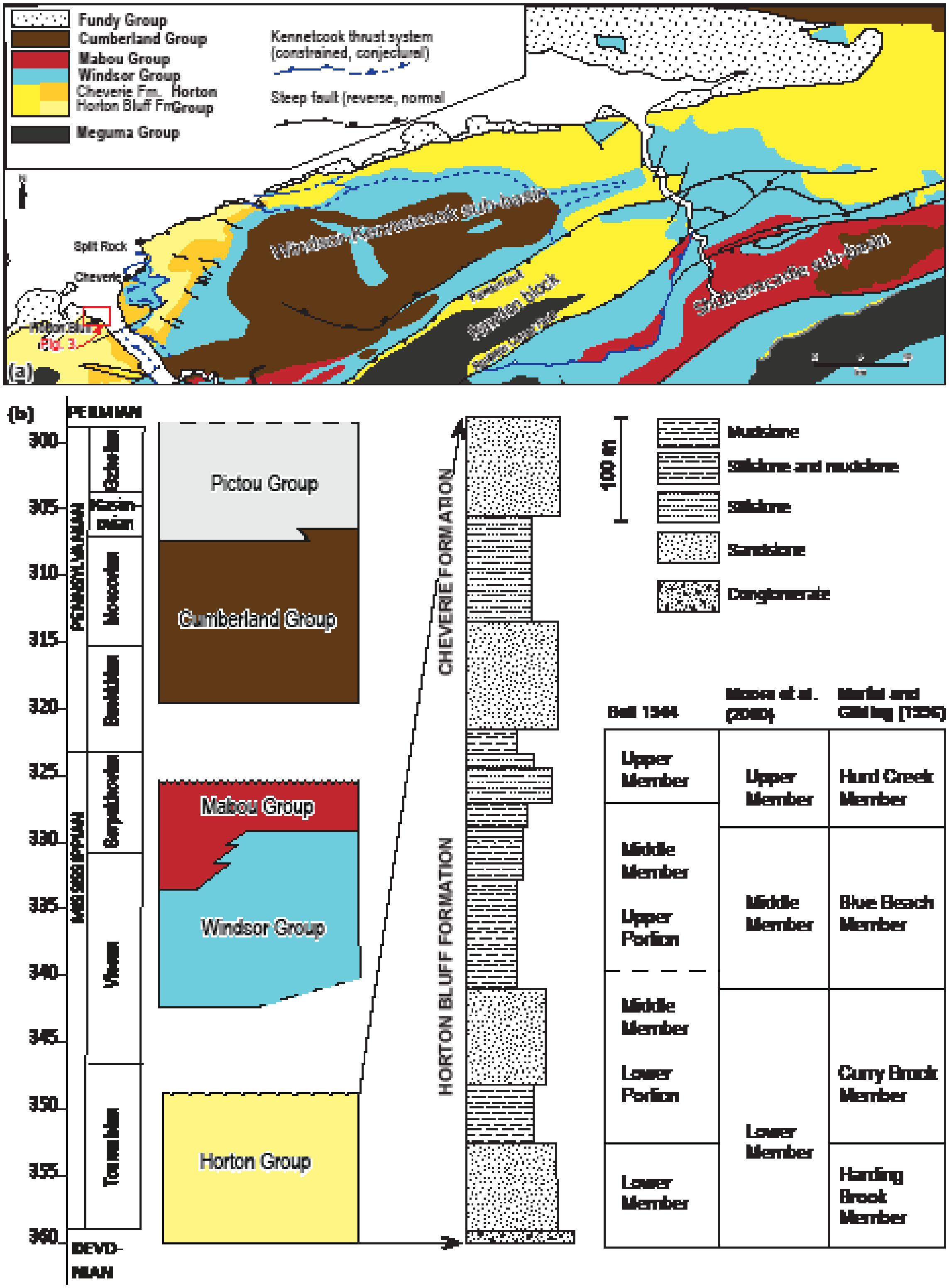

Figure 2.2. Windsor-Kennetcook subbasin in Nova Scotia
(a) map and (b) stratigraphic column. Shows major geological units and locations (modified from Waldron et al. 2010).

and recognized middle and upper members that are approximately equivalent to the Blue Beach Member and Hurd Creek Member respectively of Martel and Gibling (1996). Figure 2.2 details the relationship between different schemes; the Martel and Gibling (1996) classification is used in this paper.

The lowermost Harding Brook Member of the Horton Bluff Formation is defined by dominant sandstone with variable conglomerate, siltstone, and mudstone interpreted as the deposits of active channels (Martel & Gibling 1996). This unit is the most coarse-grained unit within the Horton Bluff Formation. The Curry Brook Member is defined by coarsening-up mudstone to sandstone cycles (Martel & Gibling 1996). The mudstone is bioturbated; organic-rich layers and siderite nodules are present. Cycles consist, from base to top, of: mudstone, alternating mudstone and planar-bedded siltstone to sandstone, and are capped by tabular coarsening-up ripple cross-laminated fine- to very coarse-grained sandstone (Martel & Gibling 1996). The Curry Brook Member is interpreted as lacustrine deposits (Martel & Gibling 1996).

The Blue Beach Member contains most of the soft-sediment deformation structures described here. It is defined by dark grey shale and mudstone, fine sandstone, dolostone, and common paleosol horizons (Moore et al. 2000). Six repeating facies are described by Martel and Gibling (1993) as: (1) grey mudstone and shale; (2) hummocky cross-stratified siltstone; (3) wave-rippled sandstone; (4) planar siltstone; (5) green mudstone; and (6) dolomite. The Blue Beach Member is interpreted by Martel and Gibling (1991) as deposited in a large, wave-dominated lake, although Wightman et al. (1993) inferred a marine influence based on the presence of agglutinated foraminifera.

The facies are organized in coarsening- and shallowing-up cycles that are interpreted to represent repeated cycles of tectonic subsidence followed by shoreline progradation (Martel & Gibling 1993). The soft-sediment deformation structures described below occur in facies (1), (2) and (4) and include dykes, microbasins, and boudins.

The Hurd Creek Member is composed of coarse grey medium- to coarse-grained sandstone (Moore et al. 2000). Cycles consist from base to top: (1) basal shale, (2) planar and lenticular siltstone and shale, (3) flaser-bedded sandstone and/or (4) interbedded rippled sandstone (Martel & Gibling 1996). Martel and Gibling (1996) interpret the Hurd Creek Member as deposited within a large wave-influenced standing body of water.

2.2.2. Cheverie Formation

The Cheverie Formation consists of three sections, which have not been distinguished as formal members. The bottom part of the formation includes thick cross-bedded, coarse-grained sandstone and conglomerate. The middle section of the formation consists of fining-up very coarse to fine sandstone and paleosols. The top section of the formation includes fining-up coarse sandstone to siltstone with carbonate nodules and conglomerate (Moore et al. 2000, Noade 2010).

Noade (2010) separated the upper section of the Cheverie Formation at Cheverie Point (Fig. 2.2), into three facies: (1) channel and overbank; (2) floodplain; and (3) abandoned channel deposits. Soft-sediment deformation structures at Cheverie include load structures, dykes, sedimentary boudins, and a large body of chaotic sediment where bedding is discontinuous and disturbed here termed intraformational breccia. Load structures and neptunian dykes occur within the mudstone, siltstone, sandstone, and paleosol of facies 2; the intraformational breccia and boudins are found within the siltstone and sandstone of facies 1.

2.2.3. Structure of the Windsor-Kennetcook subbasin

The Windsor-Kennetcook subbasin has been tectonically active periodically since its initiation in the late Devonian (Waldron et al. 2015). The subbasin is bounded to the north by the Minas Fault Zone (Fig. 2.1), a network of sub-parallel faults striking approximately east-west and separating the terranes of the Appalachians: Meguma to the south and Avalon to the north (Keppie 1982, Murphy et al. 2011). The Minas Fault Zone was active from the late Devonian to late Carboniferous, and again during Atlantic opening in the Mesozoic (Murphy et al. 2011).

South of the Minas Fault Zone, Horton Group strata are duplicated by the Kennetcook thrust system (Fig. 2.2) that climbs up-section to the southeast (Waldron et al. 2010). The Windsor-Kennetcook subbasin includes both the allochthonous hanging wall and the autochthonous footwall of the Kennetcook thrust system. The rocks in the hanging wall are intensely deformed by folds, faults, and evaporite-related structures; the footwall is less deformed, but shows faults, fractures and folds in outcrop (Waldron et al. 2005, Waldron et al. 2007, Waldron et al. 2010). Large-scale folds, faults, and unconformities are imaged in subsurface seismic profiles (Waldron et al. 2010). Waldron et al. (2010) and Javaid (2011) interpret sections that show faults that are not upwardly continuous, being truncated by local unconformities within the succession, indicating that the basin was tectonically active during deposition.

2.3. Soft-sediment deformation structures

Soft-sediment deformation structures in the Windsor-Kennetcook subbasin have been previously described only in the Horton Bluff Formation (Hesse & Reading 1978, Martel & Gibling 1993). At Horton Bluff (Fig. 2.2), interpreted as being in the footwall of the Kennetcook thrust system, strata dip gently (<20°) with few exposed folds and faults. These rocks belong to the Blue Beach Member of the Horton Bluff Formation. The Horton Bluff Formation also crops out at Split Rock (Fig. 2.2), interpreted to be in the hanging wall of the Kennetcook thrust system. Strata are more deformed at this locality, with open to tight folds attributed to multiple tectonic folding events (Waldron et al. 2007).

Soft-sediment deformation structures also occur at Cheverie (Fig. 2.2), located east of Horton Bluff, in gently dipping strata of the Cheverie Formation, interpreted to be in the footwall of the Kennetcook thrust system.

2.3.1. Microbasins

Description

At Horton Bluff, within facies (1) and (2) of Martel and Gibling (1996), are two horizons with large (>4 m^2) elliptical bodies of siltstone. Twelve such structures crop out on the wave-cut platform, shown in Figure 2.3. These structures were noted by Hesse and Reading (1978), who termed them "circular and elliptical collapse structures", but did not describe them in detail. Although not well understood, these structures are well known to the local geological community as the site is popular with student field trips (I. Spooner, Acadia University, personal communication 2013). Ten of the twelve structures occur at one stratigraphic horizon (structures 3-12 in Fig. 2.3).

All twelve structures are composed of laminated siltstone with minor interlaminated mudstone. These structures all have an elliptical shape in plan view, and appear isolated within surrounding fissile mudstone. Long axes range from 2–20 m and are all aligned, trending NNW–SSE (Fig. 2.4). Short axes, measured perpendicular to long axes, range from 1–12 m. Laminae terminate along the outlines of the bodies in truncated elliptical patterns (Fig 5a). The elliptical siltstone bodies are embedded in a layer of fissile shale (Fig 5d). This shale is up to 65 cm thick between adjacent structures, and is most thin or absent between the base of each structure (where exposed) and the competent siltstone layer below (Fig. 2.5h). Shale fissility parallels regional bedding beneath the structures, but is locally perpendicular to regional bedding between adjacent structures.

On the lateral edge of structure 8 (Fig. 2.5h) a dyke (similar to those described below) crops out. The adjacent shale shows fissility that is truncated by the edges of the dyke. This dyke shares the common NNW-SSE trend shared by the siltstone body long axes (Fig. 2.4), and dykes elsewhere in the section.

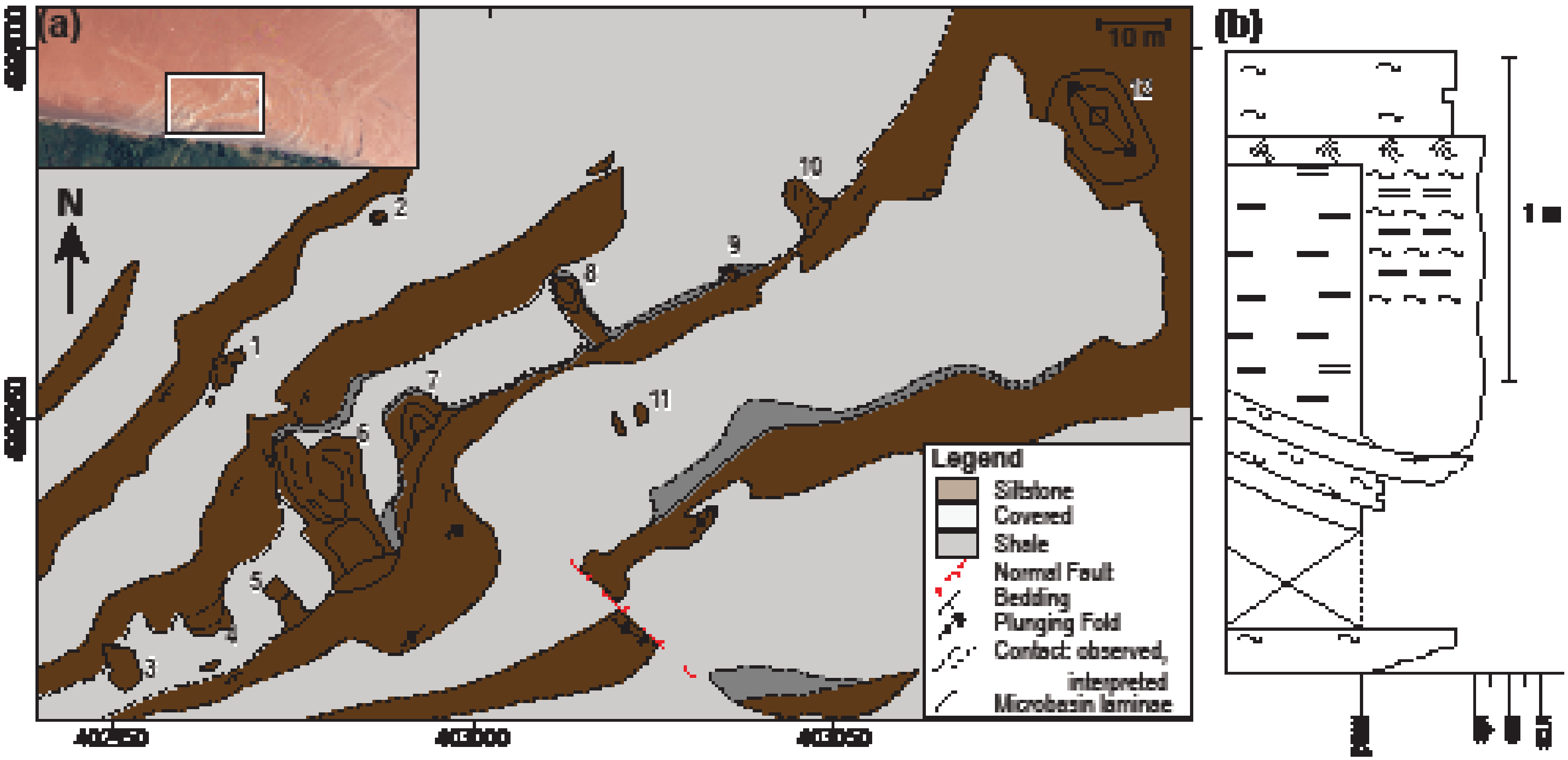

Figure 2.3. Microbasins at Horton Bluff

(a) Aerial photograph and field map of microbasins at Horton Bluff exposed at low tide. Microbasins 1 – 12 are labeled. UTM (Universal Transverse Mercator) coordinates are in North American Datum 1983; (b) stratigraphic column at Horton Bluff showing the microbasin main horizon (microbasins 3-12); legend same as Figure 2.7.

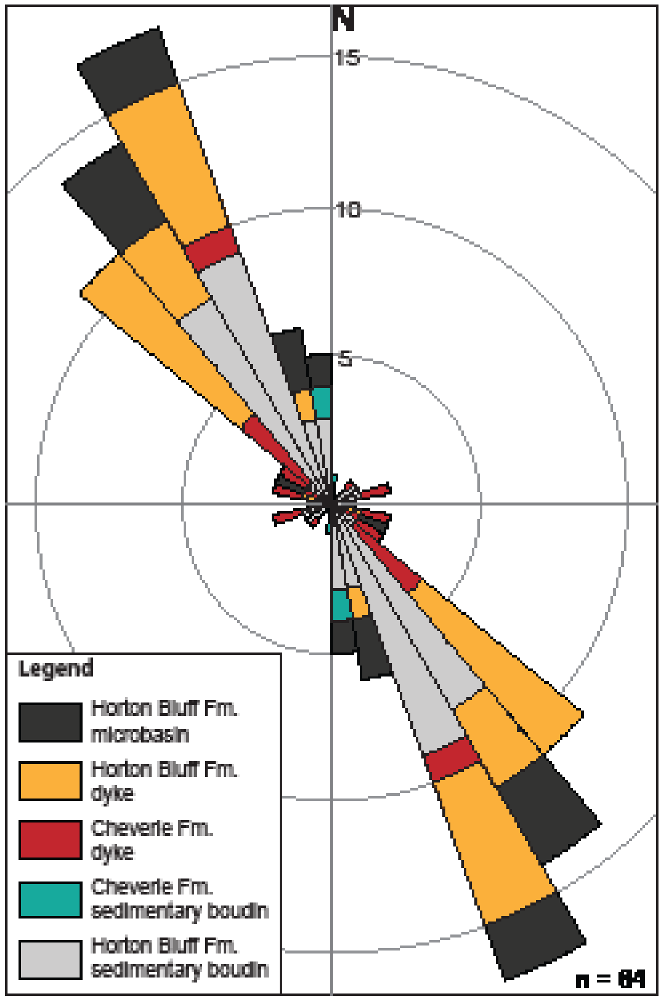

Figure 2.4. Rose diagram of all measured soft-sediment deformation structure long axes. Microbasins, sedimentary boudins, and neptunian dykes shown.

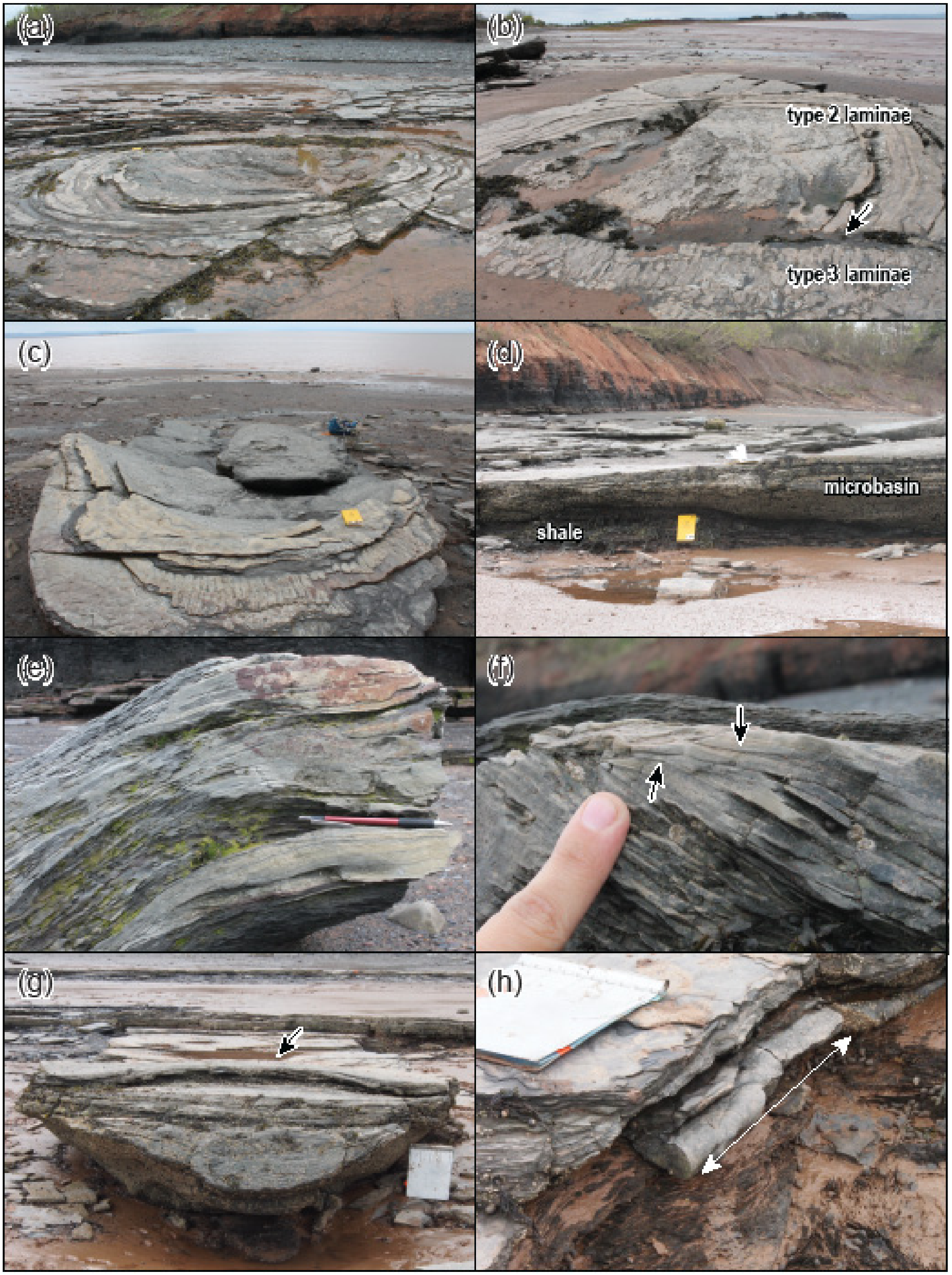
(a)
(b)
type 2 laminae
type 3 laminae
(c)
(d)
microbasin
shale
(e)
(f)
(g)
(h)

Figure 2.5. Photographs of exposed microbasins, numbered from Figure 2.3
(a) microbasin 6 showing type 2 laminae terminating in circular pattern at edges of the structure; (b) microbasin 7 showing type 3 laminae unconformably overlying type 2 laminae (arrow); (c) microbasin 9 showing laminae, including wavy laminae, terminating along the outline of the structure in a semi-circular pattern; (d) microbasin 8 showing shale of variable thickness beneath the siltstone body; (e) cross-sectional view through microbasin 5 showing dipping laminae; (f) microbasin 8 showing multiple unconformable surfaces on edges of structure (arrows); (g) side view of microbasin 8 showing convex-up laminae in the top 10 cm of the structure (arrow); (h) lateral edge of microbasin 8 with neptunian dyke parallel to long axis of microbasin (arrow) and underlying shale showing bedding-parallel fissility beneath the siltstone and bedding-perpendicular fissility at right edge of photograph. Field notebook, pencil, and clipboard for scale.

Structures 1-7, 9, and 10 (Fig. 2.3) are bowl-shaped with concave-up layers (Fig. 2.5c-g). Their maximum observed cross-sectional thicknesses range from 40 cm to 1.5 m. In cross section the structures thin laterally to zero at their edges. From base to top, each structure displays three sets of laminae: (1) bottommost layers (5–10 cm) are of approximately equal thickness across the structure; (2) middle layers (30 cm–1 m) make up the bulk of the structure, showing laminae thinning laterally from the centre; and (3) top layers (3–10 cm) have planar to wavy laminae. Unconformable surfaces are observed between set (2) laminae, where laminae above the unconformable surfaces overstep laminae below at the edges of the structures (Fig. 2.5f). Set (2) laminae also terminate at unconformable surfaces with sharp truncations against the base of set (3) laminae (Fig. 2.5b).

The majority of structures are concave-up in cross-sectional view, the top laminae being planar and flat. However, structures 8, 11, and 12 (Fig. 2.3) show variations from this geometry. Their set (1) and (2) layers are similar to structures 1-7, 9, and 10. The difference is in the top 10 cm of the structure, where set (2) and (3) laminae are convex-up, not planar (Fig. 2.5g). In plan view, these convex-up laminae are continuous across the structures.

Interpretation

The bottom 5– 10 cm of each structure shows set (1) parallel laminae, suggesting that sediment was deposited in a continuous layer prior to the initiation of the bowl-shaped structures. The gradual thickening of the set (2) laminae towards the centre of each structure, and the localized unconformable and overstep relationships around the edges of the structures, indicate that the structures formed by a synsedimentary process, where sediment was deposited during development of the bowl shape. The unconformable surfaces represent periods when tilting was rapid relative to sedimentation, allowing erosion to take place toward the margins. This process likely took place over hours or days. These relationships indicate that the structures initiated near the top of the sediment pile, when only 5–10 cm of silt had been deposited on the underlying mud layer.

The thickness of the underlying shale is dependent on the thickness of the siltstone bodies that fill the microbasins; shale is absent to very thin beneath the larger structures, which are juxtaposed against the underlying sandstone. This variability indicates that thinning of the shale occurred during filling of the structures. Between adjacent siltstone bodies, there is no siltstone but abundant shale shows changes in fissility orientation between parallel and perpendicular to regional bedding. This shale is interpreted as representing mud that locally rose diapirically between the subsiding silt-filled bowl-shaped structures.

Variations in shale thickness and fabric, together with stratigraphic relationships in the adjacent siltstone-filled depressions, clearly indicate that shale was mobilized while still close to the sediment surface. Liquidization of shale allowed denser silt to depress and displace the finer material producing the concave-up geometry of the silt beds within the microbasins.

A model for the formation of these structures is shown in Figure 2.6. Density differences, or differential loading, in wet sediment initially allowed silt laminae of set 1 to subside and displace underlying shale. Deformation and subsidence made accommodation space allowing silt laminae of set 2 to be deposited, differentially loading the underlying shale and amplifying the structure. Depositional hiatuses and variations in accommodation space towards the edges of the structures developed as mud below the structure migrated and was expelled vertically between structures. As the mud was migrating vertically, it raised the edges of the siltstone above the sediment-water interface. At these times both the mud and the silt were eroded, creating local unconformities as deformation continued. Planar and wavy laminae of set 3, deposited after cessation of deformation, cap the structures.

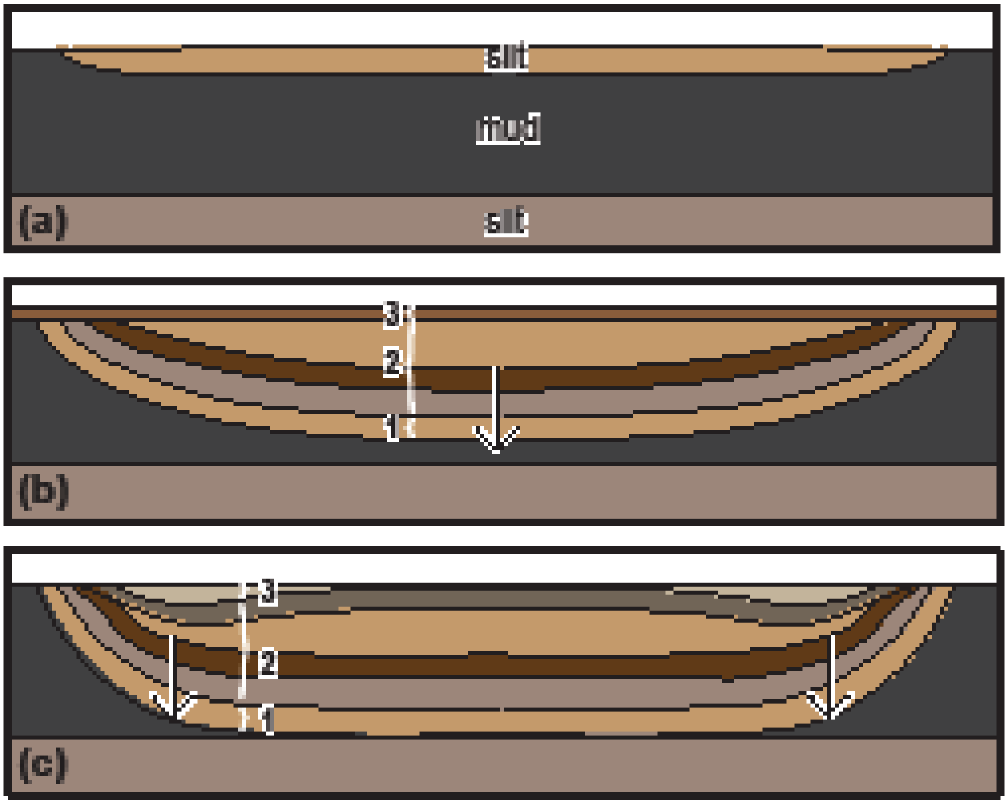

Figure 2.6. Schematic model for microbasin formation.
(a) Denser silt deposited on less dense mud; (b) silt sinks into liquidized mud below, continued subsidence coincident with deposition of silt; (c) silt welds out on competent layer below, lateral edges continue to subside with potential for complete welding of silt onto competent layer below, preserving an antiformal structure in centre. Laminae type indicated with brackets.

The domed structures (8, 11, 12) formed in the same was as those described above with an added step (Fig. 2.6). In the centre of these structures, the bottom laminae are in direct contact with the underlying competent sand layer. As the centre of the mass welded against the underlying sandstone, the laminae at the margins continued to subside, developing additional accommodation at the margins and leading to the convex-up appearance of the central portion of the structure.

The cause of localized initial subsidence is uncertain. The structures show some resemblance to hummocky cross-stratification (HCS), and it is possible that subsidence was initiated by local loading below wave-induced bedforms. However, in their progressive development, the structures depart from typical HCS geometries in showing sharply curved basal surfaces, and in displaying relatively high-angle truncation and onlap relationships principally around their edges, in contrast to the broadly developed low-angle truncations found in typical HCS. Thus although wave action may have played a part in their initiation, it is clear that progressive deformation during their development was driven by differential sediment loading. However, they also differ in geometry from typical large load structures, such as those Figure 2.d by Molina et al. (1998) and Alfaro et al. (2010), because their geometries, and particularly the internal truncations of laminae, show that they developed during deposition of their sedimentary fill, and not afterwards.

These structures show strikingly similar geometry to minibasins, characteristic of salt tectonics on continental margins (Dyson & Marshall 2005, Hudec et al. 2009, Peel 2014). Minibasins form as evaporites are expelled from beneath more dense lithologies; evaporites build into salt diapirs adjacent to these structures. Minibasins can have concave-up geometries, or can form convex-up turtle structures, analogous to those seen in structures 8, 11, and 12, as a salt weld develops. Because the structures at Horton Bluff are morphologically similar to minibasins but about three orders of magnitude smaller, the term microbasin is appropriate.

2.3.2. Load Structures

Description

Rare layers in the Cheverie Formation display load structures with more normal scale, similar to examples described by Owen (2003). For example, only three layers with load structures are observed in the Cheverie type section (Fig. 2.7), and are localized in 25 m of section. Multiple load structures of similar size and shape occur in each layer. The three layers are labeled A, B, and C; the geometry of each load structure is shown in Figure 2.7. Structures in layers A and B are 10–125 cm maximum height, composed of very fine- to fine-grained sandstone overlying mudstone. Layer C, composed of very fine sandstone, contains load structures 3–12 cm in height, overlying a layer of very fine sandstone. Beneath this layer, neptunian dykes (see below) project into underlying mudstone (Fig. 2.7).

Interpretation

Load structures have been classified geometrically by Owen (2003) as simple loads, attached pseudonodules and detached pseudonodules. All three load types are formed when more dense sediment sinks into liquidized less dense sediment below. In analogue sedimentary successions, load structures are weakened by excess pore fluid that produces liquefaction (Lowe 1975, Owen 2003, Collinson 2005). All three types of loads are observed at Cheverie: load structure layer A comprises attached pseudonodules; load layer B with undulatory bottom load surfaces, had more uneven loading of sediment compared to layers A and C, and comprises attached and detached pseudonodules; load layer C comprises simple loads.

Load structures form by density contrasts and uneven loading, where more dense sand above sinks into less dense liquidized material below. Owen (2003) shows that the complexity of the

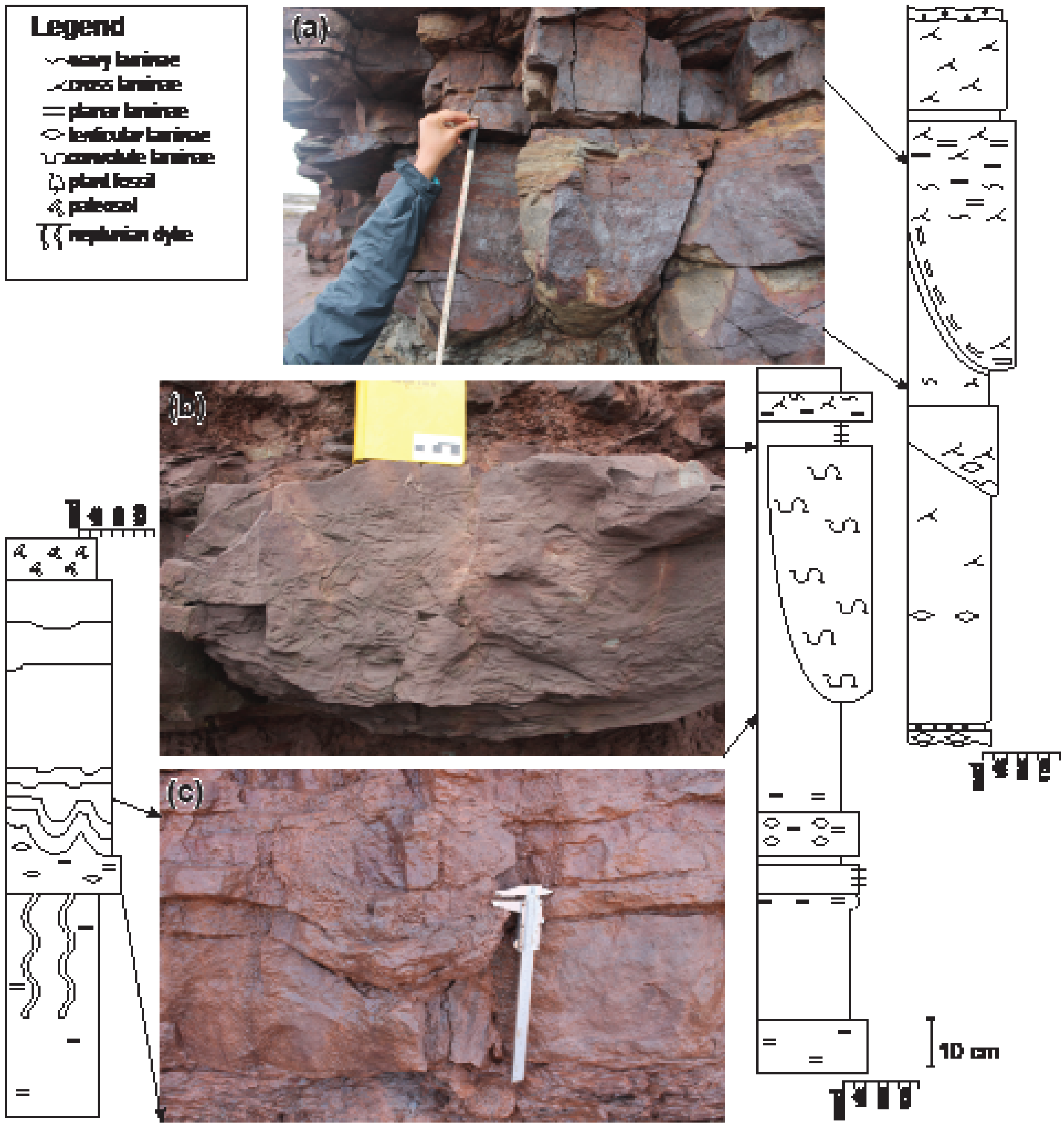

Figure 2.7. Photographs and stratigraphic columns showing Cheverie Formation load structures (a) layer A, (b) layer B, and (c) layer C. Arrows indicate extent of stratigraphic column shown in each photograph.

structures increases with stronger driving forces or longer duration of liquidization, from simple loads to attached pseudonodules to detached pseudonodules.

2.3.3. Intraformational breccia

Description

At Cheverie, a laterally discontinuous, chaotic, red/grey very fine sandstone body (Fig. 2.8) overlies 3 m of cross-stratified medium- to coarse-grained sandstone interpreted as a fluvial channel-fill, and is unconformably overlain by an undisturbed sandstone layer. The body is 2 m thick in the centre and is exposed on wave-cut platform over a visible area of 13.5 x 13 m. The structure terminates in the adjacent cliff, so its complete extent is unknown. At the base of the unit, the sandstone is nearly parallel bedded, and higher in the structure, the structure shows block-in-matrix configuration.

The degree of deformation within the structure increases from northwest to southeast. In the northwest, laminae are contorted, and no brecciation is observed. In the southeast, angular blocks of sandstone show internal laminae at variable orientations surrounded by finer sandstone matrix (Fig. 2.8b). These angular blocks are variable in size; isolated clasts range from 4 cm^2 in diameter to dimensions too large to show their complete extent within the available outcrop. The matrix is massive sandstone with no observed lamination. The structure pinches out to the northeast. Immediately overlying the structure is near horizontal sandstone bed, locally rippled, the base of which truncates the contorted laminae as shown in Figure 2.8b.

Interpretation

The limited extent and southeastward increase in deformation shows that this unit likely records a mass movement event. This structure formed at, or close to, the sediment surface as the uncon-

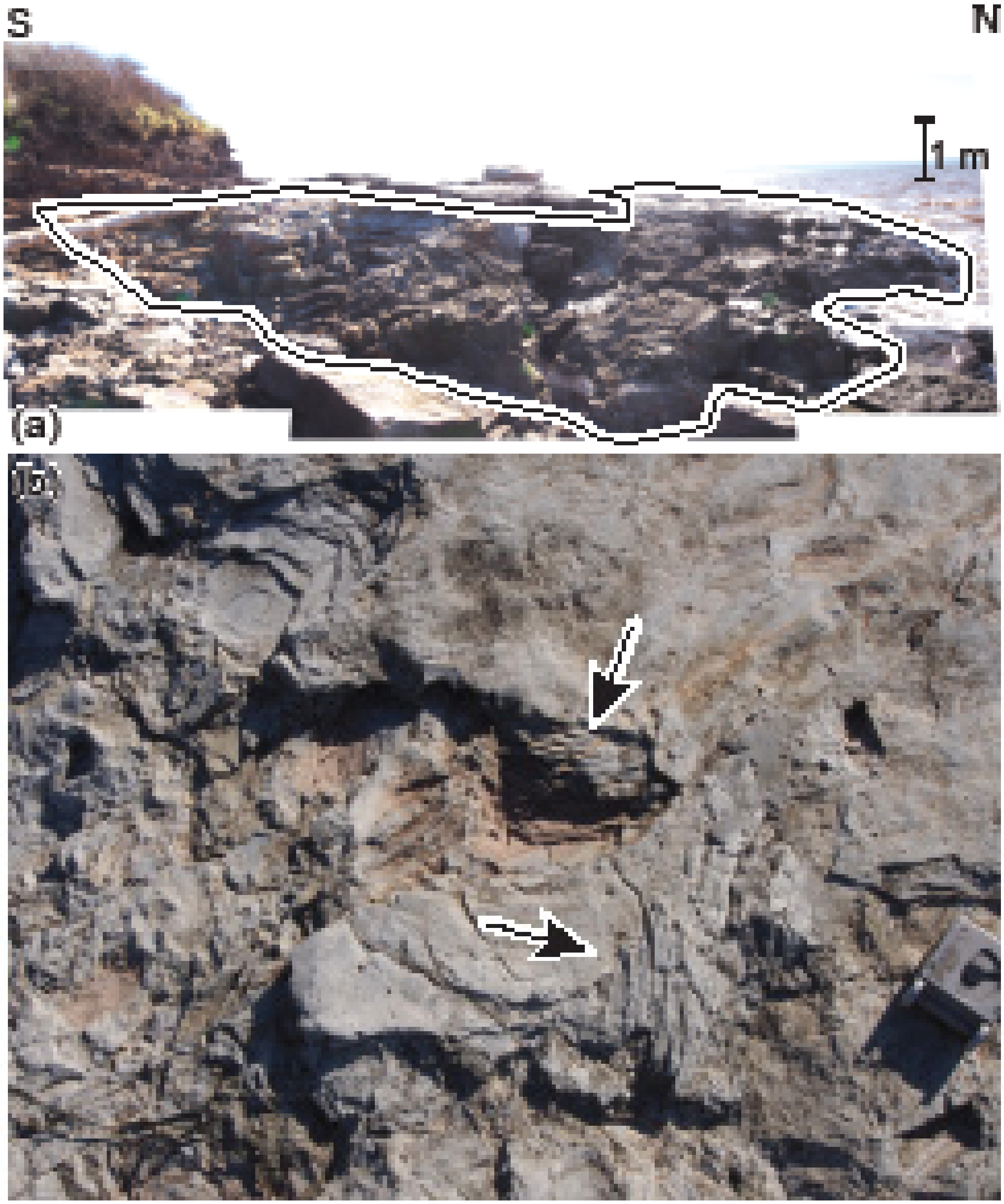

Figure 2.8. Intraformational breccia at Cheverie
(a) Panorama, line shows extent of breccia; (b) internal structure showing blocks of partially lithified silt and sand (arrows) surrounded by a sand matrix.

formable base of the overlying bed truncates it. The angular shape of the blocks and their internal parallel laminae suggest they are remnants of a continuous layer that had some cohesion, indicating partial lithification of sediment prior to failure. The lack of laminae in the matrix suggests that it was liquidized at the time of formation; fragments of original sediment were separated from others by liquidized material intruding between the fragments (Berra & Felletti 2011).

2.3.4. Neptunian dykes

Previous work

Hesse and Reading (1978) recognized over 100 parallel linear fissures striking NW–SE. They interpreted that the structures were sand volcanoes, formed by upward movement of sand with the overspill preserved atop the structures in many cases, forming lenses of sandstone. They noted that the structures were significantly folded, indicating formation before significant compaction of the host mudstone. Hesse and Reading (1978) suggested the deformation mechanism as liquefaction of sediment, and the trigger for deformation as earthquake shocks.

Martel and Gibling (1993) argue that the overspill deposits of Hesse and Reading (1978) are hummocky cross-stratified siltstone lenses, and that the structures formed by injection of siltstone down from these lenses into a host mudstone which was later compacted. Martel and Gibling (1993) report the consistent orientation of structures as parallel to wave-ripple crest orientations. They interpret the deformation mechanism as liquefaction of sediment, and the trigger for deformation as storm-wave activity paired with rapid sedimentation. In their interpretation, the parallel alignment of the dykes reflects the orientation of the paleoshoreline.

Horton Bluff Formation

Dykes in the Horton Bluff Formation occur along laterally continuous horizons associated with coarsening up cycles (facies 1 and 2 described above) in the Blue Beach Member. Examples crop out at Split Rock and Horton Bluff (Fig. 2.2). All observed dykes at Horton Bluff, and most dykes at Split Rock, occur at the base of sandstone lenses, interpreted respectively as sand volcanoes and hummocky cross stratification by Hesse and Reading (1978) and Martel and Gibling (1993).

Dykes are composed of grey siltstone with homogeneous (rarely convolute) internal structure (Figure 2.9a,b). Laterally adjacent to dykes is dark grey mudstone with bedding-parallel fissility approximately 1 m thick (Fig. 2.9a). In cross-sectional view the dykes are wide (1 - 25 cm) at the top and thin (approximately 1 cm) at the bottom. The dykes are 5 cm–1.12 m in height (average 12 cm). At Split Rock, dykes commonly bifurcate towards the bottom (Fig. 2.9b). The dykes at both Horton Bluff and Split Rock are folded ptygmatically. The folds are tight to isoclinal, with hinges parallel to the strike of the dykes in which they occur (Fig. 2.9a and b). We calculated the compaction ratio of the dykes at Horton Bluff and Split Rock from original (sinuous) height divided by present-day height. The average compaction ratio at Horton Bluff was calculated to be 2.3, identical to the result of Martel and Gibling (1993), and at Split Rock was calculated as 2.1.

The dykes are elongate, trending approximately NW–SE (Fig. 2.4) (Martel & Gibling 1993). The dykes in each horizon, at both Horton Bluff and Split Rock, are aligned parallel to each other. A less common WSW–ENE set of dykes at Split Rock cross-cuts this dominant NW–SE set.

Cheverie Formation

In the Cheverie Formation, dykes similar in appearance to those in the Horton Bluff Formation crop out in the interpreted floodplain facies. Dykes occur in multiple laterally continuous ho-

Figure 2.9. Neptunian dykes
(a) Horton Bluff, showing ptygmatic folding; inset shows bedding-parallel fissility intersected by dyke margin; (b) Split Rock, showing overlying hummocky cross-bed and downward bifurcation of dyke (arrows); and (c) Cheverie; dyke in redbeds shows less shortening by folds than (a) and (b), reflecting lesser compaction.

rizons. The dykes are composed of very fine sandstone, surrounded by bedding-parallel fissile mudstone (Fig. 2.9c). Overlying the dykes is very fine sandstone 17 cm thick with diffuse lenticular and planar laminae in its lower 5 cm; the upper part of this bed is homogeneous. The top surfaces of the dykes range from 4–12 cm wide and the dykes average 30 cm in height (ranging 12 cm–1 m). The dykes pinch downward without bifurcating and are elongate, showing a NW–SE trend similar to the dykes at Horton Bluff (Fig. 2.4). The dykes in the Cheverie Formation are ptygmatically folded but and the compaction ratio is calculated as 1.3, much less than those in the Horton Bluff Formation.

Interpretation

Hesse and Reading (1978) interpreted the dykes at Horton Bluff as products of upwelling of liquefied sediment originating from below whereas Martel and Gibling (1993) interpret the dykes to have projected down from above. Our observations clearly support Martel and Gibling (1993). The dykes in the Horton Bluff Formation and Cheverie Formation are wider at the top surface and thin downward. Dyke tops are at a constant level, and terminate at different stratigraphic intervals indicating that the siltstone projected from the top surface down into a host mudstone. They are therefore neptunian dykes in the terminology of Moretti and Sabato (2007). Load structures and thinning of beds directly above a dyke at Cheverie (Fig. 2.7c), suggest that dyke formation took place shortly after deposition of the overlying sandstone.

The neptunian dykes developed before the source sand and the surrounding mud were fully lithified, indicating a shallow depth of formation (Parnell & Kelly 2003). Sharp angular boundaries of dyke fill against surrounding mudstone, with no mixing, show that mud behaviour was brittle; convolute silt flowed in to the space created by opening of the fissure. Subsequent compaction of the mudstone buckled the siltstone and created the folded geometry of the dykes and the fissility of the mudstone. Differential compaction led to ptygmatic folding because the compaction experienced by the host mudstone was greater than the silt within the dyke (Martel & Gibling 1993, Laubach et al. 2000, Collinson 2005, Berra & Felletti 2011). In the Cheverie Formation, the compaction ratio is smaller than in the Horton Bluff Formation suggesting that there was less water when the dykes were formed. This contrast is consistent with the inferred depositional environments; neptunian dykes in the Horton Bluff Formation are within facies interpreted as subaqueous lacustrine mudstone whereas those in the Cheverie Formation were formed in a subaerial environment where water was probably lost by evaporation prior to development of dykes.

Convolute internal structure of the siltstone in the dykes clearly shows that the silt was mobile at the time of injection. In contrast, sharp contacts with adjacent shale, truncating laminae (Fig. 2.9a), show that the shale behaved in a brittle manner. Waldron and Gagnon (2011) show that ductile behaviour of coarser sediment juxtaposed with brittle mud is a strong indicator of liquidization. Martel and Gibling (1993) interpret the dykes as products of downward injection of liquidized silt due mainly to wave loading, and the preferred orientation of the dykes to bathymetric slopes associated with shorelines, as it is unlikely that fluid pressure alone could apply sufficient directed stress to produce fractures with a strong preferred orientation (Martel & Gibling 1993). However, the presence of similarly oriented dykes in the subaerial Cheverie Formation casts doubt on these interpretations. Folding of the dykes shows that the surrounding mud was not fully compacted at the time of dyke injection, suggesting that high strain rates were necessary for formation of the fractures. These observations, and the similarity in orientation between the dykes and other structures observed (Fig. 2.4), suggest that their formation was controlled by stresses associated with tectonic processes, possibly acting in addition to wave action and paleoslope as envisaged by Martel and Gibling (1993).

2.3.5. Sedimentary boudins

Description

Within interbedded siltstone and mudstone sediments at Horton Bluff, Split Rock, and Cheverie are ribbed features on bedding surfaces. Examples were described by Waldron et al. (2007) at Split Rock, who interpreted them as structures produced by extension in sediments that were incompletely cemented, kinematically equivalent to boudins that are more usually described in metamorphic rocks.

In plan view, these structures are 1–20 mm wide, and create a pattern of parallel hatching on bedding surfaces (Fig. 2.10a). These always occur in multiples, and at Split Rock, crop out on most visible siltstone horizons (Fig. 2.10b). The dominant trend across all localities is NW–SE, displayed in the composite rose diagram in Figure 2.4.

Thin sections cut perpendicular to the trace of lineations on bedding surfaces show a layer of segmented siltstone and sandstone (Fig. 2.10c). Between the siltstone and sandstone segments is mudstone. The boudins layers range 1–5 mm thick. Individual boudins are 2 mm–2 cm wide. The contact on lateral surfaces between silt boudins and the adjacent clay is gradational in some layers and sharp in others.

There is strong crystallographic preferred orientation of the majority of clay minerals in thin sections. Clay minerals are aligned parallel to bedding across the entire section, except between the sedimentary boudins. Between boudins in the same layer, clay minerals are oriented preferentially perpendicular to bedding.

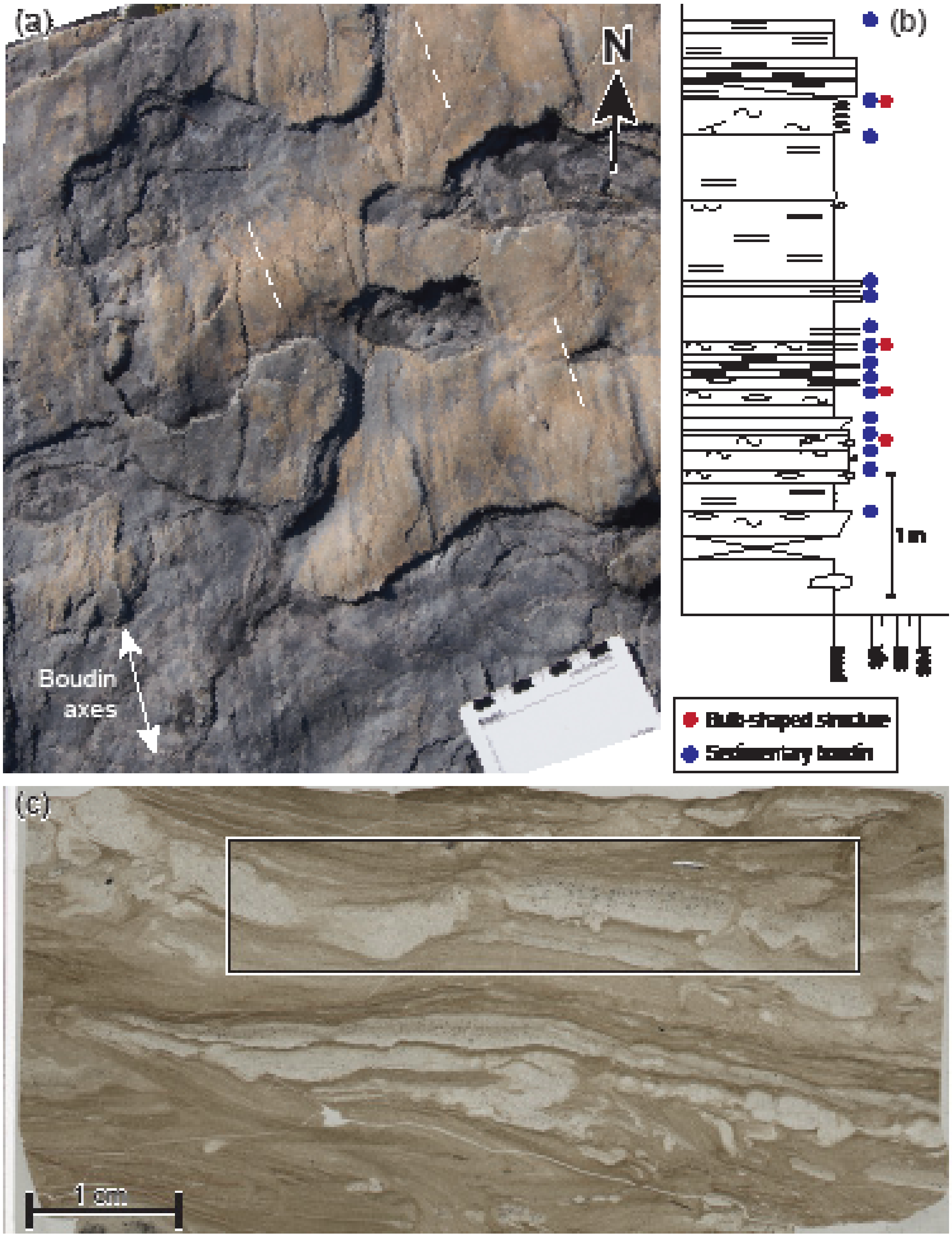

Figure 2.10. Sedimentary boudins
(a) crop out as parallel hatchmarks on the surface of bedding (dashed lines); (b) stratigraphic column at Split Rock showing sedimentary boudins and bulb structure horizons (Legend the same as Figure 2.7); (c) thin section through sedimentary boudins horizon, boudins outlined.

Interpretation

The observations support the interpretation of Waldron et al. (2007) that the structures are produced by boudinage of continuous layers. These structures are extensional and result from semi-brittle deformation of partially lithified material. These structures likely formed by extension of more rigid siltstone and sandstone; created space was filled by finer-grained sediment. As there is both a brittle and ductile component to these structures, they likely formed prior to complete lithification of sediment. After some time, compaction led to the alignment of clay minerals parallel to bedding except in boudin layers. In between sedimentary boudins, the clay was protected from compaction, resulting in no dominant crystallographic preferred orientation parallel to bedding. Clays that are aligned perpendicular to bedding may have been aligned by flow into the space initially created in the boudinage event, or by later tectonic compression.

The precise depth of formation of these structures is difficult to determine. There are no erosional surfaces indicating shallow-water initiation. It is possible that these structures formed at a significant depth. The structures are aligned across multiple horizons in all three localities, indicating the direction of extension was similar in each instance. Recurring events related to deformation of sediment could cause these structures to form.

2.3.6. Bulb structures

Description

At Split Rock (Fig. 2.2), in the Horton Bluff Formation, many interlaminated siltstone and mudstone layers with cross-laminae are less than 1 cm thick (see the stratigraphic column in Fig. 2.10b). At multiple intervals within these layers are siltstone protuberances that superficially resemble small load structures as seen in many examples of lacustrine sediment (Hempton & Dewey 1983, Alfaro et al. 2002, Owen 2003, Ezquerro et al. 2015) where concave-up bodies of coarser sediment protrude down into underlying finer material. In contrast, the structures described here are convex-up bodies of coarser grained material protruding upward into mud. These structures have been described rarely in the literature. Hempton and Dewey (1983) and Scott and Price (1988) described similar structures from lacustrine sediments in southern Turkey calling them “cycloids”. Rodriguez-Pascua et al. (2000) termed these same structures from southeast Spain “mushroom-like silts”. Nikolaeva (2009) described similar structures in northwest Russia and termed them "bulb-shaped structures". In this paper we refer to them simply as bulb structures.

In plan view, the bulb structures are 1–5 mm diameter and appear as sub-angular siltstone polygons with quasi-equal sides and rounded corners (Fig. 2.11a). They occur in groups within a mudstone matrix. These groups cover areas approximately 25 cm^2 on the tops of siltstone beds. These structures occur in a section that is unequivocally upright, and contains no evidence of overturned bedding. The layers displaying bulb structures include one horizon that is cut by neptunian dykes and contains sedimentary boudins (see above).

Thin sections were cut from hand samples with surface exposure of these structures. In each case, at least five additional layers display the same or similar structures within the sample. In cross section, the structures are convex-up siltstone bodies, partially surrounded by mudstone (Fig. 2.11b). Beneath each bulb structure layer is an interval of planar-laminated fine siltstone to mudstone 5–10 mm thick. Within these mudstone and siltstone intervals are isolated bodies of silt 0.3–3 mm thick. The bottom surface of each bulb layer is undulatory and locally may show conventional load structures or neptunian dykes, initiating from the same horizon, penetrating downwards (Fig. 2.11b).

All siltstone layers bearing bulb structures thin and pinch out laterally. The thickest part of the layer is where the bulb structures are observed. In the bulb-bearing layers, sediment shows variations in sorting and grain size; better sorted sediment occurs within the bulb areas. Within the

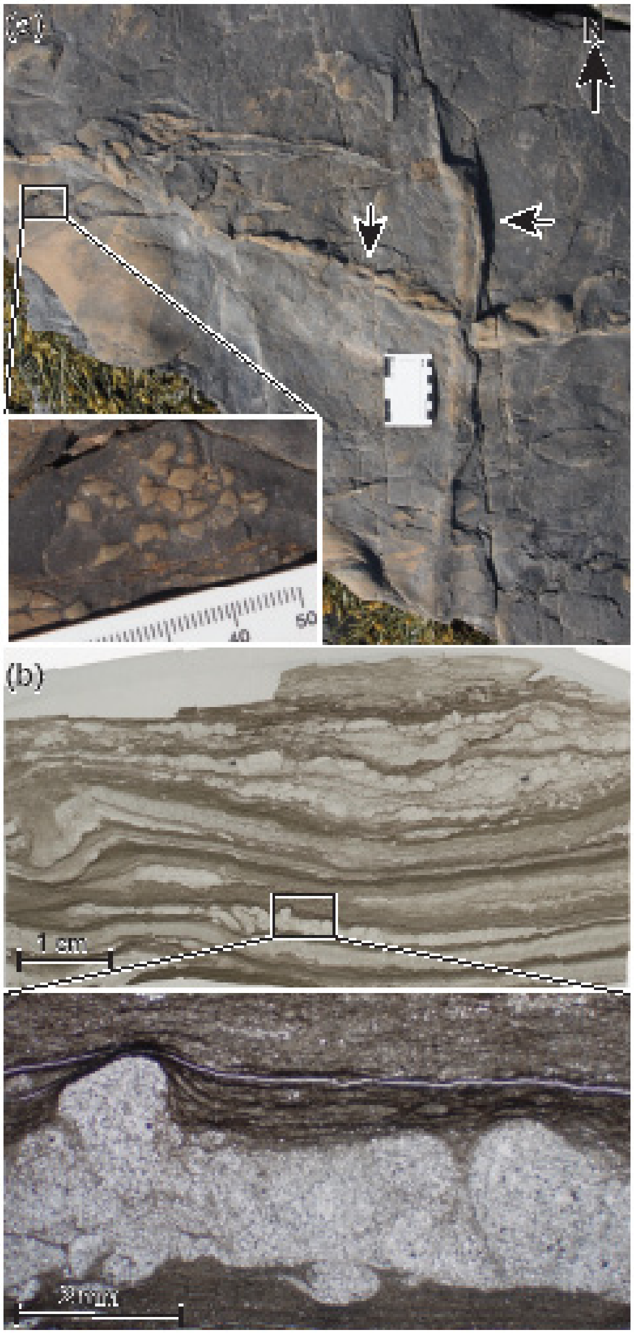

Figure 2.11. Bulb structures
(a) bulb structure layer with two neptunian dykes (arrows) cropping out on surface of bedding; inset shows enlargement of bulb structures; (b) thin section perpendicular to bedding showing multiple layers with convolute laminae, bulb structures, dykes, and lenticular silt bodies; inset showing enlargement of fine mudstone laminae draped above and dyke below bulb structure layer.

individual bulbs, grains are coarsest and most sorted at the top surface. Sorting decreases towards the base of each bulb.

The contact between the bulb structures and the overlying material is sharp, although laterally equivalent parts of the same surface may be gradational where bulb structures are absent. Immediately overlying most bulb structure layers is very fine laminated shale. In thin section the shale is dark grey to black in colour and at high magnification individual grains are not resolved. The shale is most thin immediately above a bulb, and thickens away from the bulb (Fig. 2.11b). These very fine shale laminae are only observed immediately above bulb horizons. Overlying bedded material, typically 5–10 mm thick, grades upward from siltstone to mudstone, separates each bulb layer from the next.

Interpretation

The bulb structures show no evidence of exposure at the sediment surface and are therefore interpreted to have developed post-depositionally within the sediment pile. Silt was likely deposited with uniform thickness, and was later deformed, pinching out laterally as a result of sediment flow into the bulbs. The contorted nature of the silt indicates that sediment was likely liquidized during formation of the bulbs. Flow of water within the layers and between the larger silt grains during liquidization led to the observed localized variations in grain size and sorting.

Permeability between layers of different lithologies affects the drainage of pore fluid (van Rensbergen et al. 2003), as long as loading and burial increase. If sealed by an impermeable layer above, sediment compaction is inhibited and overpressuring develops (Collinson 2005); as a result, liquidization can occur at varying levels of a sediment pile (Maltman & Bolton 2003). In the examples described here, upward migration of fluid was probably halted by the layers of fine impermeable mud seen overlying the bulb structures, allowing overpressure to develop in the underlying undercompacted silt. This allowed the upward migration of liquidized silt into the overlying mud creating the draped appearance at the top of each bulb.

2.4. Discussion

2.4.1. Timing

The soft-sediment deformation structures at Horton Bluff, Cheverie, and Split Rock initiated at different levels in the sediment pile, and could have formed at very different times in the depositional history. It is possible to classify the structures into two groups: those that were exposed at the sediment surface and those that formed later. Microbasins, load structures, intraformational breccia, and neptunian dykes show evidence, such as erosional surfaces, indicating that all formed near the sediment-water interface. Bulb structures and sedimentary boudins likely formed some time after burial, as there are no erosional surfaces to indicate exposure at the sediment surface. Furthermore, in the case of bulb structures, an overlying unbreached layer of mud was necessary for their formation. This indicates these structures formed after some amount of burial and probably after at least partial lithification. Figure 2.12 shows schematically how different structures may have formed at different times in the accumulating sediment pile. Those structures that are interpreted to form near or at the sediment surface are shown at the top surfaces, whereas those that formed later are shown within the layers.

2.4.2. Triggering mechanisms

Potential causes of liquidization have been suggested by multiple authors (Sims 1975, Hempton & Dewey 1983, Allen 1986, Rossetti 1999, Kang et al. 2010, Owen & Moretti 2011) and include: meteorite impact, permafrost thawing, tides, tsunamis, groundwater fluctuations, storm waves, rapid sediment loading, and earthquakes. Each will be considered in turn as a possible driver for soft-sediment deformation in the Horton Group.

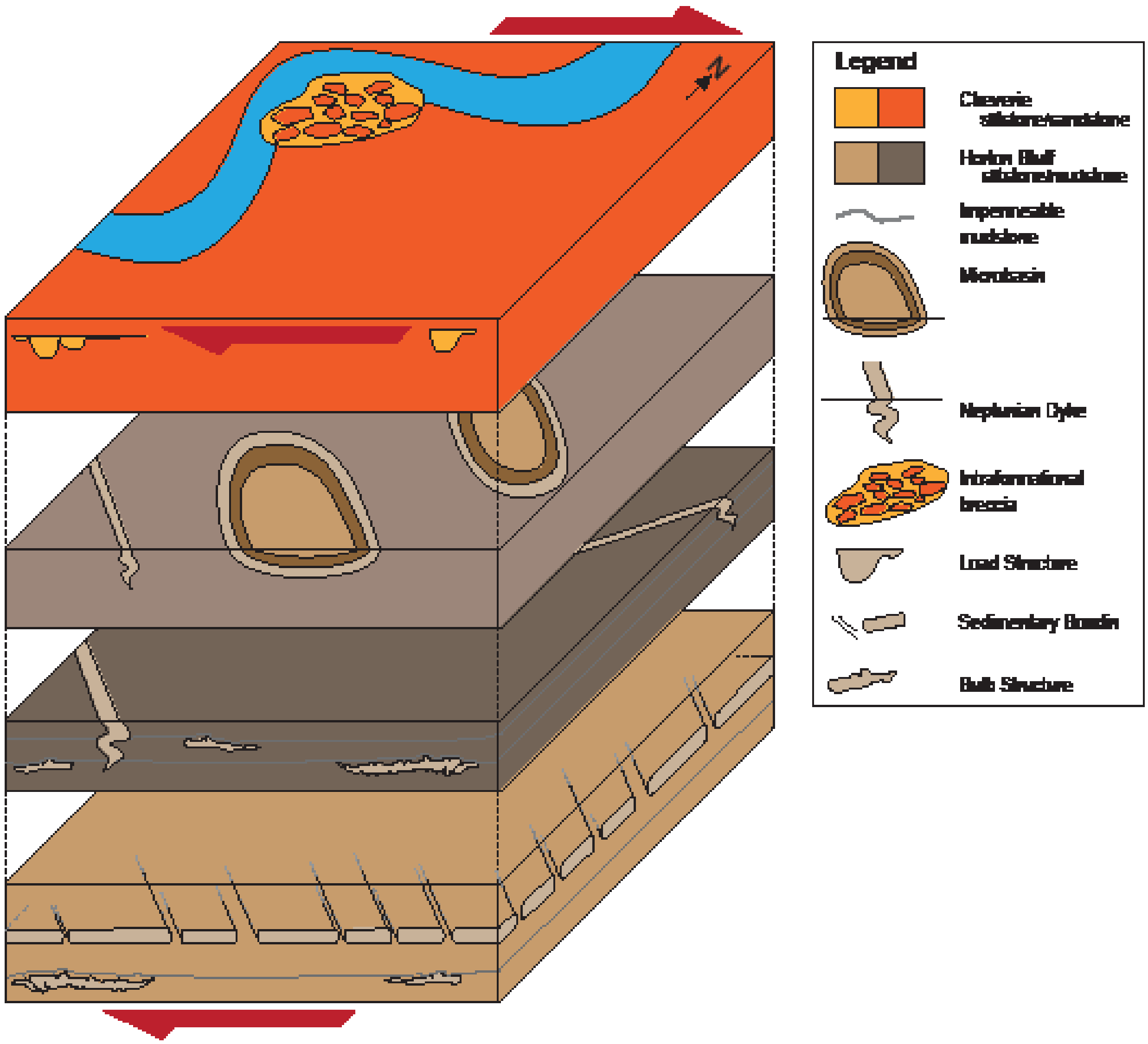

Figure 2.12. Time-exploded diagram of all soft-sediment deformation structures described. Structures interpreted as forming at the sediment-water interface shown on top surfaces. Structures interpreted as forming within the sediment pile shown in the centres of the packages.

Meteorite impacts can trigger formation of large geological structures, water escape structures, sediment dykes, faulting, and large-scale slump features (Long 2004, French & Koeberl 2010). Syndepositional deformation structures in the Horton Group occur on multiple stratigraphic horizons, indicating that the deformation structures in the area are attributed to multiple events. Meteorite impacts are therefore not likely the cause for deformation.

Permafrost thawing releases large amounts of high-pressured melt-water that can induce liquidization of sediment (Krull & Reta Ilack 1995, Harris et al. 2000). At the time of deposition of sediments, Nova Scotia was at an equatorial latitude (Calder 1998, Murphy & Rice 1998) and would not have been subject to permafrost cycles.

In tidal environments, density differentiation in grains, non-uniform confining pressure, or fluid flow within sediment can result in soft-sediment deformation (Gatmiri 1990). The absence of large-scale tidal features from the Horton Group, and especially from the subaerial Cheverie Formation, suggests that any tidal influence on the physical sedimentology was minor.

A tsunami could trigger liquidization of sediment, and a noticeable change in facies would be an indicator for such an event (Benson et al. 1997). Detailed stratigraphic sections and depositional environments suggested for the Horton Bluff and Cheverie Formations (Martel & Gibling 1996, Noade 2010) correlate stratigraphically across the Windsor-Kennetcook subbasin, and no tsunami deposits have been identified in either formation.

A rise in the water table could increase water pressure, forming soft-sediment deformation structures (Holzer & Pampeyan 1981, Holzer & Clark 1993, Hermanrud et al. 2013). The preferred orientation of the structures observed, and their occurrence in subaqueous facies, indicate that groundwater fluctuations are likely not the cause of soft-sediment deformation.

Storm waves are capable of inducing liquidization by sediment remobilization during storms; direct impact of breaking waves and cyclic stresses of wave trough/crest pressure differences could induce deformation (Dalrymple 1979, Owen 1987, Kerr & Eyles 1991, Alfaro et al. 2002). At Horton Bluff, dykes occur beneath hummocky cross-stratified lenses deposited by storms in shallow water, leading Martel and Gibling (1993) to interpret the dykes as products of storm activity, their preferred orientation being controlled by paleoslope. Although the preferred orientation in the Horton Bluff Formation could have been controlled by paleoslope, those in the Cheverie Formation occur within terrestrial floodplain deposits, indicating the neither waves or paleoslope were important in their formation (Fig. 2.4). We therefore infer that the consistent preferred orientation of microbasins, sedimentary boudins, and neptunian dykes, across locations and contrasting sedimentary environments, indicates a tectonic control other than paleoslope alone.

Extremely rapid deposition of sediment may lead to a build-up of pore pressure creating soft-sediment deformation structures (Maltman and Bolton, 2003; Hermanrud et al., 2013). Rapid sediment loading is a possible trigger of dominantly ductile deformation structures with potential liquidization components such as load structures. However, structures with both brittle and ductile components (e.g. neptunian dykes and intraformational breccia) require high strain rates unlikely to have been caused by even the most rapid sediment loading. In addition, rapid sediment loading would not produce the strong NW–SE preferred orientation (Fig. 2.4). These arguments indicate that rapid sediment loading was not the primary cause of liquidization.

Cyclic shaking of the ground caused by earthquakes can trigger liquefaction of sediment (Obermeier 1996). Liquidization during earthquake shaking occurs when sediment is completely saturated, and typically occurs at depths from 1–10 m in alluvial deposits and up to 1 m in lacustrine deposits (Obermeier 2009). Several criteria have been proposed for assessing the likelihood of a seismically-triggered origin for soft-sediment deformation structures: large aerial extent, lateral continuity, vertical repetition, restriction to single stratigraphic intervals, proximity to an active seismic zone, and similarity to features formed in recent earthquakes (Hobbs 1907, Eisbacher

1970, Sims 1975, Hempton & Dewey 1983, Owen & Moretti 2011, Wallace & Eyles 2015). In the Horton Group, deformed horizons are haphazardly distributed at all the sites, and all deformation structures occur in multiple stratigraphic horizons. The microbasins, the most unique of the deformation structures, occur at two different horizons. Between these deformed horizons, strata are undeformed. The contacts between deformed and undeformed layers are sharp, indicating that each horizon represents a separate event. Dykes present in one of these horizons (Fig. 2.5h) suggest a common trigger for both structures. Faults, active during deposition, terminate at unconformities within the Horton Group indicating that this was a tectonically active environment. All of these observations are consistent with seismic triggering.

Lab experiments performed by Moretti et al. (1999) created load structures and water escape structures similar to those at the field localities mentioned here. Liquidization-induced microbasins are similar in size and shape to craters caused by the 1886 Charleston South Carolina earthquake (Obermeier et al. 1990, Obermeier 2009, Bastin et al. 2015). For these reasons, seismic triggers are likely to have been responsible for the varied and abundant soft-sediment deformation structures observed in the Horton Group.

Most modern earthquakes that create soft-sediment deformation structures are of >7.0 Magnitude (Kawakami & Asade 1966, Iwasaki 1986, Obermeier 2009). The Minas Fault Zone acted as a transform fault during Mississippian time (Murphy et al. 2011, Waldron et al. 2015). It, and related faults, was probably responsible for seismic events capable of generating soft-sediment deformation structures during development of the Maritimes Basin.

Plint (1985) attributed soft-sediment deformation structures in younger, Pennsylvanian rocks in New Brunswick, approximately 100 km northwest of the study area, to earthquakes associated with dextral strike-slip on the Minas Fault Zone. The preferred orientations of structures described here (Fig. 2.4) are all consistent with tectonic stress associated with the Minas Fault Zone. The Minas Fault Zone was dominantly dextral from the Late Devonian to late Carboniferous (Murphy et al. 2011). Dextral strike-slip on this E–W fault would have produced a NE-SW extension direction, perpendicular to the observed dykes, microbasins, and sedimentary boudins that are elongated NW–SE. Thus movement along faults associated with the Minas Fault Zone could have provided the tectonic stress necessary to produce the observed orientations, and the seismic trigger for inducing liquidization of sediment; slopes associated with the tectonically unstable environment of deposition may also have contributed to soft-sediment deformation.

2.4.3. Tectonic deformation and overpressure

Bulb structures and sedimentary boudins are unlike the other structures described here in that they do not show sediment-water interface interactions such as erosion, onlap, or layer collapse (Taki & Pratt 2012). Thin mud layers in particular consistently overlie bulb structures. Bulb structures and sedimentary boudins potentially formed deeper in the sediment pile and later in the history of sedimentation. To mobilize and form these soft-sediment deformation structures, the buried sediment probably became liquidized as a result of overpressure (Maltman & Bolton 2003), a condition that occurs when pore fluid pressure exceeds hydrostatic pressure in a pocket of sediment (Maltman 1994, Jolly & Lonergan 2002). A fluid-saturated bed can become overpressured when rapidly buried or horizontally compressed, while fluid is trapped in pore spaces between sediment grains (Jolly & Lonergan 2002). Overpressuring commonly occurs in environments where the sediments are overlain or enclosed by low-permeability mudstones, or other effective seals (Jolly & Lonergan 2002). At Horton Bluff, Cheverie, and Split Rock, overpressuring is interpreted at locations with interfingered mudstone and siltstone.

Stress-related mechanisms commonly induce overpressured conditions in sedimentary basins (Osborne & Swarbrick 1997). Changes in the stress state of a unit can result from burial of sediment (vertical compression) or tectonic forces (horizontal compression or extension). Horizontal stress changes can generate and dissipate overpressure rapidly in tectonically active areas by increasing pore pressure, simulating rapid burial (Osborne & Swarbrick 1997). Shear stress may induce collapse of grains (static liquefaction), which can raise pore pressure (Duranti & Hurst 2004). This process can occur late, in contrast to syndepositional liquefaction immediately following deposition (Duranti & Hurst 2004).

2.5. Conclusion

Products of soft-sediment deformation within Horton Group strata are common. Liquidization of sediment is the likely mechanism of weakening, that allowed the sediment to be deformed, producing multiple deformation structures including microbasins, load structures, bulb structures, neptunian dykes, intraformational breccia, and sedimentary boudins at Horton Bluff, Split Rock and Cheverie in Nova Scotia. Microbasins, neptunian dykes, load structures, and the intraformational breccia formed at or near the sediment surface, whereas bulb structures and boudins likely formed deeper in the sediment pile. Soft-sediment deformation was probably induced by a combination of storm wave action, paleoslope orientation, and seismic activity. Movement along the Minas Fault Zone in this area possibly induced soft-sediment deformation through seismic shaking and overpressured conditions, and led to strong preferred orientation of the resulting structures. Evidence for overpressure early in the history of the subbasin has implications for the behaviour of fluids and therefore for the modeling of basin history.

Acknowledgements

Field research was supported by a grant from Triangle Petroleum; we thank Peter Hill for his support. Hayley Pothier and Maryam Dzulkefli assisted in the field. We acknowledge helpful discussions with Ian Spooner. We are appreciative of the helpful comments from L. Kennedy, M. Moretti, J. M. Molina and an anonymous reviewer.

2.6. References

Alfaro, P., Delgado, J., Estevez, A., Molina, J. M., Moretti, M. & Soria, J. M. 2002. Liquefaction and fluidization structures in Messinian storm deposites (Bajo Segura Basin, Betic Cordillera, southern Spain). *International Journal of Earth Sciences* **91**, 505-513.

Alfaro, P., Gibert, L., Moretti, M., Garcia-Tortosa, F. J., Sanz de Galdeano, C., Galindo-Zaldivar, J. & Lopez-Garrido, A. C. 2010. The significance of giant seismites in the Plio-Pleistocene Baza palaeo-lake (S Spain). *Terra Nova* **22**(3), 172-179.

Allen, J. R. L. 1986. Earthquake magnitude-frequency, epicentral distance, and soft-sediment deformation in sedimentary basins. *Sedimentary Geology* **46**(1–2), 67-75.

Alsop, G. I. & Marco, S. 2011. Soft-sediment deformation within seismogenic slumps of the Dead Sea Basin. *Journal of Structural Geology* **33**, 433-457.

Bastin, S. H., Quigley, M. C. & Bassett, K. 2015. Paleo-liquefaction in Christchurch, New Zealand. *Geological Society of America Bulletin* **Pre-Issue Publication**.

Bell, W. A. 1929. *Horton-Windsor District, Nova Scotia. 155*. Memoir Geological Survey of Canada.

Bell, W. A. 1944. Carboniferous rocks and fossil floras of northern Nova Scotia. *Canada Geological Survey Memoir* **238**.

Benson, B. E., Grimm, K. A. & Clague, J. J. 1997. Tsunami Deposits beneath Tidal Marshes on Northwestern Vancouver Island, British Columbia. *Quaternary Research* **48**(2), 192-204.

Berra, F. & Felletti, F. 2011. Syndepositional tectonics recorded by soft-sediment deformation and liquefaction structures (continental Lower Permian sediments, Southern Alps, Northern Italy): Stratigraphic significance. *Sedimentary Geology* **235**(3–4), 249-263.

Boehner, R. C. & Giles, P. S. 1993. *Geology of the Antigonish Basin, Antigonish County, Nova Scotia. 8*. Department of Natural Resources.

Calder, J. H. 1998. The Carboniferous evolution of Nova Scotia. In: *Geological Society, London, Special Publications* **143**, 261-302.

Collinson, J. 2005. Post-depositional sedimentary structures. In: *Encyclopedia of Geology* (edited by Selley, R. C., Cocks, L. R. M. & Plimer, I. R.). Elsevier, Oxford, 602-611.

Craggs, S., Keighley, D., Waldron, J. W. F. & Park, A. 2015. Salt tectonics in an intracontinental transform setting: Cumberland and Sackville basins, southern New Brunswick, Canada. *Basin Research*, 1-18.

Dafoe, L. T., Shaw, J., Jauer, C., Giles, P. S., Waldron, J. W. F. & Potter, D. P. 2016. New insights into the Bedrock and Quaternary Geology of St. George's Bay from a vertical integration of marine datasets, offshore western Newfoundland. *Bulletin of Canadian Petroleum Geology* **64**(1), 1.

Dalrymple, R. W. 1979. Wave-induced liquefaction: a modern example from the Bay of Fundy. *Sedimentology* **26**, 835-844.

Duranti, D. & Hurst, A. 2004. Fluidization and injection in the deep-water sandstones of the Eocene Alba Formation (UK North Sea). *Sedimentology* **51**(3), 503-529.

Dyson, I. A. & Marshall, T. R. 2005. *Neoproterozoic salt nappe complexes and salt-withdrawal mini-basins in the Amadeus Basin. Proceedings: Central Australian Basins Symposium Special Publication 2*. Northern Territory Geological Survey.

Eisbacher, G. H. 1970. Contemporaneous faulting and clastic intrusions in the Quirke Lake Group, Elliot Lake, Ontario. *Canadian Journal of Earth Sciences* **7**(2), 215-225.

Ezquerro, L., Moretti, M., Liesa, C. L., Luzon, A. & Simon, J. L. 2015. Seismites from a well core of palustrine deposits as a tool for reconstructing the palaeoseismic history of a fault. *Tectonophysics* **655**, 191-205.

French, B. M. & Koeberl, C. 2010. The convincing identification of terrestrial meteorite impact structures: What works, what doesn't, and why. *Earth-Science Reviews* **98**(1–2), 123-170.

Gatmiri, B. 1990. A simplified finite element analysis of wave-induced effective stresses and pore pressures in permeable sea beds. *Geotechnique* **40**(1), 15-30.

Gibert, L., Sanz de Galdeano, C., Alfaro, P., Scott, G. & López Garrido, A. C. 2005. Seismic-induced slump in Early Pleistocene deltaic deposits of the Baza Basin (SE Spain). *Sedimentary Geology* **179**(3–4), 279-294.

Gibling, M. R., Culshaw, N., Rygel, M. C. & Pascucci, V. 2008. Chapter 6 The Maritimes Basin of Atlantic Canada: Basin Creation and Destruction in the Collisional Zone of Pangea. In: *Sedimentary Basins of the World 5* (edited by Miall, A. D.). Elsevier, 211-244.

Hamblin, A. P. & Rust, B. R. 1989. Tectono-sedimentary analysis of alternate-polarite half-graben basin-fill successions: Late Devonian-Early Carboniferous Horton Group, Cape Breton Island, Nova Scotia. *Basin Research* **2**, 239-255.

Harris, C., Murton, J. & Davies, M. C. R. 2000. Soft-sediment deformation during thawing of ice-rich frozen soils: results of scaled centrifuge modelling experiments. *Sedimentology* **47**(3), 687-700.

Hempton, M. R. & Dewey, J. F. 1983. Earthquake-induced deformational structures in young lacustrine sediments, East Anatolian Fault, southeast Turkey. *Tectonophysics* **98(**3–4), T7-T14.

Hermanrud, C., Venstad, J. M., Cartwright, J., Rennan, L., Hermanrud, K. & Nordgard Bolas, H. M. 2013. Consequences of water level drops for soft sediment deformation and vertical fluid leakage. *Mathematical Geosciences* **45**, 1-30.

Hesse, R. & Reading, H. G. 1978. Subaqueous clastic fissure eruptions and other examples of sedimentary transposition in the lacustrine Horton Bluff Formation (Mississippian), Nova Scotia, Canada. In: *Special Publication of the International Association of Sedimentologists 2* (edited by Matter, A. & Tucker, M. E.) **no. 2**, 241-257.

Hibbard, J. & Waldron, J. W. F. 2009. Truncation and translation of Appalachian promontories: mid-Paleozoic strike-slip tectonics and basin initiation. *Geology* **37**, 487-490.

Hobbs, W. H. 1907. Origin of ocean basins in the light of the new seismology. *Geological Society of America Bulletin* **18**, 233-250.

Holzer, T. L. & Clark, M. M. 1993. Sand boils without earthquakes. *Geology* **21**(10), 873-876.

Holzer, T. L. & Pampeyan, E. H. 1981. Earth fissures and localized differential subsidence. *Water Resources Research* **17**(1), 223-227.

Hudec, M. R., Jackson, M. P. A. & Schultz-Ela, D. D. 2009. The paradox of minibasin subsidence into salt: Clues to the evolution of crustal basins. *Geological Society of America Bulletin* **121**(1-2), 201-221.

Iwasaki, T. 1986. Soil liquefaction studies in Japan: state-of-the-art. *Soil Dynamics and Earthquake Engineering* **5**(1), 2-68.

Javaid, K. M. 2011. Development and structure of the Kennetcook-Windsor basin, Nova Scotia, Atlantic Canada. Unpublished M.Sc. thesis, University of Alberta.

Jolly, R. J. H. & Lonergan, L. 2002. Mechanisms and controls on the formation of sand intrusions. *Journal of the Geological Society, London* **159**, 605-617.

Kang, H.-C., Paik, I. N., Lee, H. I., Lee, J. E. & Chun, J.-C. 2010. Soft-sediment deformation structures in Cretaceous non-marine deposits of southeastern Gyeongsang Basin, Korea: occurrences and origin. *Island Arc* **19**, 628-646.

Kawakami, F. & Asade, A. 1966. Damage to the ground and earth structures by the Niigata earthquake of June 16, 1964. *Soil and Foundation* **6**(1), 14-30.

Keppie, J. D. 1982. The Minas Geofracture. In: *Special Paper - Geological Association of Canada* (edited by St-Julien, P. & Beland, J.). Geological Association of Canada, Toronto, 263-280.

Kerr, M. & Eyles, N. 1991. Storm-deposited sandstones (tempestites) and related ichnofossils of the Late Ordovician Georgian Bay Formation, southern Ontario, Canada. *Canadian Journal of Earth Sciences* **28**, 266-282.

Knight, I. 1983. Geology of the Carboniferous Bay St. George subbasin, Western Newfoundland. *Mineral Development Division Department of Mines and Energy, Government of Newfoundland and Labrador* **Memoir 1**.

Krull, E. S. & Reta Ilack, G. J. 1995. Clastic dikes as evidence for discontinuous permafrost paleoclimate in Permian coal measures, Allan Hills Antarctica. *Geological Society of America Abstracts with Programs* **27**, A265.

Laubach, S. E., Schultz-Ela, D. D. & Tyler, R. 2000. Differential compaction of interbedded sandstone and coal. In: *Forced folds and fractures* (edited by Cosgrove, J. W.) **169**. Geological Society of London, London, 51-60.

Long, D. G. F. 2004. The tectonostatigraphic evolution of the Huronian basement and the subsequent basin fill: geological constraints on impact models of the Sudbury event. *Precambrian Research* **129**(3–4), 203-223.

Lowe, D. R. 1975. Water escape structures in coarse-grained sediments. *Sedimentology* **22**(2), 157.

Lynch, G., Keller, J. V. A. & Giles, P. S. 1998. Influence of the Ainslie Detachment on the stratigraphy of the Maritimes Basin and mineralization in the Windsor Group of northern Nova Scotia. *Economic Geology* **93**, 703-718.

Maltman, A. J. 1994. Introduction and overview. In: *The Geological Deformation of Sediments* (edited by Maltman, A. J.). Chapman and Hall, London, 1-35.

Maltman, A. J. & Bolton, A. 2003. How sediments become mobilized. In: *Subsurface Sediment Mobilizations* (edited by Van Rensbergen, P., Hillis, R. R., Maltman, A. J. & Morley, C. K.). Geological Society, London. Special Publication 216, 9-20.

Martel, A. T. & Gibling, M. R. 1991. Wave-dominated lacustrine facies and tectonically controlled cyclicity in the Lower Carboniferous Horton Bluff Formation, Nova Scotia, Canada. In: *Lacustrine Facies Analysis* (edited by Anadon, P., Cabrera, L. & Kelts, K.). Blackwell Publising Ltd., Halifax, 223-243.

Martel, A. T. & Gibling, M. R. 1993. Clastic dykes of the Devono-Carboniferous Horton Bluff Formation, Nova Scotia: storm-related structures in shallow lakes. *Sedimentary Geology* **87**, 103-119.

Martel, A. T. & Gibling, M. R. 1996. Stratigraphy and tectonic history of the Upper Devonian to Lower Carboniferous Horton Bluff Formation, Nova Scotia. *Atlantic Geology* **32**, 13-38.

Molina, J. M., Alfaro, P., Moretti, M. & Soria, J. M. 1998. Soft-sediment deformation structures induced by cyclic stress of storm waves in tempestites (Miocene, Guadalquivir Basin, Spain). *Terra Nova* **10**(3), 145-150.

Moore, R. G., Ferguson, S. A., Boehner, R. C. & Kennedy, C. M. 2000. Bedrock geology map of the Wolfville-Windsor area, NTS Sheet 21H/01 and part of 21A/16, Hants and Kings Counties, Nova Scotia. In: *Nova Scotia Department of Natural Resources Mineral Resource Branch Open File Map ME 2000-3, Version 2 scale 1: 50 000*.

Moretti, M., Alfaro, P., Caselles, O. & Canas, J. A. 1999. Modelling seismites with a digital shaking table. *Tectonophysics* **304**(4), 369-383.

Moretti, M. & Sabato, L. 2007. Recognition of trigger mechanisms for soft-sediment deformation in the Pleistocene lacustrine deposits of the Sant'Arcangelo Basin (Southern Italy): Seismic shock vs. overloading. *Sedimentary Geology* **196**(1–4), 31-45.

Murphy, J. B. & Rice, R. J. 1998. Stratigraphy and depositional environment of the Horton Group in the St. Marys Basin, central mainland Nova Scotia. *Atlantic Geology* **34**, 1-25.

Murphy, J. B., Waldron, J. W. F., Kontak, D. J., Pe-Piper, G. & Piper, D. J. W. 2011. Minas Fault Zone: Late Paleozoic history of an intra-continental orogenic transform fault in the Canadian Appalachians. *Journal of Structural Geology* **33**, 312-328.

Nikolaeva, S. B. 2009. Seismites in Late Pleistocene and Holocene deposits of the northwestern Kola region (northern Baltic Shield). *Russian Geology and Geophysics* **50**, 644-650.

Noade, J. E. 2010. Stratigraphy of the Cheverie Formation type section, Cheverie, Hants County, Nova Scotia, Dalhousie University Unpublished B.Sc. thesis.

Obermeier, S. F. 1996. Use of liquefaction-induced features for paleoseismic analysis — An overview of how seismic liquefaction features can be distinguished from other features and how their regional distribution and properties of source sediment can be used to infer the location and strength of Holocene paleo-earthquakes. *Engineering Geology* **44**(1–4), 1-76.

Obermeier, S. F. 2009. Chapter 7 Using Liquefaction-Induced and Other Soft-Sediment Features for Paleoseismic Analysis. In: *International Geophysics 95* (edited by James, P. M.) **Volume 95**. Academic Press, 497-564.

Obermeier, S. F., Jacobson, R. B., Smoot, J. P., Weems, R. E., Gohn, G. S., Monroe, J. E. & Powars, D. S. 1990. *Earthquake-induced liquefaction features in the coastal setting of South Carolina and in the fluvial setting of the New Madrid seismic zone. U. S. Geological Survey professional paper: 1504*. U. S. Geological Survey, Washington.

Osborne, M. J. & Swarbrick, R. E. 1997. Mechanisms for generating overpressure in sedimentary basins: a reevaluation. *AAPG Bulletin* **81**(6), 1023-1041.

Owen, G. 1987. Deformation processes in unconsolidated sands. In: *Defomration of sediments and sedimentary rocks* (edited by Jones, M. E. & Preston, R. F.) **29**. Geological Society, London, Special Publications 29, 11-24.

Owen, G. 2003. Load structures: gravity-driven sediment mobilization in the shallow subsurface. *Geological Society, London, Special Publications* **216**(1), 21-34.

Owen, G. & Moretti, M. 2011. Identifying triggers for liquefaction-induced soft-sediment deformation in sands. *Sedimentary Geology* **235**, 141-147.

Park, A. F., Keighley, D. G., St. Peter, C. & Wilson, P. 2010. Overstep and imbrication along a sidewall ramp and its relationship to a hydrocarbon play in Tournasian rocks of the Moncton Basin; the Peck Creek section, Albert Mines area, southeastern New Brunswick. *Bulletin of Canadian Petroleum Geology* **58**(3), 268-282.

Parnell, J. & Kelly, J. 2003. Remobilization of sand from consolidated sandstones: evidence from mixed bitumen-sand intrusions. In: *Subsurface Sediment Mobilization* (edited by Van Rensbergen, P., Hillis, R. R., Maltman, A. J. & Morley, C. K.) **216**. Geological Society, London. Special Publication 216, 503-513.

Peel, F. J. 2014. How do salt withdrawal minibasins form? Insights from forward modelling, and implications for hydrocarbon migration. *Tectonophysics* **630**, 222-235.

Plint, A. G. 1985. Possible earthquake-induced soft-sediment faulting and remobilization in Pennsylvanian alluvial strata, southern New Brunswick, Canada. *Canadian Journal of Earth Sciences* **22**, 907-912.

Rodriguez-Pascua, M. A., Calvo, J. P., De Vicente, G. & Gomez-Gras, D. 2000. Soft-sediment deformation structures interpreted as seismites in lacustrine sediments of the Prebetic Zone, SE Spain, and their potential use as indicators of earthquake magnitudes during the Late Miocene. *Sedimentary Geology* **135**(1-4), 117-135.

Roliff, W. A. 1962. The Maritimes Carboniferous Basin of Eastern Canada. *Proceedings of the Geological Association of Canada* **14**, 21-41.

Rossetti, D. D. F. 1999. Soft-sediment deformation structures in late Albian to Cenomanian deposits, São Luís Basin, northern Brazil: evidence for palaeoseismicity. *Sedimentology* **46**(6), 1065-1081.

Scott, B. & Price, S. 1988. Earthquake-induced structures in young sediments. *Tectonophysics* **147**, 165-170.

Sims, J. D. 1975. Determining earthquake recurrence intervals from deformational structures in young lacustrine sediments. *Tectonophysics* **29**(1–4), 141-152.

St. Peter, C. 1993. Maritimes Basin evolution: key geologic and seismic evidence from the Moncton subbasin of New Brunswick. *Atlantic Geology* **29**, 233-270.

Taki, H. E. & Pratt, B. R. 2012. Syndepositional tectonic activity in an epicontinental basin revealed by deformation of subaqueous carbonate laminites and evaporites: seismites in Red River strata (Upper Ordovician) of southern Saskatchewan, Canada. *Bulletin of Canadian Petroleum Geology* **60**(1), 37-58.

van de Poll, H. W., Gibling, M. R. & Hyde, R. S. 1995. Upper Paleozoic Rocks. In: *Geology of the Appalachian Caledonian Orogen in Canada and Greenland* (edited by Williams, H.). Geological Survey of Canada, 449-455.

van Rensbergen, P., Hillis, R. R., Maltman, A. J. & Morley, C. K. 2003. Subsurface sediment mobilization: introduction. In: *Geological Society of London, Special Publication 216* (edited by van Rensbergen, P., Hillis, R. R., Maltman, A. J. & Morley, C. K.) **216**, 1-8.

Waldron, J. W. F. 2004. Anatomy and evolution of a pull-apart basin, Stellarton, Nova Scotia. *Geological Society of America Bulletin* **116**(1-2), 109-127.

Waldron, J. W. F., Barr, S. M., Park, A. F., White, C. E. & Hibbard, J. 2015. Late Paleozoic strike-slip faults in Maritime Canada and their role in the reconfiguration of the northern Appalachian orogen. *Tectonics* **34**(8), 1661-1684.

Waldron, J. W. F. & Gagnon, J.-F. 2011. Recognizing soft-sediment structures in deformed rocks of orogens. *Journal of Structural Geology* **33**, 271-279.

Waldron, J. W. F., Roselli, C. & Johnston, S. K. 2007. Transpressional structures on a Late Paleozoic intracontinental transform fault, Canadian Appalachians. In: *Tectonics of Strike-Slip Restraining and Releasing Bends* (edited by Cunningham, W. D., and Mann, P.). Geological Society, London, Special Publications 290, 367-385.

Waldron, J. W. F., Roselli, C., Utting, J. & Johnston, S. K. 2010. Kennetcook thrust system: late Paleozoic transpression near the southern margin of the Maritimes Basin, Nova Scotia. *Canadian Journal of Earth Sciences* **47**, 137-159.

Waldron, J. W. F., Rygel, M. C., Gibling, M. R. & Calder, J. H. 2013. Evaporite tectonics and the late Paleozoic stratigraphic development of the Cumberland Basin, Appalachians of Atlantic Canada. *Geological Society of America Bulletin* **125**(5-6), 945-960.

Waldron, J. W. F., Schofield, D. I., Murphy, J. B. & Thomas, C. W. 2014. How was the Iapetus Ocean infected with subduction? *Geology* **42**, 1095-1098.

Waldron, J. W. F., White, J. C., MacInnes, E. & Roselli, C. 2005. Transpression and transtension along a continental transform fault: Minas Fault Zone, Nova Scotia. *Geological Association of Canada - Mineralogical Association of Canada - Canadian Society of Petroleum Geologists - Canadian Society of Soil Sciences Joint Meeting - Halifax, May 2005. Field Trip B7.*

Wallace, K. & Eyles, N. 2015. Seismites within Ordovician–Silurian carbonates and clastics of Southern Ontario, Canada and implications for intraplate seismicity. *Sedimentary Geology* **316**(0), 80-95.

Wightman, W. G., Scott, D. B., Medioli, F. S. & Gibling, M. R. 1993. Carboniferous marsh foraminifera from coal-bearing strata at the Sydney basin, Nova Scotia: A new tool for identifying paralic coal-forming environments. *Geology* **21**, 631-634.

Wilson, P., White, J. C. & Roulston, B. V. 2006. Structural geology of the Penobsquis salt structure; late Bashkirian inversion tectonics in the Moncton Basin, New Brunswick, Eastern Canada. *Canadian Journal of Earth Sciences = Revue Canadienne des Sciences de la Terre* **43**(4), 405-419.

Chapter 3. Synsedimentary and tectonic deformation of the Carboniferous Anguille and Codroy Groups, Bay St. George subbasin, southwest Newfoundland

The late Paleozoic Maritimes Basin of Atlantic Canada is stratigraphically and structurally complex. The Bay St. George subbasin, a subbasin within the Maritimes Basin in Newfoundland, shows synsedimentary, salt-related, and tectonic structures in coastal outcrops. The northern and southern subbasin were previously interpreted as having drastically different structural styles, but key outcrops in both locations show similar structures. Soft-sediment deformation structures and salt-related structures at Boswarlos and Ship Cove in the northern subbasin are similar to those at Cape Anguille and Capelin Cove in the southern subbasin. Liquidization of sediment during deposition of the Anguille Group and early Codroy Group was common in the Bay St. George subbasin. Gypsum outcrops with strong foliation interbedded with siltstone breccia and limestone is common along the coast. A primary salt weld at Ship Cove and a secondary salt weld at Capelin Cove suggest salt was moving during and after deposition of the Codroy and Barachois Groups. The Snakes Bight Fault, the major brittle structure onshore, shows evidence of tectonic inversion late in the subbasin history. These new interpretations lead to a better understanding of the deformation history of the entire Maritimes Basin.

3.1. Introduction

The late Devonian to Permian Maritimes Basin (Fig. 3.1) is a large (400 km maximum diameter) and deep (>12 km) sedimentary basin; it formed in the Appalachian orogen following Devonian (Acadian) orogenic events, during a period of complex tectonics involving significant transtension (Calder 1998, Gibling et al. 2008, Hibbard & Waldron 2009, Waldron et al. 2015). It comprises many subbasins having similar stratigraphic elements (Boehner & Giles 1993, Murphy et al. 2011, Waldron et al. 2015, Waldron et al. 2017) summarized in Figure 3.2. Deformation within the Maritimes Basin included periods of folding, faulting, salt tectonism, uplift, and erosion

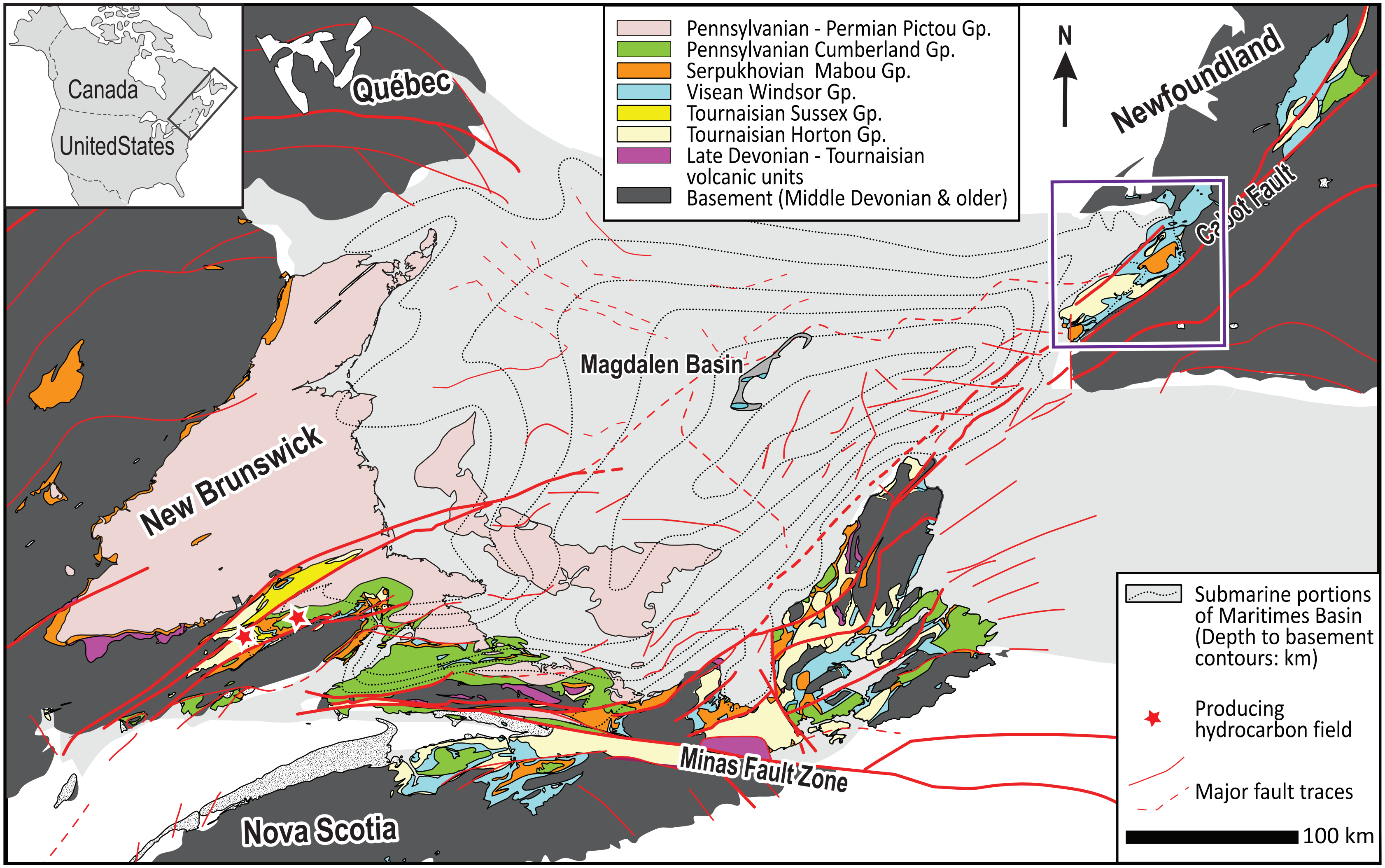

Figure 3.1. Map of the Maritimes Basin of Atlantic Canada.
Inset shows Fig. 3.3, the location of the Bay St. George subbasin. Modified from Waldron et al. (2015).

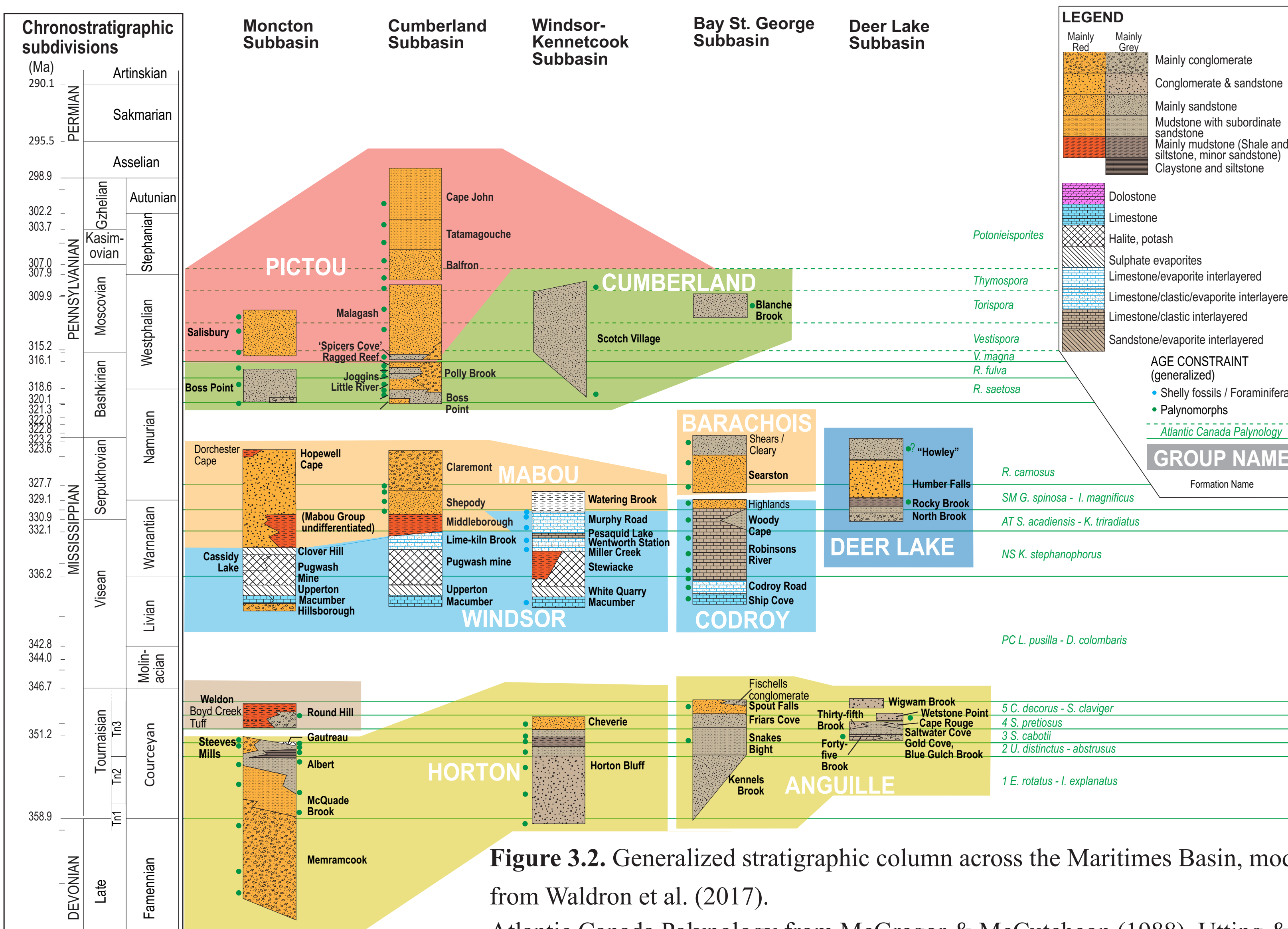

Figure 3.2. Generalized stratigraphic column across the Maritimes Basin, modified from Waldron et al. (2017).
Atlantic Canada Palynology from McGregor & McCutcheon (1988), Utting & Giles (2004), and Allen et al. (2013).

(Knight 1983, Hamblin & Rust 1989, Calder 1998, Waldron 2004, Wilson et al. 2006, Waldron et al. 2013a, Waldron et al. 2015, Gibling et al. in press 2018). Phases of subsidence and inversion led to the deposition of stratigraphic sequences separated by unconformities, and significant lateral and vertical facies variation between and within the subbasins (St. Peter 1993).

The Bay St. George subbasin (BSGSB), within the larger Maritimes Basin in Atlantic Canada (Fig. 3.3), displays significantly deformed Carboniferous strata, both onland and offshore. Previous work in this subbasin includes predominantly stratigraphic work in onland portions by Knight (1983) and Utting and Giles (2008), and geophysical interpretations offshore by Kilfoil (1988), Miller et al. (1990), Hall et al. (1992), and Dafoe et al. (2016). In this chapter we focus on the tectonic and stratigraphic evolution of the Bay St. George subbasin as exposed on land. Chapter 4 will examine offshore relationships.

For this paper, we did not attempt to remap the entire subbasin, but key outcrops of highly deformed strata were remapped and reinterpreted. Synsedimentary features previously undescribed, including soft-sediment deformation structures and salt structures, are here documented in detail. Brittle structures that cut across these ductile structures are also here described at key locations. Our results show that soft-sediment deformation, salt tectonics, and tectonic inversion played major roles in the evolution of the subbasin.

3.2. Regional Geology

3.2.1. Stratigraphy

Stratigraphic units within the Bay St. George subbasin have been described in detail by Knight (1983) and Utting and Giles (2008) who mapped late Paleozoic units ranging from the mainly Tournaisian Anguille Group to the Serpukhovian Barachois Group.

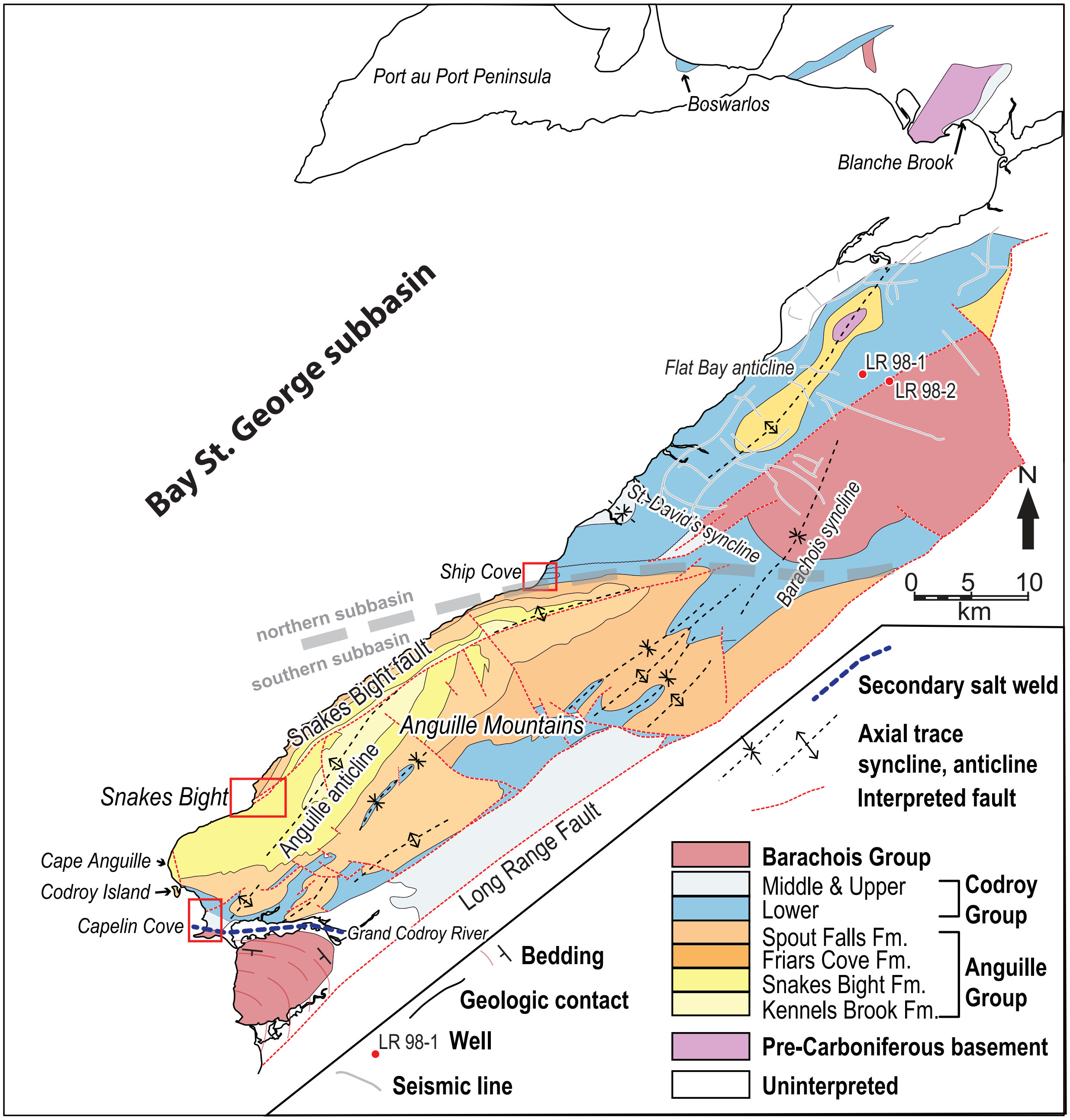

Figure 3.3. Bay St. George subbasin geologic map and generalized stratigraphy, modified from Knight (1983).
Onshore seismic lines shown in grey, locations of Figures 3.19, 3.20, and 3.24 in red boxes.

Anguille Group

The lowest stratigraphic unit within the BSGSB is the late Devonian to Tournaisian Anguille Group, equivalent to the Horton Group elsewhere in the Maritimes Basin, which unconformably overlies Proterozoic to early Paleozoic rocks assigned to the Humber Zone of the Appalachian Orogen (Fig. 3.3) (Williams 1979). The Anguille Group typically comprises basal alluvial, medial lacustrine, and upper alluvial units (Bell 1948, Knight 1983, Hamblin & Rust 1989, St. Peter 1993, Gibling et al. 2008, Gibling et al. in press 2018).

However, the stratigraphic succession differs between the northern and southern parts of the subbasin (Fig. 3.3). The thickness of the Anguille Group is dramatically different in the north and south. For example, Knight (1983) noted 150–200 m of Anguille Group strata in the Flat Bay anticline, in the north of the subbasin, contrasting with 2000 to >4900 m of Anguille Group farther south in the Anguille Mountains (Fig. 3.3). In the northern subbasin, the Anguille Group is represented only by the thin Fischells conglomerate exposed in the core of the Flat Bay anticline (Fig. 3.3), where it is interpreted to overlie Mesoproterozoic basement of the Humber Zone. In the Anguille Mountains of the southern subbasin, Knight (1983) separated the Anguille Group into four formations: Kennels Brook, Snakes Bight, Friars Cove, and Spout Falls.

The Kennels Brook Formation comprises red and grey pebbly sandstone, conglomerate, slate, and rare mudstone interpreted as originating in a meandering river and floodplain environment (Cote 1964, Knight 1983). This unit rarely crops out onshore, and is only seen at Snakes Bight and at the core of the Anguille Mountains (Fig. 3.3). Its base is not seen.

The overlying Snakes Bight Formation crops out along the southwest coast, south of Snakes Bight (Fig. 3.3), and can be traced inland to the Anguille Mountains. The Snakes Bight Formation comprises interbedded black mudstone, siltstone, and grey sandstone. This unit can be correlated to the Horton Bluff Formation in Nova Scotia (Fig. 3.2) based on similar Tournaisian spore assemblages (*Spelaeotriletes cabotii* and *Umbonatisporites distinctus–obstrusus* subzones of the

Vallatisporites vallatus Assemblage Zone) (Utting et al. 1989, Martel et al. 1993, Utting & Giles 2004, Waldron et al. 2017). Both units are interpreted as products of deposition in wave-dominated lakes that existed during periods of basin under-filling (Knight 1983, Martel & Gibling 1996).

The Friars Cove Formation is grey sandstone, conglomerate, and shale with minor carbonate and redbeds, interpreted as fluvial-deltaic deposits (Knight 1983). This unit crops out above the Snakes Bight Formation along the southwest coast and in the Anguille Mountains. This unit can be correlated to the lithologically comparable Cheverie Formation in Nova Scotia (Fig. 3.2) as they are both in the Tournaisian 3 *Spelaeotriletes pretiosus* Spore Assemblage Zone (Utting & Giles 2004, Waldron et al. 2017).

The Spout Falls Formation comprises red and grey sandstone with minor siltstone and conglomerate interpreted as braided stream deposits (Knight 1983). This unit is observed at Ship Cove in the northern part of the subbasin and near Snakes Bight (Fig. 3.3). Spores from the Tournaisian 3 *Colatisporites decorus–Schopfites claviger* Spore Assemblage Zone place this unit as younger than most of the exposed Horton Group in Nova Scotia, but comparable to parts of the Sussex Group of southern New Brunswick (Utting & Giles 2004, St. Peter & Johnson 2009, Waldron et al. 2017). The contact between the Spout Falls Formation and the Ship Cove Formation is well displayed at Ship Cove (Fig. 3.4).

Codroy Group

The overlying Codroy Group, approximately equivalent to the Windsor Group and lower parts of the Mabou Group elsewhere in the Maritimes Basin (Fig. 3.2), contains dominantly marine shale, limestone, and evaporite, and represents the only fully marine incursion into the Maritimes Basin in the late Paleozoic (Gibling et al. 2008). In the BSGSB the Codroy Group is further subdivided into four formations: Ship Cove, Codroy Road, Robinsons River, and Woody Cape (Knight 1983).

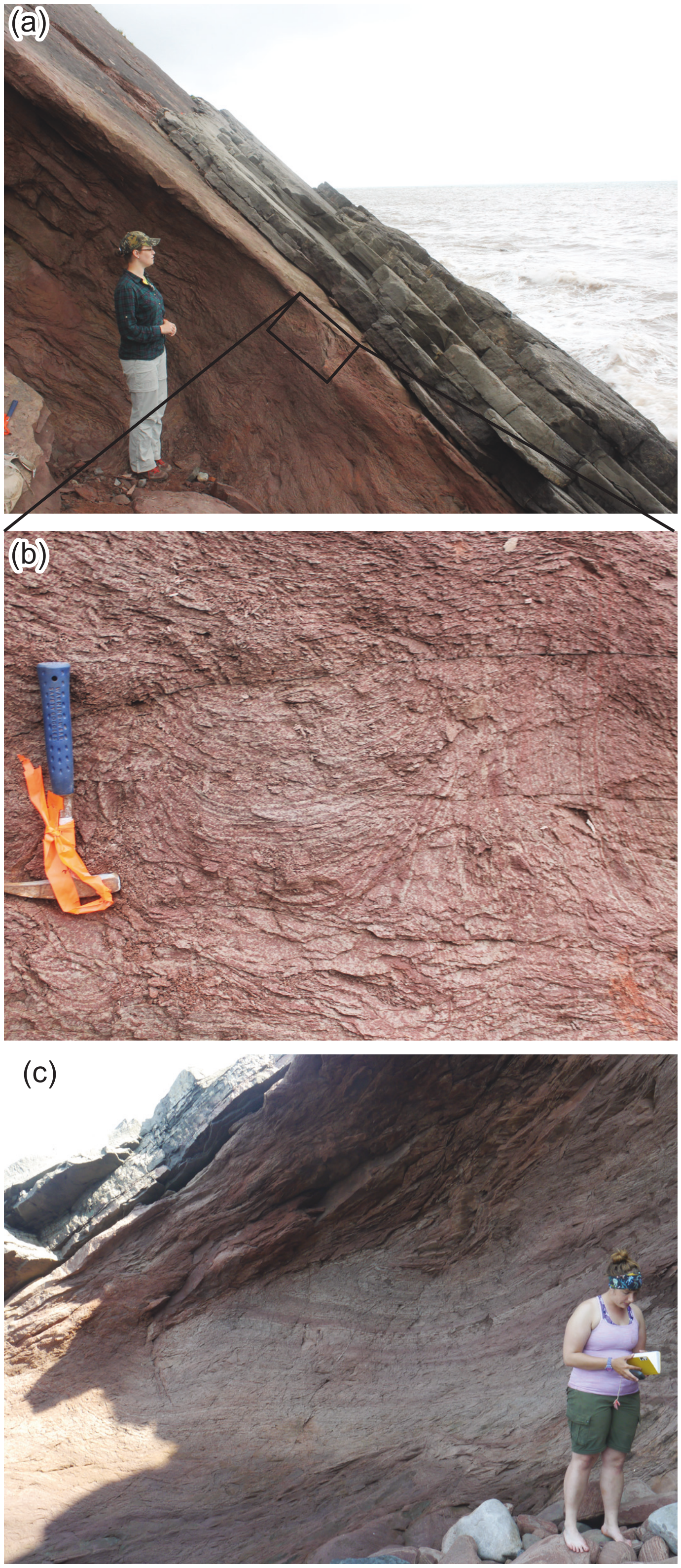

Figure 3.4. Spout Falls Formation and Ship Cove Formation contact.
(a) South side of contact, (b) inset showing soft-sediment folds, (c) north side of contact shows soft-sediment folds truncated by Ship Cove limestone.

The Ship Cove Formation comprises packstone, oolitic limestone, and minor sandstone. The contact between the Anguille Group and the Ship Cove Formation is exposed at Ship Cove in the north, and on Codroy Island in the south (Fig. 3.3). The Ship Cove Formation can be correlated to the Macumber Formation in Nova Scotia; both are within the Viséan *Lycospora pusilla–Densosporites columbaris* Spore Assemblage Zone (Utting & Giles 2004, 2008, Waldron et al. 2017). An unconformable contact between Humber Zone strata and Ship Cove Formation is seen at Boswarlos on the Port au Port Peninsula (Fig. 3.3).

The Codroy Road Formation comprises red siltstone, sandstone, siltstone breccia, limestone, and significant evaporite. It is interpreted by Knight (1983) as products of an alluvial plain to marginal marine environment. This unit is observed at multiple sites in the subbasin, and has been significantly affected by salt movement as described below. Knight (1983) describes six dominant lithologies: red siltstone and sandstone, multicoloured laminated siltstone, grey evaporitic shale, grey and blue/black mudstone and siltstone, evaporite, and carbonate (Knight 1983). Bell (1948) logged this unit as at least 244 m thick in coastal exposure between Cape Anguille and Capelin Cove (Fig. 3.3). Knight (1983) logged 145 m of Codroy Road Formation in Fischells Brook, and 300 m in the Codroy Valley. In 1980–1982, approximately 950 m of drill core acquired through the Pronto-Norada Newfoundland Potash Joint Venture in the Flat Bay anticline area (Fig. 3.3) was logged by Carter and Anderle (2012; D. Carter, Geoscientists Nova Scotia, personal communication 2017). Anhydrite replaces gypsum within a few hundred feet of burial (Murray 1964). The core was dominantly halite (of various colours, interbedded with clay), anhydrite, siltstone, and limestone from the Codroy Road Formation (Fig, 3.5). These observations, together with reports by Rhoden (1998) and Dimmel (2001), suggest that outcrop sections the Codroy Road Formation have been substantially thinned by evaporite solution.

The Robinsons River Formation consists of red sandstone, siltstone, and conglomerate, interpreted as floodplain deposits, with interbedded carbonates and minor evaporites. Knight (1983) described the Robinsons Rive Formation as a >5000 m thick unit that crops out at Ship Cove, in

Figure 3.5. Core photograph from.LR-98-1 showing dominantly halite and mudstone showing different breccia textures and ratios of halite to mudstone increasing with depth:
(a) dominantly brittle mudstone with halite-filled vugs, (b) brecciated mudstone with halite surrounding mudstone clasts, (c) dominantly halite breccia with mudstone clasts.

the Codroy Valley, and along the southwestern coast. The Robinsons River Formation is subdivided by Knight (1983) into four lithological units: Jeffrey's Village, Highlands, Mollichignick, and Overfall Brook. The Jeffrey's Village member, ~1400 m thick in the Flat Bay anticline (Fig. 3.3), consists of shale, mudstone, siltstone, sandstone, conglomerate, minor evaporites, and minor carbonates. The Jeffrey's Village Member contains spores (Fig. 3.2) from both the Viséan PC *Lycospora pusilla–Densosporites columbaris* and NS *Knoxisporites stephanephorus* Spore Assemblage Zones (Utting & Giles 2004, 2008). The Highlands Member, >1200 m thick in the St. David's syncline (Fig. 3.3) comprises red sandstone, conglomerate, and red siltstone. The Highlands Member contains spores from the SM *Grandispora spinosa–Ibrahimispores magnificus* Spore Assemblage Zone (Utting & Giles 2004, 2008), making it a lateral equivalent of the lower Mabou Group in Nova Scotia (Fig. 3.2). The Mollichignick Member, at least 2275 m thick in the Grand Codroy River (Fig. 3.3), consists of red siltstone, red and grey sandstone, and pebbly sandstone. Utting and Giles (2004) place the Mollichignick Member in the Viséan to Serpukhovian AT *Schopfipollenites acadiensis–Knoxisporites triradiatus* Spore Assemblage Zone.

The Woody Cape Formation consists of approximately 690 m of green and grey mudstone, siltstone, and sandstone interpreted as deltaic deposits (Knight 1983). The Woody Cape Formation is within the *S. acadiensis–K. triradiatus* Spore Assemblage Zone (Utting & Giles 2004, 2008, Waldron et al. 2017) suggesting correlation with the upper Windsor Group of Nova Scotia (Fig. 3.2). This unit only crops out along the southwestern coast at Capelin Cove (Fig. 3.3).

Overlying the Codroy Group are red conglomerate, sandstone, siltstone, and coal measures of the Barachois Group (Knight 1983, Gibling et al. 2008, Utting & Giles 2008) that crop out in the south and east of the subbasin (Fig. 3.3). The lowest unit within the Barachois Group is the ~2500 m thick Searston Formation, comprising grey sandstone, siltstone, and significant coal measures attributed to meandering river, floodplain, and swamp environments of deposition (Knight 1983). This formation spans the SM *G. spinosa–I. magnificus* and *Reticulatisporites carnosus* Spore Assemblage Zones of Serpukhovian age (Utting & Giles 2004, 2008, Waldron et al.

2017), suggesting correlation with the Pomquet Formation of the Mabou Group on Cape Breton Island.

The Overfall Brook Member, >345 m thick immediately west of the Long Range Fault (Fig. 3.3) is composed of massive crossbedded and pebbly sandstone assigned by Knight (1983) to the Robinsons River Formation of the Codroy Group. Utting and Giles (2008) assign the Overfall Brook Member to the Barachois Group based on the presence of spores from the Serpukhovian *Reticulatisporites carnosus* Assembage Zone (Fig. 3.2).

Higher strata of the Barachois Group were undivided by Knight (1983), but include the increasingly coal-dominated Shears/Cleary unit of Utting and Giles (2008) that is within the Serpukhovian *R. carnosus* Spore Assemblage Zone. These strata correlate to the enigmatic 'Howley Beds' of the Deer Lake subbasin (Hyde et al. 1988, Utting & Giles 2004, 2008). The younger Barachois Group strata contain conglomerate, sandstone, mudstone, and coal seams deposited in a fluvial and possibly lacustrine environment (Bell 1948, Baird & Coté 1964, Solomon 1987).

The Blanche Brook unit crops out near Boswarlos (Fig. 3.3), and comprises dominantly mudstone, sandstone, conglomerate, and significant coal measures deposited in a floodplain environment (Baird & Coté 1964, Solomon 1987, Hyde et al. 1991). This contentious unit is placed within undivided Barachois Group by Knight (1983) and Hyde et al. (1991) correlative to Moscovian (Pennsylvanian) rocks of the Cumberland Group in Nova Scotia (Fig. 3.2). However, newer palynological work by Utting and Giles (2008) suggests that the Blanche Brook unit is much younger and is correlated to the Cumberland Group of Nova Scotia.

3.2.2. Structure and deformation

The BSGSB is bounded to the south and east by the NE–SW striking Long Range Fault (Fig. 3.3), part of the Cabot Fault system. Waldron et al. (2015) suggest the Cabot Fault was active from ~370 Ma to ~310 Ma, and represents a major controlling fault of the oblique releasing bend forming the Maritimes Basin. Carboniferous strata in the BSGSB unconformably overlie Ordovician strata on Port au Port Peninsula (Fig. 3.3) and continue to dip to the southeast as far as the Long Range Fault; leading Knight (1983), Kilfoil (1988), Miller et al. (1990), Hall et al. (1992) to interpret the Bay St. George subbasin as a half-graben.

Folds in the BSGSB trend dominantly NE–SW, parallel to the Long Range Fault, and are typically doubly plunging (Knight 1983). The major folds onshore include the Flat Bay anticline and Barachois syncline (Fig. 3.3) in the northern subbasin, and the Anguille anticline in the southern subbasin. Knight (1983) in the Bay St. George subbasin and Hyde et al. (1988) in correlative rocks in the Deer Lake subbasin in northwest Newfoundland (Fig. 3.1) noted tight- to- isoclinal mesoscopic folds in the Anguille Group, and suggested intense tectonic deformation prior to Codroy Group deposition.

Abundant faults strike approximately NE–SW, parallel to the Appalachian orogen (Knight 1983); major faults include the Long Range Fault and the Snakes Bight Fault (Fig. 3.3). Several smaller NE–SW faults separate Codroy Group strata from Barachois Group strata. Knight (1983) measured faults striking E–W in two key locations: Ship Cove and Capelin Cove (Fig. 3.3). At Ship Cove, multiple E–W faults separate Robinson River Formation from Codroy Road Formation. The E–W fault at Capelin Cove separates Searston Formation (Barachois Group) to the south, and Woody Cape Formation (Codroy Group) to the north.

Knight (1983) suggested that the northern subbasin is less structurally complex than the south due to a shallow depth to basement. In the south, Hobson and Overton (1973) used old seismic refraction data to suggest the presence of up to 6 km of Carboniferous strata in the subbasin. Kilfoil (1988) used magnetic and gravity data to determine a depth to basement in the Bay St. George subbasin as up to 12 km offshore and 3 km onshore. Marillier et al. (1989) confirmed this interpretation using the NW–SE striking deep seismic Lithoprobe line 98-4 southwest of Codroy (Fig. 3.1). Durling and Marillier (1993) used seismic reflection data in the Gulf of St. Lawrence just offshore of the Bay St. George subbasin to estimate a depth to the base of the Horton Group ranging 2 km to >10 km from north to south.

3.3. Methods

The most recent on-land structural study in the Bay St. George subbasin was carried out by Knight (1983) who noted structures produced by both soft-sediment deformation and strike-slip tectonics. Since then, there have been significant advances in the study of soft-sediment deformation and salt tectonics. For example, Alfaro et al. (2016) compile recent studies of soft-sediment deformation, including a study (Snyder and Waldron 2016, Chapter 2 of this thesis) of soft-sediment deformation in Tournaisian strata of Nova Scotia. Jackson and Hudec (2017) provide a review of modern advances in salt tectonics. The effects of these processes are most apparent in the Tournaisian Anguille Group and the lower formations within the Viséan Codroy Group (Fig. 3.2). Our descriptions focus on structures visible in selected well-exposed coastal sections of these units, and are aided by the lithological descriptions provided by Knight (1983) and Utting and Giles (2008). We remapped key coastal outcrops at Ship Cove, Capelin Cove, and Snakes Bight; we prepared detailed field maps at 1:10 000 scale to portray previously undescribed tectonic and evaporite-related structures. Orientations of structures including bedding, cleavage, fold hinges, faults, and soft-sediment structures were noted and uploaded into the geographic information system ArcGIS. Key outcrops displaying soft-sediment deformation structures and salt structures were documented photographically. Fold axes were determined using stereographic projections plotted by Orient software. Stratigraphic columns, maps, and cross sections were constructed by projecting observations parallel to fold axes in areas of detailed mapping.

Vulcan Minerals shot five onland 2-D seismic surveys in the 1980s to aid in the exploration of salt and gypsum deposits (Fig. 3.3). For this paper, we have acquired and reinterpreted these SEG-Y data from the Flat Bay anticline area, together with associated well information from the same area.

3.4. Soft-sediment deformation structures

3.4.1. Introduction

Soft-sediment deformation structures are structures that form soon after deposition of sediment and before complete lithification. In the Bay St. George subbasin, Knight (1983) noted the presence of soft-sediment folds at Cape Anguille and Codroy Island (1983). In selected areas of complete exposure we have systematically described abundant soft-sediment deformation structures in the Snakes Bight Formation, Friars Cove Formation (Anguille Group), and the Ship Cove Formation (Codroy Group). These structures include soft-sediment folds, bulb structures, sedimentary boudins, and clastic dykes.

3.4.2. Observations

Soft-sediment folds

Soft-sediment folds comprise strata that are complexly folded and alternate between concave- and convex-up geometries (Rossetti 1999, Kang et al. 2010). The Snakes Bight Formation at Cape Anguille displays spectacular examples of soft-sediment folds at a range of scales (Fig. 3.6). The folded layers are composed of interlaminated siltstone and mudstone (Fig. 3.7). No cleavage is observed in the folded area. Above and below these convolute layers are undeformed strata. Contacts above deformed strata are sharp. In some locations, rafts of folded laminae are surrounded by larger scale folds (Fig. 3.6).

Individual folds range from <1 to 75 cm measured perpendicular to regional bedding, and are tight to isoclinal. At outcrop scale, hinges of the folds appear as approximately similar folds (Class 2 of Ramsay and Huber (1987); both sandstone and mudstone layers are thickened in fold hinges. In many cases, sandstone layers show class 1C geometry while adjacent mudstone shows

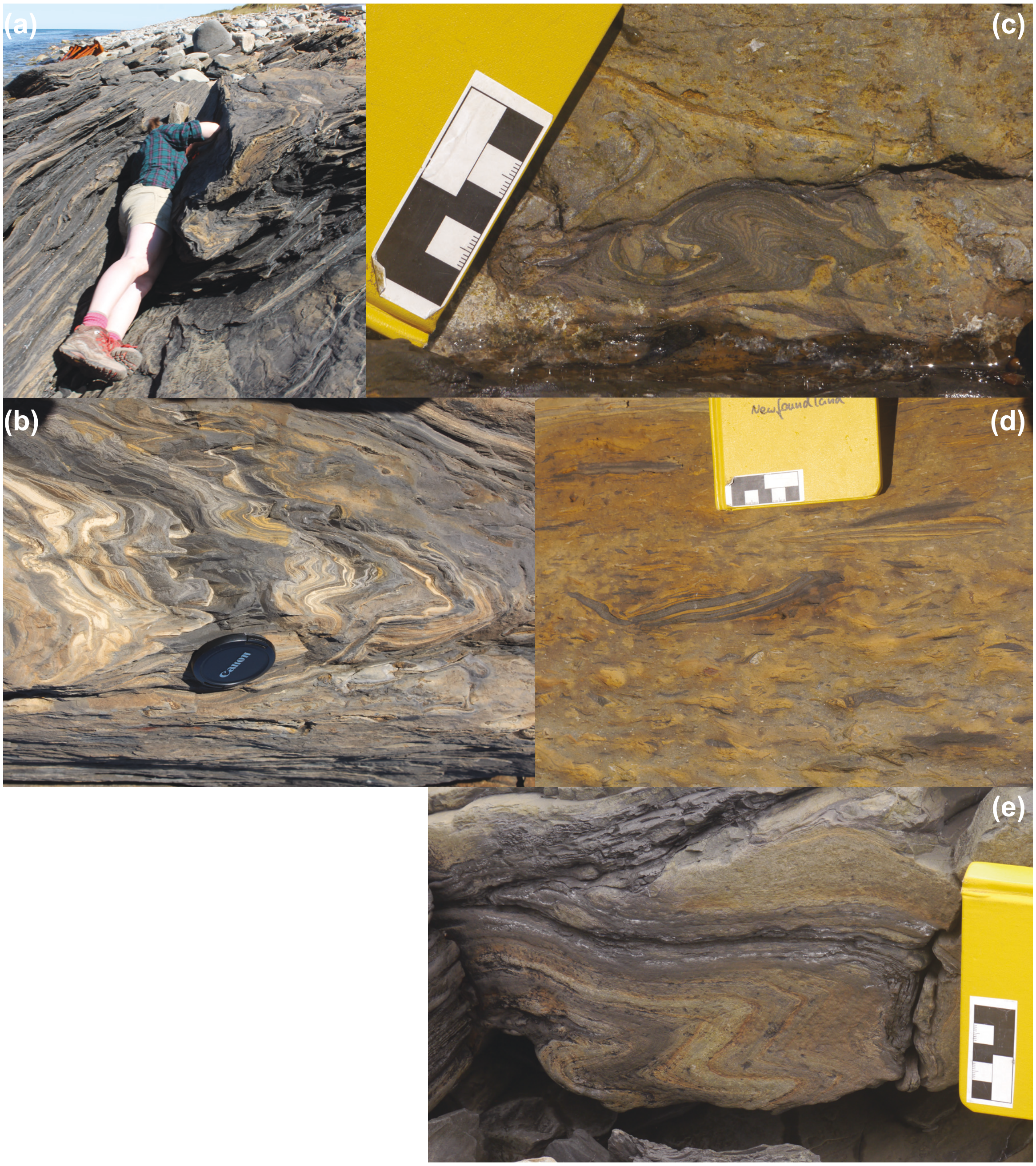

Figure 3.6. Soft-sediment folds at Cape Anguille.
(a) large recumbent fold closing west; (b) s and m folds; (c) raft of folded laminae within large-scaled folded material; (d) rafts of mudstone and siltstone within soft-sediment-folded siltstone groundmass; (e) hinges of soft-sediment folds showing class 1C geometry in sandstone and class 3 geometry in mudstone.

class 3, showing that the sand was stronger than mud during deformation, the normal condition for clastic sedimentary rocks deformed at low temperature. However, close examination reveals cases where sandstone shows class 3 geometry (Fig. 3.6e), showing that it was weaker than adjacent mudstone at the time of deformation; Waldron and Gagnon (2011) cite this geometry as a clear indicator of deformation while sand was liquidized. As shown by a stereographic projection (Fig. 3.8), folds plunge gently to the NNE. Their axial surfaces strike dominantly southwest and dip moderately to the northwest (Fig. 3.9). Viewed down plunge these folds are commonly s-folds, verging WNW. Hyde et al. (1988) described similar tight to isoclinal folds with shallow plunge in Anguille Group strata in the Deer Lake subbasin.

Soft-sediment folds are also observed at Ship Cove in the Spout Falls Formation (Fig. 3.3). The contact between the Spout Falls Formation and the overlying Ship Cove Formation is sharp (Fig. 3.4). The inset photograph in Figure 3.4b shows folded laminae immediately below the contact. On the north side of the same contact, the red sandstone of the Spout Falls Formation shows larger-scale folded bedding truncated by sandstone (Fig. 3.4c).

On Codroy Island (Fig. 3.3), in dominantly grey, medium-bedded wackestone of the Ship Cove Formation (Codroy Group), large folded intervals are interlayered with packages of undeformed strata (3.11), similar geometrically to the clastic successions at Cape Anguille. Undeformed strata dip moderately southeast (~42°). Truncations indicate that this package is right-way-up and youngs to the south. Interlayered with the undeformed strata are intervals of large metre-scale tight to isoclinal folds (Fig. 3.11). Thicknesses of deformed packages range 5 cm to >1 m. The hinges of these folds plunge to the northeast at less than 10°. The coarser layers are dominantly class 1C folds, and the fine-grained materials in between are class 3 folds of Ramsay (1967). Fold axial surfaces are near-parallel to regional bedding.

At Boswarlos (Fig. 3.3), an angular unconformity between Humber Zone strata below and Ship Cove Formation above is exposed. Above the unconformity is dominantly very-fine grained

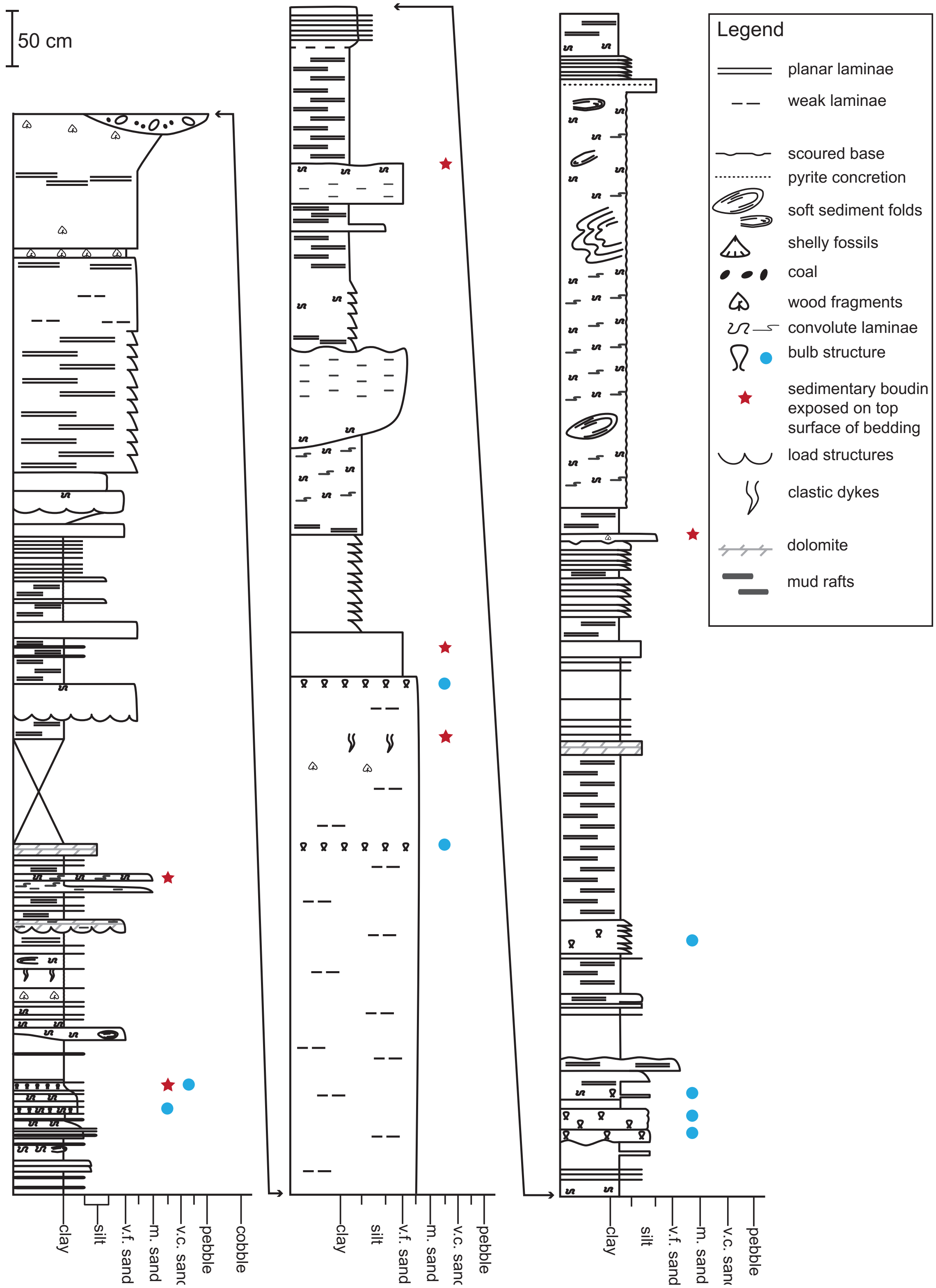

Figure 3.7. Stratigraphic column measured at Cape Anguille highlighting frequency of soft-sediment structures.

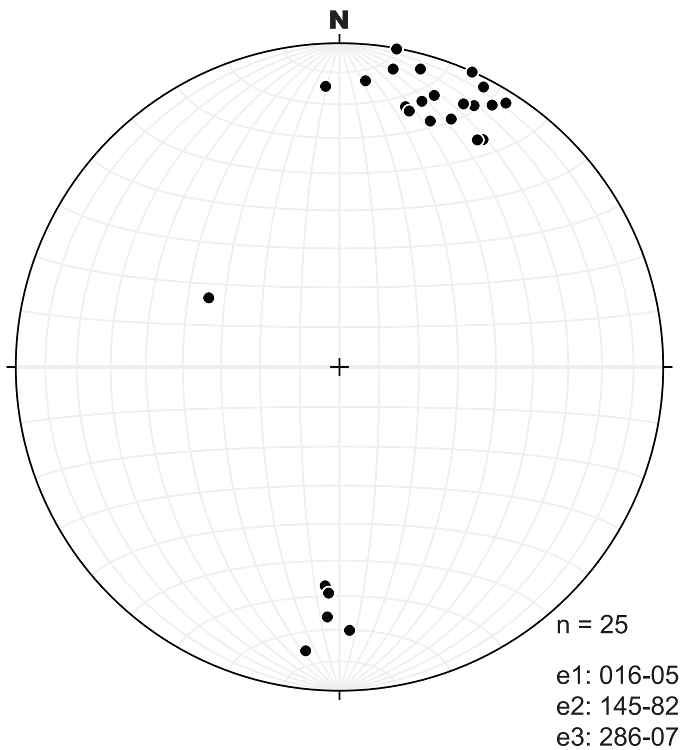

Figure 3.8. Hinges of soft-sediment folds measured at Cape Anguille plotted on an equal area projection.
Average fold hinge orientation is 016-05 NE. Bingham eigenvectors shown as e1, e2, e3. Best fit great circle orientation is 016/83 SE.

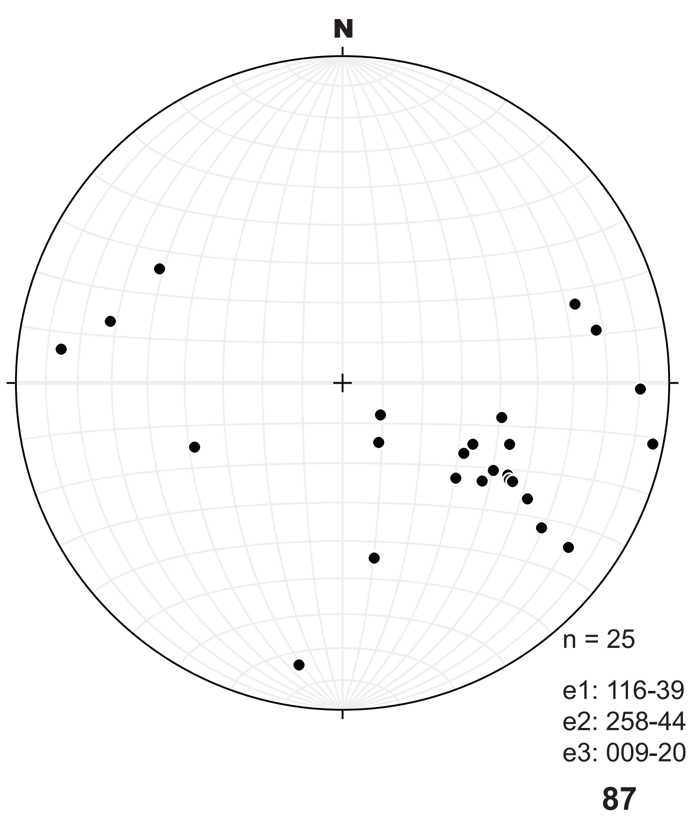

Figure 3.9. Poles to axial surfaces measured at Cape Anguille plotted on an equal area projection.
Average axial surface orientation 206/51 NW. Bingham eigenvectors shown as e1, e2, and e3.

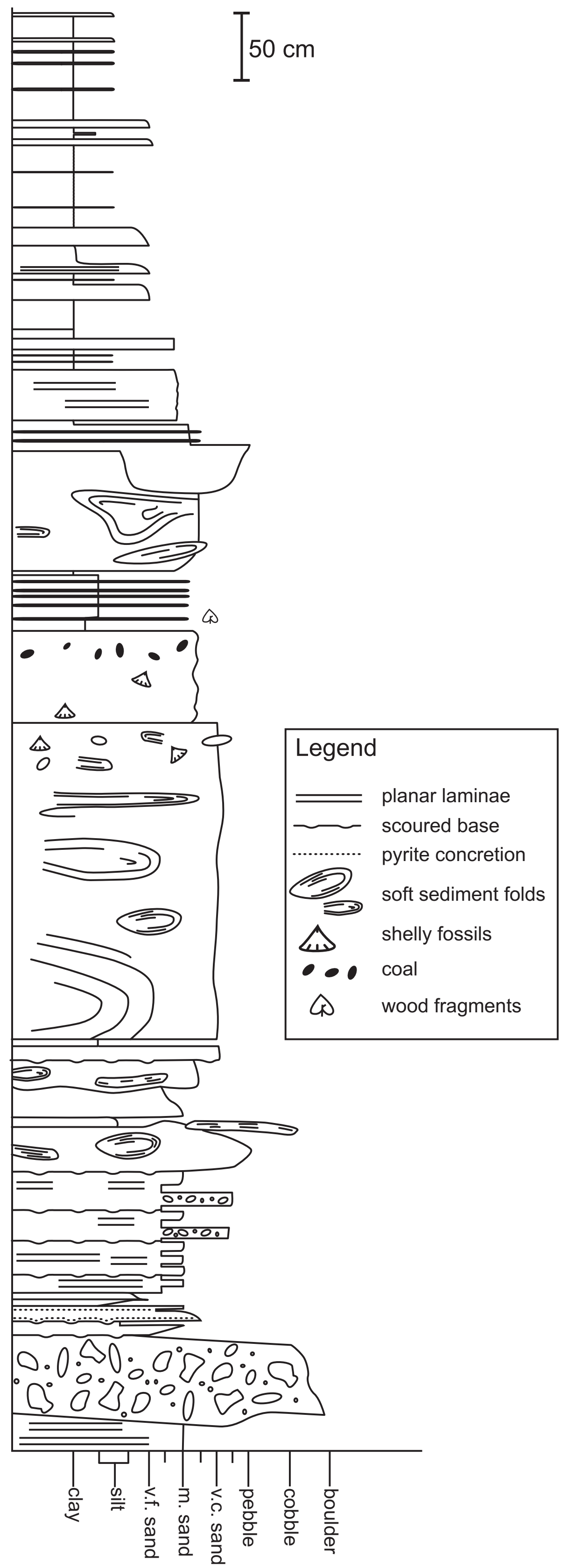

Figure 3.10. Stratigraphic column measured at Boswarlos.

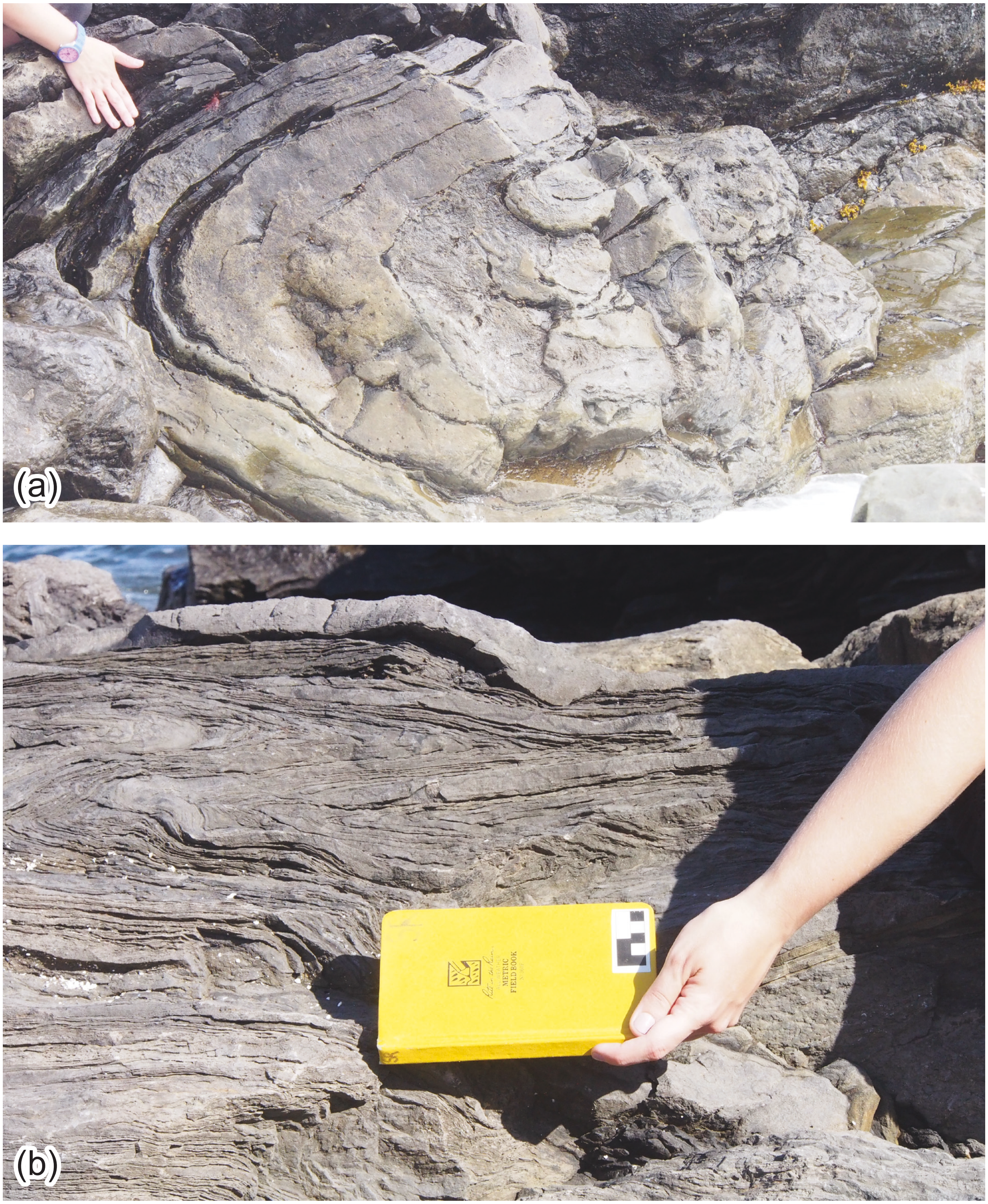

Figure 3.11. Soft-sediment folds on Codroy Island.

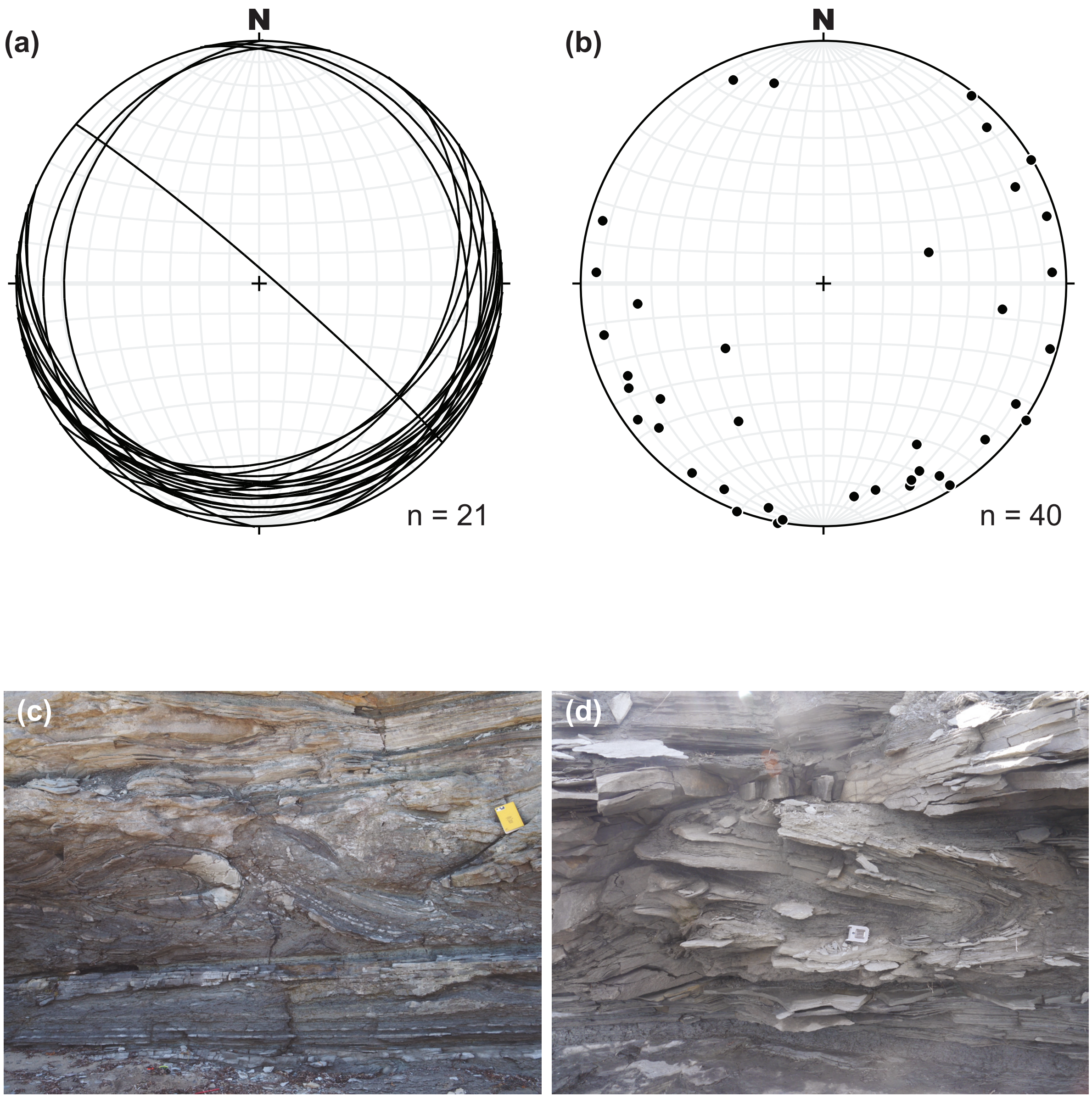

Figure 3.12. Soft-sediment folds at Boswarlos (a) Equal area projection of axial surfaces; (b) equal area projection of fold axes; (c)(d) photographs of soft-sediment folds including a sheath fold.

to pebbly limestone dipping sub-horizontally (~05°) to the southwest. A detailed stratigraphic column (3.10) shows four intervals exhibiting soft-sediment folds. These folds comprise tight to isoclinal class 2 (similar) folds, some of which have curved hinges, resembling sheath folds (Fig. 3.12). Fold hinges plunge gently, displaying a girdle distribution when plotted together on a spherical projection (Fig. 3.12). Plunge of fold hinges on the sheath fold shown in Figure 3.12c range from 06° to 53° and the folds close to the north and east. Axial surfaces dominantly dip gently south-southwest, and strike east-southeast. Shear at base of the soft-sediment folds and thinning of limbs indicate transport to the west. The presence of highly deformed sheath folds suggest that these structures were produced by larger amounts of deformation than those at Cape Anguille, Ship Cove, and Codroy Island.

Sedimentary boudins

Within interbedded siltstone and mudstone at Cape Anguille (Fig. 3.7) are ribbed features exposed on bedding top surfaces. In plan-view these structures are 1–10 mm wide, and create a pattern of parallel hatching on bedding surfaces (Fig. 3.13). These invariably occur in multiples and are commonly found on the top of siltstone and sandstone beds; intervening layers of mudstone do not show traces of the ribbed features. The contact between the ribbed features and the adjacent sediment is gradational. The contacts above and below beds with the ribbed features are parallel; there are no erosional features at the bedding surface. At microscopic scale, the spaces between the structures are filled by mudstone. These structures show preferential orientation, trending dominantly N–S and NE–SW (Fig. 3.13c). Sedimentary boudins crosscut bulb structures (described below). Sedimentary boudins are at an oblique angle to fold hinges at Cape Anguille, consistent with dextral movement.

Examples of sedimentary boudins are described by Waldron et al. (2007) and Snyder and Waldron (2016) (Chapter 2 in this thesis) in correlative rocks in the Windsor-Kennetcook subbasin in Nova Scotia. These authors interpreted the structures as produced by extension in incompletely

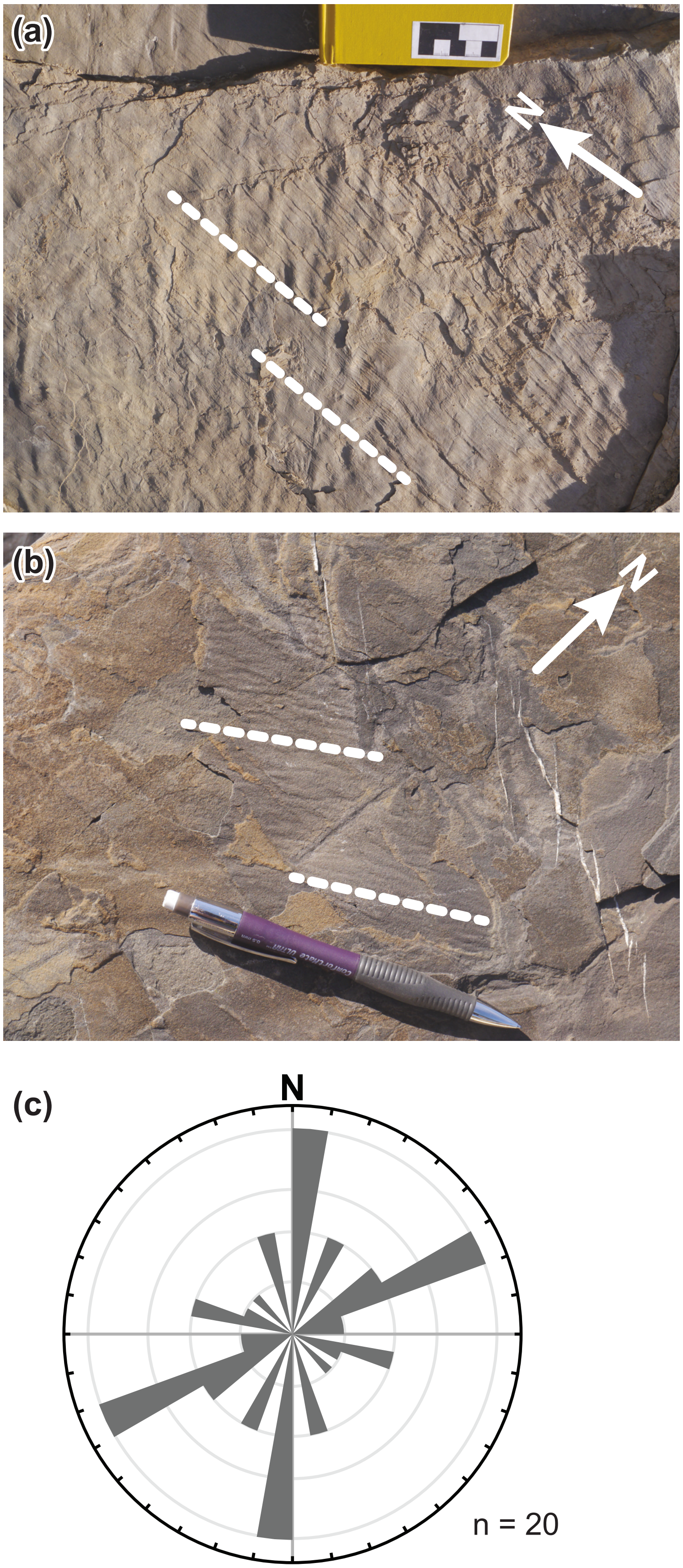

Figure 3.13. Sedimentary boudins at Cape Anguille. (a)(b) ribbed features on the tops of bedding. Dashed lines show boudin surfaces; (c) Circular histogram showing boudin trends on bedding.

cemented sediment. The observations above support a similar interpretation for the Bay St. George subbasin structures to those of Waldron et al. (2007) and Snyder and Waldron (2016) that the sedimentary boudins formed by extension of partially lithified more rigid siltstone and sandstone.

Clastic dykes

Clastic dykes are common in siltstone interlaminated with mudstone layers (Fig. 3.7). Dykes are composed of grey siltstone and are laterally adjacent to dark grey mudstone showing bedding-parallel fissility. The dykes are elongate, trending dominantly NE–SW (Fig. 3.14), but some sections show perpendicular dykes trending NW–SE. The dykes range from 4–14 cm in height, and 5 mm–14 cm wide on the top surfaces of beds. The dykes narrow and in some instances bifurcate with depth. These clastic dykes are very similar in appearance to those described by Snyder and Waldron (2016) (Chapter 2 in this thesis) in the Windsor-Kennetcook subbasin in Nova Scotia.

The clastic dykes at Cape Anguille crosscut sedimentary boudins and soft-sediment folds (Fig. 3.14). The top surface of one sandstone bed shows a bedding-parallel fault (219/23 NW) and clastic dykes on the same surface. The sandstone fill of the clastic dyke appears in positive relief overprinting slickenlines (254-14 SW) shown in Figure 3.14d. The clastic dyke must therefore be younger than the slickenlines on the fault which indicates that the dyke formed after the fault moved.

Bulb structures

At multiple intervals in the Snakes Bight Formation at Cape Anguille (Fig. 3.7) are siltstone protuberances on the tops of bedding surfaces. In plan-view, these structures are approximately 1–5 cm in diameter and appear as rounded siltstone polygons that occur in groups within a mudstone matrix. Cross-bedding in sandstone beds immediately above one layer with the structures at Cape

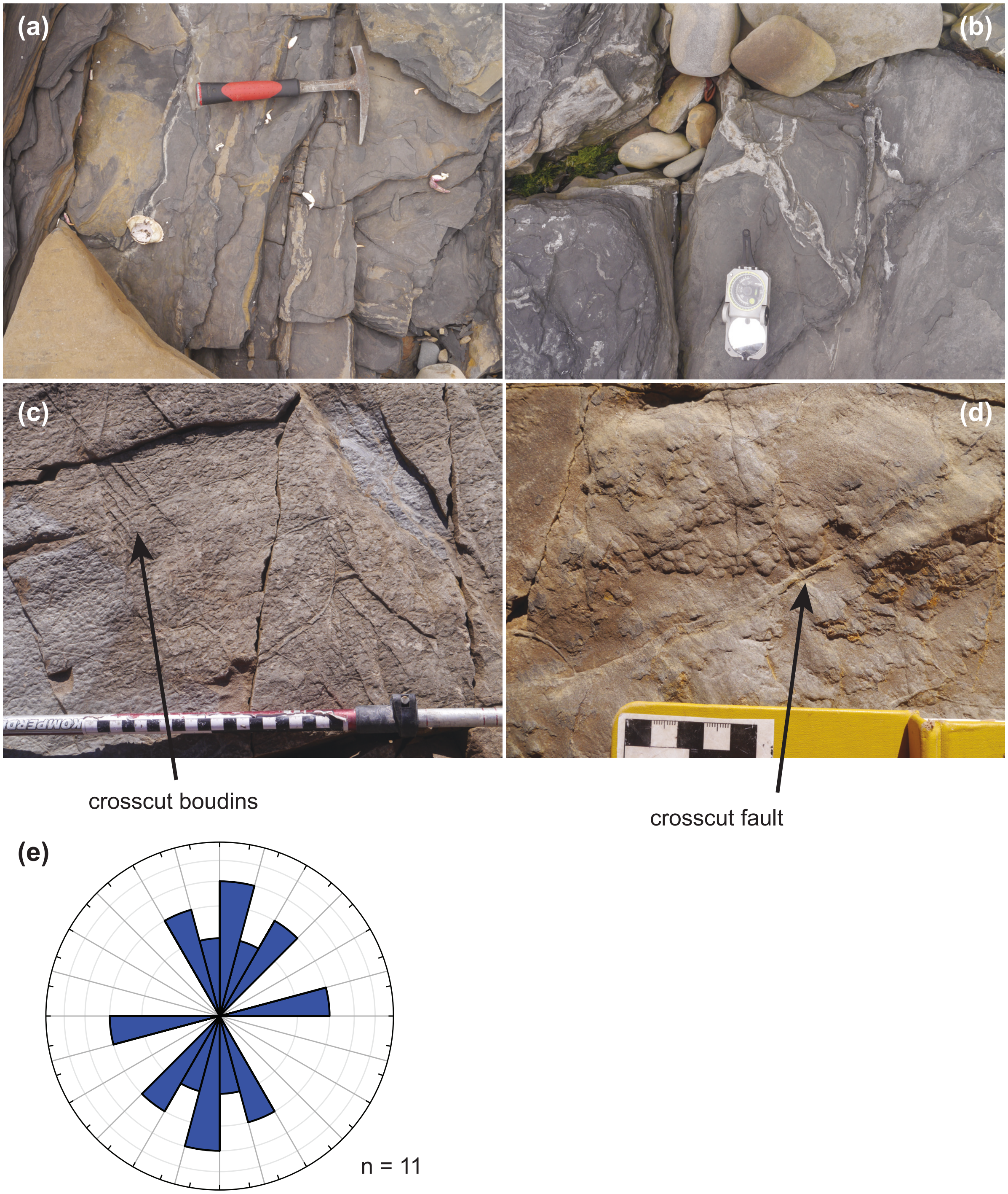

Figure 3.14. Clastic dykes at Cape Anguille.
(a)(b) Clastic dykes on the tops of bedding at Cape Anguille trend NE-SW and NW-SE; (c) Clastic dyke crosscutting sedimentary boudin; (d) clastic dyke crosscutting bedding-parallel fault; (e) circular histogram showing clastic dyke trends on bedding.

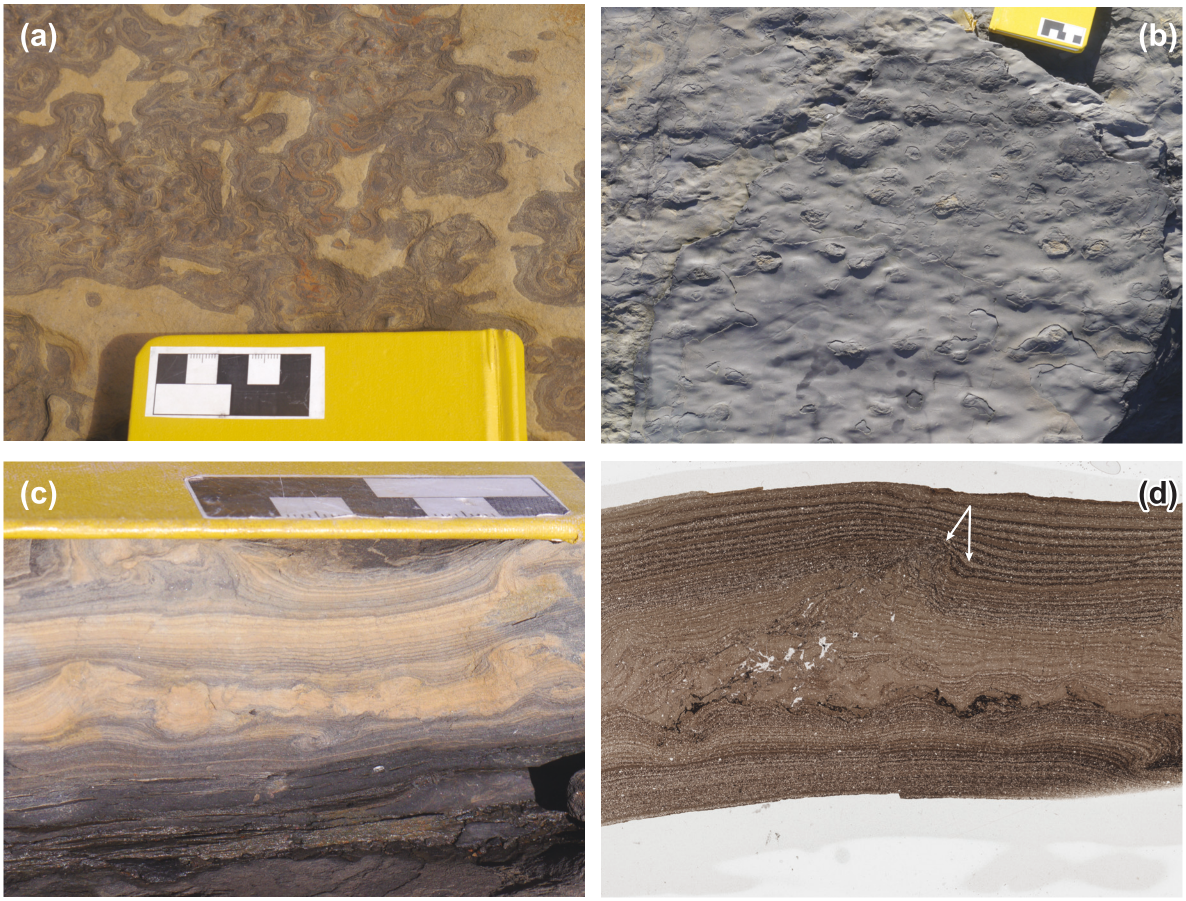

Figure 3.15. Bulb structures at Cape Anguille.
(a)(b) plan view as polygons on the tops of bedding; (b) in cross-sectional view in outcrop, and (d) in cross sectional view in thin section; arrows point to thickness changes in mud immediately adjacent and overlying a bulb.

Anguille indicates these beds are upright. These groups cover the entirety of the tops of siltstone beds; in some locations three or more square metres of exposed structures crop out (Fig. 3.15). Clastic dykes and sedimentary boudins crosscut the structures (Fig. 3.15b).

In cross-sectional view, these structures range 1–10 cm in height (Fig. 3.15c). The structures themselves are convex-up siltstone bodies surrounded by mudstone. Overlying the structures are laminated mudstone and siltstone that are thicker adjacent to these convex-up structures, and thinner immediately above the most convex part of the structure as shown in thin section (Fig. 3.15d). These laminae show uniform dip and thickness laterally with the exception of immediately above the siltstone protuberances where they are convex-up and thinner. The bottom surface of the deformed layer is undulatory and locally may show conventional load structures or soft-sediment folds (Fig. 3.15d).

The structures described above superficially resemble conventional load structures noted, for example, by Hempton and Dewey (1983) in Turkey, Alfaro et al. (2002) and Ezquerro et al. (2015) in Spain, Owen (2003) and Collinson (2005) in England, and Moretti et al. (1999) in a physical simulation; the structures differ in their being ‘upside-down’. Similar structures have been described with variable names: 'cycloids' by Hempton and Dewey (1983) and Scott and Price (1988), 'mushroom-like silts' by Rodríguez-Pascua et al. (2000), 'bulb-shaped structures' by Nikolaeva (2009) and 'bulb structures' by Snyder and Waldron (2016), which is the term used here.

3.4.3. Interpretation

Soft-sediment structures provide information on early deformation of sedimentary rocks in tectonically active environments such as strike-slip systems, pull-apart basins, and sedimentary basins cut by faults (Hempton & Dewey 1983, Plint 1985, Rossetti 1999, Sibson 2003, Berra & Felletti 2011, Waldron & Gagnon 2011, Snyder & Waldron 2016). Liquidization (liquefaction and/or fluidization) is the most common deformation mechanism for soft-sediment deformation structures; liquidized and partially lithified sediments are able to form these unique structures (Maltman 1994, Maltman & Bolton 2003, van Loon & Mazumder 2011). However, Waldron and Gagnon (2011) show that soft-sediment deformation can be induced both by down-slope, gravity-driven processes and by movement on underlying tectonic faults, or by combinations of the two, in which tectonic activity produces steep topographic slopes.

The geometries of folds in both the Anguille Group and Codroy Group examples clearly indicates that sediments were unlithified at the time of deformation, but does not clearly indicate whether tectonism or topographic slope, or some combination of the two, provided the necessary differential stress to deform the sediments. Folded beds at Cape Anguille and Codroy Island show preferential fold hinge orientations within the overall plane of bedding (Fig. 3.8, 3.11) suggesting overall tectonic control. At Cape Anguille the folds trend NNE, have a gentle plunge, and are commonly s-folds verging WNW when looking down plunge. The folds at this location likely formed during movement of mobilized sediment towards the WNW, initiated when the location was tectonically active. The rafts of folded laminae within the larger mass of folded material at this location also suggest multiple periods of deformation. Partially lithified layers imply breakage, preservation, and incorporation of rafts into a larger folded system.

Because soft-sediment folds are observed in the Snakes Bight, Spout Falls, and Ship Cove Formations, we suggest that the subbasin was tectonically active throughout deposition of the Anguille Group and that deformation continued into deposition of the Ship Cove Formation of the Codroy Group. However, the Ship Cove Limestone overlying the Spout Falls Formation at Ship Cove is uniform with no soft-sediment structures. This suggests that the trigger for deposition did not affect the entire subbasin, and therefore that soft-sediment deformation was the result of multiple local events.

Sedimentary boudins are interpreted as structures produced by extension parallel to bedding in sediments that were incompletely cemented, kinematically equivalent to boudins that are more usually described in metamorphic rocks (Chapter 2 in this thesis). These structures are extensional and result from semi-brittle extension of more rigid siltstone and sandstone; created space was filled by more ductile sediment. As there is both a brittle and ductile component to these structures, they likely formed after some lithification of sediment but prior to complete lithification. The sedimentary boudins and bulb structures also show no evidence of exposure at sediment surfaces; we interpret the sedimentary boudins and bulb structures as having formed post-depositionally within the sediment pile.

All other soft-sediment deformation structures crosscut the bulb structures, indicating that the bulbs formed soon after deposition. Bulb structures are interpreted as being comparable to those described by Snyder and Waldron (2016) (Chapter 2 in this thesis) in the Windsor-Kennetcook subbasin. In these examples, silt was deposited in layers of uniform thickness and was later deformed by pinching out laterally as a result of sediment flow into the bulbs. The contorted nature of the silt in the bulb structures indicates that sediment was likely liquidized during formation of the bulbs. Flow of water within the layers and between the larger silt grains during liquidization led to the observed localized variations in grain size described above.

Clastic dykes of siltstone show downward thinning and terminate at different stratigraphic levels, indicating that the siltstone was sourced from the overlying sediment down into a host mudstone. The dykes likely developed before the surrounding mud was fully lithified; the contact between siltstone and adjacent shale is sharp which suggests brittle deformation at a shallow depth of formation (Parnell & Kelly 2003). Waldron and Gagnon (2011) show that ductile behaviour in coarser sediment in contact with brittle mud is a strong indicator of sediment liquidization; they suggest that when mud acts more rigid than coarser sediment, the coarser sediment behaved as a fluid with a lower yield stress than the mud.

3.5. Evaporite-related and tectonic structures

3.5.1. Introduction

Large-scale tectonic structures onshore have been noted by Knight (1983). The most widely recognized structures are the Flat Bay anticline, the Barachois syncline, the Anguille anticline, and the Snakes Bight Fault. The Flat Bay anticline and the adjacent Barachois syncline represent the most recognized structures in the north of the subbasin. The Anguille anticline and the Snakes Bight Fault are the dominant structure in the south subbasin. We remapped and reinterpreted two detailed sections from Ship Cove and Capelin Cove to compare structural style in the north and south of the subbasin. We also compare the structures present in the Anguille Group compared to those in the Codroy Group.

3.5.2. Observations

Drilling data

Mineral exploration directed at gypsum, potash, and halite in the Codroy Group in the Flat Bay anticline area (Fig. 3.3) has produced a significant amount of drilling data. Leeson Resources Inc. LR-98-1 and LR-98-2 (Fig. 3.3) were drilled in the northern part of the subbasin along Fischells Brook and penetrated 681 m and 359 m of Carboniferous strata, respectively (Rhoden 1998). Drill core contains sandstone, siltstone, mudstone, conglomerate, and an increasing amount of evaporites (gypsum and halite) with depth; halite is the dominant lithology below ~360 m in LR-98-1 and LR-98-2 (Rhoden 1998). Immediately above the Ship Cove Formation, the Codroy Road Formation is logged as thick foliated intervals of dominantly halite and anhydrite with frequent limestone bands. The thick halite package contains bands and/or inclusions of mudstone and siltstone that make up between 2 and 40% of the drilled section (Fig. 3.5). We infer that stratigraphic sections exposed in outcrop, now devoid of halite, originally contained significantly larger proportions of evaporite.

Seismic reflection data

To investigate the extent and geometry of Carboniferous strata in the subsurface, time-migrated 2-D seismic reflection data acquired from the Newfoundland and Labrador Department of Natural Resources were examined (Fig. 3.3). The data are of poor to moderate quality, and we have not attempted any reprocessing of the original seismic data. Initial horizon identification and interpretations were made by comparison with maps, drill core, and data from offshore BSGSB (Chapter 4 in this thesis).

Groups of reflections consistently picked include a base reflector (horizon BA) that represents the boundary between bright but poorly coherent reflections below and coherent reflections above. Above horizon BA is a reflective interval that defines antiform-synform pairs (Fig. 3.16). The reflective interval above horizon BA shows significant variations in two-way travel time (TWTT) between reflections across the seismic profile, interpreted to indicate thickness changes. There are significant thickness increases between reflections from the southwest to southeast (Fig. 3.16). Thickness between reflections increases near the hinge of the syncline; thickness between reflections decreases near the hinge of the anticline.

The base of the reflective interval overlying horizon BA is a reflection that can be traced across most lines, here termed horizon TS (Fig. 3.16). In Figure 3.16, on the NW to SE seismic profile, horizon TS is in direct contact with horizon BA. On the SW end of the SE–SW seismic profile in Figure 3.16, a convex-up zone of incoherent reflections is imaged between horizon BA and horizon TS. Horizon TS appears bound the incoherent zone by downlapping directly onto horizon BA. To the southeast, reflections overlying horizon TS, dipping moderately to the southeast, change dip to parallel the subhorizontal horizon BA.

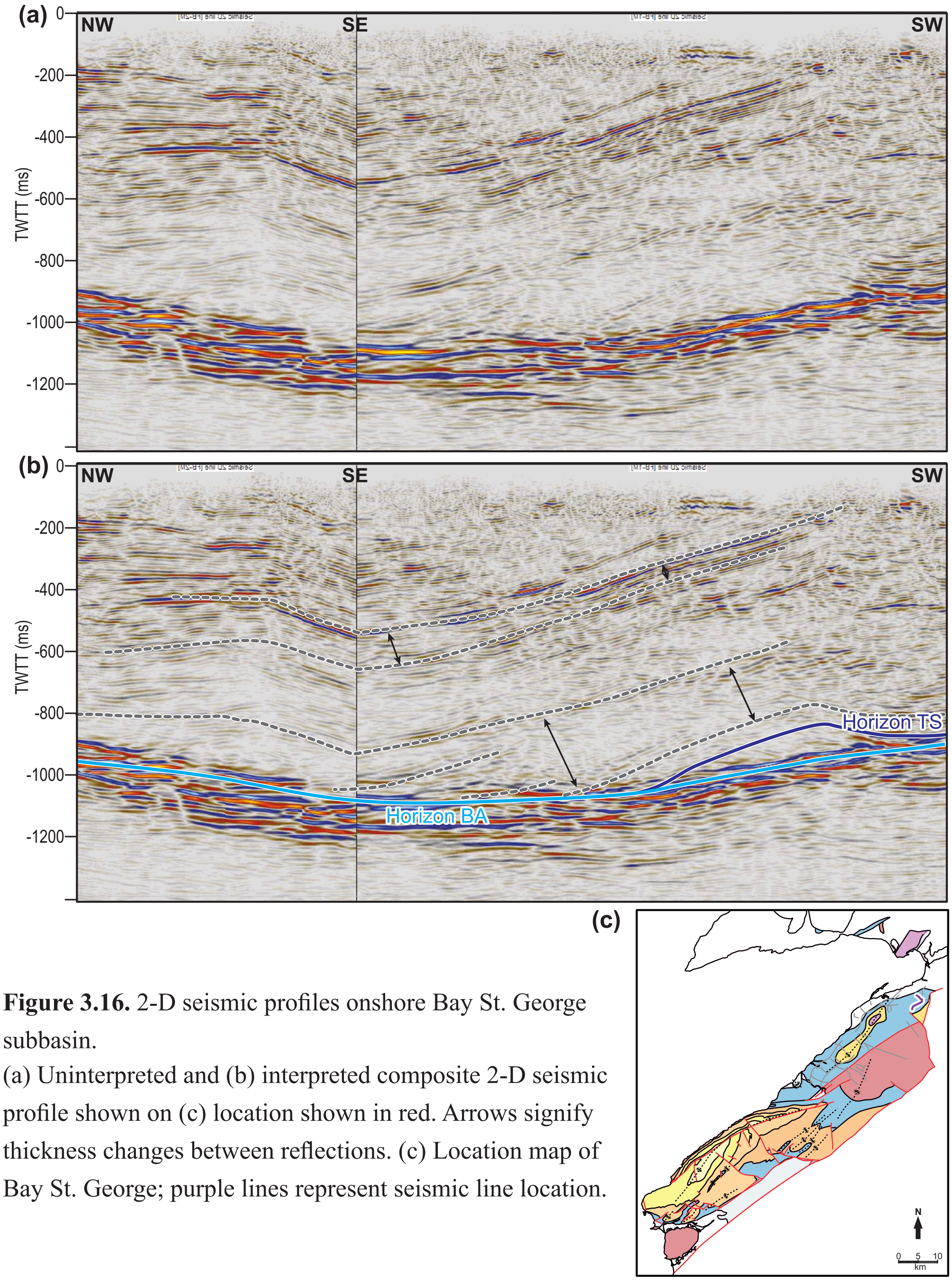

Figure 3.16. 2-D seismic profiles onshore Bay St. George subbasin.
(a) Uninterpreted and (b) interpreted composite 2-D seismic profile shown on (c) location shown in red. Arrows signify thickness changes between reflections. (c) Location map of Bay St. George; purple lines represent seismic line location.

Evaporites are commonly incoherent on seismic profiles (Jackson & Hudec 2017). The incoherent core of the anticline in Figure 3.16 is likely filled with Codroy Road Formation evaporites. The interpreted evaporites are absent in the centre of the syncline, leaving horizon BA and horizon TS in direct contact.

Rhoden (1998) examined drill core from LR 98-1 and LR 98-2 east of the Flat Bay anticline, and interpreted a salt-expulsion minibasin. The geometries on these seismic lines are similar to salt-related structures on passive continental margins (Hudec et al. 2009) where expulsion of evaporites is caused by younger sediment subsiding into an evaporite-filled layer forming synclines. Lateral thickness changes record differential subsidence during sedimentation. Once the salt becomes mobilized, it collects into adjacent salt-cored anticlines (Jackson & Vendeville 1994, Ge et al. 1997, Hudec & Jackson 2004, Hudec & Jackson 2007, Hudec et al. 2009, Garcia et al. 2012, Jackson & Hudec 2017). Due to the presence of evaporites beneath an anticline in Figure 3.16, we interpret the structure as a salt-cored anticline and adjacent salt-expulsion minibasin.

The surface where material above and below the evaporite package is in direct contact represents a salt weld (Jackson & Talbot 1991). Therefore we interpret a primary salt weld underlying the salt-expulsion minibasin in Figure 3.16.

Ship Cove

Ship Cove (Fig. 3.3) is a spectacular section that includes a >10 m high sea-stack ~50 m offshore, a cobble beach, and kilometres of continuous outcrop. This section was mapped by Knight (1983) as a continuous conformable succession spanning the Spout Falls, Ship Cove, Codroy Road, and Robinsons River Formations. We remapped this area and created a detailed section measured from the top of the Ship Cove Formation into the base of the Codroy Road Formation (Fig. 3.17). In this section, laminated limestone, mudstone, massive conglomerate, gypsum, and multicoloured weakly foliated siltstone breccia (Fig. 3.18) alternate. At a larger scale, a cross

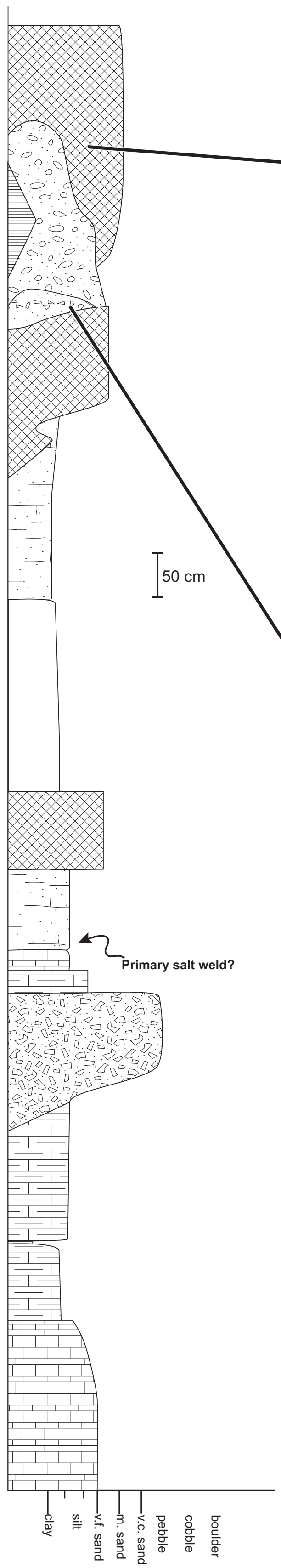

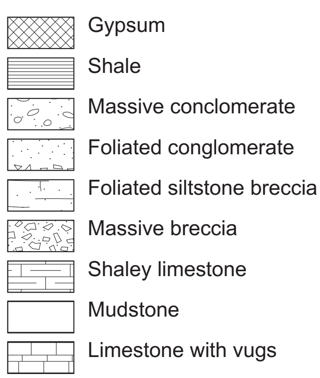

Figure 3.17. Stratigraphic Column and photographs of the Codroy Road Formation at Ship Cove.
Photographs show gypsum surrounded by siltstone breccia (above), and an angular conglomerate layer parallel to the gypsum foliation (below).

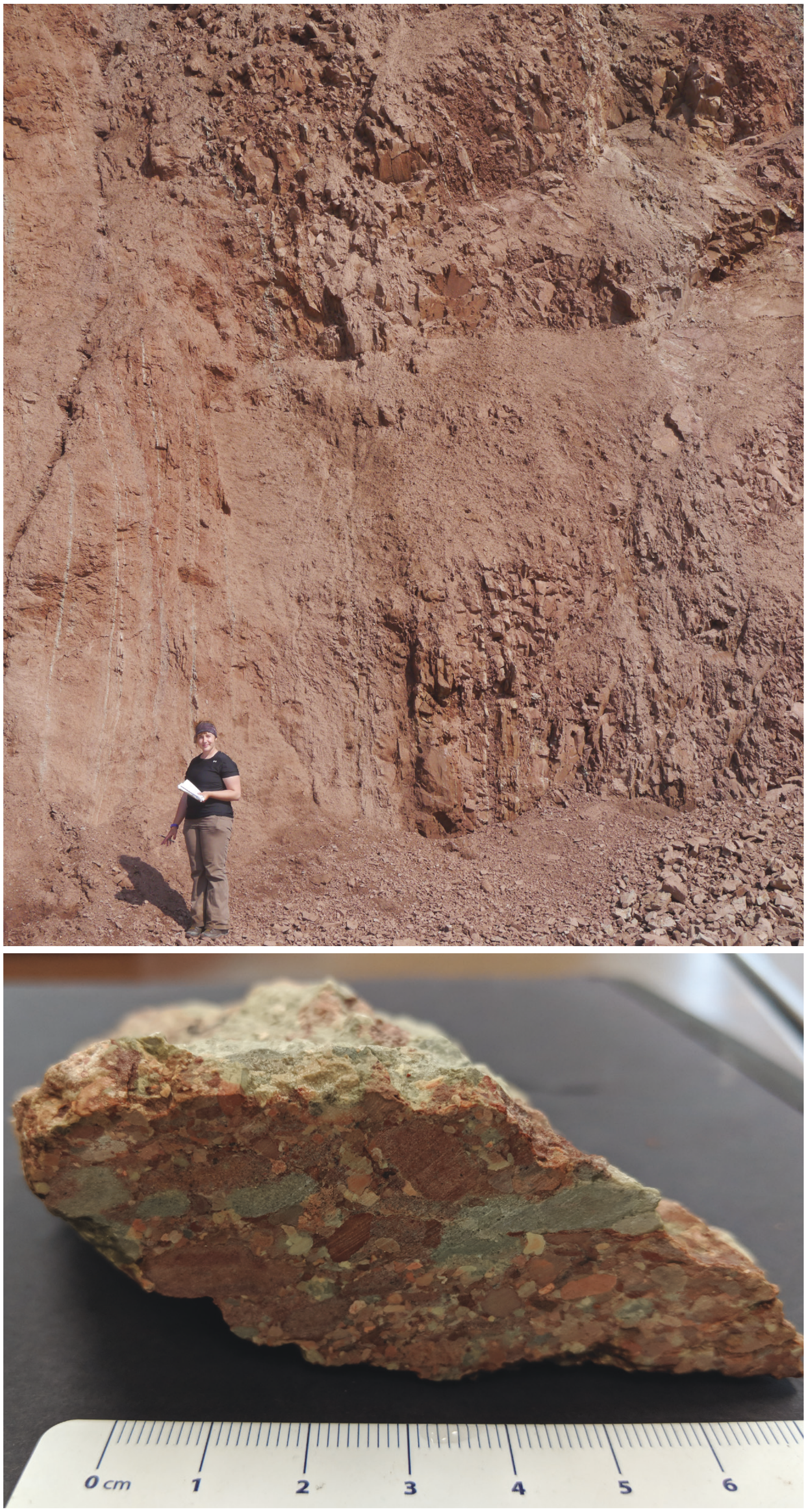

Figure 3.18 . Photographs of siltstone breccia.
(a) outcrop view siltstone breccia showing near vertical foliation and (b) cut hand sample showing dominantly siltstone clasts.

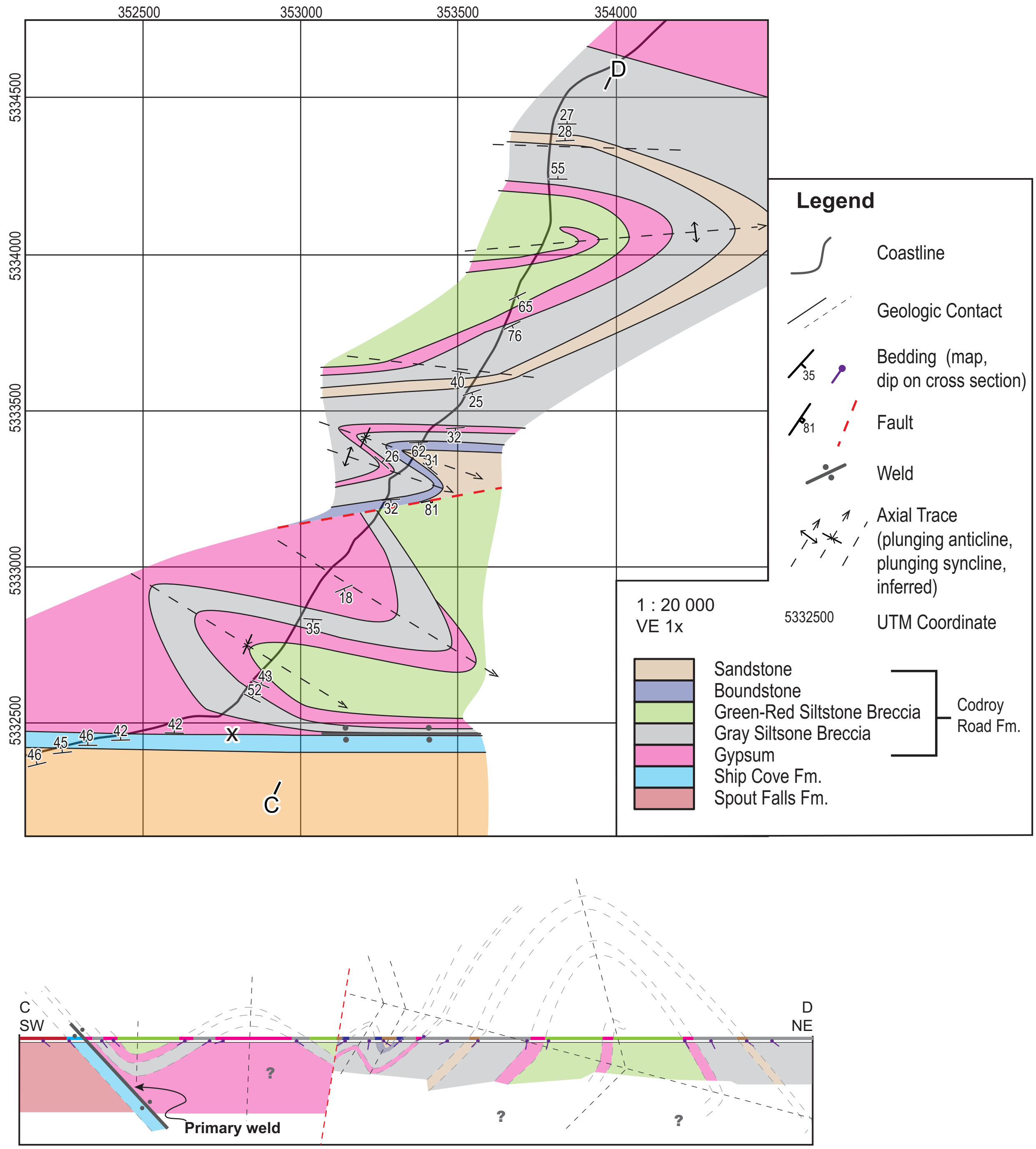

Figure 3.19. New geologic map and cross section of Ship Cove in the northern subbasin. Exposure along coast is nearly continuous. X represents location of Fig. 3.17.

section (C–D in Fig. 3.19) along the coast, perpendicular to major fold axes, shows alternating thick sections of foliated siltstone breccia, gypsum, and minor carbonates. Within the siltstone breccia packages, thin beds of gypsum are found. The gypsum sections have varying texture, but consistently show foliated dark and light bands.

At small and large scale there are alternating packages of siltstone breccia, gypsum, and minor carbonates. This suggests that the Codroy Road Formation was deposited during cyclic changes in the depositional environment. Giles (1981) interpreted correlative rocks from the Windsor Group in the Shubenacadie subbasin in Nova Scotia and noted similar cycles at mesoscopic and macroscopic scale.

Map and cross-sectional views show uniformly dipping Spout Falls and Ship Cove Formation. Above these units, map relationships require that the thickness of the overlying Codroy Road Formation gypsum varies dramatically when traced laterally, which suggests the presence of an evaporite structure. It is interpreted that expulsion of evaporites along the top of the Ship Cove Formation created the thickened evaporite package shown in the cross section in Figure 3.19. The parallel contact between the Ship Cove Formation limestone and an overlying siltstone breccia and gypsum likely represents a surface where evaporites were expelled or dissolved forming a primary weld.

In the overlying Codroy Road Formation, a series of anticline–syncline pairs comprise the remainder of the section. Interbedded boundstone, sandstone, siltstone breccia, and gypsum form a large anticline further north. Gypsum outcrops near the core of the large anticline are steep at water-level and are folded about a near-horizontal secondary axial trace, suggesting the presence of tectonic refolded folds.

Capelin Cove Section

One of the most structurally complex coastal sections in the BSGSB extends from Stormy Point to Cape Anguille (Fig. 3.3). Knight (1983) mapped this section, interpreting many near-vertical faults separating Searston, Woody Cape, Codroy Road, Friars Cove, and Snakes Bight Formations. For this study, the Capelin Cove section was remapped (Fig. 3.20). The Codroy Road Formation was separated into 3 mappable siltstone breccia units, 2 separate gypsum-dominated packages, and 2 black limestone packages (Fig. 3.20, 3.21).

A yellow-orange breccia unit cropping out at the northern end of the section is mapped by Knight (1983) as Jeffreys Village Member. This unit unconformably overlies the Codroy Road Formation. Within the Jeffreys Village Member, an internal unconformity separates a breccia below, with dolomitic matrix, pebble-sized limestone and gypsum clasts, from a conglomerate above, with sandy matrix and clasts of variable lithology including pebble-sized gabbro and amphibolite higher in the section.

To the south of the Capelin Cove section are sandstone, dark shale, siltstone, and rare gypsum beds of the Woody Cape Formation. One sandstone bed within the Woody Cape Formation has quartz pseudomorphs after halite (Fig. 3.22) suggesting the Woody Cape Formation was likely deposited subaqueously in hypersaline water. Crossbedding and climbing ripples in the sandstone provide unequivocal way-up indicators. This package of rock has variable dip, ranging from steeply dipping (~75° south) and younging to the south, to near horizontal (~07° north), to overturned (~58° south) and younging to the north (Fig. 3.21).

The contact between Woody Cape Formation and Searston Formation to the south comprises a near-vertical brecciated zone exposed in the cliff. The contact zone is ~5.5 m wide, and strikes approximately E–W (250°) (Fig. 3.23). Within this zone is fine-grained very poorly consolidated breccia and gouge. Broken sandstone layers are present near the edges of the zone, with orien-

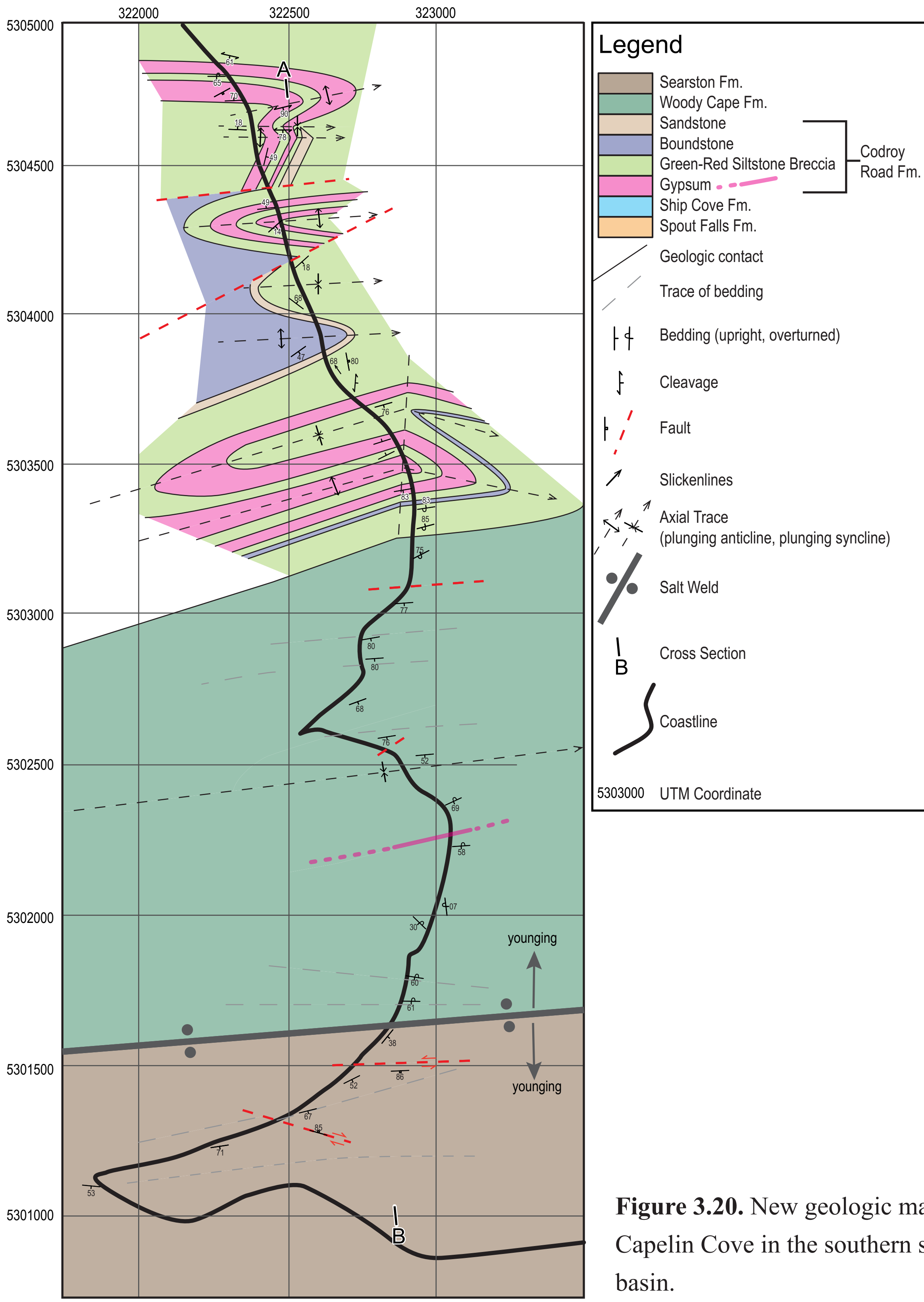

Figure 3.20. New geologic map of Capelin Cove in the southern sub-basin.

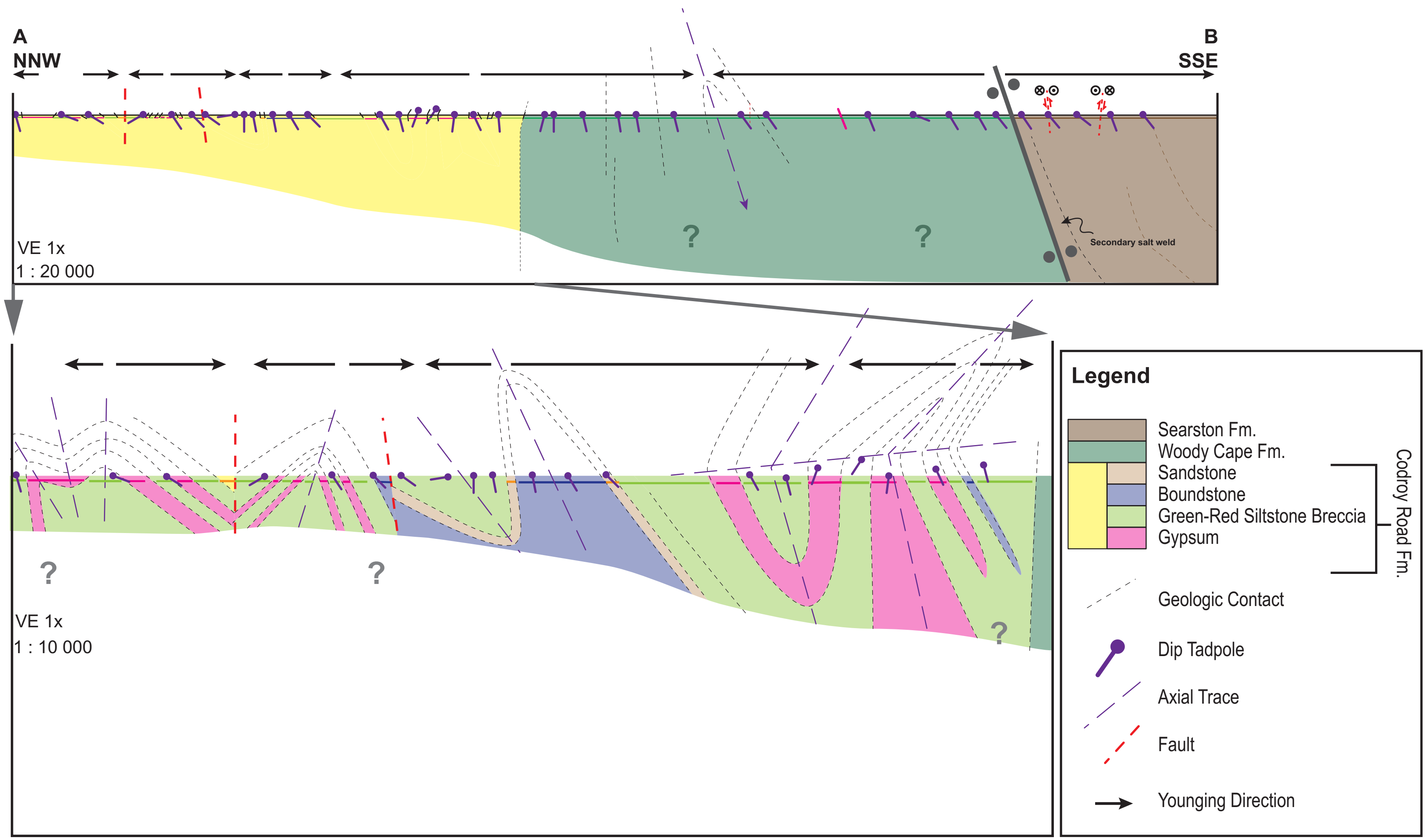

Figure 3.21. Cross section of Capelin Cove. Inset shows detailed mapping in the Codroy Road Formation.

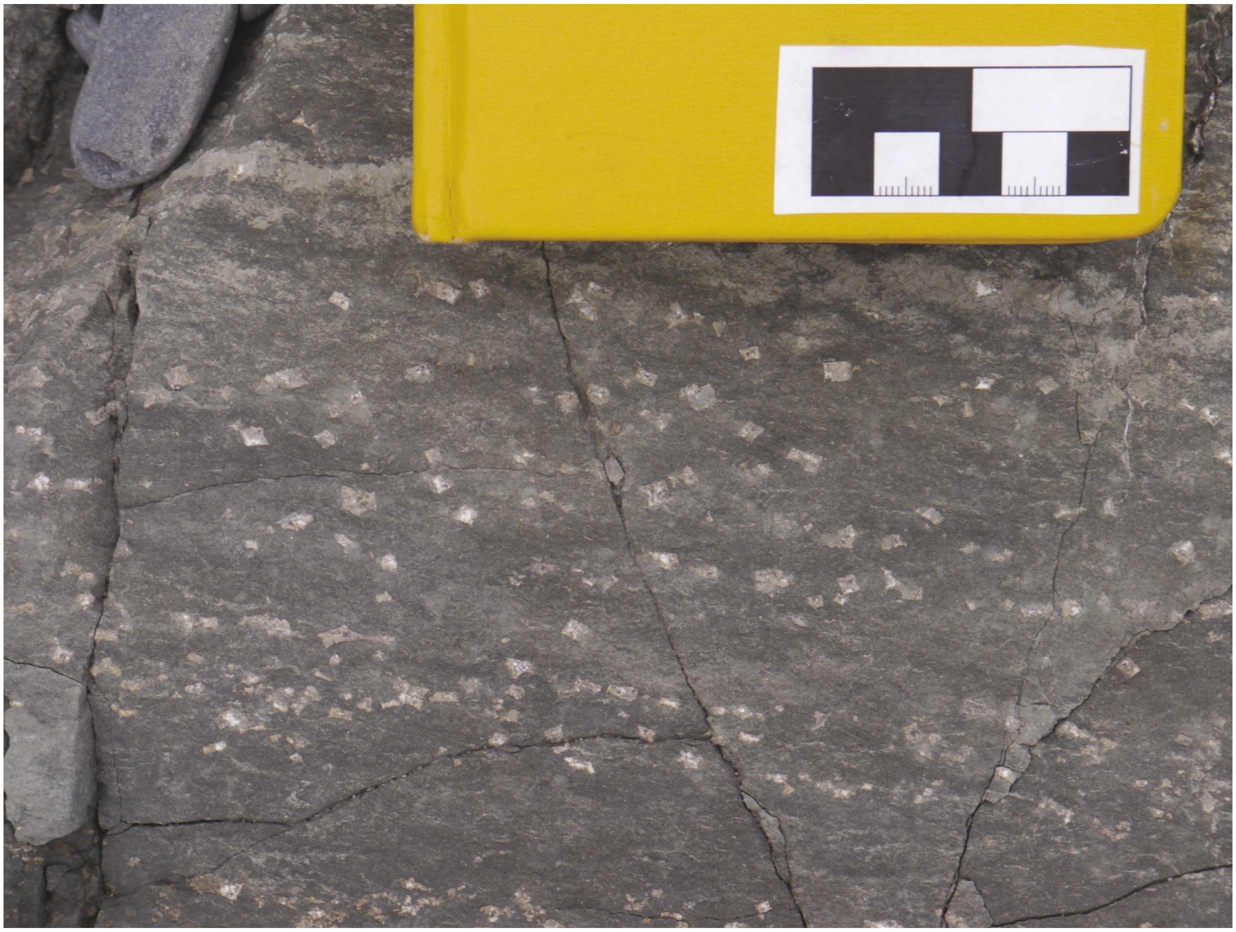

Figure 3.22. Photograph of halite pseudomorphs in outcrop taken from the Woody Cape Formation.

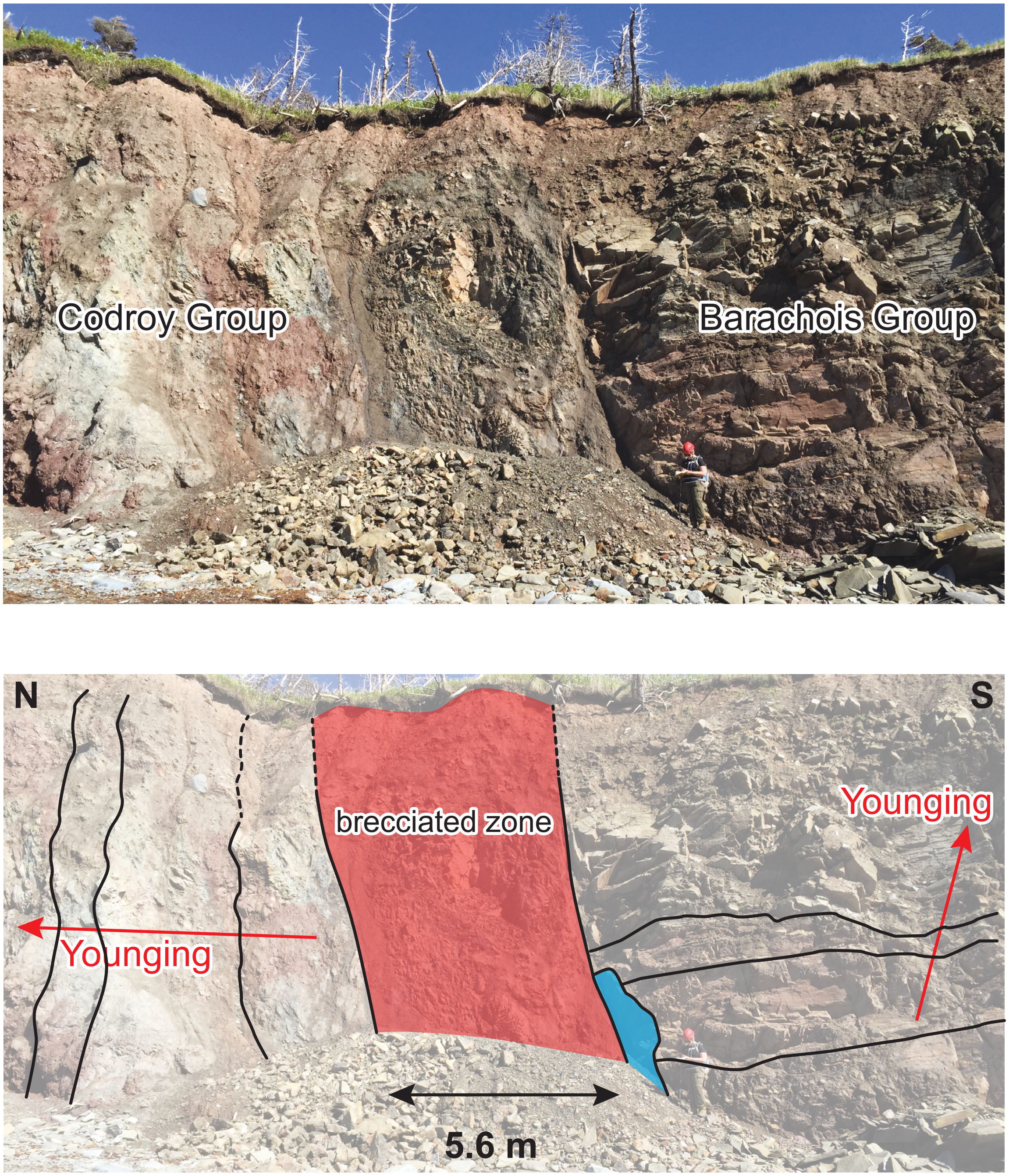

Figure 3.23. Secondary salt weld at Capelin Cove.
(a) Photograph and (b) interpreted photograph of brecciated zone and younging direction of bedding on either side of the zone. Martin for scale: 1.7 m.

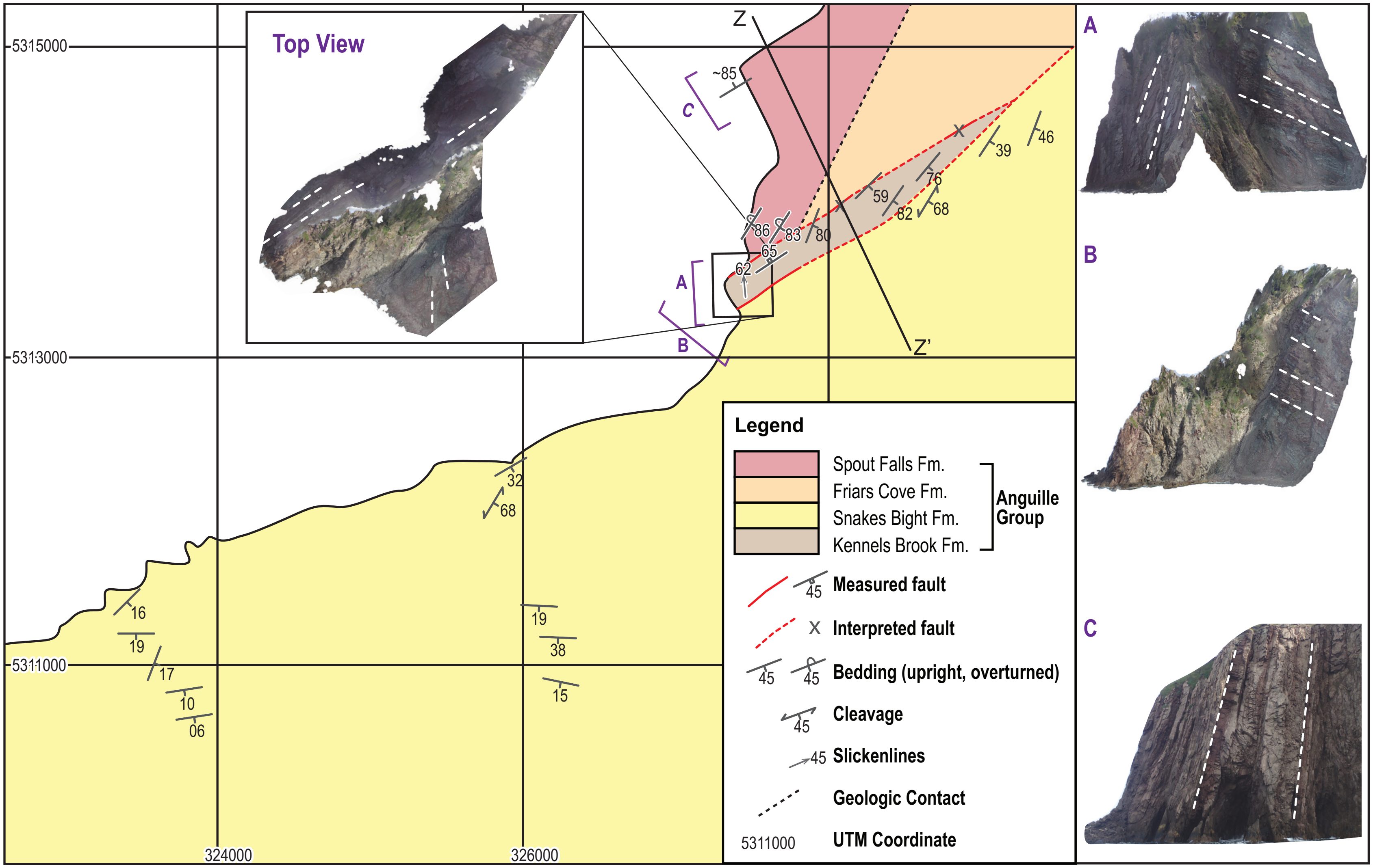

Figure 3.24. Map and photos of Snakes Bight.
Vertical orthomosaic photos have traces of bedding traced on in white dashed lines highlighting the difference in orientations. Z-Z' is the line of cross section for Fig. 3.25.

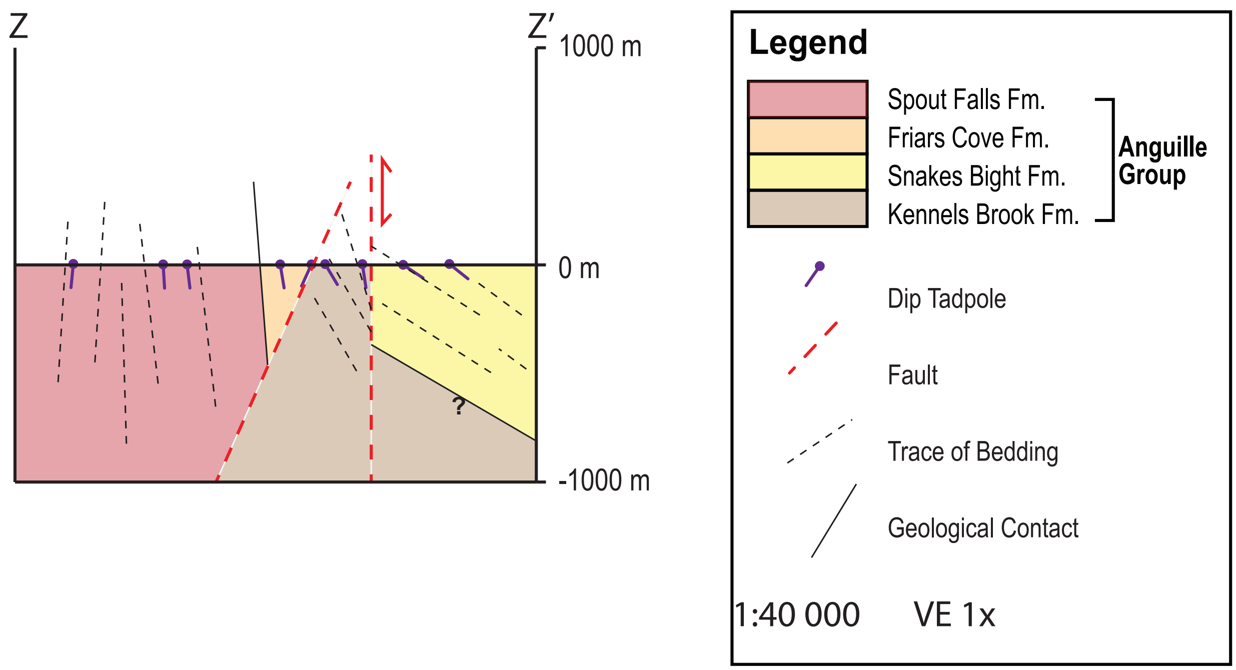

Figure 3.25. Cross section of Snakes Bight (Z-Z' in Fig. 3.24).

tations subparallel to bedding in the adjoining units. Multiple surfaces on the competent rocks display slickenlines and deformation bands.

To the south of the brecciated zone are sandstone, siltstone, and coal measures of the Searston Formation that dip 50°– 60° and young to the southeast. Searston Formation rocks measured inland also young to the south and east forming a synclinal elliptical pattern that can be traced offshore (Fig. 3.3).

Snakes Bight and Kennels Cove

The Snakes Bight Fault (Fig. 3.3) is the largest fault onshore in the Bay St. George subbasin separating Carboniferous stratigraphy. The fault comes onshore at Snakes Bight, striking NE–SW. Knight (1983) mapped the Snakes Bight Fault as striking more E–W at Ship Cove and near the boundary between the southern and northern subbasins (Fig. 3.3). Figure 3.24 shows a detailed map of the Snakes Bight area. A vertical orthomosaic of Snakes Bight, made in the photogrammetry program Agisoft Photoscan, shows bedding orientation differences on either side of a narrow fault-bounded section. To the west is slightly overturned red sandstone of the Spout Falls Formation, the youngest formation in the Anguille Group, that youngs to the west. View C, north of Snakes Bight, shows the Spout Falls Formation, steeply dipping and younging to the west. To the east of the faults are moderately inclined mudstone and siltstone of the Snakes Bight Formation younging to the east. The fault-bounded area in the centre consists of moderately to steeply dipping grey conglomerate and sandstone of the Kennels Brook Formation, the oldest formation in the Anguille Group, that youngs to the east.

At two locations (marked with an x in Figure 3.24), brecciated rocks with no measurable bedding are noted. At the shore, a fault dipping moderately to the northwest shows slickenlines suggesting dip-slip across the fault. In view B in Figure 3.24, a second fault strikes NE and dips nearly vertically. Z-Z' in Figure 3.25 shows a cross section perpendicular to both faults. The hanging wall of the fault contains the Kennels Brook and Snakes Bight Formations.

3.5.3. Interpretation

The Codroy Road Formation in outcrop comprises siltstone, gypsum, and limestone facies together with multicoloured siltstone breccia. However, a large proportion of halite is revealed in this Formation by drilling and other subsurface data. Multicoloured halite mixed with mud is extensive in drill core (Fig. 3.5). We here suggest that the multicoloured siltstone breccia seen in outcrop is in fact the residual material left after halite was dissolved or expelled. This indicates that the thickness of the Codroy Road Formation is significantly larger than previously described from outcrop. The variation in thickness of the Codroy Road Formation between Ship Cove and Capelin Cove (~120 m to ~300 m respectively) is interpreted to result from varying percentages of impurities when the salt was deposited.

The contact between Woody Cape Formation and Searston Formation was interpreted by Knight (1983) as a steeply dipping fault. However, the diametrically opposed younging directions of the formations on either side make reconstruction of fault offsets very difficult. In contrast, the configuration of two oppositely younging, steeply dipping formations separated by breccia, closely resembles the geometry of secondary salt welds observed in seismic profiles of passive continental margins (Jackson & Hudec 2017).

A secondary salt weld represents a usually steeply dipping zone where salt has been expelled. The brecciated zone would represent the material left after salt was expelled vertically. Secondary salt welds are rare in outcrop. However, the structure at Capelin Cove resembles secondary salt welds described by Rowan et al. (2012) in the La Popa Basin in Mexico and by Thomas and Waldron (2017) at Little Judique, Cape Breton Island in rocks of comparable age in the Maritimes Basin. It is therefore interpreted that the contact separating Woody Cape Formation and

Searston Formation is a secondary salt weld, not a fault. Rocks within the brecciated salt weld zone are incompetent and easily eroded. Inland, the expression of the secondary salt weld could route through Grand Codroy River (Fig. 3.3), which follows the strike of the feature and is a low elevation area with poor exposure suggesting the presence of evaporites. Bedding measurements from the Searston Formation inland (Fig. 3.3) form an elliptical pattern south of the secondary salt weld suggesting that the Searston Formation strata are within a salt-expulsion minibasin, similar to the structure east of the Flat Bay anticline in the northern subbasin.

3.6. Discussion

3.6.1. Extensional geometry of the Bay St. George subbasin

The Bay St. George subbasin formed during Devonian subsidence and strike-slip motion along major NE–SW faults, such as the Long Range Fault, that created the Maritimes Basin (Gibling et al. 2008, Hibbard & Waldron 2009, Waldron et al. 2015). Initial deposition into the Bay St. George half-graben started with the Tournaisian Anguille Group. The Anguille Group is dramatically thicker in the southern subbasin compared to the northern subbasin. In the hanging wall of the Snakes Bight Fault, a thick package of Kennels Brook, Snakes Bight, Friars Cove, and Spout Falls Formations are exposed in the Anguille anticline and surrounding area. The southern subbasin is dominated by the oldest Carboniferous stratigraphy in the subbasin. This suggests that the Snakes Bight Fault was a normal, SE-side down growth fault during the Tournaisian. Continuing movement allowed accumulation of much thicker Anguille Group strata on the SE sides.

3.6.2. Soft-sediment deformation

The Snakes Bight, Friars Cove, Spout Falls, and Ship Cove Formations record a history of soft-sediment deformation indicating deformation during deposition of sediment. Soft-sediment folds and clastic dykes represent structures that likely formed soon after deposition. Bulb structures are very commonly cross-cut by other soft-sediment structures suggesting continuing liquidization during deposition of younger sediment. As the complexly folded beds and bulb structures occur in multiple sections within the Snakes Bight Formation and into the Friars Cove Formation, we conclude that the subbasin was tectonically active throughout deposition of these units.

At Cape Anguille, soft-sediment folds shed light on the timing of deformation. For example, the rafts of folded laminae within larger masses of convolutely folded material (Fig. 3.6d) formed when partially-lithified layers broke and became part of a larger folded system. The structures in these rafts would have formed in an initial deformation event; the rafts separated and became incorporated into the larger soft-sediment fold in a later deformation event. The coarser sediment slid down-slope when wet, and the overlying fine-grained sediment isoclinal folds show preferred orientations. The observations at Cape Anguille suggest that the subbasin was tectonically active throughout deposition of the Anguille Group. Soft-sediment folds are frequently observed in the overlying Ship Cove Formation suggesting that the subbasin remained tectonically active into the Viséan.

The bulb structures and ~N–S preferentially-oriented sedimentary boudins do not show evidence of interaction with the sediment-water interface, which suggests that they formed deeper in the sediment pile during a period of overpressure. Overpressure liquidizes a fluid-saturated bed if rapidly buried or horizontally compressed (Maltman 1994, Jolly & Lonergan 2002, Maltman & Bolton 2003, Taki & Pratt 2012). In sedimentary basins, either rapid burial of sediment or tectonic strain can induce overpressured conditions (Osborne & Swarbrick 1997). Therefore, rapid burial of the Snakes Bight Formation, and/or tectonism leading to preferentially oriented structures and overpressured conditions in which bulb structures and sedimentary boudins formed.

Orientations of the some soft-sediment structures are oblique to major fold hinges in the subbasin, consistent with dextral strike-slip movement during subbasin formation and subsequent deformation (Fig. 3.8) as suggested regionally by Knight (1983), Kilfoil (1988), Miller et al. (1990) and Hall et al. (1992).

Soft-sediment structures are not the only features at acute angles to major basin faults. Large-scale tectonic folds in the subbasin, including the Anguille anticline, the Flat Bay anticline, and the Barachois syncline are also *en echelon* to the Long Range Fault. These likely formed after deposition of the Barachois Group as the subbasin continued to undergo dextral strike-slip motion. The orientation of these Anguille Group and Ship Cove Formation structures are consistent with deposition and deformation in an area of rapid basin subsidence in an environment undergoing deformation that involved a large component of strike-slip as interpreted in the Windsor-Kennetcook, Cumberland, and Sackville subbasins (Knight 1983, Waldron et al. 2013b, Snyder & Waldron 2016, Gibling et al. in press 2018).

3.6.3. Timing of evaporite movement

Onshore outcrops record a complex salt-tectonic history. Some salt structures formed synkinematically with brittle and ductile structural features, apparent in the Codroy Road Formation in outcrop. The Codroy Road Formation, overlying the Ship Cove Formation, contains significant halite in the subsurface and siltstone breccia and gypsum in outcrop. In drill core, impure halite is interbedded with anhydrite and rare limestone. Our interpretation of the Codroy Road Formation is that the siltstone breccia represents salt-expulsion residue where the halite has been completely removed and only the clastic impurities remain.

An angular unconformity observed in seismic profiles and in outcrop at Ship Cove between the Spout Falls Formation and the overlying Ship Cove Formation suggest that the environment that had existed during deposition of the Anguille Group continued to be tectonically active.

On the seismic profiles in Figure 3.16, thicknesses between reflections increases down-dip into a syncline where no evaporites remain, representing a primary salt weld. The secondary salt weld at Capelin Cove separates the Codroy Group from the Barachois Group, both affected by salt expulsion. We suggest that Codroy Road Formation salt was moving from the Viséan to the Serpukhovian.

3.6.4. Tectonic inversion

The map pattern of the southern Bay St. George subbasin shows thick Anguille Group strata exposed at the surface at a higher structural level than its position in the northern subbasin, suggesting that that Snakes Bight Fault has a more complicated history than that of a simple Tournaisian normal fault as described above (Fig. 3.3). The Snakes Bight Fault shows reverse separation at present suggesting that Anguille Group was uplifted on the SE side and was rotated to near-vertical.

Palinspastic reconstructions of the Northern Appalachians constructed by Waldron et al. (2015) discuss displacement of Tournaisian to Serpukhovian rocks in northern Nova Scotia and suggest that tectonic wedging in the central Maritimes Basin occurred at ~330 Ma, before significant movement along the Minas Fault Zone (Fig. 3.1). Tectonic inversion in the Bay St. George subbasin likely occurred during this time.

3.6.5. Strike-slip

Folds related to salt-expulsion at Ship Cove and Capelin Cove (Fig. 3.19, 3.20) show fold axes trending dominantly ESE and ENE respectively. These orientations are consistent with Pennsylvanian dextral transpression of the Maritimes Basin, noted by Waldron et al. (2007), Waldron et al. (2015), and Gibling et al. (in press 2018). Steep faults, striking generally ENE at both Ship

Cove and Capelin Cove, crosscut all units indicating that they moved the late in the subbasin history. The orientations of these structures are consistent with dextral transpression on E–W faults.

3.7. Conclusions

Soft-sediment deformation structures are common in the Snakes Bight, Friars Cove, Spout Falls, and Ship Cove Formations of the Anguille and Codroy Groups. These structures, found in the northern and southern subbasin, suggest that the Bay St. George subbasin was tectonically active early in its history. The orientations of these structures are consistent with transtension related to Maritimes Basin extension and subbasin development. During and after deposition of the Codroy Road Formation, deformation was dominantly related to salt movement. Salt structures displaced material of the Codroy Road Formation of the Codroy Group and the Searston Formation of the Barachois Group, suggesting that deformation continued throughout formation of the subbasin. Salt-related structures mapped in outcrop are oriented consistently with dextral transpression on E–W faults.

Knight (1983) concluded that the southern Bay St. George subbasin was significantly more deformed than the northern Bay St. George subbasin. Soft-sediment deformation structures of similar style occur at Boswarlos in the north and Cape Anguille in the south. Salt-related structures at Ship Cove in the north and Capelin Cove in the south are also similar in style. Therefore, we conclude that structures in the northern subbasin are very similar to those in the southern subbasin.

The Bay St. George subbasin was tectonically active during the entirety of its formation. The final stage of deformation included significant faulting, including inversion of the major Snakes Bight Fault, bringing a thick package of Anguille Group strata to the surface in the southern subbasin. These new interpretations lead to a better understanding of deformation of Bay St. George subbasin and the entire Maritimes Basin.

Acknowledgements

Field research was supported by a grant from the Government of Newfoundland and Labrador Petroleum Exploration Enhancement Program. We thank the Newfoundland and Labrador Department of Natural Resources for access to the onshore SEG-Y data. Parts of this work were supported by the University of Alberta in the form of a Teaching Assistantship. We thank L. Kennedy for her thoughtful comments. Lauren Eggleston and Martin Schwangler assisted in the field.

3.8. References

Alfaro, P., Delgado, J., Estevez, A., Molina, J. M., Moretti, M. & Soria, J. M. 2002. Liquefaction and fluidization structures in Messinian storm deposites (Bajo Segura Basin, Betic Cordillera, southern Spain). *International Journal of Earth Sciences* **91**, 505-513.

Alfaro, P., Moretti, M. & Owen, G. 2016. Special Issue: the environmental significance of soft-sediment deformation. *Sedimentary Geology* **344**, iii-iv.

Allen, J. P., Fielding, C. R., Rygel, M. C. & Gibling, M. R. 2013. Deconvolving signals of tectonic and climatic controls from continental basins: an example from the late Paleozoic Cumberland Basin, Atlantic Canada. *Journal of Sedimentary Research* **83**(10), 847-872.

Baird, D. M. & Coté, P. R. 1964. *Lower Carboniferous sedimentary rocks in southwestern Newfoundland and their relations to similar strata in western Cape Breton Island.* Canadian Institute of Mining and Metallurgy.

Bell, W. A. 1948. Early Carboniferous Strata of St. Georges Bay Area, Newfoundland. In: *Geological Survey Bulletin No. 10*. Mines and Geology Branch, Department of Mines and Resources, 51.

Berra, F. & Felletti, F. 2011. Syndepositional tectonics recorded by soft-sediment deformation and liquefaction structures (continental Lower Permian sediments, Southern Alps, Northern Italy): Stratigraphic significance. *Sedimentary Geology* **235**(3–4), 249-263.

Boehner, R. C. & Giles, P. S. 1993. Geology of the Antigonish Basin, Antigonish County, Nova Scotia. In: *Nova Scotia Department of Natural Resources, Mines and Energy Branch, Memoir* **8**.

Calder, J. H. 1998. The Carboniferous evolution of Nova Scotia. In: *Geological Society, London, Special Publications* **143**, 261-302.

Collinson, J. 2005. Post-depositional sedimentary structures. In: *Encyclopedia of Geology* (edited by Selley, R. C., Cocks, L. R. M. & Plimer, I. R.). Elsevier, Oxford, 602-611.

Cote, P. R. 1964. Lower Carboniferous sedimentary rocks of the Horton Group in parts of Cape Breton Island, and their relation to similar strata of the Anguille Group in southwestern Newfoundland, University of Ottawa.

Dafoe, L. T., Shaw, J., Jauer, C., Giles, P. S., Waldron, J. W. F. & Potter, D. P. 2016. New insights into the Bedrock and Quaternary Geology of St. George's Bay from a vertical integration of marine datasets, offshore western Newfoundland. *Bulletin of Canadian Petroleum Geology* **64**(1), 1.

Dimmel, P. 2001. *Potential for Mining Salt in Western Newfoundland.* Department of Mines and Energy; Government of Newfoundland and Labrador.

Durling, P. & Marillier, F. 1993. Structural elements of the Magdalen Basin, Gulf of St. Lawrence, from seismic reflection data. Geological Survey of Canada Paper 93-1D, Canada, 147-154.

Ezquerro, L., Moretti, M., Liesa, C. L., Luzon, A. & Simon, J. L. 2015. Seismites from a well core of palustrine deposits as a tool for reconstructing the palaeoseismic history of a fault. *Tectonophysics* **655**, 191-205.

Garcia, S. F. d. M., Letouzey, J., Rudkiewicz, J.-L., Danderfer Filho, A. & Frizon de Lamotte, D. 2012. Structural modeling based on sequential restoration of gravitational salt deformation in the Santos Basin (Brazil). *Marine and Petroleum Geology* **35**(1), 337-353.

Ge, H., Jackson, M. P. A. & Vendeville, B. C. 1997. Kinematics and dynamics of salt tectonics driven by progradation. *AAPG Bulletin* **81**(3), 398-423.

Gibling, M. R., Culshaw, N., Pascucci, V., Waldron, J. W. F. & Rygel, M. C. in press 2018. The Maritimes Basin of Atlantic Canada: Basin Creation and Destruction during the Paleozoic Assembly of Pangea. In: *Sedimentary Basins of the World* (edited by Miall, A.) **5**.

Gibling, M. R., Culshaw, N., Rygel, M. C. & Pascucci, V. 2008. Chapter 6 The Maritimes Basin of Atlantic Canada: Basin Creation and Destruction in the Collisional Zone of Pangea. In: *Sedimentary Basins of the World 5* (edited by Miall, A. D.). Elsevier, 211-244.

Giles, P. S. 1981. *Major Transgressive-Regressive Cycles in Middle to Late Visean Rocks of Nova Scotia. Mineral Resources Division Report of Activities 1981*, Nova Scotia Department of Mines and Energy.

Hall, J., Langdon, G., Roberts, B., Hawkins, D., Fagan, A., Knight, I. & Kilfoil, G. 1992. Reflection seismic imaging of the Carboniferous Bay St. George subbasin, onshore western Newfoundland: a reappraisal of Paleozoic stratigraphic thickness. *Bulletin of Canadian Petroleum Geology* **40**(4), 321-334.

Hamblin, A. P. & Rust, B. R. 1989. Tectono-sedimentary analysis of alternate-polarite half-graben basin-fill successions: Late Devonian-Early Carboniferous Horton Group, Cape Breton Island, Nova Scotia. *Basin Research* **2**, 239-255.

Hempton, M. R. & Dewey, J. F. 1983. Earthquake-induced deformational structures in young lacustrine sediments, East Anatolian Fault, southeast Turkey. *Tectonophysics* **98**(3–4), T7-T14.

Hibbard, J. & Waldron, J. W. F. 2009. Truncation and translation of Appalachian promontories: mid-Paleozoic strike-slip tectonics and basin initiation. *Geology* **37**, 487-490.

Hudec, M. R. & Jackson, M. P. A. 2004. Regional restoration across the Kwanza Basin, Angola: Salt tectonics triggered by repeated uplift of a metastable passive margin. *AAPG Bulletin* **88**(7), 971-990.

Hudec, M. R. & Jackson, M. P. A. 2007. Terra infirma: Understanding salt tectonics. *Earth-Science Reviews* **82**(1–2), 1-28.

Hudec, M. R., Jackson, M. P. A. & Schultz-Ela, D. D. 2009. The paradox of minibasin subsidence into salt: Clues to the evolution of crustal basins. *Geological Society of America Bulletin* **121**(1-2), 201-221.

Hyde, R. S., Kalkreuth, W. D. & Utting, J. 1991. Petrology, palynology, and depositional environments of coals of the Upper Carboniferous Barachois Group (Westphalian A and C), southwestern Newfoundland. *Canadian Journal of Earth Sciences* **28**(12), 1905-1924.

Hyde, R. S., Miller, H. G., Hiscott, R. N. & Wright, J. A. 1988. Basin architecture and thermal maturation in the strike-slip Deer Lake Basin, Carboniferous of Newfoundland. *Basin Research* **1**(2), 85-105.

Jackson, M. P. & Hudec, M. R. 2017. *Salt tectonics: Principles and practice.* Cambridge University Press.

Jackson, M. P. A. & Talbot, C. J. 1991. *A Glossary of Salt Tectonics. No. 91-4*. Bureau of Economic Geology Geological Circular The University of Texas at Austin.

Jackson, M. P. A. & Vendeville, B. C. 1994. Regional extension as a geologic trigger for diapirism; with Suppl. Data 9401. *Geological Society of America Bulletin* **106**(1), 57-73.

Jolly, R. J. H. & Lonergan, L. 2002. Mechanisms and controls on the formation of sand intrusions. *Journal of the Geological Society, London* **159**, 605-617.

Kang, H.-C., Paik, I. N., Lee, H. I., Lee, J. E. & Chun, J.-C. 2010. Soft-sediment deformation structures in Cretaceous non-marine deposits of southeastern Gyeongsang Basin, Korea: occurrences and origin. *Island Arc* **19**, 628-646.

Kilfoil, G. J. 1988. An integrated gravity, magnetic, and seismic interpretation of the Carboniferous Bay St. George subbasin, western Newfoundland, Memorial University of Newfoundland.

Knight, I. 1983. Geology of the Carboniferous Bay St. George subbasin, Western Newfoundland. *Mineral Development Division Department of Mines and Energy, Government of Newfoundland and Labrador* **Memoir 1**.

Maltman, A. J. 1994. Introduction and overview. In: *The Geological Deformation of Sediments* (edited by Maltman, A. J.). Chapman and Hall, London, 1-35.

Maltman, A. J. & Bolton, A. 2003. How sediments become mobilized. In: *Subsurface Sediment Mobilizations* (edited by Van Rensbergen, P., Hillis, R. R., Maltman, A. J. & Morley, C. K.). Geological Society, London. Special Publication 216, 9-20.

Martel, A. T. & Gibling, M. R. 1996. Stratigraphy and tectonic history of the Upper Devonian to Lower Carboniferous Horton Bluff Formation, Nova Scotia. *Atlantic Geology* **32**, 13-38.

Martel, A. T., McGregor, D. C. & Utting, J. 1993. Stratigraphic significance of Upper Devonian and Lower Carboniferous miospores from the type area of the Horton Group, Nova Scotia. *Canadian Journal of Earth Sciences* **30**(5), 1091-1098.

McGregor, D. C. & McCutcheon, S. R. 1988. Implications of spore evidence for Late Devonian age of the Piskahegan Group, southwestern New Brunswick. *Canadian Journal of Earth Sciences* **25**(9), 1349-1364.

Miller, H. G., Kilfoil, G. & Peavy, S. T. 1990. An integrated geophysical interpretation of the Carboniferous Bay St. George Subbasin, Western Newfoundland. *Bulletin of Canadian Petroleum Geology* **38**(3), 320-331.

Moretti, M., Alfaro, P., Caselles, O. & Canas, J. A. 1999. Modelling seismites with a digital shaking table. *Tectonophysics* **304**(4), 369-383.

Murphy, J. B., Waldron, J. W. F., Kontak, D. J., Pe-Piper, G. & Piper, D. J. W. 2011. Minas Fault Zone: Late Paleozoic history of an intra-continental orogenic transform fault in the Canadian Appalachians. *Journal of Structural Geology* **33**, 312-328.

Murray, R. C. 1964. Origin and diagenesis of gypsum and anhydrite. *Journal of Sedimentary Petrology* **34**(3), 512-523.

Nikolaeva, S. B. 2009. Seismites in Late Pleistocene and Holocene deposits of the northwestern Kola region (northern Baltic Shield). *Russian Geology and Geophysics* **50**, 644-650.

Osborne, M. J. & Swarbrick, R. E. 1997. Mechanisms for generating overpressure in sedimentary basins: a reevaluation. *AAPG Bulletin* **81**(6), 1023-1041.

Owen, G. 2003. Load structures: gravity-driven sediment mobilization in the shallow subsurface. *Geological Society, London, Special Publications* **216**(1), 21-34.

Parnell, J. & Kelly, J. 2003. Remobilization of sand from consolidated sandstones: evidence from mixed bitumen-sand intrusions. In: *Subsurface Sediment Mobilization* (edited by Van Rensbergen, P., Hillis, R. R., Maltman, A. J. & Morley, C. K.) **216**. Geological Society, London. Special Publication 216, 503-513.

Plint, A. G. 1985. Possible earthquake-induced soft-sediment faulting and remobilization in Pennsylvanian alluvial strata, southern New Brunswick, Canada. *Canadian Journal of Earth Sciences* **22**, 907-912.

Ramsay, J. G. & Huber, M. I. 1987. *The techniques of modern structural geology Volume 2: folds and fractures*. Academic Press Orlando.

Rhoden, H. N. 1998. *Preliminary evaluation of Fischells Brook rock-salt deposit in western Newfoundland, a mining project to supply the Atlantic-coast road de-icing market.*, St. John's Newfoundland.

Rodríguez-Pascua, M. A., Calvo, J. P., De Vicente, G. & Gómez-Gras, D. 2000. Soft-sediment deformation structures interpreted as seismites in lacustrine sediments of the Prebetic Zone, SE Spain, and their potential use as indicators of earthquake magnitudes during the Late Miocene. *Sedimentary Geology* **135**(1–4), 117-135.

Rossetti, D. D. F. 1999. Soft-sediment deformation structures in late Albian to Cenomanian deposits, São Luís Basin, northern Brazil: evidence for palaeoseismicity. *Sedimentology* **46**(6), 1065-1081.

Rowan, M. G., Lawton, T. F. & Giles, K. A. 2012. Anatomy of an exposed vertical salt weld and flanking strata, La Popa Basin, Mexico. *Geological Society, London, Special Publications* **363**(1), 33-57.

Scott, B. & Price, S. 1988. Earthquake-induced structures in young sediments. *Tectonophysics* **147**, 165-170.

Sibson, R. H. 2003. Brittle-failure controls on maximum sustainable overpressure in different tectonic regimes. *AAPG Bulletin* **87**(6), 901-908.

Snyder, M. E. & Waldron, J. W. F. 2016. Unusual soft-sediment deformation structures in the Maritimes Basin, Canada; possible seismic origin. *Sedimentary Geology* **344**, 145-159.

Solomon, S. M. 1987. Sedimentology and fossil-fuel potential of the Upper Carboniferous Barachois Group, western Newfoundland.

St. Peter, C. 1993. Maritimes Basin evolution: key geologic and seismic evidence from the Moncton subbasin of New Brunswick. *Atlantic Geology* **29**, 233-270.

St. Peter, C. J. & Johnson, S. C. 2009. *Palynological Data for Late Devonian–Carboniferous Strata of the Maritimes Basin of Southeastern New Brunswick (NTS 21 H/9, 10, 14, 15, 16 and 21 I/01, 02). Minerals, Policy and Planning Division, Open File*

Taki, H. E. & Pratt, B. R. 2012. Syndepositional tectonic activity in an epicontinental basin revealed by deformation of subaqueous carbonate laminites and evaporites: seismites in Red River strata (Upper Ordovician) of southern Saskatchewan, Canada. *Bulletin of Canadian Petroleum Geology* **60**(1), 37-58.

Thomas, A. K. & Waldron, J. W. F. 2017. Faults in the late Paleozoic Antigonish sub-basin, Nova Scotia, reinterpreted as potential salt welds. In: *Program with Abstracts - Geological Association of Canada; Mineralogical Association of Canada: Joint Annual Meeting* **40**, Kingston, Ontario, 376.

Utting, J. & Giles, P. S. 2004. Biostratigraphical implications of new palynological data from the MIssissippian of Newfoundland and Nova Scotia, Canada. In: *Memoirs of the Association of Australasian Palaeontologists* **29**, 115-160.

Utting, J. & Giles, P. S. 2008. Palynostratigraphy and lithostratigraphy of Carboniferous Upper Codroy Group and Barachois Group, southwestern Newfoundland. *Canadian Journal of Earth Sciences* **45**(1), 45-67.

Utting, J., Keppie, J. D. & Giles, P. S. 1989. Palynology and stratigraphy of the Lower Carboniferous Horton Group, Nova Scotia. In: *Contributions to Canadian Paleontology* **396**. Geological Survey of Canada Bulletin, 117-143.

van Loon, A. J. & Mazumder, R. 2011. Can once lithified rocks later undergo soft-sediment deformation. *Sedimentary Geology* **238**, 101-105.

Waldron, J. W. F. 2004. Anatomy and evolution of a pull-apart basin, Stellarton, Nova Scotia. *Geological Society of America Bulletin* **116**, 109-207.

Waldron, J. W. F., Barr, S. M., Park, A. F., White, C. E. & Hibbard, J. 2015. Late Paleozoic strike-slip faults in Maritime Canada and their role in the reconfiguration of the northern Appalachian orogen. *Tectonics* **34**(8), 1661-1684.

Waldron, J. W. F. & Gagnon, J.-F. 2011. Recognizing soft-sediment structures in deformed rocks of orogens. *Journal of Structural Geology* **33**, 271-279.

Waldron, J. W. F., Giles, P. S. & Thomas, A. K. 2017. *Correlation chart for Late Devonian to Permian stratified rocks of the Maritimes Basin, Atlantic Canada.*

Waldron, J. W. F., Roselli, C. & Johnston, S. K. 2007. Transpressional structures on a Late Paleozoic intracontinental transform fault, Canadian Appalachians. In: *Tectonics of Strike-Slip Restraining and Releasing Bends* (edited by Cunningham, W. D., and Mann, P.). Geological Society, London, Special Publications 290, 367-385.

Waldron, J. W. F., Rygel, M. C., Gibling, M. R. & Calder, J. H. 2013a. Evaporite tectonics and the late Paleozoic stratigraphic development of the Cumberland basin, Appalachians of Atlantic Canada. *Geological Society of America Bulletin*.

Waldron, J. W. F., Rygel, M. C., Gibling, M. R. & Calder, J. H. 2013b. Evaporite tectonics and the late Paleozoic stratigraphic development of the Cumberland Basin, Appalachians of Atlantic Canada. *Geological Society of America Bulletin* **125**(5-6), 945-960.

Williams, H. 1979. Appalachian Orogen in Canada. *Canadian Journal of Earth Sciences* **16**, 792-807.

Wilson, P., White, J. C. & Roulston, B. V. 2006. Structural geology of the Penobsquis salt structure: late Bashkirian inversion tectonics in the Moncton Basin, New Brunswick, eastern Canada. *Canadian Journal of Earth Sciences* **43**, 405-419.

Chapter 4. Salt tectonics in a strike-slip basin: Bay St. George subbasin, Newfoundland, Canada

The late Paleozoic Maritimes Basin of Atlantic Canada formed during strike-slip and extensional motion along NE–SW striking faults, and comprises multiple subbasins filled between the late Devonian and early Permian. The complex stratigraphy includes the evaporite-rich Middle Mississippian Codroy Group. In southern Newfoundland, the Bay St. George subbasin of the Maritimes Basin exhibits numerous salt-related structures evident in bathymetric data, aeromagnetic maps, and seismic profiles. Three groups of peaks are picked on seismic profiles, tied to the bathymetric and aeromagnetic maps, and correlated with the Mississippian stratigraphy. The base group of reflections is the interpreted basal anhydrite, a unit near the base of the evaporite-bearing Codroy Road Formation. A reflector near the top of an evaporite package and a middle anhydrite reflector, within the middle Codroy Road Formation, are also traced across the geophysical datasets. Salt structures imaged include salt-cored anticlines, salt-expulsion minibasins and salt welds. Novel techniques including trough-surface tracking and successive horizon flattening suggest that the dominant salt-movement direction varied between the centre of the subbasin and the ends. Faults, including a flower structure and a tectonic wedge in the central subbasin, separate these salt structures. The brittle structures suggest tectonic inversion in the subbasin after deposition of the Upper Mississippian Barachois Group.

4.1. Introduction

The Maritimes Basin (Fig. 4.1) in Atlantic Canada comprises a complex network of variably connected or isolated subbasins filled between the late Devonian and early Permian (Calder 1998, Gibling et al. 2008, Waldron et al. 2013, Waldron et al. 2015, Gibling et al. in press 2018). The Maritimes Basin likely formed during significant strike-slip motion in the Appalachians, reactivating a regional releasing bend on the NE–SW trending Laurentian continental margin (Thomas 1977, 1991, Hibbard & Waldron 2009, Waldron et al. 2013, Waldron et al. 2015).

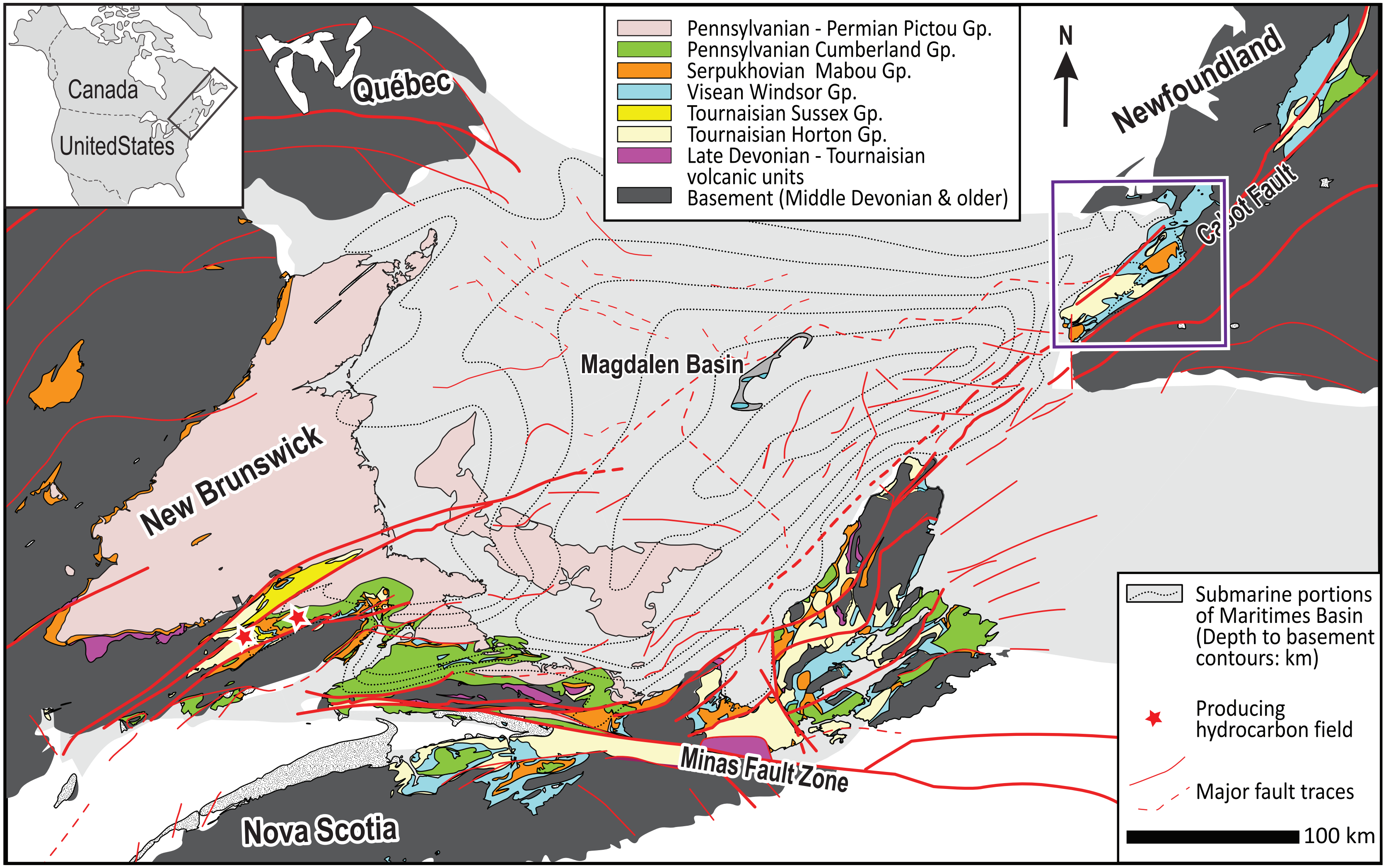

Figure 4.1. Map of the Maritimes Basin location and coverage.
Inset shows Fig. 4.4, the location of the Bay St. George subbasin. Modified from Waldron et al. (2015).

The history of the Maritimes Basin includes repeated cycles of subsidence and exhumation. These cycles influenced thermal maturation, diagenesis, and migration of hydrocarbons and mineralizing fluids in all subbasins. The Maritimes Basin contains significant known and potential resources of evaporites, coal, oil, and natural gas (Bell 1958, Utting & Hamblin 1991, Bibby & Schimeld 2000, Wilson & White 2006, Hu & Dietrich 2010, Dietrich et al. 2011, Gibling et al. in press 2018), the distributions of which are strongly influenced by both strike-slip and salt tectonics. Exploitation of resources in the Maritimes Basin dates back over 100 years; most offshore seismic data acquisition and exploration drilling occurred dominantly in the 1970s and 1980s (Hu & Dietrich 2010). The recent bathymetry, gravity, and aeromagnetic surveys have added to the exploration effort (Hayward et al. 2014, Dafoe et al. 2016).

Salt has played a prominent role in the tectonics of the Maritimes Basin, but most structural analyses (Bell 1948, Belt 1969, Knight 1983, Peavy 1985, Kilfoil 1988, Miller et al. 1990, Hall et al. 1992, Langdon & Hall 1994), predated advances that have revolutionized salt tectonics in the last 20 years (summarized by Hudec & Jackson (2007). Halokinesis of evaporites in the Maritimes Basin created many salt structures (Bell & Howie 1990, Durling & Marillier 1993b, Langdon & Hall 1994, Rhoden 1998, Dimmel 2001, Boehner et al. 2003, Waldron 2004, Wilson & White 2006, Wilson et al. 2006, Giles 2008, Waldron et al. 2013, Craggs et al. 2015, Dafoe et al. 2016); salt diapirs in Nova Scotia, Cape Breton Island, southeast New Brunswick, and western Newfoundland have been mined for rock salt, gypsum, and potash (Bell 1948, Goodman 1952, Bell 1958, Boehner 1986, Adams 1991, Boehner & Giles 1993, Calder 1998, Rhoden 1998, Boehner et al. 1999, Kontak et al. 2000). The timing of salt movement across the Maritimes Basin was variable, but generally coincided with maximum deposition rate, suggesting that salt expulsion formed significant accommodation space (Waldron & Rygel 2005, Waldron et al. 2013, Gibling et al. in press 2018).

In this paper we apply a modern salt-tectonics analysis to provide new insight into the history of the subbasin by integrating and re-interpreting data from 36 two-dimensional seismic lines, high-resolution bathymetric data, aeromagnetic surveys, and the outcrop studies described in Chapter 3.

4.2. Regional geology

4.2.1. Composite Maritimes Basin

Stratigraphy

Many stratigraphic units can be correlated between most of the subbasins that comprise the Maritimes Basin (Fig. 4.2); distinctive marker units occur offshore and onshore. Basin fill is interpreted as dominantly terrestrial, but includes the Viséan (Middle Mississippian) Codroy and laterally equivalent Windsor Groups, that include evaporite-rich units representing the only fully marine incursion into the basin. Evaporite units include halite, gypsum, and anhydrite in major evaporite cycles in the lower and middle Codroy Group (Giles 1981, Giles & Boehner 2001, Giles 2008, Giles 2009).

Structure

Maritimes Basin tectonics are complex; most authors are in agreement that regional fault motion and early subsidence occurred in a dextral zone of transtension or oblique rifting in the late Devonian (Bradley 1982, Hibbard & Waldron 2009, Waldron et al. 2015, Pinet et al. 2018, Gibling et al. in press 2018). NE–SW faults, near-parallel to the Appalachian Orogen, are the dominant brittle structures (Waldron et al. 2015). Steep E–W striking dextral faults and NW–SE striking sinistral faults are common in parts of the present-day Gulf of St. Lawrence and across Nova Scotia (McCutcheon & Robinson 1987, Hibbard & Waldron 2009, Waldron et al. 2015). Ductile structures in the Maritimes Basin include large- and small-scale folds and salt structures recorded in nearly every subbasin (Knight 1983, Durling & Marillier 1993b, a, Durling et al. 1995, Roselli

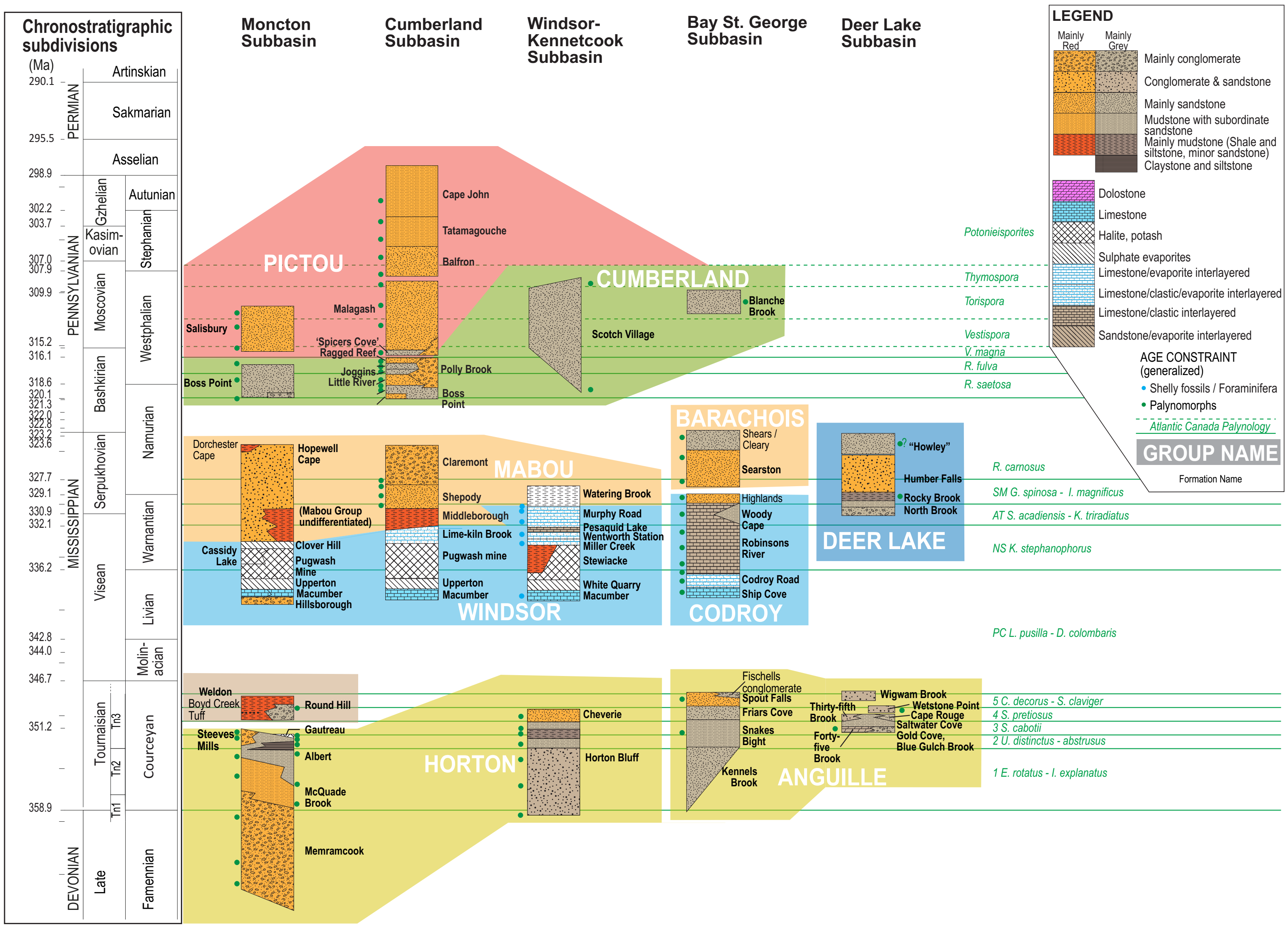

Figure 4.2. Stratigraphic chart across subbasins within the Maritimes Basin, modified from Waldron et al. (2017). Atlantic Canada Palynology from McGregor & McCutcheon (1988), Utting & Giles (2004), and Allen et al. (2013).

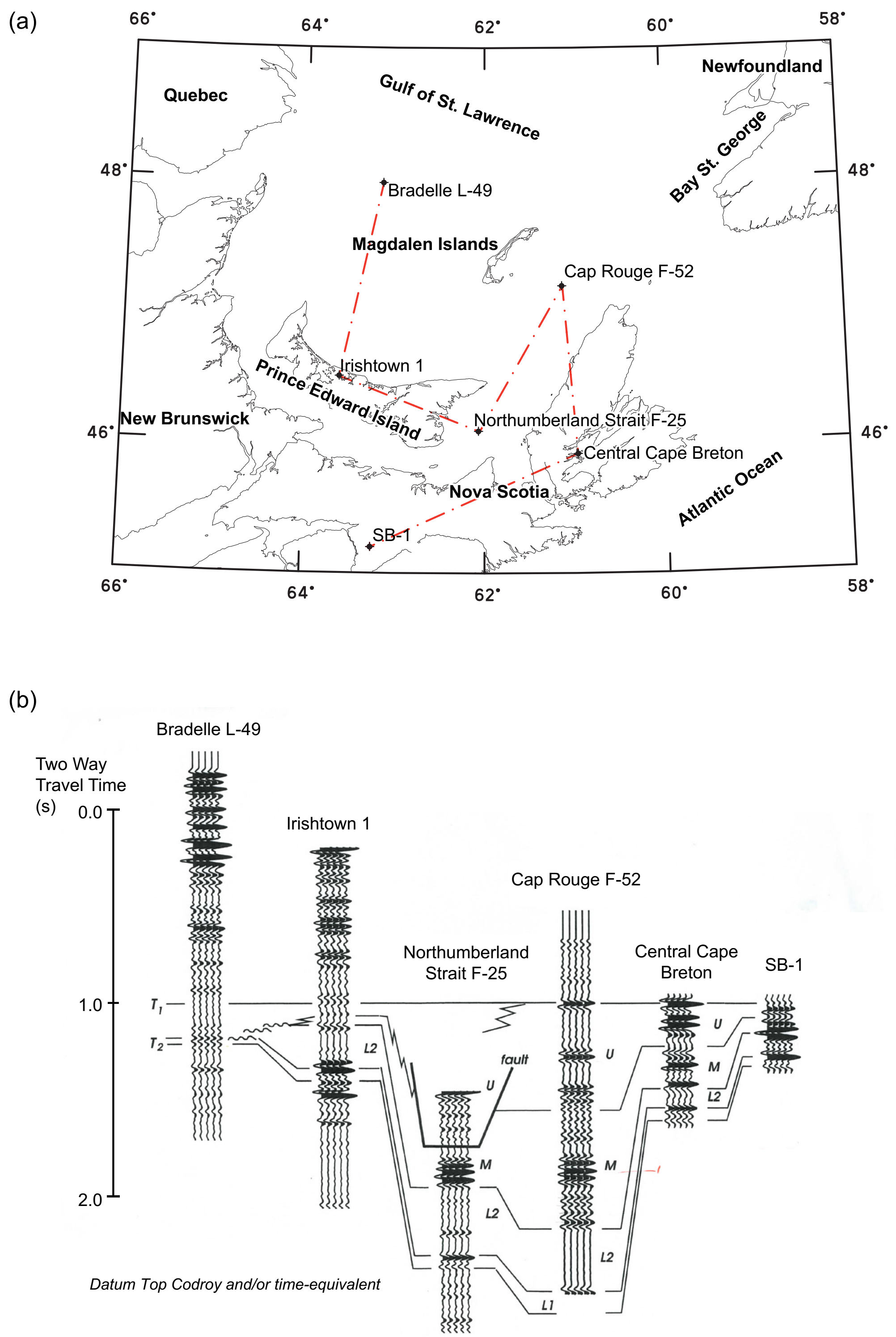

Figure 4.3. Offshore wells in the Maritimes Basin.
(a) map of central Maritimes Basin showing location of wells offshore after Giles & Utting (2001); (b) synthetic seismograms of the wells in (a) correlated across offshore Maritimes Basin which were used to aid in linking reflectors to geology in the Bay St. George subbasin (P. Durling personal communication 2018).

2003, Waldron 2004, Martel & Durling 2005, Waldron et al. 2005, Waldron et al. 2010, Craggs et al. 2013, Waldron et al. 2013, Hayward et al. 2014, Dafoe et al. 2016, Snyder & Waldron 2016, Eggleston 2017, Gibling et al. in press 2018).

The early structural phase of the basin in the late Devonian to early Mississippian is related to partially connected fault-bounded depocenters filled with continental clastic deposits of the Anguille Group and equivalents (Dietrich et al. 2011, Pinet et al. 2018). This interpretation is based dominantly on onshore field observations of faults in New Brunswick and Nova Scotia (Hibbard & Waldron 2009, Waldron et al. 2015), and offshore observations of normal faults in seismic profiles (Durling & Marillier 1993b). This phase of transtension was likely responsible for the initial rapid subsidence of the Maritimes Basin following the Acadian Orogeny (Murphy & Keppie 2005, Hibbard & Waldron 2009, Hayward et al. 2014).

From the Middle Mississippian to the early Permian, deformation is related to deposition and subsequent mobilization of the Viséan Codroy Group and equivalents (Gibling et al. 2008, Waldron et al. 2013, Pinet et al. 2018). Deformation post-dating the Anguille Group is recorded mainly by shortening structures, basin inversion, and salt structures (Wilson et al. 2006, Waldron et al. 2013). During this stage, many subbasins within the Maritimes Basin show features indicative of salt movement, including salt diapirs and salt-expulsion minibasins. Several kilometres of evaporites were deposited during this stage (Waldron & Rygel 2005, Waldron et al. 2013, Craggs et al. 2015).

Following deposition of the Codroy Group, there was thermal subsidence and regional strike-slip along major NE–SW and E–W faults (Durling & Marillier 1990, Waldron et al. 2007, Murphy et al. 2011). Viséan to Permian Barachois and younger rocks were deposited while Codroy Group evaporites remained mobile (Waldron et al. 2015).

Deformation from the late Carboniferous to Permian consisted of basin inversion related to dextral transpression on NE–SW strike-slip faults and the E–W Minas Fault (Fig. 4.1) are well documented in outcrop and seismic data in Quebec and Nova Scotia (Jutras et al. 2003, Murphy & Keppie 2005, Murphy et al. 2011, Pinet et al. 2018).

4.2.2. Central Maritimes Basin

Stratigraphy

The majority of the central Maritimes Basin lies offshore, where previous work dominantly consists of interpretations of well, seismic, and ship-track magnetic data (Durling & Marillier 1993b). The region southwest of the Bay St. George subbasin (Fig. 4.1) and underlying most of the Gulf of St. Lawrence, is the largest (~25 000 km^2) and deepest (up to 12 km) part of the overall Maritimes Basin (Bradley 1982, Durling & Marillier 1993b). Bradley (1982), Durling and Marillier (1993), and most subsequent authors use the term Magdalen Basin to represent the central, deepest part of the Maritimes Basin. However, Giles and Lynch (1993) and Giles (2008) use "Magdalen Basin" to refer to a much larger area, including on-land exposures in New Brunswick, Nova Scotia, and Newfoundland. We therefore refer to the offshore depocentre simply as the central Maritimes Basin. The central Maritimes Basin connects laterally and transitionally into multiple subbasins, including the Bay St. George subbasin, with no bounding faults.

The Magdalen Islands (Fig. 4.3), a group of islands in the central Gulf of St. Lawrence, represents the onshore component of the central Maritimes Basin (Giles 2008). Onshore outcrops on the Magdalen Islands include conglomerate, sandstone, siltstone, shale, limestone, evaporites, and volcanics interpreted as Anguille, Codroy, and possibly Barachois Group equivalents (Barr et al. 1985, Bell & Howie 1990, Giles 2008). Offshore, the stratigraphy is known from exploratory wells including: Cap Rouge, Wellington #1, Irishtown #1, and Shubenacadie SB-1 wells (Fig. 4.3) (Rehill et al. 1995, Giles & Utting 1999, 2001, Wilson & White 2006, Hayward et al. 2014).

Structure

Structures in the central Maritimes Basin, near the Magdalen Islands, have been interpreted from seismic, gravity, and magnetic data by Durling and Marillier (1993b), Hayward et al. (2001) and Hayward et al. (2014). The Magdalen Basin contains multiple grabens and half-grabens; bounding faults include offshore extensions of onshore faults mapped in New Brunswick and Quebec (Durling & Marillier 1993b). Grabens were initially filled with Horton Group (Anguille Group) deposited during a phase of regional extension (Durling & Marillier 1993b, Hayward et al. 2014). Above the Horton Group strata are Windsor Group (Codroy Group) strata including significant evaporites (Bradley 1982, Hayward et al. 2014). Halokinesis is responsible for many structures in the central Maritimes Basin including salt diapirs up to 8 km high (Durling & Marillier 1990, Durling & Marillier 1993b, Hayward et al. 2001, Hayward et al. 2014, Gibling et al. in press 2018); many salt structures in the Magdalen Basin are similar to those in the Cumberland subbasin in Nova Scotia (Waldron et al. 2013, Craggs et al. 2015).

4.2.3. Onshore Bay St. George subbasin

Stratigraphy

The Bay St. George subbasin (Fig. 4.4) represents the portion of the central Maritimes Basin that extends into western Newfoundland. Strata in the Bay St. George subbasin unconformably overlie rocks of the Humber Zone, the westernmost terrane of the Canadian Appalachians (Williams 1979, Stockmal et al. 1998, Waldron et al. 1998). This unconformity can be observed onshore at Port au Port Peninsula (Fig. 4.4).

The fill of the Bay St. George subbasin can be divided into three main groups exposed onshore in outcrop: the Anguille Group, Codroy Group, and Barachois Group. The early Tournaisian to early Viséan Anguille Group contains mudstone, siltstone, sandstone, and conglomerate interpreted as being from fluvial and lacustrine environments.

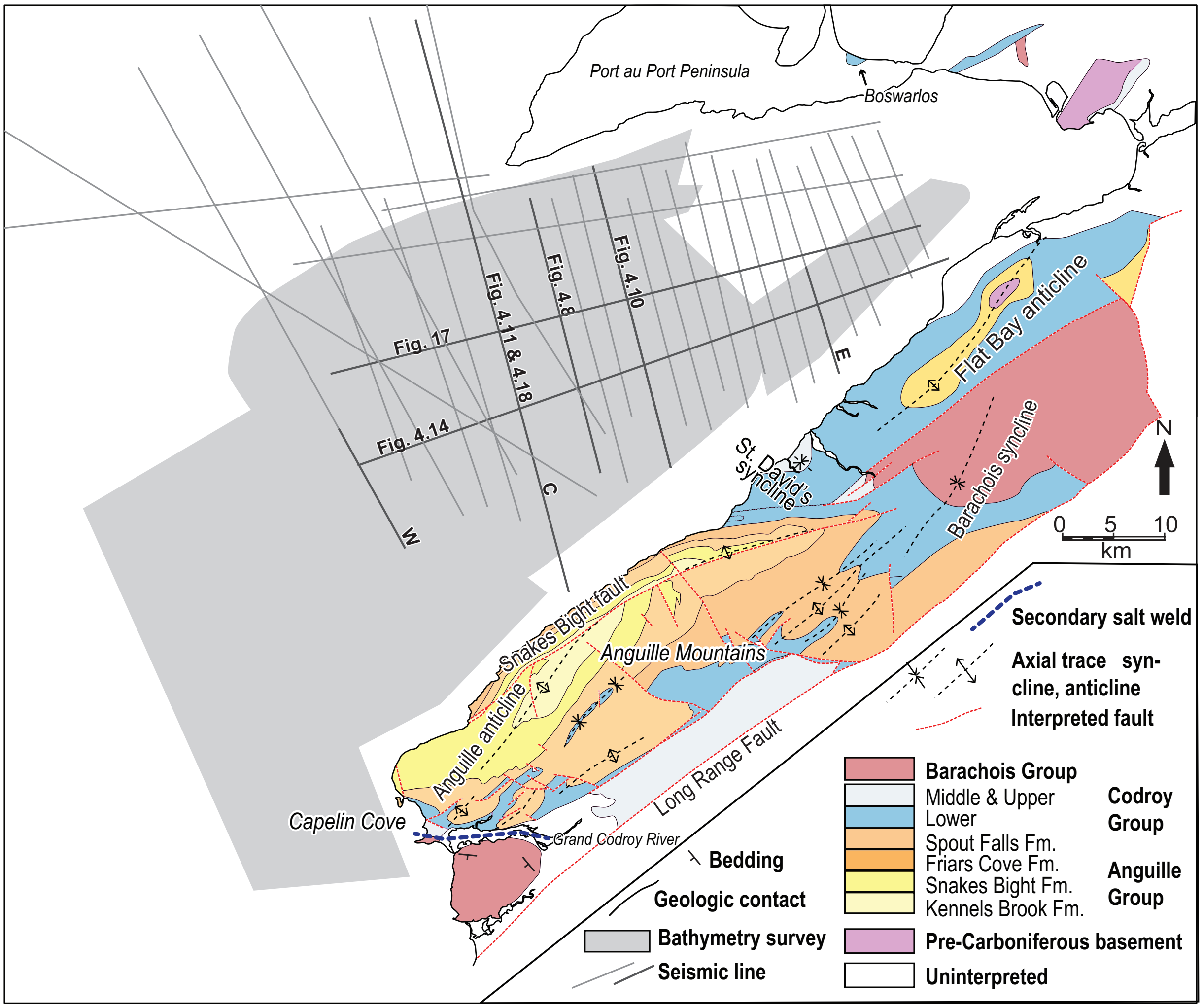

Figure 4.4. Geologic map of the onshore Bay St. George subbasin of Knight (1983). Units include the Anguille Group, Codroy Group, and Barachois Group. Bathymetric data extent, seismic lines, and key outcrop locations are shown. Aeromagnetic map extent covers the entire map area.

The unconformably overlying middle Viséan to Serpukhovian Codroy Group comprises interbedded limestone, siltstone breccia, gypsum, anhydrite, and salt. The Codroy Group is interpreted as recording cyclic marine conditions (Knight 1983). The basal unit of the Codroy Group is the relatively uniform ~15–20 m thick limestone of the Ship Cove Formation, correlated with the Macumber Formation of Nova Scotia and New Brunswick (Fig. 4.2). Evaporites of the Codroy Road Formation overlying the Ship Cove Formation were a major influence on the sedimentological and structural development of subbasins within the Maritimes Basin (Hamblin & Rust 1989, Boehner 1992, Craggs et al. 2013, Waldron et al. 2013). In Chapter 3 of this thesis, it is suggested that onshore outcrops of siltstone breccia, gypsum, and minor limestone of the Codroy Road Formation are the remnants of a much larger package of evaporite-dominated stratigraphy.

Unconformably overlying the Codroy Group is the Serpukhovian Barachois Group. The Barachois Group comprises a thick succession of sandstone, pebbly sandstone, coal-bearing grey siltstone, mudstone, and represents a return to a dominantly fluvial depositional environment (Knight 1983, Utting & Giles 2008).

Structure

Onshore, the Bay St. George subbasin (Fig. 4.4) shows significant deformation. These structures were initially studied by Bell (1948) and later Knight (1983), who described large-scale folds and faults. The major onland ductile structural features (Fig. 4.4) noted by these authors include the open, doubly plunging Anguille anticline, Flat Bay anticline, and Barachois syncline (Bell 1948, Knight 1983). The axes of these, and many other mesoscopic folds, trend NE–SW.

The major onland brittle structures are the NE–SW striking Long Range Fault, the southeastern subbasin boundary, and the Snakes Bight Fault (Fig. 4.4) that cuts across the Anguille anticline (Bell 1948, Knight 1983). Knight (1983) mapped other mesoscopic to macroscopic faults striking NE–SW, NW–SE, and E–W shown in Figure 4.4.

Some structures previously interpreted as tectonic folds or faults onshore are here reinterpreted as resulting from salt movement (Chapter 3, this thesis). For example, folds at key locations within the Codroy Road Formation along the coast are interpreted to result from significant salt expulsion. At Ship Cove (Fig. 4.4), the contact between the Ship Cove and the Codroy Road Formations(Codroy Group) is interpreted as a primary salt weld. Knight (1983) interpreted a ~6 m wide near-vertical brecciated zone at Capelin Cove (Fig. 4.4) as a fault, separating Woody Cape Formation (Codroy Group) to the north and Searston Formation (Barachois Group) to the south. Beds on either side of this zone young in opposite directions. We suggest that this zone represents a secondary salt weld (Chapter 3 in this thesis); a salt diapir separated the oppositely younging Woody Cape and Searston Formations and was completely expelled.

4.2.4. Offshore Bay St. George subbasin

Stratigraphy

The stratigraphy offshore in the Bay St. George subbasin is poorly known as no wells have penetrated the entire Carboniferous stratigraphy. Kilfoil (1988) and Hall et al. (1992) used residual gravity, magnetic, and seismic data to suggest a 3–4 km thick package of Carboniferous sediment offshore. Burden and Williams (1996) described stratigraphy in only one well, St. George's Bay A-36, which penetrated 320 m of Carboniferous stratigraphy, an unconformity, and 1984 m of underlying Ordovician strata. Drill cores collecting near-surface bedrock in the bay contain spores from the *Grandispora spinosa–Ibrahimispores magnificus* (SM) Zone (Utting & Giles 2008, Opdyke et al. 2012), Serpuhhovian in age, that correlate to the Upper Codroy Group (Utting & Giles 2008, Dafoe et al. 2016).

Structure

The structure offshore has been interpreted using dominantly geophysical techniques. Kilfoil (1988), Miller et al. (1990), and Hall et al. (1992) used seismic, gravity, and aeromagnetic data to interpret offshore structures. Dafoe et al. (2016) integrated gravity, aeromagnetic, bathymetric, and seismic data to identify Quaternary and Paleozoic features and made preliminary inferences of the geometry of salt bodies and major faults in the subbasin.

Seismic reflection profiling has been the geophysical technique most used to interpret subsurface structure. Dafoe et al. (2016) picked two reflectors on seismic profiles: a top salt reflector, representing an average top of Codroy Road Formation evaporite, and a base Codroy Group reflector representing an average base of Codroy Road Formation salt. Because the top salt reflector picked was not one continuous reflection, the top salt pick of Dafoe et al. (2016) cut across reflections. As a result, the top salt of Dafoe et al. (2016) did not correspond to a single stratigraphic surface.

Previous authors all agree that the Bay St. George subbasin is half-graben dipping to the southeast, bounded to the southeast by the Long Range Fault, and unconformably overlying Ordovician strata (Kilfoil 1988, Miller et al. 1990, Hall et al. 1992). The main offshore Carboniferous structures described by Kilfoil (1988), Miller et al. (1990), and Dafoe et al. (2016) include: salt-cored anticlines, synclines, and faults that strike dominantly NE–SW with both reverse and normal separation. The orientations of many structures are at an acute angle (*en echelon*) to the Long Range Fault suggesting that the subbasin was formed in a dextral strike-slip environment and experienced concurrent salt expulsion and tectonism.

In this chapter, we describe salt-related and brittle structures in the Bay St. George subbasin in detail, in order to define the deformation history. We pick horizons on seismic data in the Carboniferous stratigraphy that can be identified in other datasets. We attempt to tie salt-related and brittle structures to tectonic episodes. Novel methods of tracking the direction of salt movement are used in this paper; by tracing the varying location of trough points upwards in a minibasin, and tracking bulk salt movement direction. By using all data types, we are able to build on the process of Dafoe et al. (2016) and overcome the difficulty correlating reflectors between adjacent seismic sections.

4.3. Datasets

4.3.1. Seismic data

Seven conventional 2-D seismic surveys in offshore Bay St. George were carried out between 1973 and 1995 by Gulf, Hunt Oil, Marathon Oil, and Talisman Energy Inc. (Fig. 4.4). The data were migrated after acquisition using post-stack time migration. We have not attempted any re-processing of the original seismic data, and we interpret the seismic data in the time domain. The migrated data were imported in SEG-Y format into Petrel for interpretation and integration with the other geophysical datasets. Seafloor multiples and pull-up features are artifacts common in the dataset, but intersecting lines from different surveys can typically be tied without difficulty.

4.3.2. Aeromagnetic Data

Dumont and Jones (2003 a-p) published 16 maps at 1:100 000 scale showing the total magnetic field and its second vertical derivative, data collected by the Geological Survey of Canada and the Newfoundland and Labrador Department of Natural Resources. The aeromagnetic maps image stratigraphically controlled variations in the magnetic susceptibility. The second vertical derivative maps (Fig. 4.5) are here mainly used in interpretation as they emphasize near-seafloor magnetic contrasts, assisting interpretation of seafloor geology. The second vertical derivative maps were imported as raster images into Petrel and then draped over the bathymetric surface.

4.3.3. Bathymetric data

The Geological Survey of Canada collected multibeam sonar data in the offshore Bay St. George subbasin from 1995 to 1997 using an EM-1000 system (Shaw et al. 1997). The Marine Institute, Memorial University, collected multibeam sonar data from 2011 to 2015 using an EM-170 Kongsberg Multibeam sonar system (Fig. 4.4). We georeferenced and imported these high-resolution (5 m grid) data into Petrel for integration with seismic data (Fig. 4.6). To integrate the bathymetric data with the seismic data, the bathymetric data were converted from the depth domain to the time domain.

4.3.4. Data integration

Quaternary and older bedrock features are well imaged by the bathymetric and aeromagnetic maps (Fig. 4.5, 4.6). The Quaternary deposits, principally of glacial origin, are most common in the inner part of Bay St. George, and are distinguished from bedrock features using the techniques described by Dafoe et al. (2016). Bedrock ridges on the bathymetric data and magnetic anomalies on the aeromagnetic maps are stratigraphically controlled. Figure 4.7 shows one such bedrock ridge traced on the bathymetric data. This bedrock ridge corresponds to an easily identifiable seismic reflection. The bedrock ridge is imaged on the aeromagnetic map as a strong linear negative anomaly (Fig. 4.7c).

Vertical exaggeration and hill shading at variable orientations help to highlight bedrock ridges on the bathymetric data. Linear bedrock ridges and depressions are here mapped and where possible correlated to horizons traced in the seismic data. The aeromagnetic maps are draped onto the bathymetric data in Petrel to increase the precision of tracing bedrock features intersecting the surface (Fig. 4.7). Where the bedrock ridge is not visible on the bathymetric data, magnetic lineations are followed and vice versa. The bathymetric, aeromagnetic, and seismic data assist in correlating horizons between the seismic sections to better constrain the 3-D structure.

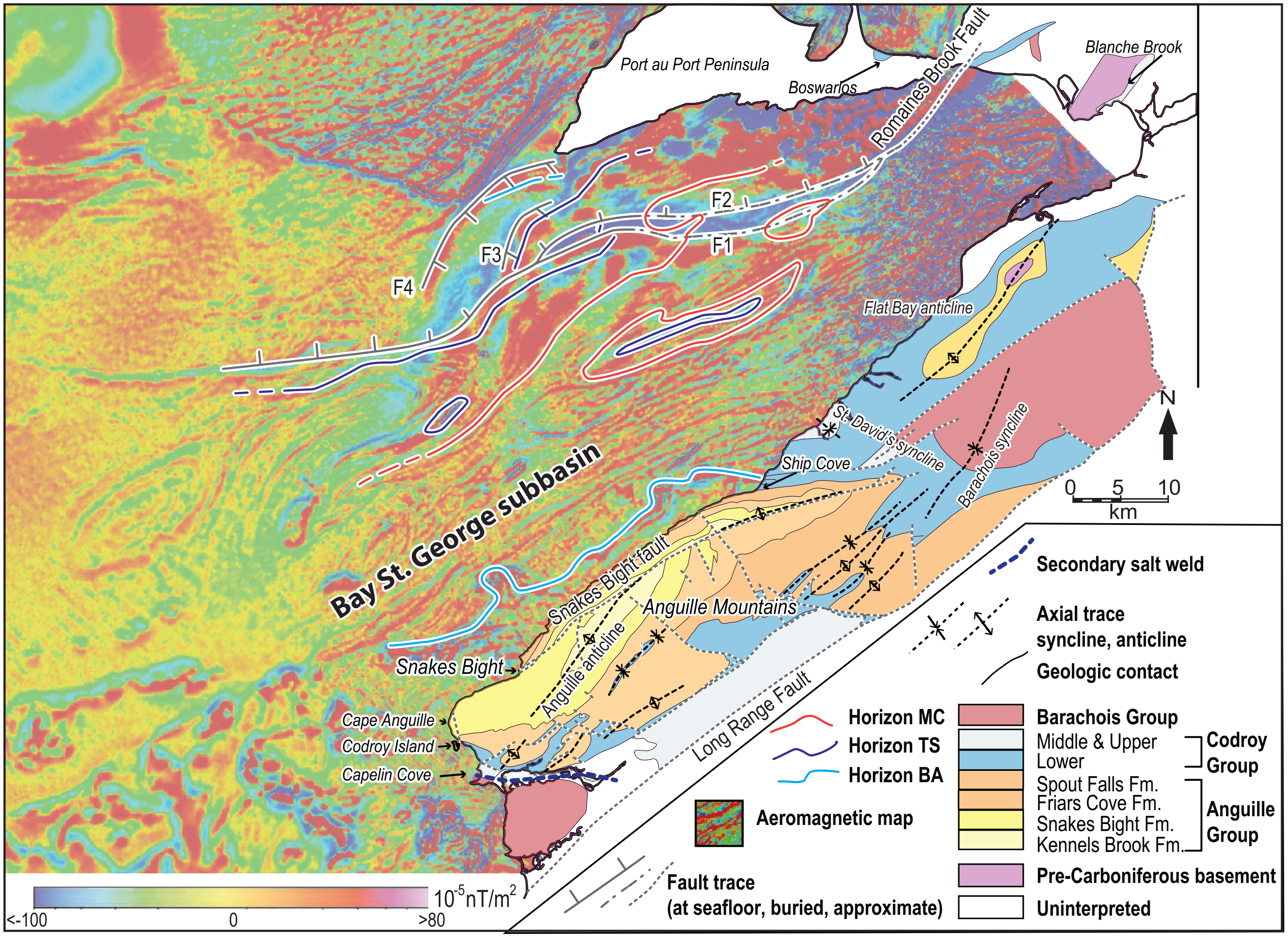

Figure 4.5. Geological map of onshore Bay St. George subbasin after Knight (1983) and second vertical derivative aeromagnetic map of offshore subbasin. Named faults F1-F4 and horizons BA, TS, and MC traced offshore.

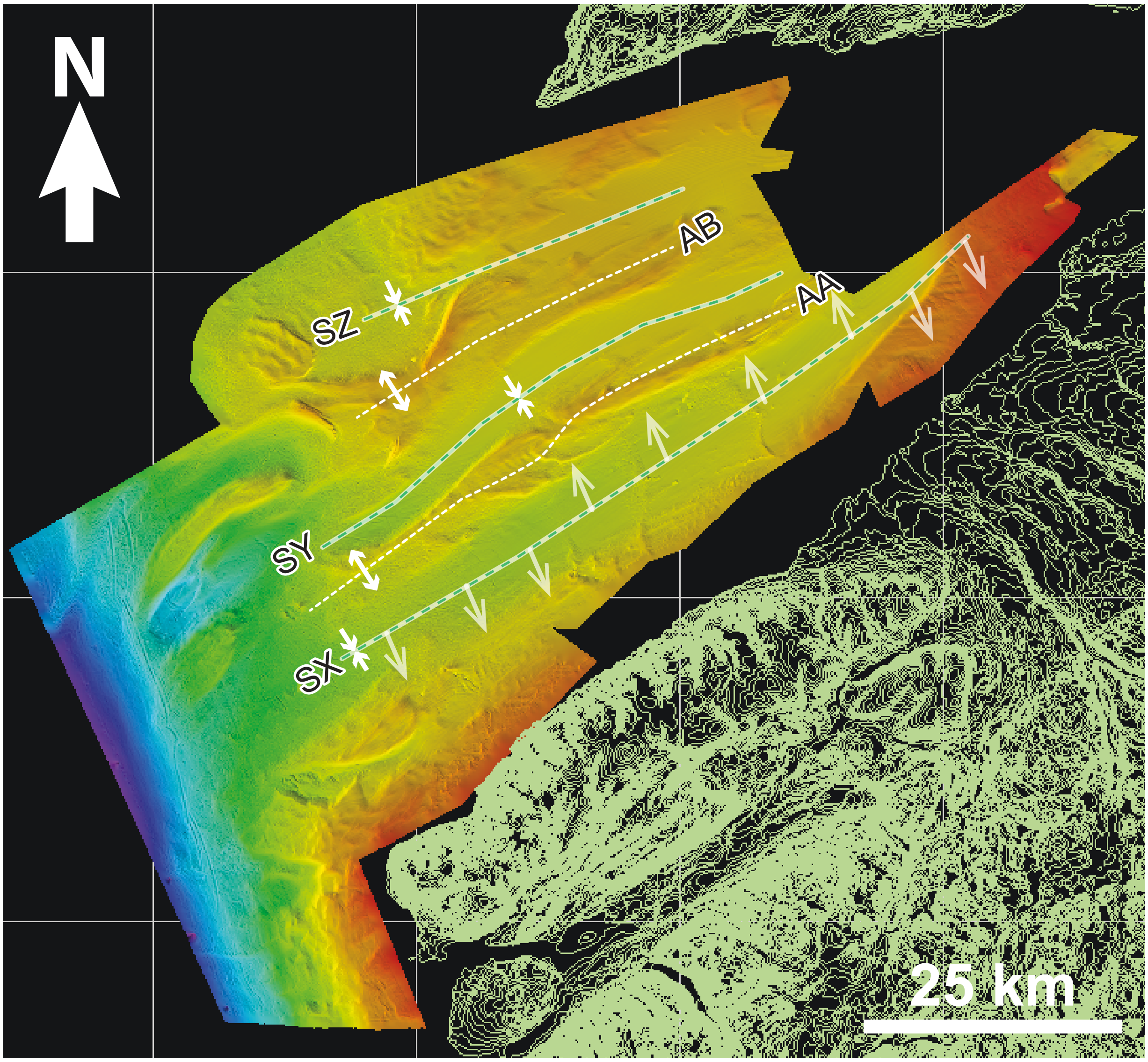

Figure 4.6. Top view of high-resolution bathymetric data showing bedrock features. Green dashed lines represent syncline trough-surface traces on bathymetric surface. Arrows on syncline SX indicate dominant salt movement direction. White dashed lines are anticline axial traces.

4.4. Stratigraphic interpretation

4.4.1. Introduction

The 2-D seismic lines spanning Bay St. George show strong reflections that are well imaged and can be traced across most profiles. Three groups of reflections that we are confident represent Carboniferous strata were picked consistently. Two of the picked horizons can also be correlated to features visible on the bathymetric data and aeromagnetic maps.

Although seismic reflections can be correlated across the offshore subbasin, and the geologic structure can be interpreted based on reflection geometry, no wells penetrated the entire stratigraphic column offshore. Arguments based on reflection character, and long-distance correlations with wells elsewhere in the Maritimes Basin, must be used for interpretation. A synthetic seismogram generated by correlating wells across the Maritimes Basin aids in the interpretation of seismic in areas lacking well control (Fig. 4.3).

4.4.2. Anguille Group

Below horizon BA, the lowest picked reflection, are unresolvable reflections that could not be traced across the subbasin. These reflections likely represent Tournaisian Anguille Group and/or Ordovician Humber Zone reflectors noted by Dooley and Schreurs (2012), Dafoe et al. (2016), and systematically mapped by White (2018) further north. The Ordovician units are represented in southwest Newfoundland by uniform-thickness carbonate shelf deposits (Waldron & van Staal 2001). Ordovician seismic horizons picked by White (2018) around the Port au Port Peninsula maintain constant thickness between reflectors. Reflections below horizon BA, two of which are picked for clarity in Figure 4.8, converge upwards and are truncated near horizon BA creating an angular discordance. As the strata below the angular discontinuity vary in thickness, it is likely that the strata immediately underlying horizon BA belong to the Anguille Group and not the older Humber Zone.

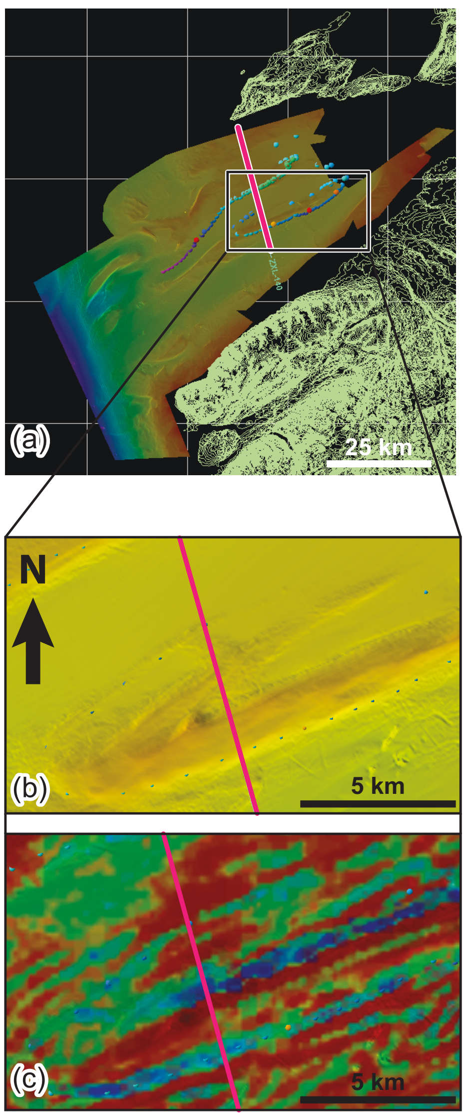

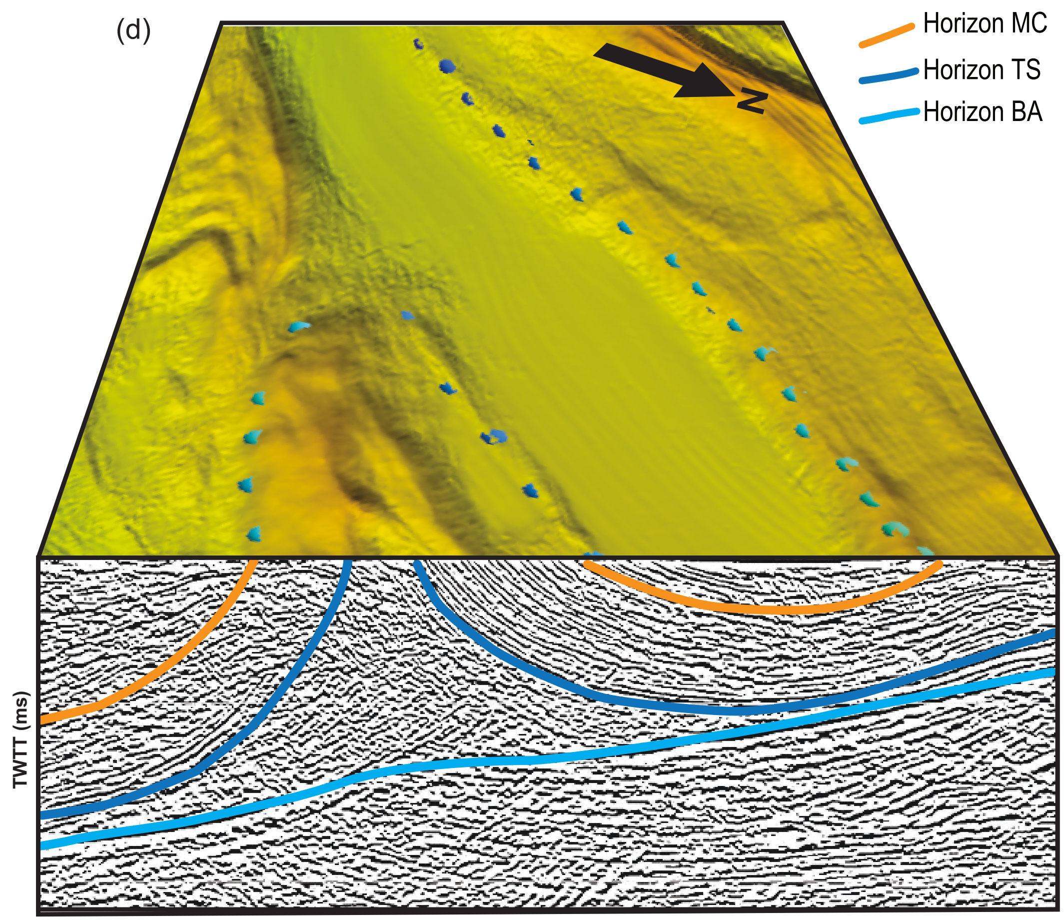

Figure 4.7. Geophysical data integration.
(a) High-resolution bathymetry showing points picked along a ridge corresponding to a picked seismic reflector; (b) inset showing bedrock anticlinal ridge on bathymetry and (c) aeromagnetic data where ridge corresponds to magnetic low; (d) box diagram showing intersection of bathymetry and an intersecting seismic profile. The basal anhydrite (light blue), above salt (dark blue), and middle-to-upper Codroy reflector (orange). The bedrock picks on the bathymetry correlate to the middle-to-upper Codroy reflector.

4.4.3. Horizon BA ("basal anhydrite")

The most obvious group of reflections across all lines is at the base of the well-imaged portion of the seismic data. Horizon BA is chosen in a set of peaks dipping approximately south-southeast (00° to 35° dip) from the seafloor in the northern Bay St. George subbasin to ~2500 ms two-way travel time (TWTT) in the southern subbasin (Fig. 4.9). On some lines there are up to five strong reflections, but on most there are two. We attempted to consistently pick the shallowest peak in the package as horizon BA

A comparable set of strong reflections underlying incoherent reflections in Carboniferous strata was described in the Moncton subbasin in New Brunswick by Wilson et al. (2006), the Windsor-Kennetcook subbasin Nova Scotia by Waldron et al. (2010), the Cumberland subbasin in Nova Scotia by Waldron et al. (2013), and the Bay St. George subbasin by Durling and Marillier (1993b) and Dafoe et al. (2016). In all these areas it has been interpreted as representing the Macumber Formation, at the base of the Windsor Group (equivalent to the Ship Cove Formation of the Codroy Group). These peaks are similar in reflection character to our horizon BA. Drilling in the Moncton and Windsor-Kennetcook subbasins confirms the presence of a thin limestone unit at the base of this group of strong reflections in these subbasins (Wilson et al. 2006, Waldron et al. 2010).

To place BA more precisely within the basal stratigraphy of the Codroy group, it is helpful to compare equivalent sections elsewhere in the Maritimes Basin where deformation is less intense. For example, Giles and Utting (2001) logged a thick (~160 m) anhydrite package near the base of the equivalent Windsor Group in the Shubenacadie #1 well, the Cap Rouge F-52 well, and onshore central Cape Breton Island (Fig. 4.3). This anhydrite is underlain by a basal limestone (Macumber Formation equivalent to the Ship Cove Formation) and overlain by a thick halite package in all the wells. If horizon BA represented the Ship Cove Formation, it would represent a contact from evaporite to limestone, as interpreted by Durling and Marillier (1993) and Dafoe et al. (2016), and would be expected to show a negative reflection due to the decrease in acoustic

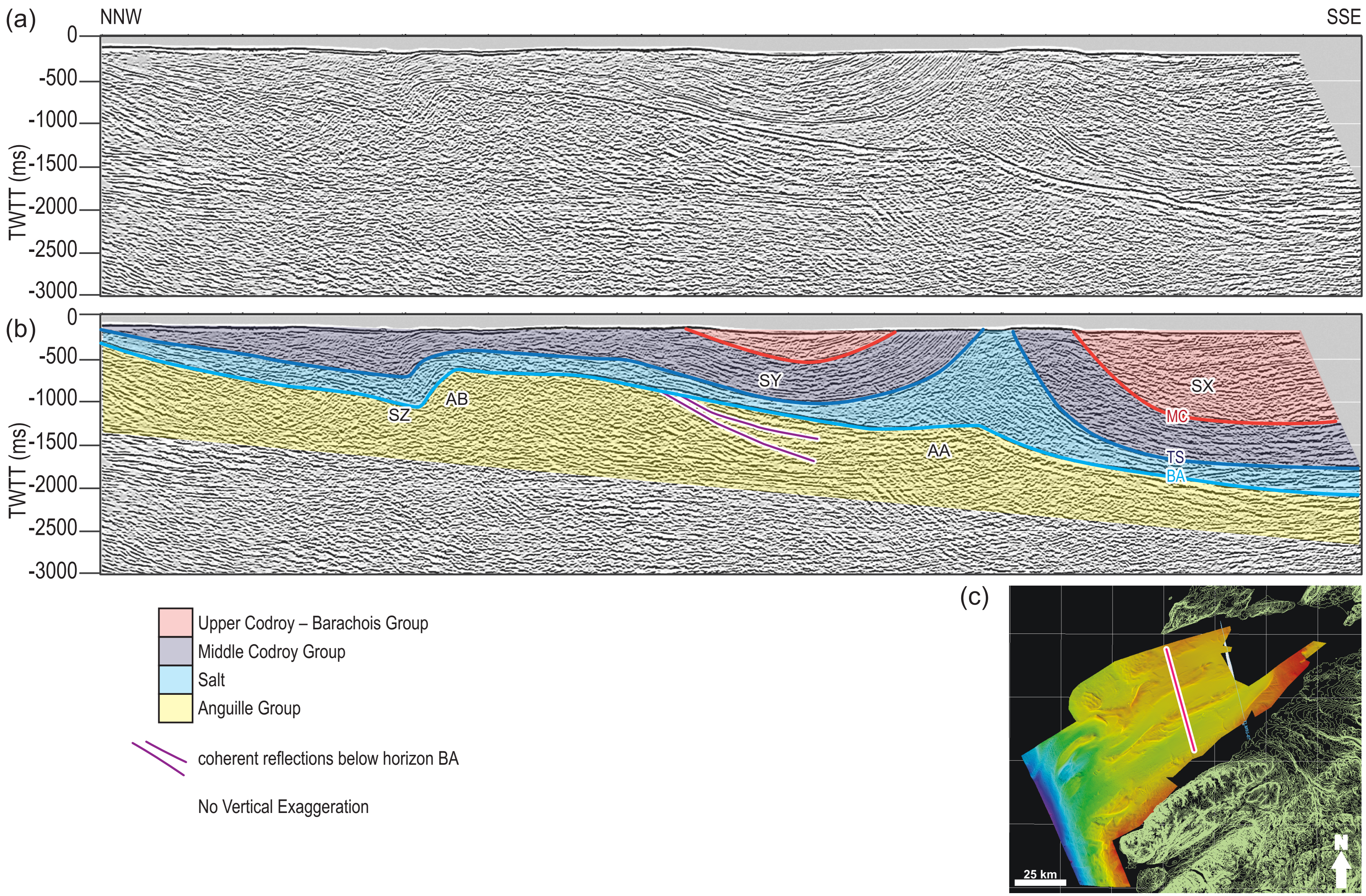

Figure 4.8. NNW-SSE seismic line
(a) uninterpreted and (b) interpreted shown on (c) location map.

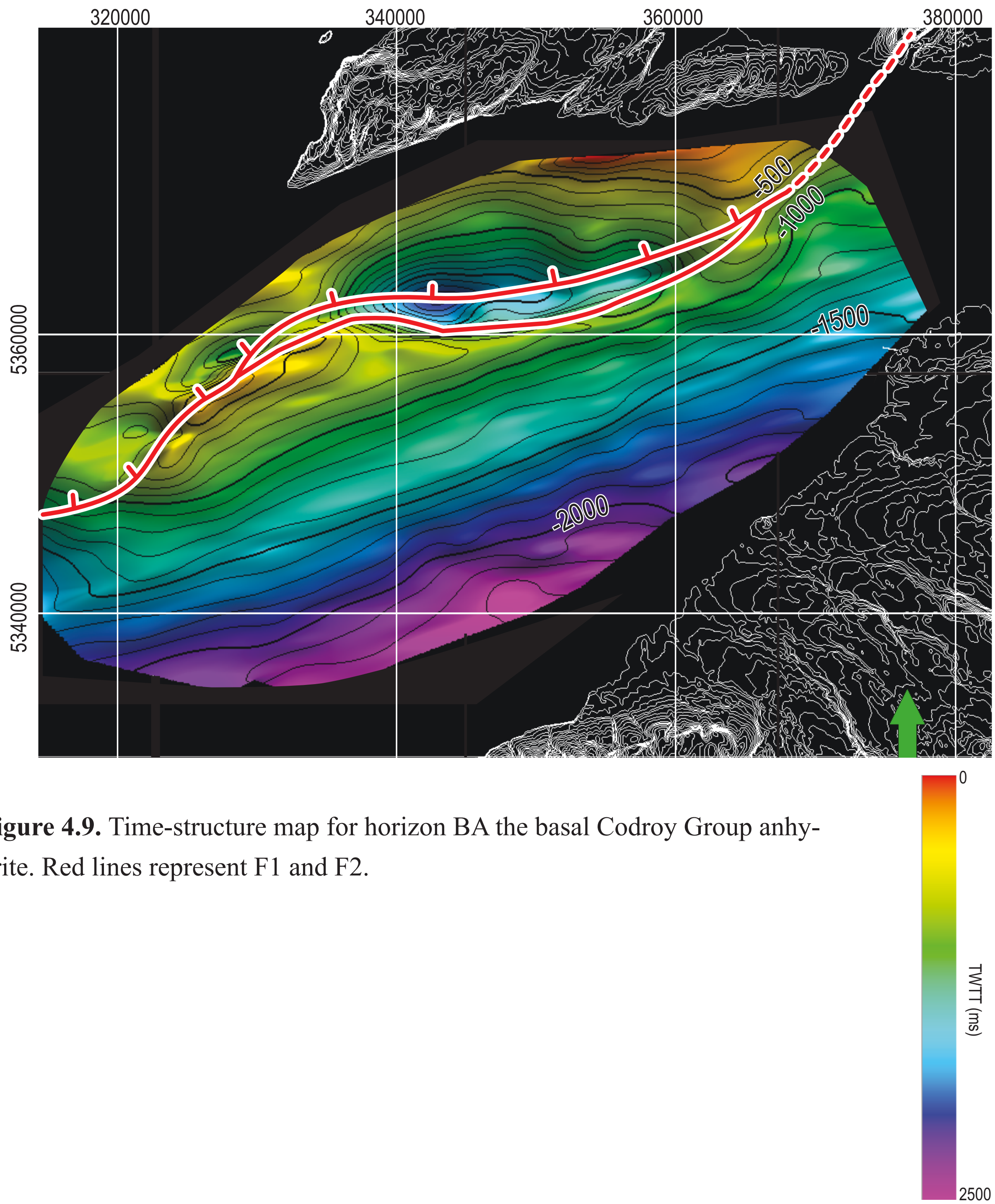

Figure 4.9. Time-structure map for horizon BA the basal Codroy Group anhydrite. Red lines represent F1 and F2.

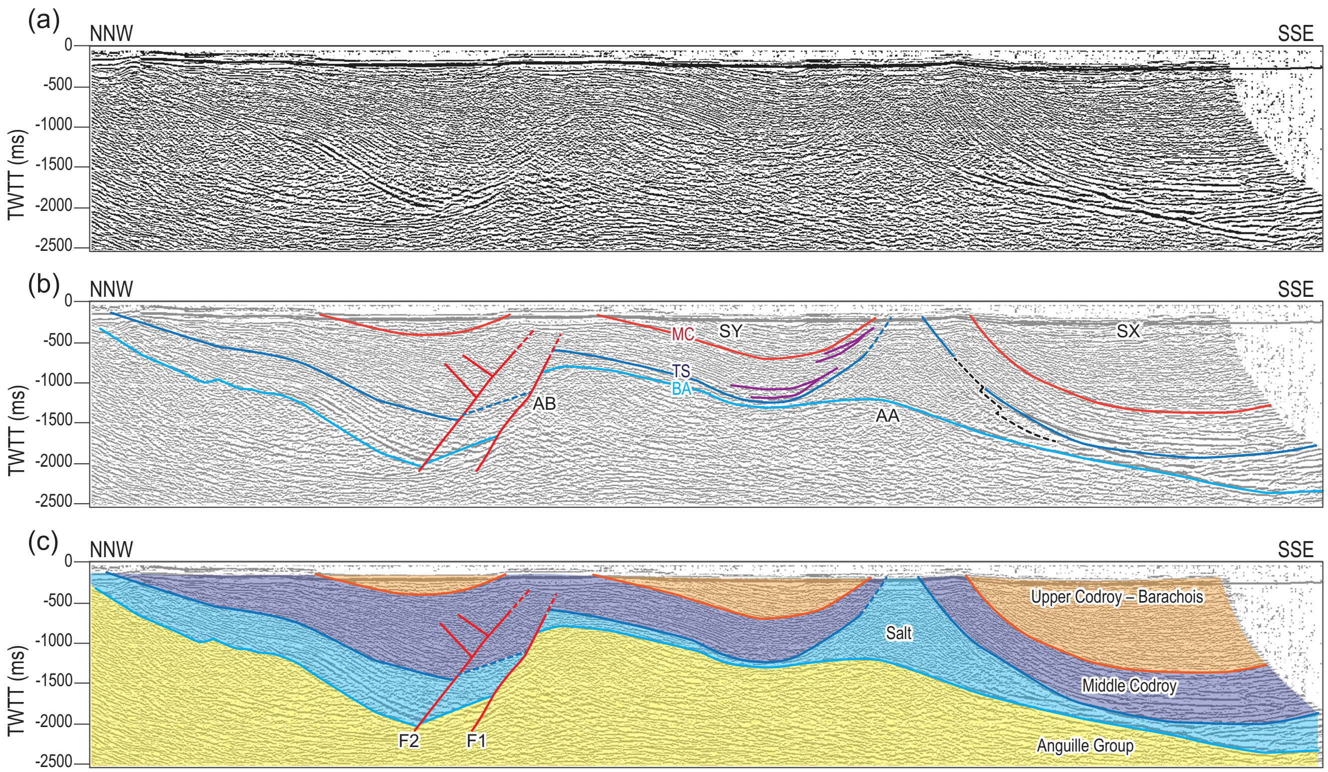

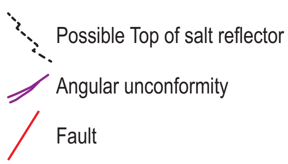

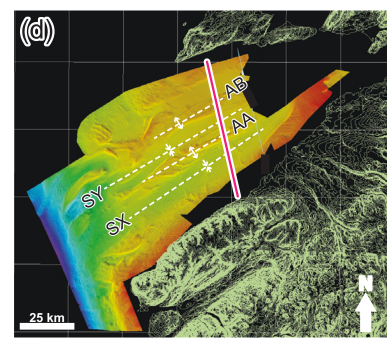

Figure 4.10. NNW–SSE seismic profile.
(a) uninterpreted, (b) traced labelling horizons BA, TS, MC, the locations of major anticlines and synclines and wedge unconformities adjacent to top salt reflector shown in purple, and (c) interpreted seismic sections showing interpreted geology and labelling major faults F1 and F2 from (d) location map showing seismic profile location in pink and axial traces of SX, AA, and SY.

impedance at a contact of anhydrite on limestone. It is more likely that the strong positive reflection identified as BA on the seismic profiles corresponds to the top of the thick anhydrite package. This interpretation is based on the increase in acoustic impedance at a contact from halite to anhydrite that would be expected with the two sediment velocities and densities. Horizon BA is therefore interpreted as the top of the basal anhydrite layer within the lower Codroy Group. The thickness variations, represented by the changing number of successive strong reflections in this group across all seismic lines, can be explained by a variably thick anhydrite unit rather than a uniform limestone unit as previously interpreted.

Horizon BA commonly rises slightly in the profiles, beneath the thickest package of evaporites. These features are interpreted as "pull-up" artifacts, resulting from under-estimation during processing of the effect of high-velocity evaporites in the overlying section.

The top of the basal anhydrite is probably exposed in a complexly deformed section at Ship Cove, described in Chapter 3. None of the interpreted seismic profiles extends close to the shore in this area, but a strong negative magnetic anomaly comes ashore at this point (Fig. 4.5). This anomaly can be traced offshore for >40 km as a sinuous line tentatively identified as horizon BA in Figure 4.5.

4.4.4. Evaporites

Above horizon BA are regions with incoherent structure and chaotic reflection character. Reflections have generally low amplitude and are laterally discontinuous. Incoherent regions range from 0 to >750 ms TWTT thick on NNW–SSE seismic lines, forming anticlinal features (Fig. 4.7d). The anticlines can be correlated between adjacent NNW–SSE lines, showing that they trend subparallel to the WSW–ENE lines, and are marked by multiple parallel elongate ridges on the bathymetric data (Fig. 4.6). The anticlines are laterally discontinuous and plunge both NE and SW. The dips of well-imaged reflections adjacent to the incoherent anticlines range from

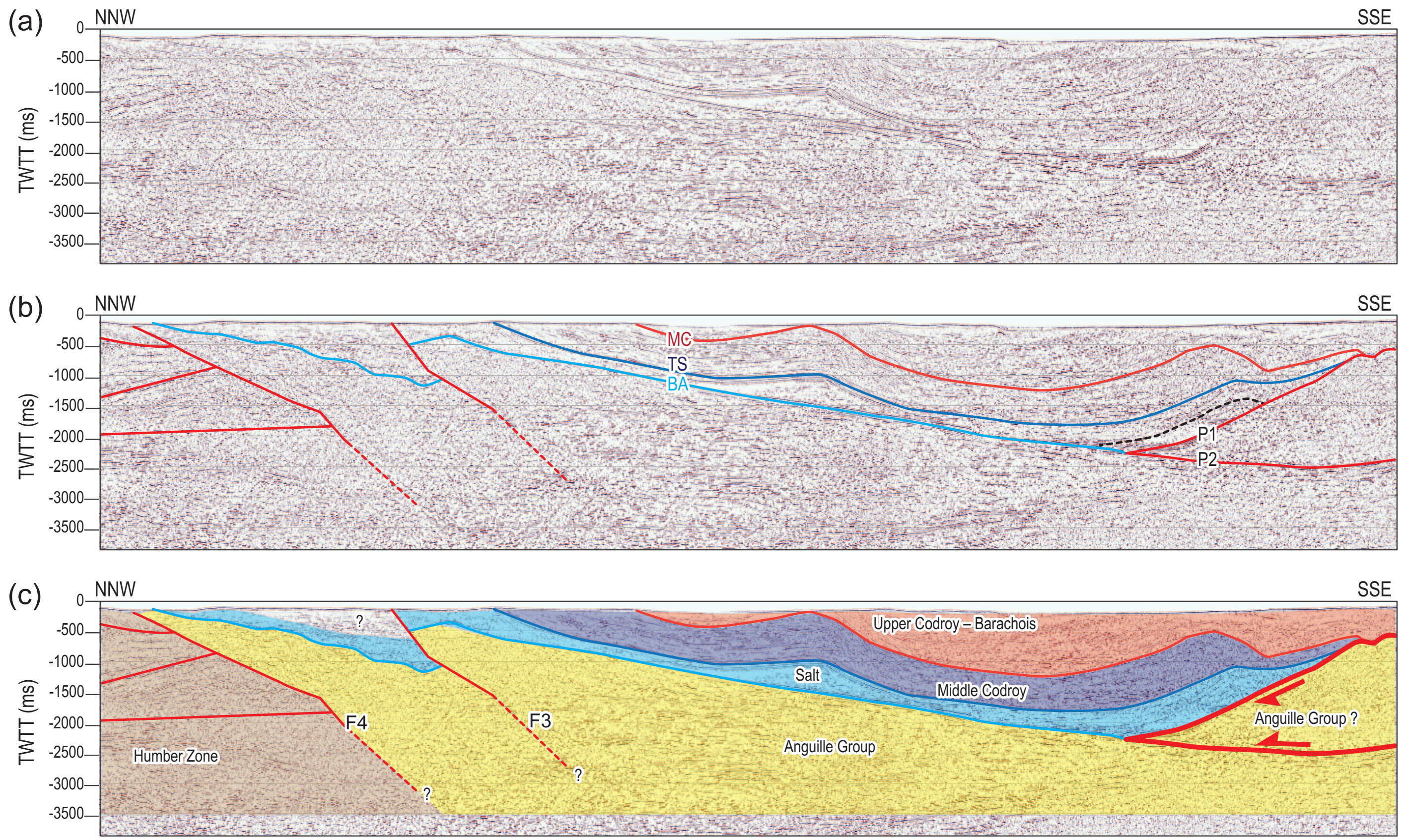

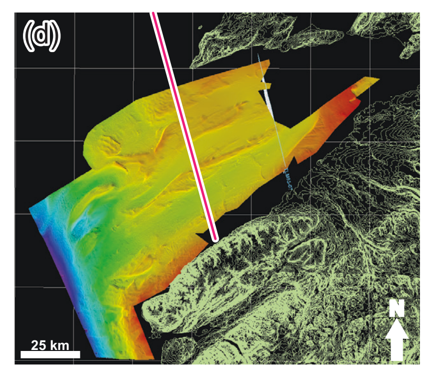

Figure 4.11. NNW–SSE seismic profile.

(a) Uninterpreted (b) with traced horizons, and (c) with interpreted geology shown on (d) location map. Faults are shown in red. Humber Zone rocks are separated by the Carboniferous Bay St. George subbasin by two synthetic graben-bounding faults. Black dashed line represents another 'top of salt' horizon. To the SSE a tectonic wedge filled with Anguille Group with/without Codroy Group strata.

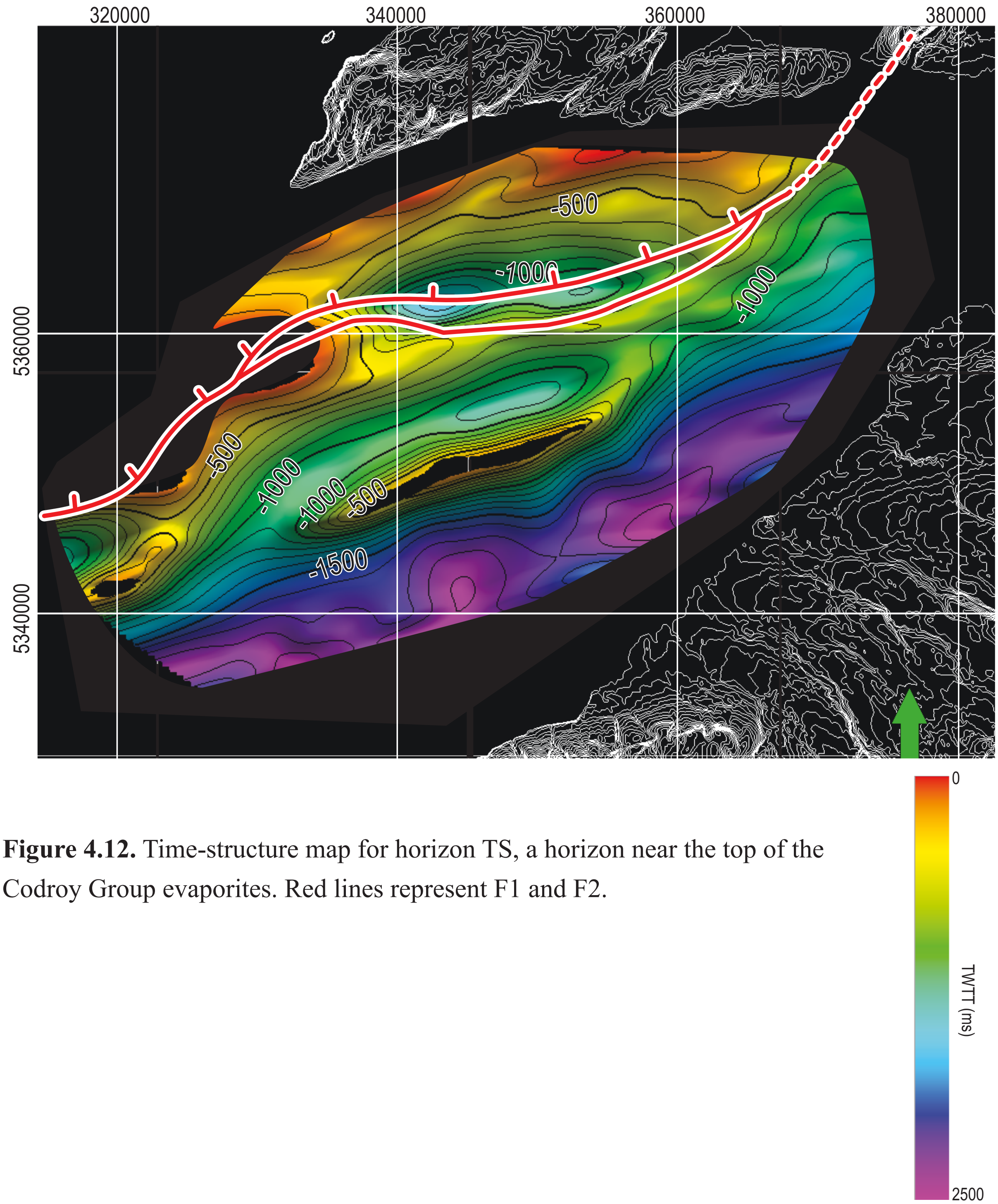

Figure 4.12. Time-structure map for horizon TS, a horizon near the top of the Codroy Group evaporites. Red lines represent F1 and F2.

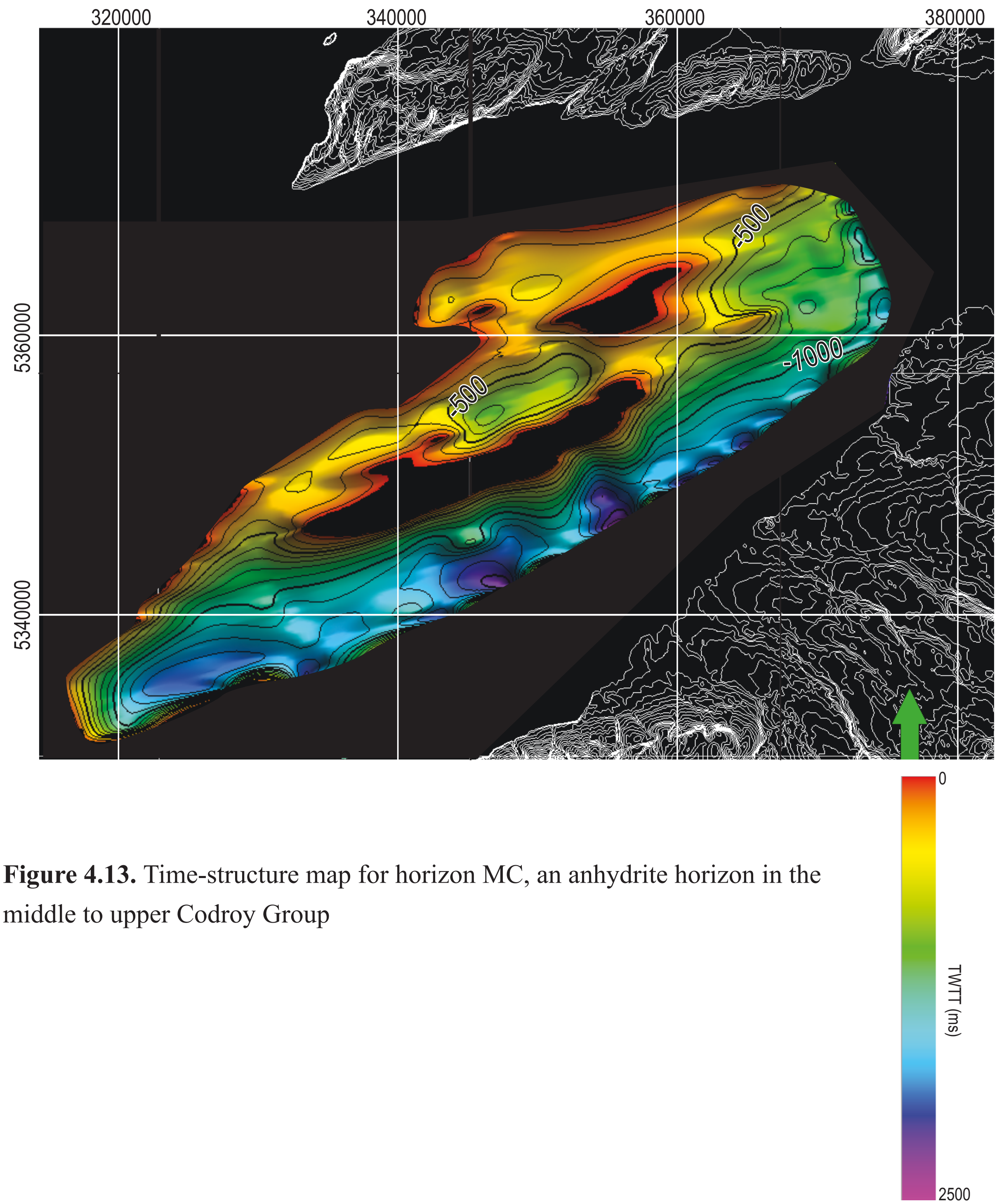

Figure 4.13. Time-structure map for horizon MC, an anhydrite horizon in the middle to upper Codroy Group

parallel to horizon BA to near vertical (00° – 80°). We interpret these variably dipping, typically incoherent reflections, as dominantly representing evaporites of the Codroy Road Formation.

4.4.5. Horizon TS

Multiple 'top of salt' reflectors are shown in Figure 4.10 and 4.11. Based on on-land observations (Chapter 3 in this thesis), the Codroy Road Formation could contain interbedded non-halite strata (ex. anhydrite, sandstone, or limestone), encased roof blocks, and/or subsalt material, so it is likely that these reflections represent other rock-types that are partially or completely encased in salt. Sedimentary strata that onlap salt diapir flanks represent strata that were deposited horizontally, and later eroded during salt diapir formation, indicating that salt was moving at different times in the geologic history (Fig. 4.10).

Horizon TS, a reflector typically immediately above the Codroy Group evaporites, likely represents a limestone bed in the lower to middle Codroy Group boundary above which evaporite occurrence is minor (Fig. 4.2).

Where horizon TS intersects the seafloor, a strong bedrock ridge is apparent on the bathymetric data. This bedrock ridge can be traced and corresponds to a positive magnetic anomaly on the aeromagnetic map (Fig. 4.5). On the seismic profiles, horizon TS is a strong peak with variable dip ranging from sub-horizontal to near vertical across the subbasin. The depth of this horizon ranges from the seafloor, where strata are near vertical, to approximately 2000 ms TWTT in the south central subbasin (Fig 4.12). On NNW–SSE seismic lines, horizon TS delineates two synclines separated by an anticline (SX and SY on Fig. 4.10). Along the flanks of the anticline, horizon TS in many cases intersects the seafloor and disappears above the seismic profile. Tracing horizon TS on the bathymetric data and aeromagnetic data allowed more precise picking on either side of anticline AA (Fig. 4.10). To the north, horizon TS is cut by moderately dipping discontinuities interpreted as faults (F1 and F2 Fig. 4.10).

4.4.6. Lower to middle Codroy Group

Above horizon TS are coherent reflections similar in character to horizon TS; most reflections overlying horizon TS are near parallel. Adjacent to anticline AA (Fig. 4.10), reflections show angular discordances (Fig. 4.10b). Strata in this package do not form bedrock ridges on the bathymetric data. However, magnetic anomalies parallel bedrock ridges formed by lower stratigraphy (Fig. 4.5). Therefore, linear magnetic anomalies that parallel the bathymetric highs can be traced on the aeromagnetic maps. Hayward et al. (2014) interpreted similar magnetic anomalies in the Bay St. George subbasin as representing salt- and iron-rich sedimentary rocks brecciated during salt mobilization. This package likely represents clastic, limestone, and minor evaporites of the lower to middle Codroy Group.

4.4.7. Horizon MC

Horizon MC, a third reflection picked across the subbasin, is consistently visible in the seismic profiles. Horizon MC is truncated by the seafloor adjacent to anticlines in many profiles (e.g. AA in Fig. 4.10). An obvious bedrock structure represented by a set of two ridges is present on the bathymetric data and corresponds to horizon MC. This bedrock structure is imaged on the aeromagnetic maps as a strong negative linear anomaly (Fig. 4.7). By following the linear magnetic anomaly and the bathymetric high, we can confidently pick horizon MC on both limbs of anticlines AA and AB (Fig 4.10). Horizon MC is picked as the deepest reflection in a set of three peaks. The dip of horizon MC varies from parallel to gently dipping horizon BA, to steeply dipping (00° – 75°). This reflection ranges in depth from intersecting the seafloor when steeply dipping, to approximately 1500 ms TWTT in the south-central subbasin (Fig. 4.13).

Figure 4.3 shows a set of three peaks on synthetic seismograms created from wells across the Maritimes Basin (P. Durling pers. comm. 2018). In these seismograms, three conspicuous peaks correspond to drilled anhydrite layers in the middle Codroy Group (Giles & Utting 2001). The

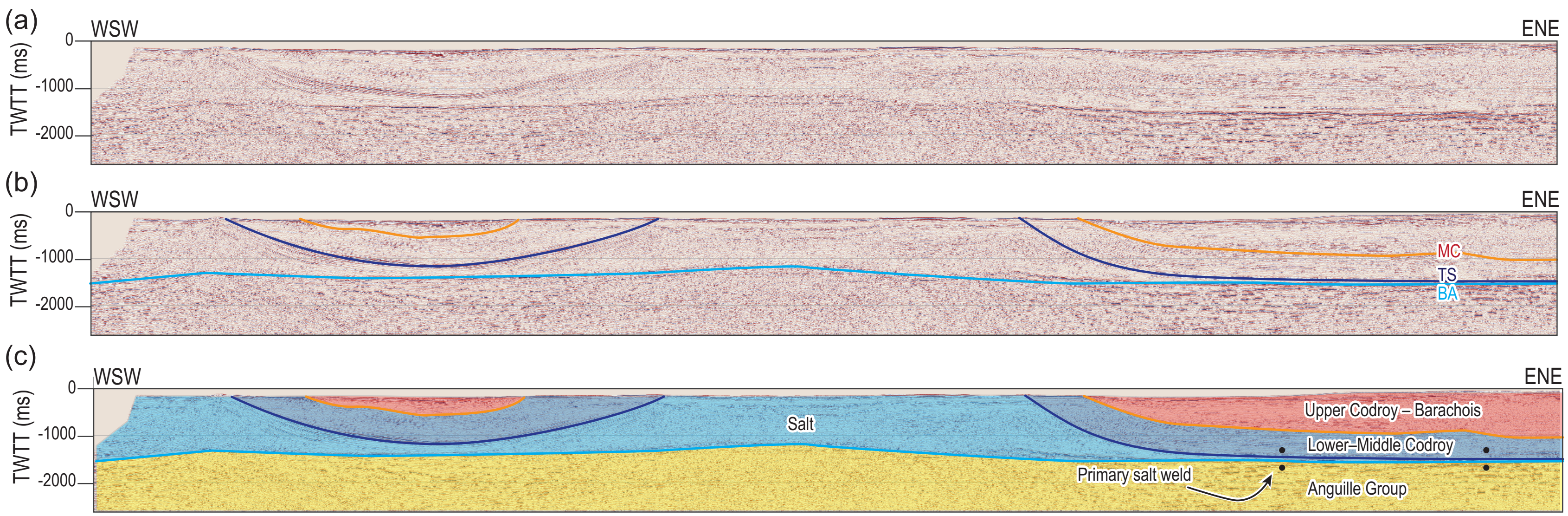

Figure 4.14. WSW – ENE seismic line

(a) Uninterpreted and (b) interpreted shown on (d) location map. A primary salt weld is marked underlying the southeastern minibasin.

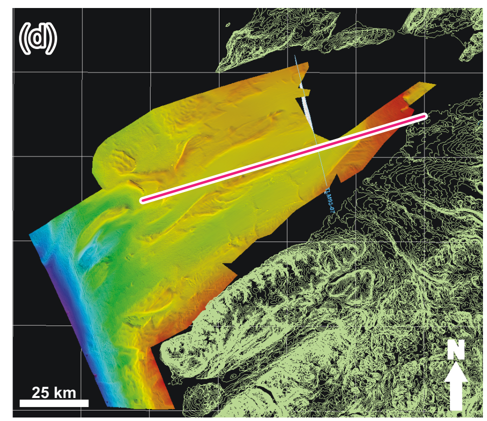

lowest peak can be correlated with horizon MC. We therefore suggest that horizon MC corresponds to the top of an anhydrite package in the middle Codroy Group (Fig. 4.3).

4.4.8. Middle Codroy to Barachois Group

Overlying horizon MC are continuous coherent reflections that are typically sub-parallel to horizon MC. These reflections become unresolvable near the surface due to seismic artifacts including seafloor multiples. This apparently conformable package of strata is interpreted as representing the middle Codroy Group to the Barachois Group.

4.5. Structures

4.5.1. Salt-cored anticlines

Two elongate structures trending ENE–WSW, parallel to the shoreline (Fig. 4.6), are the most obvious structures shown on the bathymetric surface and in the NNW–SSE seismic profiles. The structures narrow upward and all overlying reflections dip away from the centre forming high aspect-ratio ellipses in plan view. Following Dafoe et al. (2016), they are interpreted as salt-cored anticlines (AA and AB in Fig. 4.8).

Figure 4.8 shows a cross-sectional view and Figure 4.14 an oblique view through these salt structures. Horizon TS intersects the seafloor dipping away from the salt-cored anticlines in all directions. Down dip, beneath the intervening synclines that separate the salt structures, horizon TS approaches and merges with horizon BA (see next section). The dips of horizon TS on the sections indicate that the anticline AA is doubly plunging. Anticline AB is more complex. In Figure 4.8, a continuous anticline-syncline pair is shown. Further east this salt anticline is cut by steep faults dipping NNW (F1 and F2 in Fig. 4.10).

4.5.2. Synclines: salt-expulsion minibasins

Adjacent to the salt-cored anticlines are synclines filled with suprasalt material of the Codroy Group and Barachois Group. Three dominant synclines are elongated parallel to the major graben-bounding faults (Fig. 4.6). On NNW–SSE seismic lines, perpendicular to the fold axes of these synclines, apparent dips of reflections decrease from the flanks to the hinge zone, and from the base to the top. On WSW–ENE seismic lines, apparent dips of reflections decrease to parallel with the basal anhydrite in both directions, indicating that these are doubly plunging synclines. Strata within the synclines appear thicker in the hinge region and thinner at the flanks. At the edges of synclines, angular unconformities are shown where underlying reflections are truncated by overlying reflections (Fig. 4.10).

The hinge zones of these synclines are broad. Figure 4.15 shows three NNW–SSE seismic profiles intersecting the southern syncline SX (Fig. 4.10), where the lowest points (trough points) of reflections change location with depth. Trough points can be connected to create trough surface traces. Figure 4.6 shows the southern syncline trough surface trace and its apparent dip direction in map view. In the west, the trough surface dips to the southeast; in the centre the trough surface dips northwest, and in the east the trough surface dips southeast.

The geometry of these structures is similar to salt-expulsion minibasins on passive continental margins, including the Gulf of Mexico (Hudec & Jackson 2007, Hudec et al. 2009), Brazil (Ge et al. 1997, Garcia et al. 2012), Angola (Spathopoulos 1996, Hudec & Jackson 2004, Jackson & Hudec 2005) and eastern Canada (Enachescu 1992, Jackson & Vendeville 1994, Albertz et al. 2010), where expulsion of evaporites causes subsidence forming synclines. Salt-expulsion minibasins form synkinematically as sediment is deposited above the salt and salt is gradually expelled by sediment loading through time; the resulting accommodation space is filled by younger sediments (Trusheim 1960, Jackson & Talbot 1991, Peel 2014, Callot et al. 2016). Salt expelled beneath the minibasins is typically collected adjacent to the minibasins as salt-cored anticlines or salt diapirs (Koyi et al. 2008, Peel 2014, Callot et al. 2016, Duffy et al. 2017, Jackson & Hudec 2017).

The elliptical shape of minibasins in the Bay St. George subbasin is well displayed on the aeromagnetic and bathymetric maps (Fig. 4.5, 4.6). Elliptical salt-expulsion minibasins are common in other subbasins within the Maritimes Basin including the Cumberland subbasin (Waldron et al. 2013), the Moncton subbasin (Wilson et al. 2006), and the Sackville subbasin (Craggs et al. 2015). Elliptical minibasins are observed in locations where salt expulsion was tectonically controlled, particularly in strike-slip zones (Koyi 1998, Koyi et al. 2008, Jahani et al. 2009, Callot et al. 2016).

4.5.3. Salt welds

Underlying the salt-expulsion minibasins, on multiple seismic profiles (ex. Fig. 4.14), horizon TS is in direct contact with horizon BA; the Codroy Group evaporites are absent. Surfaces where there has been a near-complete removal of an autochthonous salt layer are termed primary salt welds (Jackson & Talbot 1991, Wagner III & Jackson 2011). In Chapter 3, salt welds are described in outcrop. For example, at Ship Cove (Fig. 4.4) a primary salt weld crops out at the contact between the Ship Cove Formation and overlying Codroy Road Formation. A corresponding primary salt weld is imaged in Figure 4.14 in the subsurface, for example, where horizon TS and horizon BA are parallel to the dip of underlying and overlying strata, and all the autochthonous Codroy Group salt has been expelled.

4.5.4. High-angle faults

High-angle faults are the most obvious brittle structures interpreted on the bathymetric data, aeromagnetic maps, and on the seismic profiles. Many high-angle faults have been described by Dafoe et al. (2016), including an offshore extension of the SW striking Romaines Brook Fault

(Fig. 4.5), which crops out onshore, and is interpreted as a reverse fault later affected by dextral strike slip (Williams 1985, Palmer et al. 2002, Dafoe et al. 2016).

The southwest end of the interpreted Romaines Brook Fault merges into two large high-angle faults (F1 and F2 in Fig. 4.10 and F1/F1a of Dafoe et al. (2016). These faults cut horizons BA and TS, but do not intersect horizon MC. The the southernmost fault, F1, strikes WSW and dips NNW. The northern fault, F2, has a more complicated geometry. The basal part of this fault strikes WSW and dips NNW; F2 branches where the fault is more shallow. In Figure 4.16A, F2 has one antithetic fault branch forming a Y-shape, whereas in Figure 4.10, F2 has two antithetic branches. The throw on these faults decreases to zero towards the east and west.

The separation on faults F1 and F2, where they crosscut horizon BA, is normal. Upwards along faults (ex. 500 to 750 TWTT on Fig. 4.16), above horizon TS, a positive-relief structure is observed where the faults diverge into multiple Y-shapes. Reflections are cut by the branching faults. Reflections with similar character, on either side of faults, appear to show reverse separation (Fig. 4.16B). These faults are here interpreted as a positive flower structure. Positive flower structures have been described in other subbasins within the Maritimes Basin including the Windsor-Kennetcook subbasin in Nova Scotia (Waldron et al. 2007, Waldron et al. 2010) and the Moncton subbasin in New Brunswick (Eggleston 2017).

Two parallel SSE dipping normal faults are observed on NNW–SSE seismic lines that extend to the NNW, past the Port au Port Peninsula (F3 and F4 in Fig. 4.11). To the northwest of F4 are early Paleozoic rocks of the Humber Zone interpreted by White (2018) and to the southeast are Carboniferous Maritimes Basin strata described here. The younger strata in the hanging wall indicate that F4 has normal separation. F3 separates Carboniferous stratigraphy in the hanging wall and footwall. Horizon BA is cut by F3 and shows reverse separation.

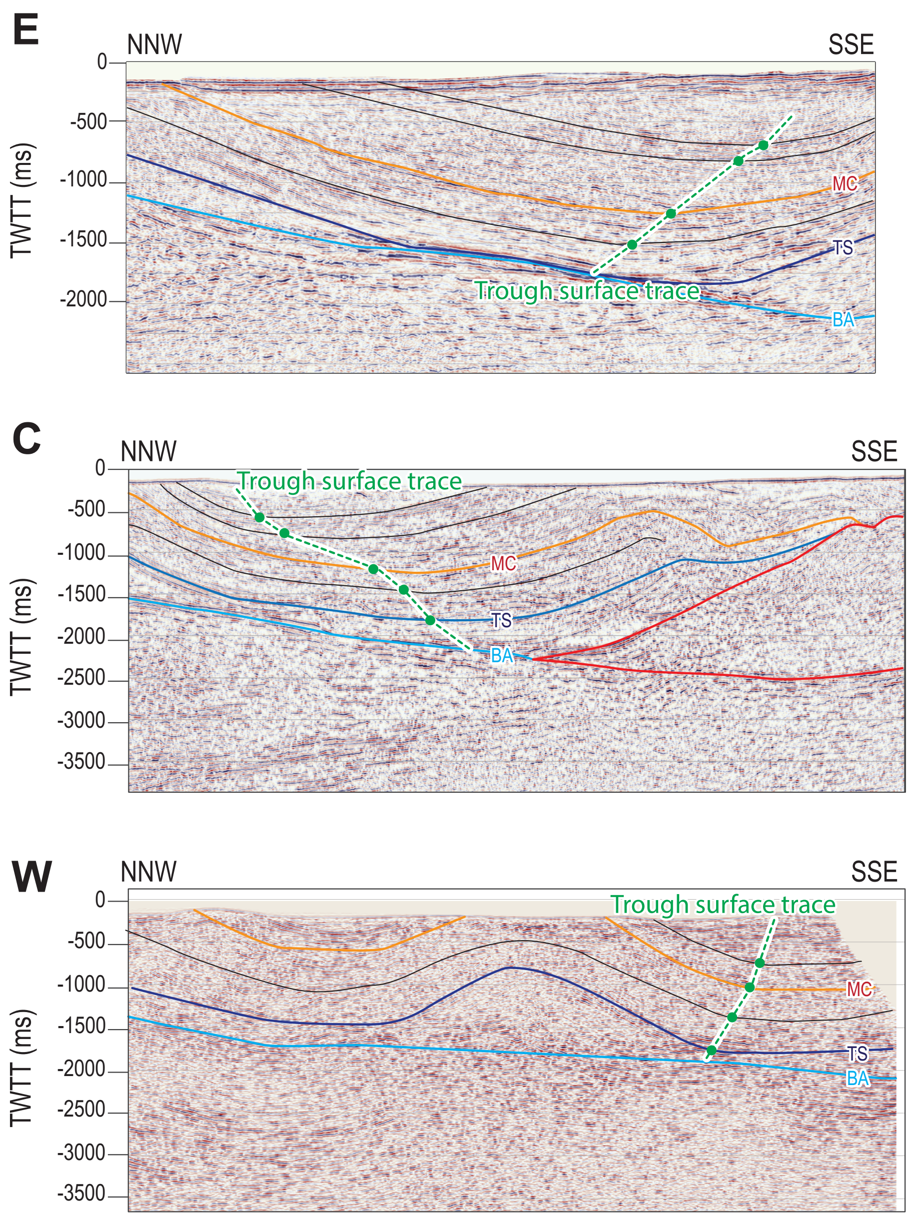

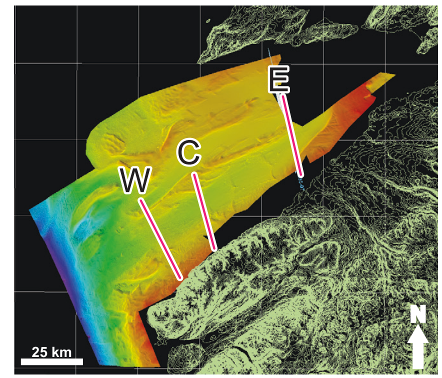

Figure 4.15. Lines W, C, and E on a map and on seismic lines showing examples of trough points migrating with decreased depth.
Line W show and axial trace that migrates NNW to SSE with decreased depth. Line C shows an axial trace that migrates SSE to NNW with decreased depth. Line E shows an axial trace that migrates NNW to SSE with decreased depth.

4.5.5. Low angle faults

Other faults offshore include a west-verging reverse fault duplicating stratigraphy above the salt that does not intersect the basal anhydrite in the central subbasin (F9 in Fig. 4.17). The same seismic profile shows another set of faults that are similar in geometry to an imbricate fan (F5-F8), connecting with a décollement above the basal anhydrite, likely within the lower Codroy Group. Dips of F5 to F8 vary from 00° to ~30° W. Reflections bounded by the faults in this structure are truncated and show reverse separation.

4.5.6. Tectonic wedge

At the SSE end of multiple seismic lines located in the central subbasin, a unique triangular feature is imaged (Fig. 4.11). SSE of anticline AA, horizon BA dips gently SSE as far as a point where it appears to branch into two reflectors (Fig. 4.11). A concave-up reflection (P1 on Fig. 4.11b) extends SSE with moderate apparent dip, shallowing to ~500 ms TWTT at the end of the seismic profile. The second reflection (P2 on Fig. 4.11b) continues from the branch point with gentle apparent dip to the SSE to the end of seismic profile. Between P1 and P2 (Fig. 4.11b) is a triangular region in which reflections dip NNW, parallel to P1, and appear to be truncated by P2.

Immediately overlying the tip of this triangle are incoherent reflections interpreted as salt (Fig. 4.11). Above the salt, horizons TS, MC, and many other subparallel reflections form anticline-syncline pairs that are truncated to the SSE by the steep side of the triangle (P1 on Fig. 4.11b). Figure 4.18b is a simplified interpretation of the same seismic profile with additional reflections traced in order to highlight, from north to south: a salt-cored anticline, a salt-expulsion minibasin, an asymmetric anticline with a salt body immediately above P1, and a syncline-anticline pair truncated by P1.

This triangle is interpreted as a tectonic wedge inserted above the basal anhydrite (horizon BA). P1 and P2 on Figure 4.18 represent the base and roof faults of this tectonic wedge. The reflec-

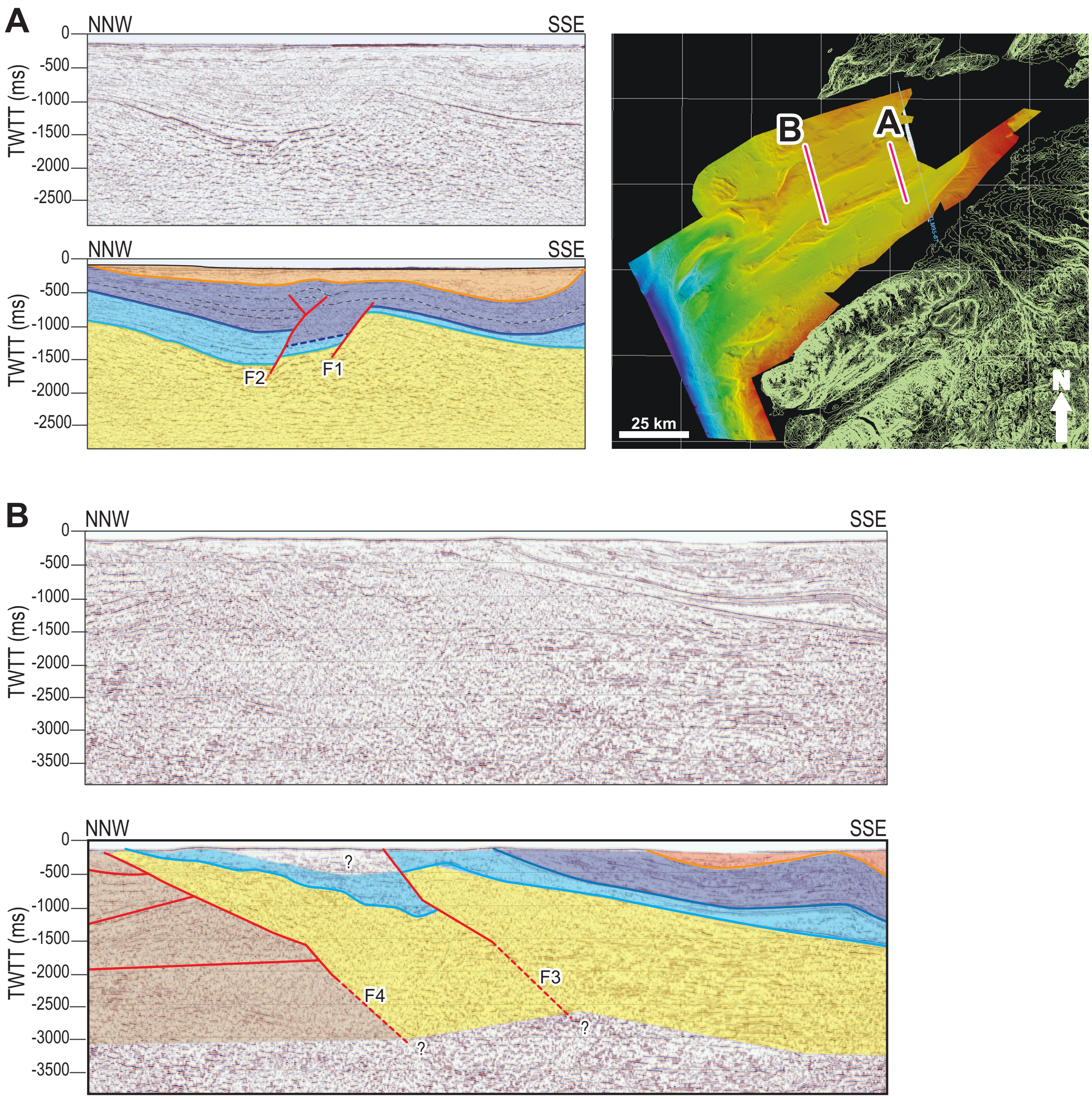

Figure 4.16. Evidence for inversion in Bay St. George.
Line A shows normal faults striking ENE separating the basal anhydrite, and a positive flower structure at the shallowest depth of the fault extent. Line B shows thicker hanging wall sediment across a fault that initiated as a normal fault and now has reverse separation.

tions truncated by P2 are inside the triangle, and reflections truncated by P1 are above the triangle (Fig. 4.18). P1, the roof fault, cuts both horizon TS and MC, meaning it cuts across salt, anhydrite, and higher Carboniferous stratigraphy.

Tectonic wedges have been described elsewhere in the Maritimes Basin, including the Antigonish subbasin by Durling et al. (1995), the Moncton subbasin by Wilson & White (2006), the Windsor-Kennetcook subbasin by Waldron et al. (2010), and the Sackville subbasin by Eggleston (2017).

In Figure 4.5, the aeromagnetic map shows a sinuous negative magnetic anomaly, tentatively identified as horizon BA, striking NE–SW and intersecting the coast at Ship Cove, where the interpreted primary weld crops out onshore (Fig. 4.4, see Chapter 3 of this thesis). This negative anomaly is intersected only at the extreme south end of the seismic profile shown in Figure 4.11, where the tectonic wedge is imaged. This negative anomaly is likely indicates that the salt weld extends offshore close to the top of the tectonic wedge. Its sinuous character probably reflects complex folding and expulsion of evaporites associated with emplacement of the wedge. The lack of seismic profiles in this area precludes more detailed interpretation of its geometry.

4.6. Discussion

4.6.1. Evaporite expulsion and sedimentation

The minibasins identified in the Bay St. George subbasin are elliptical in map view and asymmetric in cross section. Hudec et al. (2009) suggested that mechanisms other than pure density-driven subsidence are responsible for the development of asymmetrical minibasins. These mechanisms can include shortening, extension, or location on a bathymetric slope. Jackson and Hudec (2005) and Hudec et al. (2009) used trough point tracking techniques in Angola and the Gulf of Mexico respectively to differentiate between pure density-driven subsidence and tectonically controlled subsidence. In the Kwanza Basin, Angola, Jackson and Hudec (2005) suggested that migration of minibasin depocenters reflected the unidirectional movement of salt during deposition of younger sediments.

These techniques are here applied to the Bay St. George subbasin with exa,ples in Figure 4.15. Trough points in minibasins represent the location with the greatest total salt expulsion or dissolution at a given time. Figure 4.15 shows the variation of trough point positions with depth in successive minibasins. Tracking successive trough points upwards within minibasins likely records the direction of bulk salt movement. On NNW–SSE seismic profiles W and E (Fig. 4.15), trough points migrate SSE through time indicating that salt was dominantly moving to the SSE. Between W and E, on seismic profile C (Fig. 4.15) in the relative centre of the subbasin, the trough points migrate NNW, indicating salt in this area was dominantly moving NNW.

The seismic lines where trough points migrate NNW through time (seismic profile C in Fig. 4.15b) correspond to those that display the tectonic wedge. This suggests that the salt moved dominantly NNW during emplacement of the tectonic wedge. Where trough points migrate SSE on successive reflections (seismic profiles W and E in Fig. 4.15) the tectonic wedge is absent.

A main assumption of salt tectonics is that sediment deposited above the crest of a rising salt-cored anticline is thin and suprasalt sediment in a salt-expulsion minibasins is thick where expulsion is most rapid. A refinement of trough-point tracking involves recording the locus of maximum sediment thickness through successive stratigraphic units in a minibasin. Figure 4.19 shows the result of flattening traced reflections on seismic profiles perpendicular to the main fold axis of the minibasins. In order to highlight the positions of greatest subsidence rate, arrows are drawn where the sediment is thickest between traced reflections. These arrows represent the locus of maximum subsidence during the increments of time between the traced reflections. Tracking the displacement of arrows through time shows the general minibasin migration direction. As seismic profiles W and E in Figure 4.19 are successively flattened, arrows migrate generally to the SSE. Seismic profile C is more complicated; arrows representing the location of maximum thickness move SSE in lower parts of the succession, but trend NNW in shallower examples. This

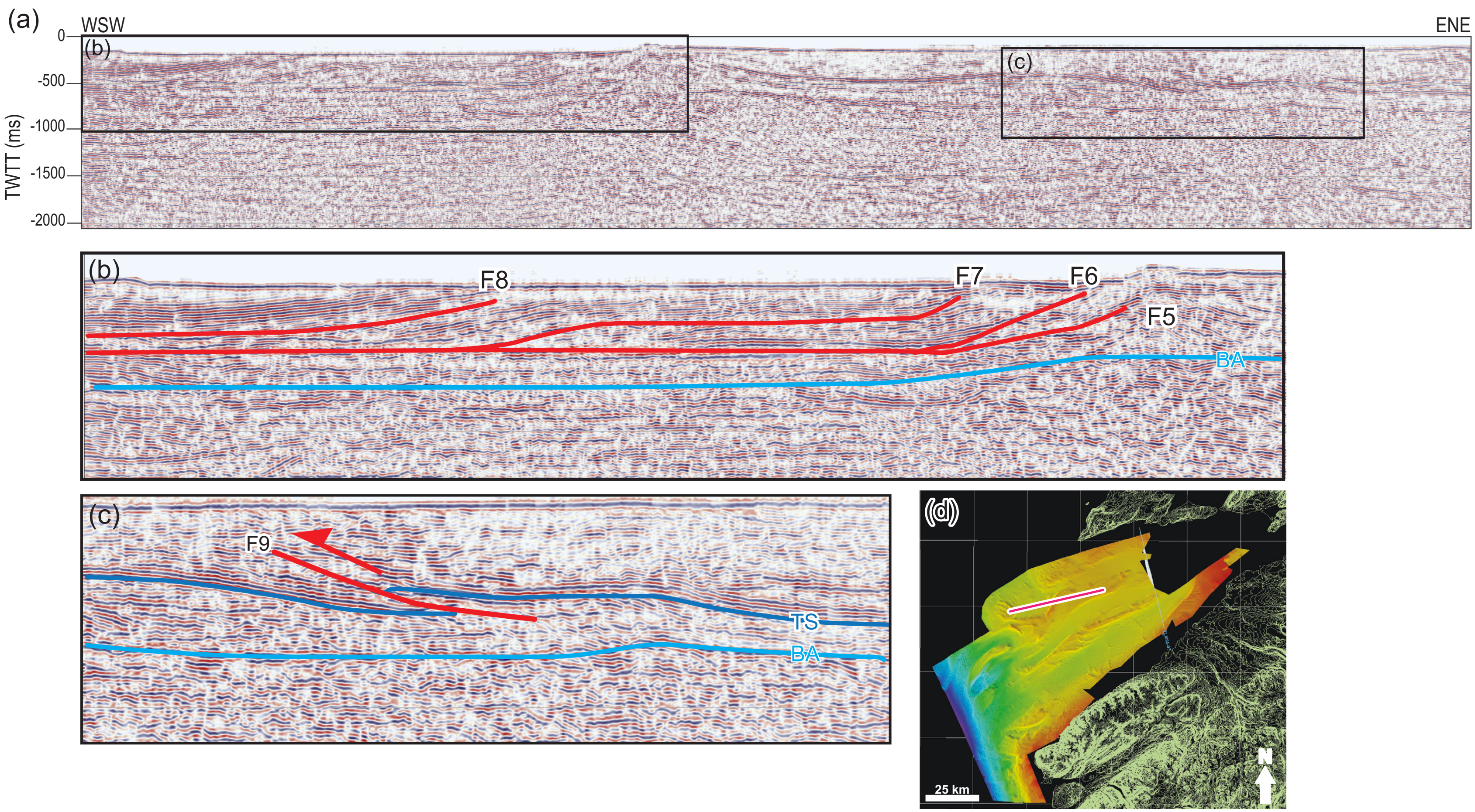

Figure 4.17. Reverse faults imaged on WSW–ENE seismic profile
(a) uninterpreted seismic profile showing locations of insets. (b) east-verging imbricate faults F5-F8; (c) interpreted inset of WSW-verging reverse fault offsetting horizon TS (d) Location map.

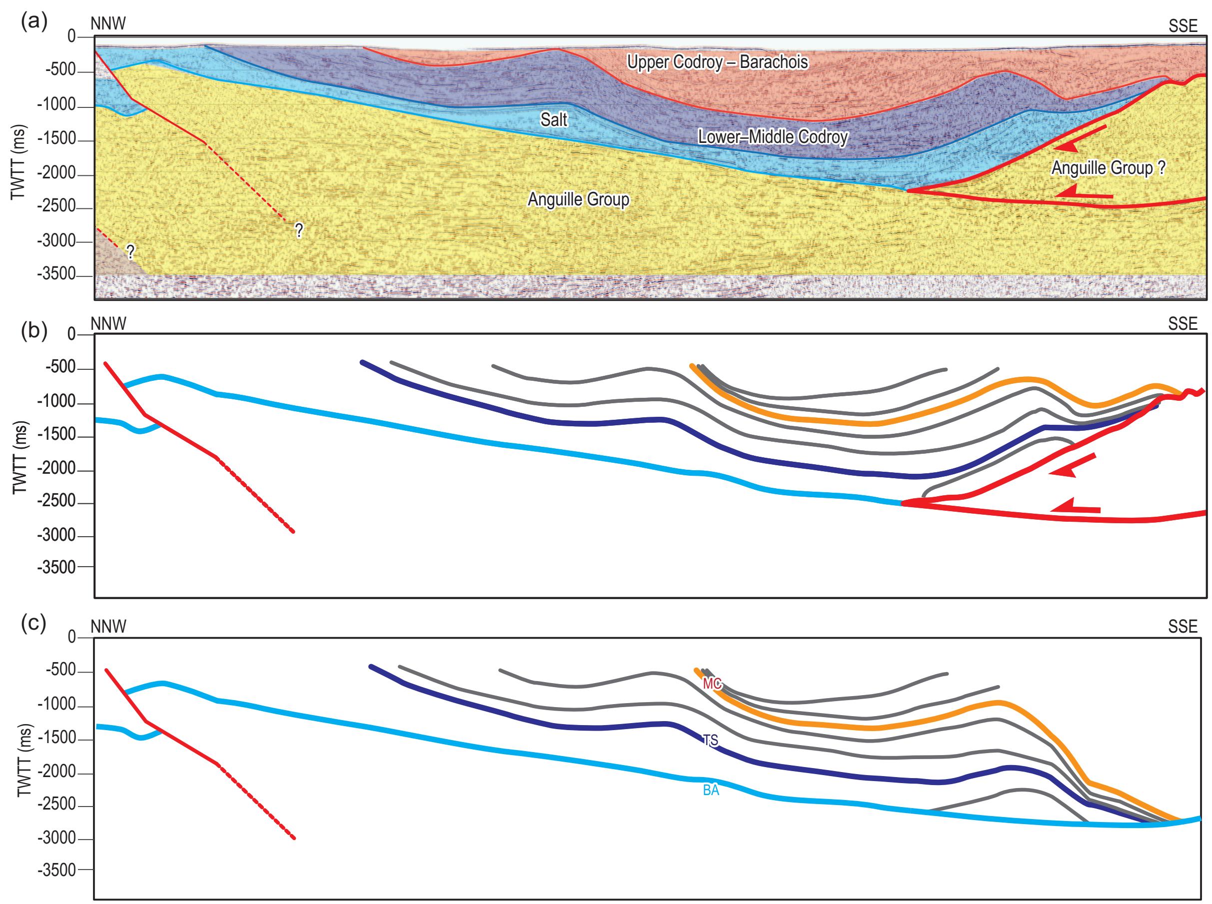

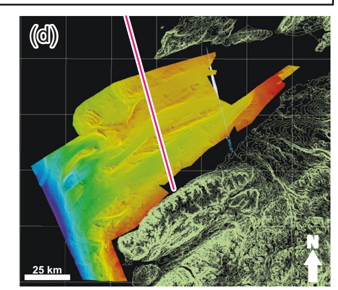

Figure 4.18. Tectonic wedge imaged on NNW–SSE seismic profile

(a) Interpreted seismic section (same as Fig. 4.11); (b) lined interpretation with extra horizons traced. (c) Tectonic wedge removed, and strata restored using vertical simple shear. (d) Location map.

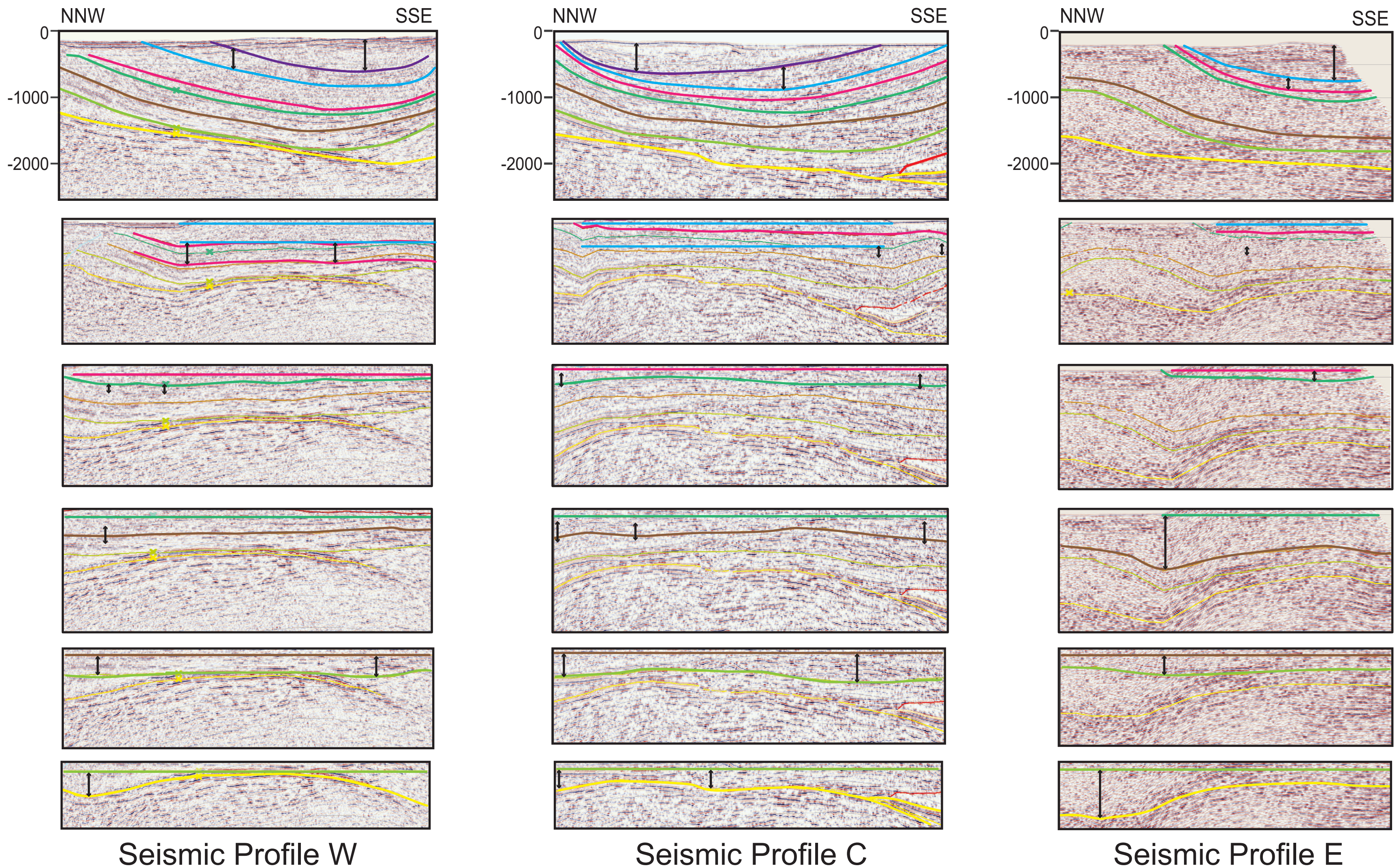

Figure 4.19. Successive flattening of horizons in minibasins.

Three columns of NNW–SSE profiles from west to east (W, C, and E in Figure 4.15). Arrows correspond to greatest thickness between picked reflections, interpreted as the position of maximum subsidence.

suggests that the tectonic wedge was inserted while salt was still moving, resulting in a change of dominant salt migration direction.

4.6.2. Fault movements and sedimentation

Growth faults

Most high-angle faults imaged have greater thickness of sediment in the hanging wall compared to the footwall. For example, F1 and F2 in Figure 4.10, and F3 and F4 in Figure 4.11, show significant thickness variations of Anguille and Codroy Group across the faults. These are therefore growth faults that formed during sedimentation. This indicates that these faults were initially active from the Tournaisian to the Viséan.

Inversion

Despite the stratigraphic evidence for normal movement during sedimentation, many faults show reverse offset of part of the succession at the present day, indicating tectonic inversion. F4 (Fig. 4.16) is a SSE-dipping normal fault with early Paleozoic rocks of the Humber Zone in the footwall and Carboniferous rocks in the hanging wall. F3 is a SSE-dipping reverse fault with Carboniferous strata in the footwall and hanging wall. The geometry of these faults suggests that F3 is a normal fault, synthetic to F4, which has been inverted and now shows reverse separation.

The basal anhydrite (horizon BA) is relatively undeformed and uniformly dipping, except where folded and faulted by F1 and F2 (Fig. 4.16), and by the tectonic wedge (see below). Horizon BA shows normal separation across both F1 and F2. At shallower depths, F2 shows reverse separation of horizon TS. The positive flower structure (Fig. 4.16A) in higher stratigraphic successions along the same faults indicates a history of inversion. These faults were initially formed by extension and later affected by contraction.

An anticline above the positive flower structure (F2), visible in the upper Codroy – Barachois Group (Fig 4.16A), has lower amplitude than the offset of strata separated across the faults at the top of the F2 flower structure. Horizon MC is not offset by F2. The reverse separation of strata below horizon MC suggests some tectonic inversion before deposition of all upper Codroy – Barachois Group strata. Adjacent to this anticline is a shallow minibasin. upper Codroy – Barachois Group strata fill this minibasin above F1 and F2, indicating that salt was likely still moving during or after movement along the faults.

4.6.3. Tectonic wedge emplacement

The complicated geometry of strata within and overlying the tectonic wedge can be interpreted by schematically retro-deforming the section. Reflections traced in Figure 4.18b overlying the tectonic wedge, are distorted by emplacement of the wedge. To remove this distortion, we remove the volume the wedge occupied at the present day by translating reflections above the wedge by vertical heterogeneous simple shear. The result (Fig. 4.18c) represents a possible geometry prior to wedge insertion. A salt-cored anticline terminating in a possible primary salt weld to the SSE is revealed. Above this primary salt weld is a salt-expulsion minibasin filled with upper Codroy and younger strata.

Insertion of the tectonic wedge from the southeast likely occurred during salt expulsion. The roof fault cuts the salt, horizon TS, horizon MC, and higher reflections. Because faults cut through strata of the Barachois Group, the tectonic wedge was likely still being inserted after deposition of this unit. The trace of the roof fault is not imaged on the bathymetry. A negative curving anomaly is visible on the aeromagnetic maps, where we tentatively identified it as horizon BA (Fig. 4.5). This negative anomaly extends southwest from Ship Cove, where a primary salt weld is mapped onshore (Chapter 3, this thesis). Only the seismic line in Figure 4.11 extends SSE of this the anomaly and the structure is poorly resolved close to the end of the line. We suggest that the sinuous geometry of the anomaly represents deformation of evaporites at the roof of the tectonic wedge. The close association of this anomaly with the location of the Snakes Bight Fault onshore strongly suggests that insertion of the tectonic wedge offshore occurred at the same time as the inversion of the Snakes Bight Fault documented in Chapter 3.

4.6.4. Deformation history

Initial deposition into the Bay St. George half-graben started with the Tournaisian deposition of the Anguille Group. Onshore, the Anguille Group is dramatically thicker in the south compared to the north (see Chapter 3 of this thesis). Offshore, it is difficult to determine the thickness of the Anguille Group as seismic reflections are unresolvable below the basal anhydrite reflector, except for a few converging reflectors that underlie the Codroy Group offshore.

Codroy Group strata were deposited after a period of tilting and erosion, preserving this angular unconformity. Deposition of the Ship Cove Formation limestone was followed by deposition of the Codroy Road Formation, which contains evaporite-rich packages. Salt movement was the major driver in subbasin deformation, forming salt structures containing Codroy Road Formation, overlain by younger middle and upper Codroy Group and Barachois Group strata, deposited synkinematically. Salt structures sourced from the Codroy Road Formation evaporites initiated soon after deposition. Strata adjacent to the Codroy Road Formation salt structures are thin, show concave up geometry, and locally contain angular unconformities. The changes in thickness and geometry define halokinetic sequences (Giles & Lawton 2002, Giles & Rowan 2012) that represent periods of salt expulsion and sediment deposition. These dramatic thickness changes, accompanied by angular unconformities on the flanks of Lower Codroy Group salt diapirs, suggest that salt was moving during deposition of the Middle to Upper Codroy Group.

The large salt-expulsion minibasins and salt-cored anticlines in the Bay St. George subbasin show doubly-plunging elliptical geometries *en echelon* to the main graben-bounding faults, noted by Dafoe et al. (2016). Structures *en echelon* to graben-bounding faults have been related to strike-slip motion on the major bounding faults in the Bay St. George subbasin (Knight 1983, Dafoe et al. 2016). Salt-cored anticlines sub-parallel to graben-bounding faults are described by Trusheim (1960) in northern Germany, by Lohmann (1979) in the Mediterranean Sea, Jackson and Talbot (1986) in the Gulf of Mexico, and many others. More rare are elliptical salt-expulsion minibasins, which have been described by Jackson (1990) in Iran, Jackson et al. (2014) in Brazil, and Waldron et al. (2013) in Nova Scotia. Minibasins with the long axis *en echelon* to major faults are typically formed in strike-slip environments (McBride et al. 1998, Koyi et al. 2008, Craggs et al. 2013, Weimer et al. 2017). The *en echelon*, doubly plunging anticlines and salt-expulsion minibasins suggest a correlation between tectonism and salt movement. The orientations of structures offshore in the Bay St. George subbasin are related to transtension on NE–SW Appalachian-trending faults, consistent with structures in the Cumberland and Sackville subbasins in Nova Scotia (Hibbard & Waldron 2009, Waldron et al. 2013, Waldron et al. 2015, Dafoe et al. 2016).

Tracing minibasin trough surface dips allows a more precise timing of tectonic wedge insertion and salt movement. It is here interpreted that where the trough surface dips southeast on syncline SX, salt was flowing dominantly south during suprasalt sediment deposition (Fig. 4.6). In the area near the tectonic wedge, trough surfaces dip northwest, indicating salt was flowing dominantly northwest. We suggest that tectonic wedge insertion occurred synkinematically with salt movement and was responsible for changes in the direction of salt expulsion.

Inversion occurred during and after deposition of the middle Codroy Group (mid-Viséan). In Figure 4.16b, the continuous middle Codroy anhydrite overlies the brittle extent of a positive flower structure with less positive relief, suggesting that inversion occurred during deposition of these units.

4.7. Conclusion

Seismic, aeromagnetic, and bathymetric data allow us to examine the spectacular and complicated offshore structure of the Bay St. George subbasin in detail. The deformation history of the Bay St. George subbasin includes significant ductile and brittle deformation; most deformation can be tied to salt deposition and/or movement. In order to trace deformation through time, determining the timing of salt movement is key.

Salt structures, including salt-cored anticlines, salt-expulsion minibasins, and salt welds, suggest that salt was mobile soon after deposition in the Viséan at least until deposition of the youngest strata in the minibasins (likely the Serpukhovian Barachois Group). Though it is interpreted that salt was mobile during most of the subbasin history, brittle deformation was also significant. Normal faults, reverse faults, and faults with both senses of separation at different depths representing tectonic inversion, are all present.

A tectonic wedge was inserted from the southeast to the northwest into Codroy Group strata during salt movement. The trace of the tectonic wedge, corresponding to a negative anomaly on the aeromagnetic data, represents the extent of this structure.

Acknowledgements

Field research was supported by a grant from the Government of Newfoundland and Labrador Petroleum Exploration Enhancement Program. We thank the Marine Institute, in particular Randy Gillespie, for access to the recently acquired bathymetry data. We thank Leprechaun Resources Ltd. for access to the offshore SEG-Y data. We are grateful for discussions with L. Kennedy from UBC, Paul Durling from Corridor Resources and Chris Jauer from the Geological Survey of Canada. Parts of this work were supported by a University of Alberta Teaching Assistantship. Lauren Eggleston and Martin Schwangler assisted in the field.

4.8. References

Adams, G. C. 1991. Gypsum and anhydrite resources in Nova Scotia. In: *Nova Scotia Department of Natural Resources, Mines and Energy Branches, Economic Geology Series 91-1*, 15.

Albertz, M., Beaumont, C., Shimeld, J. W., Ings, S. J. & Gradmann, S. 2010. An investigation of salt tectonic structural styles in the Scotian Basin, offshore Atlantic Canada: 1. Comparison of observations with geometrically simple numerical models. *Tectonics* **29**(4), TC4017.

Allen, J. P., Fielding, C. R., Rygel, M. C. & Gibling, M. R. 2013. Deconvolving signals of tectonic and climatic controls from continental basins: an example from the late Paleozoic Cumberland Basin, Atlantic Canada. *Journal of Sedimentary Research* **83**(10), 847-872.

Barr, S. M., Brisebois, D. & Macdonald, A. S. 1985. Carboniferous volcanic rocks of the Magdalen Islands, Gulf of St. Lawrence. *Canadian Journal of Earth Sciences = Revue Canadienne des Sciences de la Terre* **22**(11), 1679-1688.

Bell, J. S. & Howie, R. D. 1990. Paleozoic geology--Geologie du Paleozoique The Geology of North America **2**. Geological Society of America, United States, United States, 141-165.

Bell, W. A. 1948. Early Carboniferous Strata of St. Georges Bay Area, Newfoundland. In: *Geological Survey Bulletin No. 10*. Mines and Geology Branch, Department of Mines and Resources, 51.

Bell, W. A. 1958. *Possibilities for occurrence of petroleum reservoirs in Nova Scotia.* Province of Nova Scotia Department of Mines, Halifax.

Belt, E. S. 1969. Newfoundland Carboniferous Stratigraphy and its relation to the Maritimes and Ireland: Chapter 54: Late Orogenic Stratigraphy and Structure. In: *Memoir 12: North Atlantic: Geology and Continental Drift* (edited by Kay, M.), 734-753.

Bibby, C. & Schimeld, J. 2000. *Compilation of reservoir data for sandstones of the Devonian-Permian Maritimes Basin, Eastern Canada. Geological Survey of Canada, Open File Report 3895*.

Boehner, R. C. 1986. Salt and Potash Resources in Nova Scotia. In: *Nova Scotia Department of Mines and Energy Bulletin ME 005*, 346 p.

Boehner, R. C. 1992. An overview of the role of evaporites in the structural development of Carboniferous basins in Nova Scotia. In: *Mines and Energy Branch, Report of Activities 1991* (edited by MacDonald, D. R.) **Report 92-1**, 39-56.

Boehner, R. C., Adams, G. C. & Giles, P. S. 2003. Karst geology in the salt-bearing Windsor Group evaporites and controls on the origin of gypsum deposits in south-central Cape Breton Island, Nova Scotia. In: *Mineral Resources Branch, Report of Activities 2002*. Nova Scotia Department of Natural Resources, Report 2003-1, 9-24.

Boehner, R. C. & Giles, P. S. 1993. *Geology of the Antigonish Basin, Antigonish County, Nova Scotia. 8*. Department of Natural Resources.

Boehner, R. C., Moore, R. G. & Kennedy, C. M. 1999. Overview of the Geology and Mineral Resources of the Western Part of the Windsor (Kennetcook) Basin, Wolfville - Windsor Area (NTS 21H/01 and part of 21A/16), Hants and Kings Counties, Nova Scotia. In: *Nova Scotia Department of Natural Resources Mineral Resources Branch Report of Activities - Report 2000-1* (edited by MacDonald, D. R. & Mills, K. A.), 1-11.

Bradley, D. C. 1982. Subsidence in Late Paleozoic basins in the Northern Appalachians. *Tectonics* **1**(1), 107-123.

Burden, E. T. & Williams, S. H. 1996. *Biostratigraphy and thermal maturity of strata in NHOC – PCP St. George's A-36. Report to the Newfoundland Hunt Oil Company*.

Calder, J. H. 1998. The Carboniferous evolution of Nova Scotia. In: *Geological Society, London, Special Publications* **143**, 261-302.

Callot, J.-P., Salel, J.-F., Letouzey, J., Daniel, J.-M. & Ringenbach, J.-C. 2016. Three-dimensional evolution of salt-controlled minibasins; interactions, folding, and megaflap development. *AAPG Bulletin* **100**(9), 1419-1442.

Craggs, S., Keighley, D., Park, A. F. & Waldron, J. W. F. 2013. Stratigraphy and salt tectonics of Missisippian-Pennsylvanian strata of the northern Cumberland Basin, Maringouin Peninsula, southeastern New Brunswick. *Atlantic Geology* **49**, 24-24.

Craggs, S., Keighley, D., Waldron, J. W. F. & Park, A. 2015. Salt tectonics in an intracontinental transform setting: Cumberland and Sackville basins, southern New Brunswick, Canada. *Basin Research*, 1-18.

Dafoe, L. T., Shaw, J., Jauer, C., Giles, P. S., Waldron, J. W. F. & Potter, D. P. 2016. New insights into the Bedrock and Quaternary Geology of St. George's Bay from a vertical integration of marine datasets, offshore western Newfoundland. *Bulletin of Canadian Petroleum Geology* **64**(1), 1.

Dietrich, J., Lavoie, D., Hannigan, P., Pinet, N., Castonguay, S., Giles, P. & Hamblin, A. 2011. Geological setting and resource potential of conventional petroleum plays in Paleozoic basins in eastern Canada. *Bulletin of Canadian Petroleum Geology* **59**(1), 54-84.

Dimmel, P. 2001. *Potential for Mining Salt in Western Newfoundland.* Department of Mines and Energy; Government of Newfoundland and Labrador.

Dooley, T. P. & Schreurs, G. 2012. Analogue modelling of intraplate strike-slip tectonics: A review and new experimental results. *Tectonophysics* **574-575**, 1-71.

Duffy, O. B., Fernandez, N., Hudec, M. R., Jackson, M. P. A., Burg, G., Dooley, T. P. & Jackson, C. A. L. 2017. Lateral mobility of minibasins during shortening: Insights from the SE Precaspian Basin, Kazakhstan. *Journal of Structural Geology* **97**, 257-276.

Dumont, R. & Jones, A. 2013a. Aeromagnetic survey of offshore western Newfoundland, NTS 11-N NE, Newfoundland and Labrador--Leve aeromagnetique extracotier de l'ouest de Terre-Neuve, SNRC 11-N NE, Terre-Neuve-et-Labrador. Geological Survey of Canada : Calgary, AB, Canada, Canada.

Dumont, R. & Jones, A. 2013b. Aeromagnetic survey of offshore western Newfoundland, NTS 11-O SW, Newfoundland and Labrador--Leve aeromagnetique extracotier de l'ouest de Terre-Neuve, SNRC 11-O SW, Terre-Neuve-et-Labrador. Geological Survey of Canada : Calgary, AB, Canada, Canada.

Dumont, R. & Jones, A. 2013c. Aeromagnetic survey of offshore western Newfoundland, NTS 12-B NE, Newfoundland and Labrador--Leve aeromagnetique extracotier de l'ouest de Terre-Neuve, SNRC 12-B NE, Terre-Neuve-et-Labrador. Geological Survey of Canada : Calgary, AB, Canada, Canada.

Dumont, R. & Jones, A. 2013d. Aeromagnetic survey of offshore western Newfoundland, NTS 12-B NW, Newfoundland and Labrador--Leve aeromagnetique extracotier de l'ouest de Terre-Neuve, SNRC 12-B NW, Terre-Neuve-et-Labrador. Geological Survey of Canada : Calgary, AB, Canada, Canada.

Dumont, R. & Jones, A. 2013e. Aeromagnetic survey of offshore western Newfoundland, NTS 12-B SE, Newfoundland and Labrador--Leve aeromagnetique extracotier de l'ouest de Terre-Neuve, SNRC 12-B SE, Terre-Neuve-et-Labrador. Geological Survey of Canada : Calgary, AB, Canada, Canada.

Dumont, R. & Jones, A. 2013f. Aeromagnetic survey of offshore western Newfoundland, NTS 12-B SW, Newfoundland and Labrador--Leve aeromagnetique extracotier de l'ouest de Terre-Neuve, SNRC 12-B SW, Terre-Neuve-et-Labrador. Geological Survey of Canada : Calgary, AB, Canada, Canada.

Dumont, R. & Jones, A. 2013g. Aeromagnetic survey of offshore western Newfoundland, NTS 12-C NE, Newfoundland and Labrador--Leve aeromagnetique extracotier de l'ouest de Terre-Neuve, SNRC 12-C NE, Terre-Neuve-et-Labrador. Geological Survey of Canada : Calgary, AB, Canada, Canada.

Dumont, R. & Jones, A. 2013h. Aeromagnetic survey of offshore western Newfoundland, NTS 12-C SE, Newfoundland and Labrador--Leve aeromagnetique extracotier de l'ouest de Terre-Neuve, SNRC 12-C SE, Terre-Neuve-et-Labrador. Geological Survey of Canada : Calgary, AB, Canada, Canada.

Dumont, R. & Jones, A. 2013i. Aeromagnetic survey of offshore western Newfoundland, NTS 12-F SE, Newfoundland and Labrador--Leve aeromagnetique extracotier de l'ouest de Terre-Neuve, SNRC 12-F SE, Terre-Neuve-et-Labrador. Geological Survey of Canada : Calgary, AB, Canada, Canada.

Dumont, R. & Jones, A. 2013j. Aeromagnetic survey of offshore western Newfoundland, NTS 12-G NE, Newfoundland and Labrador--Leve aeromagnetique extracotier de l'ouest de Terre-Neuve, SNRC 12-G NE, Terre-Neuve-et-Labrador. Geological Survey of Canada : Calgary, AB, Canada, Canada.

Dumont, R. & Jones, A. 2013k. Aeromagnetic survey of offshore western Newfoundland, NTS 12-G NW, Newfoundland and Labrador--Leve aeromagnetique extracotier de l'ouest de Terre-Neuve, SNRC 12-G NW, Terre-Neuve-et-Labrador. Geological Survey of Canada : Calgary, AB, Canada, Canada.

Dumont, R. & Jones, A. 2013l. Aeromagnetic survey of offshore western Newfoundland, NTS 12-G SE and part of 12-H SW, Newfoundland and Labrador--Leve aeromagnetique extracotier de l'ouest de Terre-Neuve, SNRC 12-G SE et partie de 12-H SW, Terre-Neuve-et-Labrador. Geological Survey of Canada : Calgary, AB, Canada, Canada.

Dumont, R. & Jones, A. 2013m. Aeromagnetic survey of offshore western Newfoundland, NTS 12-H NW, Newfoundland and Labrador--Leve aeromagnetique extracotier de l'ouest de Terre-Neuve, SNRC 12-H NW, Terre-Neuve-et-Labrador. Geological Survey of Canada : Calgary, AB, Canada, Canada.

Dumont, R. & Jones, A. 2013n. Aeromagnetic survey of offshore western Newfoundland, NTS 12-I NW and part of 12-J NW, 12-O SE, 12-P SW, Newfoundland and Labrador--Leve aeromagnetique extracotier de l'ouest de Terre-Neuve, SNRC 12-I NW et partie de 12-J NW, 12-O SE, 12-P. Geological Survey of Canada : Calgary, AB, Canada, Canada.

Dumont, R. & Jones, A. 2013o. Aeromagnetic survey of offshore western Newfoundland, NTS 12-I SW, Newfoundland and Labrador--Leve aeromagnetique extracotier de l'ouest de Terre-Neuve, SNRC 12-I SW, Terre-Neuve-et-Labrador. Geological Survey of Canada : Calgary, AB, Canada, Canada.

Dumont, R. & Jones, A. 2013p. Aeromagnetic survey of offshore western Newfoundland, NTS 12-J SE, Newfoundland and Labrador--Leve aeromagnetique extracotier de l'ouest de Terre-Neuve, SNRC 12-J SE, Terre-Neuve-et-Labrador. Geological Survey of Canada : Calgary, AB, Canada, Canada.

Durling, P., Harvey, P. & Howells, K. 1995. Geophysical evidence for thrust faulting in the Carboniferous Antigonish-Mabou Subbasin, Nova Scotia.

Durling, P. & Marillier, F. 1993a. Structural elements and sedimentation patterns in the Magdalen Basin. *Atlantic Geology* **29**(1), 78-78.

Durling, P. & Marillier, F. 1993b. Structural elements of the Magdalen Basin, Gulf of St. Lawrence, from seismic reflection data. Geological Survey of Canada Paper 93-1D, Canada, 147-154.

Durling, P. W. & Marillier, F. J. Y. 1990. Structural trends and basement rock subdivisions in the western Gulf of St. Lawrence, northern Appalachians. *1990*.

Eggleston, L. K. 2017. Deformation and kinematic history of the Sackville and Moncton Sub-basins, southeastern New Brunswick, Maritimes Basin of Atlantic Canada, University of Alberta.

Enachescu, M. E. 1992. Basement extension on the Newfoundland continental margin (Canadian east coast). *Proceedings of the International Conference on Basement Tectonics* **7, Vol. 1**, 227-256.

Garcia, S. F. d. M., Letouzey, J., Rudkiewicz, J.-L., Danderfer Filho, A. & Frizon de Lamotte, D. 2012. Structural modeling based on sequential restoration of gravitational salt deformation in the Santos Basin (Brazil). *Marine and Petroleum Geology* **35**(1), 337-353.

Ge, H., Jackson, M. P. A. & Vendeville, B. C. 1997. Kinematics and dynamics of salt tectonics driven by progradation. *AAPG Bulletin* **81**(3), 398-423.

Gibling, M. R., Culshaw, N., Pascucci, V., Waldron, J. W. F. & Rygel, M. C. in press 2018. The Maritimes Basin of Atlantic Canada: Basin Creation and Destruction during the Paleozoic Assembly of Pangea. In: *Sedimentary Basins of the World* (edited by Miall, A.) **5**.

Gibling, M. R., Culshaw, N., Rygel, M. C. & Pascucci, V. 2008. Chapter 6 The Maritimes Basin of Atlantic Canada: Basin Creation and Destruction in the Collisional Zone of Pangea. In: *Sedimentary Basins of the World 5* (edited by Miall, A. D.). Elsevier, 211-244.

Giles, K. A. & Lawton, T. F. 2002. Halokinetic Sequence Stratigraphy Adjacent to the El Papalote Diapir, Northeastern Mexico. *AAPG Bulletin* **86**(5), 823-840.

Giles, K. A. & Rowan, M. G. 2012. Concepts in halokinetic sequence deformation and stratigraphy. *Geological Society Special Publications* **363**, 7-31.

Giles, P. & Lynch, G. 1993. Bedding-parallel faults, breccia zones, large-scale recumbent folds and basin evolution: the case for extensional tectonics in the onshore Magdalen Basin in Nova Scotia. *Atlantic Geology*, 81.

Giles, P. S. 1981. *Major Transgressive-Regressive Cycles in Middle to Late Visean Rocks of Nova Scotia. Mineral Resources Division Report of Activities 1981*, Nova Scotia Department of Mines and Energy.

Giles, P. S. 2008. Windsor Group (Late Mississippian) stratigraphy, Magdalen Islands, Quebec; a rare eastern Canadian record of late Visean basaltic volcanism. *Atlantic Geology* **44**, 167-185.

Giles, P. S. 2009. Orbital forcing and Mississippian sea level change: time series analysis of marine flooding events in the Visean Windsor Group of eastern Canada and implications for Gondwana glaciation. *Bulletin of Canadian Petroleum Geology* **57**(4), 449-471.

Giles, P. S. & Boehner, R. C. 2001. *Windsor Group Stratigraphy and Structure, Open File Report ME 2003-2. Geologial Mapping for Mineral Development, South-central Cape Breton Island Targeted Geoscience Initiative (TGI)*. Mineral Resources Branch, Nova Scotia Department of Natural Resources.

Giles, P. S. & Utting, J. 1999. *Maritimes Basin stratigraphy - Prince Edward Island and adjacent Gulf of St. Lawrence.*

Giles, P. S. & Utting, J. 2001. *SHELL-AMOCO Cap Rouge F-52 Gulf of St. Lawrence, eastern Canada.*

Goodman, N. R. 1952. Gypsum and Anhydrite in Nova Scotia. In: *Province of Nova Scotia Department of Mines Memoir No. 1*, 75.

Hall, J., Langdon, G., Roberts, B., Hawkins, D., Fagan, A., Knight, I. & Kilfoil, G. 1992. Reflection seismic imaging of the Carboniferous Bay St. George subbasin, onshore western Newfoundland: a reappraisal of Paleozoic stratigraphic thickness. *Bulletin of Canadian Petroleum Geology* **40**(4), 321-334.

Hamblin, A. P. & Rust, B. R. 1989. Tectono-sedimentary analysis of alternate-polarite half-graben basin-fill successions: Late Devonian-Early Carboniferous Horton Group, Cape Breton Island, Nova Scotia. *Basin Research* **2**, 239-255.

Hayward, N., Dehler, S. A., Grant, A. C. & Durling, P. 2014. Magnetic anomalies associated with salt tectonism, deep structure and regional tectonics in the Maritimes Basin, Atlantic Canada. *Basin Research* **26**(2), 320-337.

Hayward, N., Dehler, S. A. & Oakey, G. N. 2001. The structure of the northeastern Gulf of St. Lawrence, Canada: new insight from geophysical data analysis. *Canadian Journal of Earth Sciences* **38**, 1495-1516.

Hibbard, J. & Waldron, J. W. F. 2009. Truncation and translation of Appalachian promontories: mid-Paleozoic strike-slip tectonics and basin initiation. *Geology* **37**, 487-490.

Hu, K. & Dietrich, J. 2010. Petroleum reservoir potential of upper Paleozoic sandstones in the offshore Maritimes Basin, Eastern Canada. Geological Survey of Canada : Calgary, AB, Canada, Canada.

Hudec, M. R. & Jackson, M. P. A. 2004. Regional restoration across the Kwanza Basin, Angola: Salt tectonics triggered by repeated uplift of a metastable passive margin. *AAPG Bulletin* **88**(7), 971-990.

Hudec, M. R. & Jackson, M. P. A. 2007. Terra infirma: Understanding salt tectonics. *Earth-Science Reviews* **82**(1–2), 1-28.

Hudec, M. R., Jackson, M. P. A. & Schultz-Ela, D. D. 2009. The paradox of minibasin subsidence into salt: Clues to the evolution of crustal basins. *Geological Society of America Bulletin* **121**(1-2), 201-221.

Jackson, M. P. & Hudec, M. R. 2017. *Salt tectonics: Principles and practice.* Cambridge University Press.

Jackson, M. P. A. & Hudec, M. R. 2005. Stratigraphic record of translation down ramps in a passive-margin salt detachment. *Journal of Structural Geology* **27**(5), 889-911.

Jackson, M. P. A. & Talbot, C. J. 1991. *A Glossary of Salt Tectonics. No. 91-4*. Bureau of Economic Geology Geological Circular The University of Texas at Austin.

Jackson, M. P. A. & Vendeville, B. C. 1994. Regional extension as a geologic trigger for diapirism; with Suppl. Data 9401. *Geological Society of America Bulletin* **106**(1), 57-73.

Jahani, S., Callot, J.-P., Letouzey, J. & Frizon de Lamotte, D. 2009. The eastern termination of the Zagros fold and thrust belt, Iran; structures, evolution, and relationships between salt plugs, folding, and faulting. *Tectonics* **28**(6), @PaperTC6004-@PaperTC6004.

Jutras, P., Prichonnet, G. & McCutcheon, S. 2003. Alleghanian deformation in the eastern Gaspe Peninsula of Quebec, Canada. *Geological Society of America Bulletin* **115**(12), 1538-1551.

Kilfoil, G. J. 1988. An integrated gravity, magnetic, and seismic interpretation of the Carboniferous Bay St. George subbasin, western Newfoundland, Memorial University of Newfoundland.

Knight, I. 1983. Geology of the Carboniferous Bay St. George subbasin, Western Newfoundland. *Mineral Development Division Department of Mines and Energy, Government of Newfoundland and Labrador* **Memoir 1**.

Kontak, D. J., Ansdell, K. & Douglas, A. 2000. Zn-Pb mineralization associated with a mafic dyke at Cheverie, Hants County, Nova Scotia: implications for Carboniferous metallogeny. *Atlantic Geology* **36**, 7-26.

Koyi, H. 1998. The shaping of salt diapirs. *Journal of Structural Geology* **20**(4), 321-338.

Koyi, H. A., Ghasemi, A., Hessami, K. & Dietl, C. 2008. The mechanical relationship between strike-slip faults and salt diapirs in the Zagros fold-thrust belt. *Journal of the Geological Society of London* **165**(6), 1031-1044.

Langdon, G. S. & Hall, J. 1994. Devonian-Carboniferous tectonics and basin deformation in the Cabot Strait area, Eastern Canada. *AAPG Bulletin* **78**(11), 1748-1774.

Martel, T. & Durling, P. 2005. The McCully gas field; production, reserves and challenges. *Atlantic Geology* **41**(1), 71-71.

McBride, B. C., Weimer, P. & Rowan, M. G. 1998. The effect of allochthonous salt on the petroleum systems of northern Green Canyon and Ewing Bank (offshore Louisiana), northern Gulf of Mexico. *AAPG Bulletin* **82**(5B), 1083-1112.

McCutcheon, S. R. & Robinson, P. T. 1987. Geological constraints on the genesis of the Maritimes Basin, Atlantic Canada. In: *Sedimentary Basins and Basin-Forming Mechanisms* (edited by Beaumont, C. & Tankard, A. J.) **5**. Atlantic Geoscience Society Special Publications, Halifax, 287-297.

McGregor, D. C. & McCutcheon, S. R. 1988. Implications of spore evidence for Late Devonian age of the Piskahegan Group, southwestern New Brunswick. *Canadian Journal of Earth Sciences* **25**(9), 1349-1364.

Miller, H. G., Kilfoil, G. & Peavy, S. T. 1990. An integrated geophysical interpretation of the Carboniferous Bay St. George Subbasin, Western Newfoundland. *Bulletin of Canadian Petroleum Geology* **38**(3), 320-331.

Murphy, J. B. & Keppie, J. D. 2005. The Acadian Orogeny in the Northern Appalachians. *International Geology Review* **47**(7), 663-687.

Murphy, J. B., Waldron, J. W. F., Kontak, D. J., Pe-Piper, G. & Piper, D. J. W. 2011. Minas Fault Zone: Late Paleozoic history of an intra-continental orogenic transform fault in the Canadian Appalachians. *Journal of Structural Geology* **33**, 312-328.

Opdyke, N. D., Giles, P. S. & Utting, J. 2012. Magnetic stratigraphy and palynostratigraphy of the Mississippian - Pennsylvanian boundary interval in eastern North America and the stratigraphic position of the beginning of the Kiamen. *American Geophysical Union Fall Meeting* **2012**, GP13B-1124.

Palmer, S. E., Waldron, J. W. F. & Skilliter, D. M. 2002. Post-Taconian shortening, inversion and strike slip in the Stephenville area, western Newfoundland. *Canadian Journal of Earth Sciences* **39**, 1393-1410.

Peavy, S. T. 1985. A gravity and magnetic interpretation of the Bay St. George Carboniferous subbasin in western Newfoundland, Memorial University of Newfoundland Master of Science Thesis.

Peel, F. J. 2014. How do salt withdrawal minibasins form? Insights from forward modelling, and implications for hydrocarbon migration. *Tectonophysics* **630**, 222-235.

Pinet, N., Dietrich, J., Duchesne, M. J., Hinds, S. J. & Brake, V. 2018. Low-angle faulting in strike-slip dominated settings: Seismic evidence from the Maritimes Basin, Canada. *Tectonophysics* **738-739**, 33-40.

Rehill, T. A., Gibling, M. R. & Williamson, M. A. 1995. Stratigraphy of the Central Maritimes Basin, eastern Canada: non-marine sequence stratigraphy. In: *Current Research 1995-E*. Geological Survey of Canada, 221-231.

Rhoden, H. N. 1998. *Preliminary evaluation of Fischells Brook rock-salt deposit in western Newfoundland, a mining project to supply the Atlantic-coast road de-icing market.*, St. John's Newfoundland.

Roselli, C. 2003. Transpression and overthrusting in the Minas basin, Nova Scotia. Unpublished M.Sc. thesis, University of Alberta.

Shaw, J., Courtney, R. C. & Currie, J. R. 1997. Marine geology of St. George's Bay, Newfoundland, as interpreted from multibeam bathymetry and back-scatter data. *Geo-Marine Letters* **17**(3), 188-194.

Snyder, M. E. & Waldron, J. W. F. 2016. Unusual soft-sediment deformation structures in the Maritimes Basin, Canada; possible seismic origin. *Sedimentary Geology* **344**, 145-159.

Spathopoulos, F. 1996. An insight on salt tectonics in the Angola Basin, South Atlantic. *Geological Society, London, Special Publications* **100**(1), 153.

Stockmal, G. S., Slingsby, A. & Waldron, J. W. F. 1998. Deformation styles at the Appalachian structural front, western Newfoundland: implications of new industry seismic reflection data. *Canadian Journal of Earth Sciences* **35**(11), 1288-1306.

Thomas, W. A. 1977. Evolution of the Appalachain-Ouachita salients and recesses from reentrants and promontories in the continental margin. *American Journal of Science* **277**, 1233-1278.

Thomas, W. A. 1991. The Appalachian Ouachita rifted margin of southeastern North America. *Geological Societry of America Bulletin* **103**, 415-431.

Trusheim, F. 1960. Mechanism of salt migration in northern Germany. *AAPG Bulletin* **44**(9), 1519-1540.

Utting, J. & Giles, P. S. 2004. Biostratigraphical implications of new palynological data from the MIssissippian of Newfoundland and Nova Scotia, Canada. In: *Memoirs of the Association of Australasian Palaeontologists* **29**, 115-160.

Utting, J. & Giles, P. S. 2008. Palynostratigraphy and lithostratigraphy of Carboniferous Upper Codroy Group and Barachois Group, southwestern Newfoundland. *Canadian Journal of Earth Sciences* **45**(1), 45-67.

Utting, J. & Hamblin, A. P. 1991. Thermal maturity of the lower carboniferous Horton group, Nova Scotia. *International Journal of Coal Geology* **19**(1–4), 439-456.

Wagner III, B. H. & Jackson, M. P. A. 2011. Viscous flow during salt welding. *Tectonophysics* **510**, 309-326.

Waldron, J. W. & van Staal, C. R. 2001. Taconian orogeny and the accretion of the Dashwoods block: A peri-Laurentian microcontinent in the Iapetus Ocean. *Geology* **29**(9), 811-814.

Waldron, J. W. F. 2004. Anatomy and evolution of a pull-apart basin, Stellarton, Nova Scotia. *Geological Society of America Bulletin* **116**(1-2), 109-127.

Waldron, J. W. F., Anderson, S. D., Cawood, P. A., Goodwin, L. B., Hall, J., Jamieson, R. A., Palmer, S. E., Stockmal, G. S. & Williams, P. F. 1998. Evolution of the Appalachian Laurentian margin: lithoprobe results in western Newfoundland. *Canadian Journal of Earth Sciences* **35**, 1271-1287.

Waldron, J. W. F., Barr, S. M., Park, A. F., White, C. E. & Hibbard, J. 2015. Late Paleozoic strike-slip faults in Maritime Canada and their role in the reconfiguration of the northern Appalachian orogen. *Tectonics* **34**(8), 1661-1684.

Waldron, J. W. F., Roselli, C. & Johnston, S. K. 2007. Transpressional structures on a Late Paleozoic intracontinental transform fault, Canadian Appalachians. In: *Tectonics of Strike-Slip Restraining and Releasing Bends* (edited by Cunningham, W. D., and Mann, P.). Geological Society, London, Special Publications 290, 367-385.

Waldron, J. W. F., Roselli, C., Utting, J. & Johnston, S. K. 2010. Kennetcook thrust system: late Paleozoic transpression near the southern margin of the Maritimes Basin, Nova Scotia. *Canadian Journal of Earth Sciences* **47**, 137-159.

Waldron, J. W. F. & Rygel, M. C. 2005. Role of evaporite withdrawal in the preservation of a unique coal-bearing succession: Pennsylvanian Joggins Formation, Nova Scotia. *Geology* **33**(5), 337-340.

Waldron, J. W. F., Rygel, M. C., Gibling, M. R. & Calder, J. H. 2013. Evaporite tectonics and the late Paleozoic stratigraphic development of the Cumberland Basin, Appalachians of Atlantic Canada. *Geological Society of America Bulletin* **125**(5-6), 945-960.

Waldron, J. W. F., White, J. C., MacInnes, E. & Roselli, C. 2005. Transpression and transtension along a continental transform fault: Minas Fault Zone, Nova Scotia. *Geological Association of Canada - Mineralogical Association of Canada - Canadian Society of Petroleum Geologists - Canadian Society of Soil Sciences Joint Meeting - Halifax, May 2005. Field Trip B7.*

Weimer, P., Bouroullec, R., van den Berg, A. A., Lapinski, T. G., Roesink, J. G. & Adson, J. 2017. Structural setting and evolution of the Mensa and Thunder Horse intraslope basins, northern deep-water Gulf of Mexico: A case study. *AAPG Bulletin* **101**(7), 1145-1172.

White, S. E. 2018. Evolution of the Western Newfoundland Appalachian Orogen and its Foreland Basin, University of Alberta.

Williams, H. 1979. Appalachian Orogen in Canada. *Canadian Journal of Earth Sciences* **16**, 792-807.

Williams, H. 1985. Geology, Stephenville Map Area, Newfoundland (edited by Geological Survey of Canada, M. A.).

Wilson, P. & White, J. C. 2006. Tectonic evolution of the Moncton Basin, New Brunswick, Eastern Canada; new evidence from field and sub-surface data. *Bulletin of Canadian Petroleum Geology* **54**(4), 319-336.

Wilson, P., White, J. C. & Roulston, B. V. 2006. Structural geology of the Penobsquis salt structure; late Bashkirian inversion tectonics in the Moncton Basin, New Brunswick, Eastern Canada. *Canadian Journal of Earth Sciences = Revue Canadienne des Sciences de la Terre* **43**(4), 405-419.

Chapter 5. Fracture overprinting history using Markov chain analysis: Windsor-Kennetcook subbasin, Maritimes Basin, Canada

The deformation history of the Upper Paleozoic Maritimes Basin, Atlantic Canada, can be partially unraveled by examining fractures (joints, veins, and faults) that are well exposed on the shorelines of the macrotidal Bay of Fundy, in subsurface core, and on image logs. Data were collected from coastal outcrops and well core across the Windsor-Kennetcook subbasin, a subbasin in the Maritimes Basin, using the circular scan-line and vertical scan-line methods in outcrop, and FMI Image log analysis of core. We use cross-cutting and abutting relationships between fractures to understand relative timing of fracturing, followed by a statistical test (Markov chain analysis) to separate groups of fractures. This analysis, previously used in sedimentology, was modified to statistically test the randomness of fracture timing relationships. The results of the Markov chain analysis suggest that fracture initiation can be attributed to movement along the Minas Fault Zone, an E–W fault system that bounds the Windsor-Kennetcook subbasin to the north. Four sets of fractures are related to dextral strike slip along the Minas Fault Zone in the late Paleozoic, and four sets are related to sinistral reactivation of the same boundary in the Mesozoic.

5.1. Introduction

The Upper Paleozoic Maritimes Basin is large (400 km maximum diameter) and deep (>12 km), covering a portion of onshore and offshore Atlantic Canada (Fig. 5.1) (Keppie 1982, Gibling et al. 2008). This basin formed in the Appalachians, following Devonian Acadian orogenic events, probably during a period of dextral transtension (Calder 1998, Hibbard & Waldron 2009, Waldron et al. 2015) though it was subsequently affected by dextral transpression (Waldron et al. 2007, Murphy et al. 2011, Waldron et al. 2015). Later, Mesozoic deformation associated with Atlantic opening inverted some of these structures in sinistral transtension (Wade et al. 1996, Tanner & Brown 1999), although minor later inversion is suggested by Withjack et al. (2009).

The basin fill displays a wide variety of fracture systems well exposed on the shorelines of the modern macrotidal Bay of Fundy (Fig. 5.1). Fractures are also documented by subsurface core and image logs collected during exploration for oil and natural gas. This paper aims to document the spatial and temporal arrangement of fracture systems across the Windsor-Kennetcook subbasin, a subbasin within the Maritimes Basin, and relate them to the deformation of the Maritimes Basin.

Fracture types present in the Windsor-Kennetcook subbasin include: calcite-filled veins, a variety of apparently barren fractures, and small-displacement faults. Fractures with aperture widths below the limit of field measurement (approximately 2 mm) are here termed 'closed joints'. Wider, apparently open fractures are commonly visible in outcrop; however, it is difficult to determine whether an original vein-filling mineral may have been removed during recent weathering. These fractures are here characterized simply as 'joints'.

Determining fracture timing can help unravel the history of brittle deformation through time, and shed light on the state of stress at the time of fracture propagation. Simple criteria for relative timing of fractures using abutting and intersecting relationships were described by Hancock (1985) and are our main source of information on timing. For example, in cleat, consistent patterns of abutting relationships are well documented (Laubach et al. 1998). More recent work by Becker et al. (2010), Fall et al. (2015), and Laubach et al. (2016) used textural cross-cutting relationships of quartz growth in cements and fluid inclusions within those cements to reconstruct fracture history. These additional criteria are most useful when looking at subsurface samples, where vein fills are well preserved. In outcrop examples, such as those examined in this study, calcite vein fills are unreliably preserved. In these cases we have relied upon abutting and intersecting relationships to provide evidence of relative timing.

Fracture initiation has been linked to tectonic events, by many authors (Engelder 1985, Hancock 1985, Pollard & Aydin 1988). Becker et al. (2010) note that not all fracture sets reflect discrete

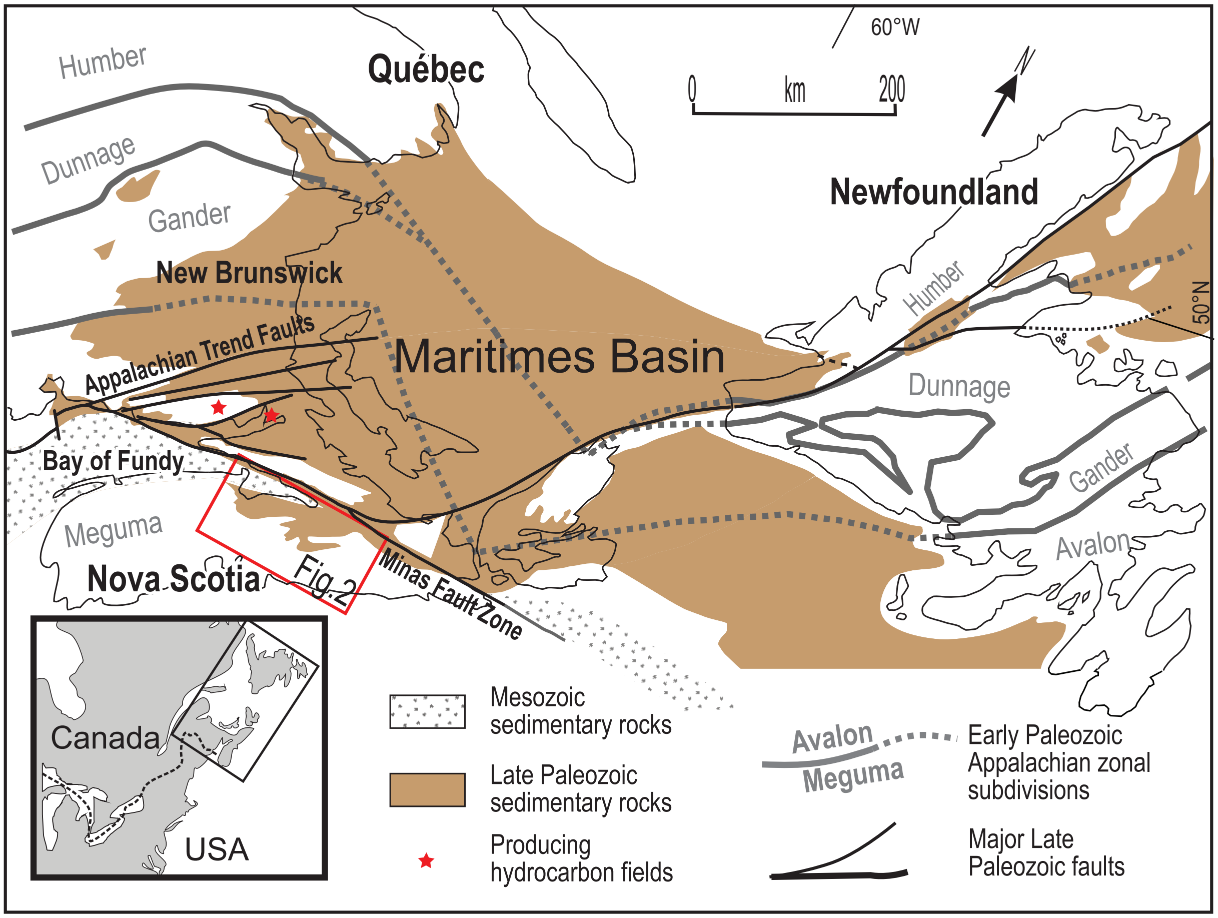

Figure 5.1. Map of Maritimes Basin in Atlantic Canada.

Location of Windsor-Kennetcook subbasin (Figure BB) is highlighted in red. Faults parallel to the Appalachian structural trend, and Minas Fault Zone shown. Modified from Snyder and Waldron (2016).

events, and that fractures may form, and remain open, over periods of millions of years. In this study, we relate relative timing relationships to tectonic episodes that deformed rocks of the Maritimes Basin over a 150 million year span.

To understand the relationship of fractures to the tectonic history of a basin, a method is needed for the interpretation of relative fracture timing. Markov chain analysis is here used to separate groups of fractures and identify overall fracture history. Markov chain analysis is a statistical procedure that investigates timing relationships between events (Reading 1986, Ching et al. 2013). This method has been used in sedimentology, in understanding facies relationships, as described by Gingerich (1969), Miall (1973), and Reading (1986). A modification of this method is here applied in the analysis of fracture timing.

5.2. Regional Geology

The late Paleozoic Maritimes Basin of Atlantic Canada is structurally complex, consisting of multiple subbasins trending generally northeast and east, and separated by uplifted basement rocks (Boehner & Giles 1993, van de Poll et al. 1995, Murphy et al. 2011, Waldron et al. 2013, Waldron et al. 2015). The basin fill comprises predominantly Carboniferous clastic sedimentary rocks together with lesser carbonates and evaporites. The Windsor-Kennetcook subbasin of the Maritimes Basin (Fig. 5.2) is located in southern mainland Nova Scotia where the macrotidal shores of the Bay of Fundy provide excellent exposure of the basin fill.

5.2.1. Stratigraphy

Basement rocks beneath the Windsor-Kennetcook subbasin belong to the early Paleozoic Meguma terrane of the Canadian Appalachians (Williams 1979). The overlying latest Devonian to Tournaisian *Horton Group* is composed of alluvial, lacustrine, and potentially marine deposits (Bell 1924, Wightman et al. 1993, Allard et al. 2006, Gibling et al. 2008, Noade 2010, Snyder &

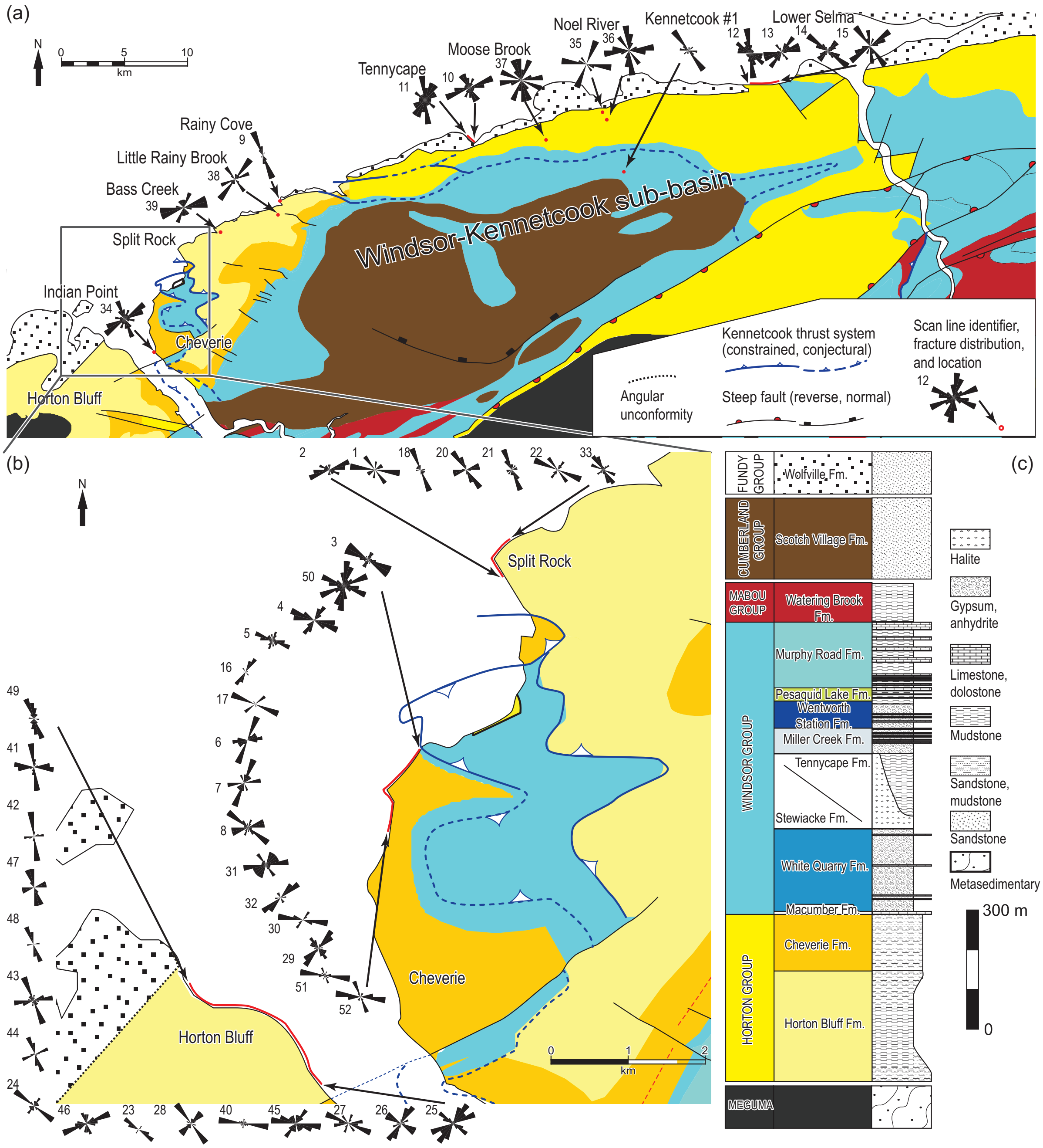

Figure 5.2. Windsor-Kennetcook subbasin

(a) map showing locations of measured rose diagrams; (b) enlarged map of Horton Bluff, Cheverie, and Split Rock showing locations of fracture circles and Kennetcook thrust; (c) stratigraphic column of units in study area modified from Waldron et al. (2010).

Waldron 2016). In the Windsor-Kennetcook subbasin, this group is divided into two formations, the lower Horton Bluff Formation and the upper Cheverie Formation (Fig. 5.2).

The overlying *Windsor Group* is dominantly marine shale, limestone and evaporite, representing the only fully marine incursion into the Maritimes Basin in the late Paleozoic (Gibling et al. 2008). In the Windsor-Kennetcook subbasin the lowermost units, the Macumber Formation and the Pembroke Breccia, are widely exposed. The Macumber Formation is a 2 – 10 m thick unit of finely laminated limestone interpreted by Schenk (1967) to have been formed in a shallow-water environment, by Savard et al. (1996) in deep water, and Lavoie et al. (1998) to have formed below storm wave base on a marine slope setting. The overlying Pembroke Breccia is an enigmatic unit composed of variably sized elongate clasts of weathered Macumber Formation within a grey to red carbonate-rich matrix (Bell 1924, Weeks 1948, Lavoie et al. 1995, Moore et al. 2000). Clasts in the breccia locally contain calcite-filled veins similar to those in the underlying Macumber Formation, suggesting that the veins were developed before breccia formation. Previous interpretations (Lavoie et al. 1998, Johnson 1999) have suggested that the breccia could have formed by slumping of microbial mats, tectonic brecciation, or solution collapse. Waldron et al. (2007) argue that the Pembroke Breccia is associated with movement in the Windsor evaporites that originally overlay the basal carbonates but became structurally interleaved during development of the Kennetcook thrust system. Overlying the Pembroke Breccia are alternations of marine limestone, evaporite, and red mudstone, characteristic lithologies of the Windsor Group (Boehner et al. 1999, Giles 2009).

The Serpukhovian *Mabou Group,* overlying the Windsor Group*,* comprises nonmarine red siltstone and sandstone (Belt 1965, Calder 1998). Unconformably overlying the Mabou Group are Bashkirian to Moscovian sandstone and shale of the *Cumberland Group* (Boehner 1996, Gibling et al. 2008), the youngest Carboniferous unit within the Windsor-Kennetcook subbasin. These two units crop out mainly in scattered inland exposures and were not investigated in this study.

Mesozoic strata in the Fundy basin area are continental red clastic rocks of the *Fundy Grou*p (Brown et al. 1995). The lowest unit of the Fundy Group is the dominantly sandstone and conglomeratic Triassic Wolfville Formation, which occurs above an angular unconformity on Horton Group strata of the Windsor-Kennetcook subbasin (Withjack et al. 1995, Wade et al. 1996, Leleu et al. 2010, Waldron et al. 2010).

5.2.2. Major faults

Steep faults striking NE–SW, parallel to the Appalachian Orogen, are common across the entire Maritimes Basin. In Nova Scotia, these faults include the Hollow and George River faults, and the Eastern Highlands Shear Zone (Fig. 5.1) (Hibbard & Waldron 2009). Hibbard and Waldron (2009) suggest that these faults, referred to as Appalachian-trend faults, (Waldron et al. 2015) were activated in the late Devonian; and that their motion was responsible for transtension at a major releasing bend in the margin of Laurentia, responsible for the formation of the Maritimes Basin.

The Minas Fault Zone, a late Paleozoic transform fault, strikes east-west through Atlantic Canada and separates the southern Meguma terrane and the northern Avalon terrane of the Appalachian Orogen (Fig. 5.1) (Keppie 1982, Murphy et al. 2011). This orientation is described as the Minas trend by Waldron et al. (2015). The Minas Fault Zone was dominantly dextral from the late Devonian to late Carboniferous (Murphy et al. 2011). It bounds the Windsor-Kennetcook subbasin to the north. In the early Mesozoic, the Minas Fault Zone was reactivated as a sinistral transtensional boundary of the Fundy half-graben during deposition of the Fundy Group (Wade et al. 1996, Tanner & Brown 1999, Withjack et al. 2009).

South of the Minas Fault Zone are duplications of Horton Group strata, generated by the Kennetcook thrust system that climbs up-section to the southeast and flattens into the Windsor evaporites (Fig. 5.2) (Waldron et al. 2010). The Windsor-Kennetcook subbasin thus includes both the allochthonous hanging wall and autochthonous footwall of the Kennetcook thrust system. The rocks in the hanging wall are steeply dipping and intensely deformed (Waldron et al. 2005, Waldron et al. 2010) by folds, faults, and evaporite-related structures. The footwall is gently dipping and less deformed but shows abundant joints, veins, faults, and folds.

In the Windsor-Kennetcook subbasin petroleum exploration has led to the acquisition of 2-D and 3-D seismic data and the drilling of 11 wells. On these seismic lines, faults dominate the otherwise planar stratigraphy in the Windsor-Kennetcook subbasin. Faults that initiate and terminate within the Horton Group indicate that the Windsor-Kennetcook subbasin was tectonically active during deposition of sediment. Murphy et al. (1994) suggest that the Minas Fault Zone was responsible for some of this synsedimentary activity. During this time interval, from Mississippian to early Pennsylvanian, faults and fractures initiated and propagated in the Windsor-Kennetcook subbasin (Waldron et al. 2015).

5.3. Economic implications

Petroleum exploration within the Maritimes Basin has focused on Lower Carboniferous rocks as both sources and reservoirs. Mississippian potential source rocks and/or unconventional reservoirs include black organic-rich shale and carbonate of the Horton Group (Bell 1958, Utting & Hamblin 1991, Bibby & Schimeld 2000, Dietrich et al. 2011). Horton Group reservoir rocks are typically sealed either by shale within the succession or by salt and anhydrite of the overlying Windsor Group (Dietrich et al. 2009). An initial discovery of petroleum in the Horton Group was made in 1909 at Stoney Creek in the Moncton subbasin of New Brunswick (Fig. 5.1) (Martel 2004, Dietrich et al. 2009). Subsequently, the 2000 discovery of natural gas at McCully (Martel & Durling 2005, Wilson & White 2006), also in the Moncton subbasin, has led to increased interest in the Horton Group as both a source and a reservoir target.

Mineral exploration and mining in the Windsor-Kennetcook subbasin targets barite, silver, gypsum, anhydrite, potash, salt, native sulphur, limestone, and dolostone in the Windsor Group

(Calder 1998, Boehner et al. 1999). Of particular interest is the Walton mine located within the study area (Fig. 5.2), a major historical producer of barite, Pb, Zn and Ag.

5.4. Data and methods

5.4.1. Overview

Fractures in the Windsor-Kennetcook subbasin are mainly perpendicular to bedding, presumably because layer-parallel anisotropy controlled fracture behavior. Most show little evidence of fracture-parallel slip, and are therefore characterized as joints and veins, or opening-mode fractures. In the following sections, fracture patterns are described across coastal outcrops and in subsurface core to determine both their overall distribution and the sequence of brittle deformation events in the area. Opening-mode fracture sets in sedimentary rocks are parallel or subparallel to each other (Pollard and Aydin 1988); they are typically interpreted as having formed perpendicular to the most tensile principal stress. In complexly fractured locales, there are multiple sets of fractures in varying orientations, which could have developed at variable times after deposition of strata. Consistent combinations of orientation and fracture type can help distinguish fracture systems.

5.4.2. Sampling locations

The study area includes coastal outcrops from Horton Bluff to Lower Selma and well-core from Kennetcook #1 and Kennetcook #2 (Fig. 5.2). It was selected because of excellent coastal exposure and proximity to exploration wells. The outcrop sites have been chosen where fractures are exposed on bedding surfaces (Fig. 5.3a, b) and in surfaces perpendicular to bedding in the adjacent cliffs. Sites were chosen in 2 – 20 cm thick siltstone, sandstone and paleosol beds within the Horton Bluff and Cheverie Formations (Horton Group), and limestone in the Macumber Forma-

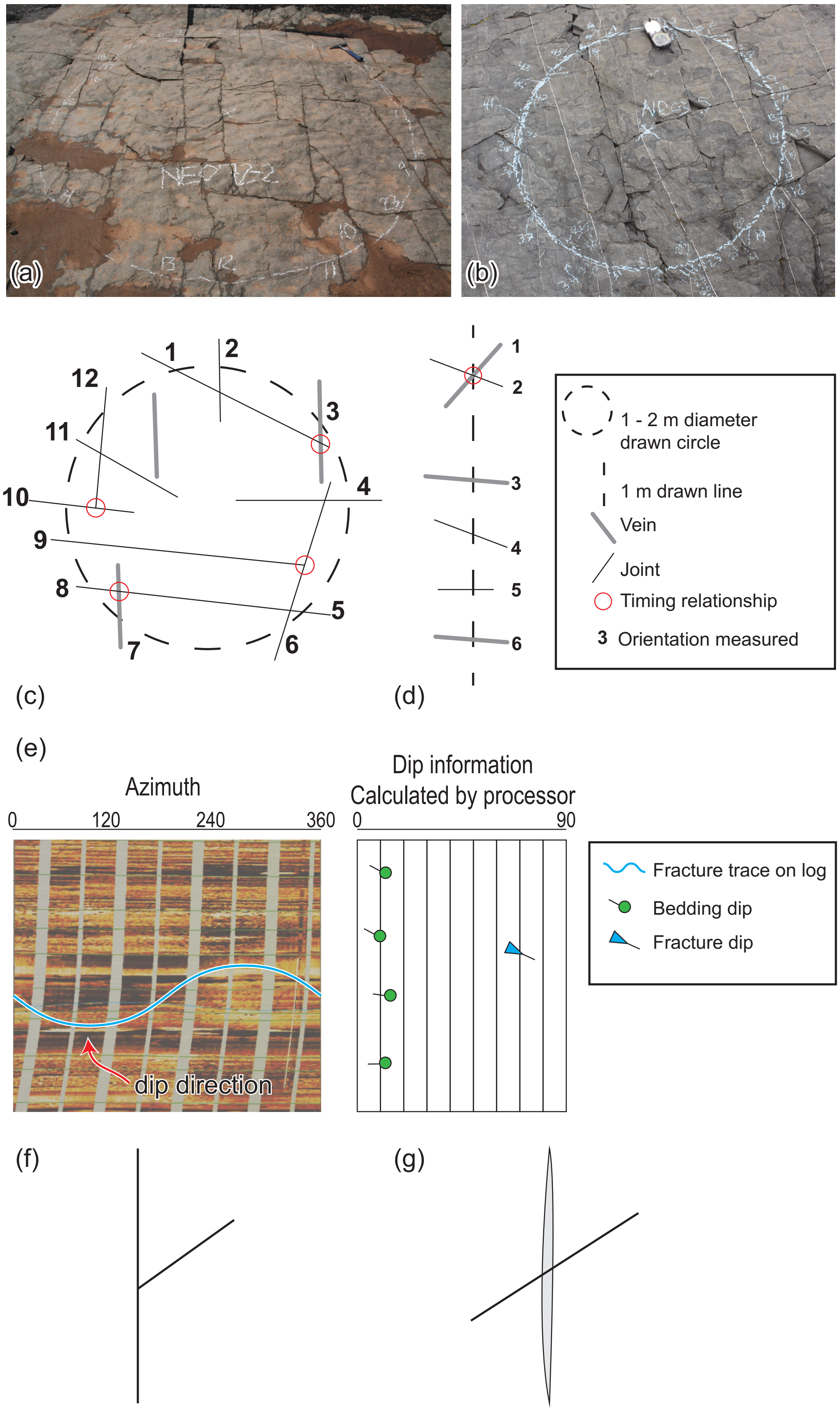
(a)
NE07-2-2
(b)
1
2
3
4
5
6
7
8
9
10
11
12
(c)
(d)
1 - 2 m diameter drawn circle
1 m drawn line
Vein
Joint
Timing relationship
3 Orientation measured
(e)
Azimuth
0
120
240
360
dip direction
Dip information
Calculated by processor
0
90
Fracture trace on log
Bedding dip
Fracture dip
(f)
(g)

Figure 5.3. Fracture data collection methods.

(a) Typical circular scan-line in the Horton Group showing open joints. (b) Circular scan-line in Horton Group showing open joints and calcite-filled veins. (c) Circular scan-line method. 1-2 m diameter circle is drawn an exposed bedding surface. Fractures intersecting the drawn circle are noted. Type, orientation, aperture width and timing relationships are recorded. (d) Vertical scan-line method. 1 m line is drawn perpendicular to bedding on exposed cliff. Fractures intersecting drawn line are noted. Type, orientation and timing relationships are recorded. (e) FMI Image log method. Fracture trace is a sinusoid wave highlighted on an image of the inside of a well. Azimuth is determined by the lowest point on the wave (dip direction) and converted to strike (right-hand-rule). The dip value is determined by the calculation: Dip = arctan (trough-to-peak amplitude of sinusoid/well-bore diameter) and was provided with the FMI data. (f) Fracture timing relationship showing a T-intersection of two open joints. The head of the T is the first fracture formed, and the second joint terminates once it hits the first fracture. (g) Fracture timing-relationship showing an open joint cross-cutting a vein; the joint post-dates the vein.

tion (Windsor Group). Fractures are typically regularly spaced, perpendicular to bedding, and terminate at lithological boundaries.

5.4.3. Data collection

To describe fracture networks fully, it is necessary to describe the fracture orientation, type, density, intensity, connectivity, extent, and aperture width (MacKay 2011a, b). In the statistical treatment of fractures, it is important to distinguish fracture *density* from fracture *intensity*. Fracture *density* measures the observed number of fractures in a region of unit size. Fracture density can be measured by counting the number of fractures intersecting a unit area or a unit volume of rock (Gauthier et al. 2012). Fracture density is often determined by counting unique points associated with fractures (e.g. fracture center points or terminations). For practical purposes when working on two-dimensional surfaces such as those observed in this study, density is commonly measured by counting the number of fracture terminations per unit area (Mauldon 1998, Rohrbaugh et al. 2002). Fracture *intensity* takes into account the size of the fractures and corresponds to the number of fractures per unit sample of length, the fracture length per unit area, or the fracture area per unit volume (Rohrbaugh et al. 2002, Singhal & Gupta 2010). Fracture intensity has the dimension $(\text{length})^{-1}$ regardless of whether length, area, or volume is considered, and incorporates both density and size of fractures (Rohrbaugh et al. 2002). On outcrop surfaces such as those considered here, fracture intensity may be assessed by counting the number of fractures intersecting a scan line.

Circular scan-line method

In outcrop studies, the geometry of rock outcrops can lead to a skewed sampling of fracture orientations. The circular scan-line method described by Heidrick and Titley (1982) and Davis et al. (2012) was chosen for the collection of data to reduce bias in two dimensions. Circles are drawn on a bedding surface and data are collected from all fractures that intersect the circumference of the circle (Fig. 5.3c). Documenting fractures in this way minimizes sampling bias resulting from the elongated geometry of the coastal outcrops (Rohrbaugh et al. 2002). The circular scan-line method measures fracture intensity, with dimension ($length^{-1}$) because it takes into account both the size and numerical abundance of fractures. Common fracture sets cross the scan-line once, and very long fracture sets are more likely to intersect the scan-line twice. Fracture sets with small spacing are also more likely to intersect the scan-line multiple times.

For this study, circles of 1–2 m diameter were drawn on bedding surfaces from 52 sites between Horton Bluff and Lower Selma (Fig. 5.2). For the majority of fractures at high angles to bedding, fracture orientations were noted as trends on bedding. In those cases where 3-D exposure was available, the strike and dip of the fracture was noted.

Relative timing of fracturing was determined from fracture intersections. Using the criteria of Hancock (1985) and Engelder and Gross (1993) when two fractures intersect, creating a T-intersection (Fig. 5.3f), the terminating fracture is interpreted to have initiated later. Some subsequent studies (Laubach & Diaz-Tushman 2009, Olson et al. 2009) have cast doubt on this criterion, suggesting that multiple sets of fractures may form T-intersections simultaneously, during bi-axial extension. In the latter case, we would expect to find no consistent T-intersections between simultaneously forming fracture sets, a prediction that is tested below. Cross-cutting relationships between veins and joints can be used as a second timing criterion, because where a vein is cut by an open joint, the vein must have formed before the joint (Fig. 5.3g).

Vertical scan-line method

Vertical scan-lines, 1 m long, were measured in cliff outcrops immediately adjacent to circular scan-lines to collect data in the third dimension (Figure 5.3d). Orientation, extent, presence/absence of fill, and fracture interactions were recorded for each fracture crossing the scan-line. Because fractures in the area of study are dominantly perpendicular to bedding, few visible fractures were intersected by vertical scan-lines. Therefore a vertical systematic measurement of fractures was attempted at only 3 locations.

FMI Image log method

Cores from the Kennetcook #1 and Kennetcook #2 wells (Fig. 5.2) were rotated when removed from the wells, making it impossible to orient fractures using the physical core samples. However Formation Micro-Imager (FMI) data, made available by Triangle Petroleum Corporation, show images of the inside of the well-bores by using shallow resistivity readings that are related to rock composition, structure, and fluid content (Ekstrom et al. 1987, Longman & Koepsell 2005). The image logs are directionally oriented. Structures (including bedding and fractures) appear on the logs as sinusoidal curves (Figure 5.3e).

5.5. Presentation of joint data

Orientation data collected using the circular scan-line, vertical scan-line, and FMI Image methods have been plotted using the program Spheristat3 (Pangaea Scientific). Rose diagrams (Fig. 5.2) display trends of fracture traces on bedding at these locations. For sites with >75 fractures, 5° bins have been used. For small data sets (n <75), many bins would contain zero or one data point; therefore a larger bin size (15°) is used.

As bedding dip increases, the fracture trend measured is increasingly affected by the tilt of strata. For beds that dip <30°, the fracture trend changes by at most ±4° if bedding is restored to horizontal by simple rotation about strike and dip. For this reason a 30° cutoff was used to separate data sets in the Markov chain analysis. This criterion effectively separates localities in the footwall (Fig. 5.4) from those in the hanging wall (Fig. 5.5) of the Kennetcook thrust. Where bedding is steeper (>30°), rotation of fractures by folding has to be taken into account. For simplicity, it is here assumed that bed dips developed from a single sub-horizontal fold generation resulting in

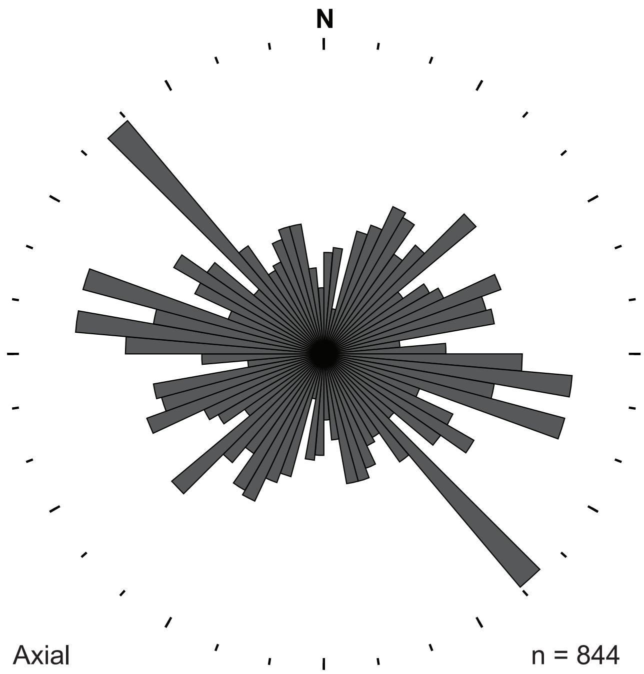

Figure 5.4. Composite rose diagram of all fractures measured from beds with dip <30°, modes at 005°, 025°, 045°, 068°, 098°, 123°, 140°, and 163°.

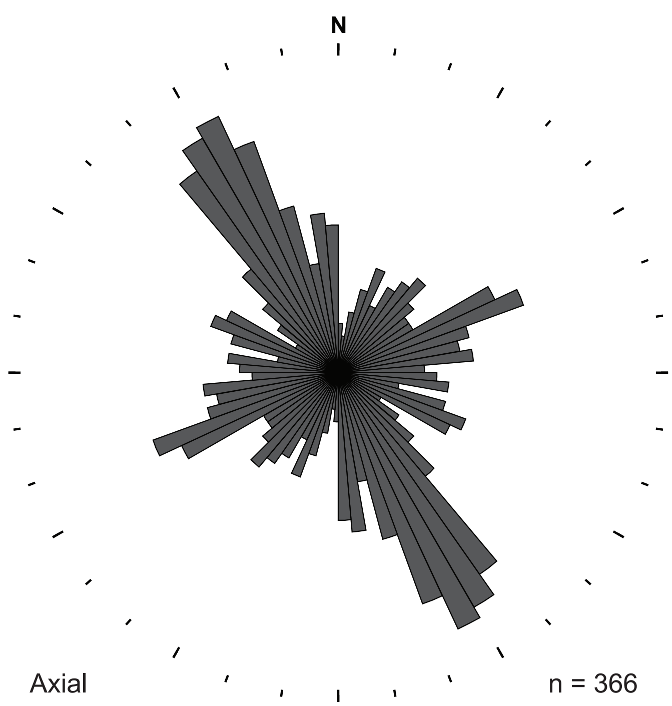

Figure 5.5. Composite rose diagram of all measured fractures from beds with dip >30°, modes NNE-SSW and ESE-WSW.

rotation about the strike of bedding, although more complex fold histories have been interpreted in some parts of the Windsor-Kennetcook subbasin (Waldron et al. 2007).

5.6. Markov chain analysis

Preliminary examination of the data shows that no completely consistent ordering describes all the observed relationships, but that some fracture sets preferentially display T-intersections or cross-cutting relationships with others. A statistical method is needed to determine whether a fracture set, when interpreted using these criteria, post-dates a differently oriented fracture set more often than expected in a random ordering, and thereby assess the significance of the observed orderings.

Markov chain analysis is a statistical procedure that investigates timing relationships between events in a time series (Reading 1986, Ching et al. 2013). This method has been used in sedimentology, in understanding facies relationships, as described by Gingerich (1969), Miall (1973), and Reading (1986), but has not been previously used to investigate fracture timing relationships, to the authors' knowledge. When used for facies relationships, the analysis examines whether one facies passes upward into another more often than would be expected in a purely random succession of facies (Reading 1986). Markov chain analysis combined with a simple hypothesis test (e.g. χ^2 test) can be used to test the randomness of facies ordering in the succession. We seek to use this method to investigate fracture orientations and their relative timing. The procedure, as it applies to fracture orientations measured within circular scan-lines, is described below and is shown in a step-by-step schematic in Figure 5.6. The null hypothesis in the following analysis is that fractures developed in a random order. The equations that follow were developed here to modify the sedimentary application of Markov chain analysis to the investigation of relative timing relationships between differently oriented fracture sets.

The first steps in a Markov chain analysis create an observed data array.

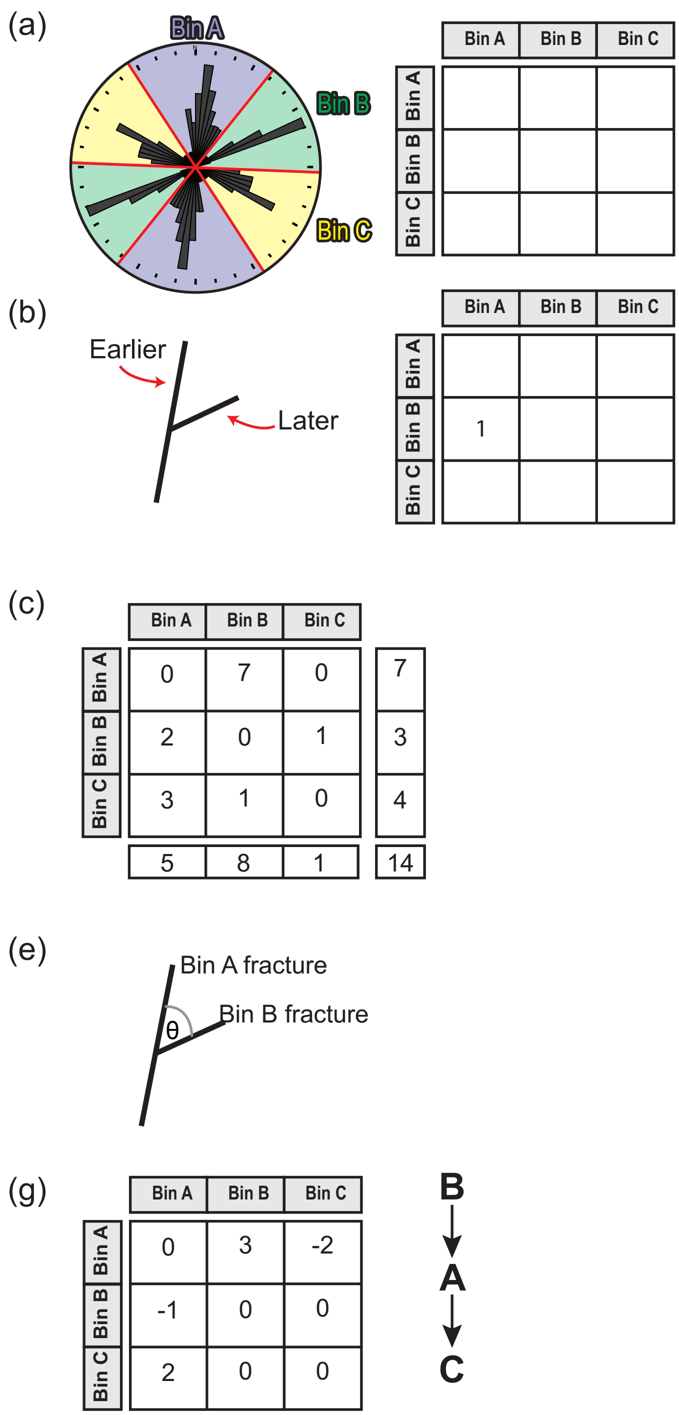

Figure 5.6. Workflow for Markov Chain analysis.

(a) Make an observed data table. Label rows and columns with bins corresponding to a composite rose diagram. (b) Tally observed timing relationships in the observed table. (c) Sum row and column tallies. (e) Determine angular relationship between fractures. Make an expected data table using Equation (3). (f) Make an observed-expected table. (g) Make a standardized residuals table using Equation (4). Using standardized residuals, create an order of events.

a. Define fracture sets and list them at the top of columns and end of rows of a square matrix such that each dominant mode is contained between the boundaries of a single bin.

b. Tally T-intersections and cross-cutting relationships. The intersection of row *a*, column *b* contains the number of times that fractures in bin *a* appear to post-date fractures in bin *b* ($O_{a,b}$).

c. Sum rows and columns individually, and total all inferred timing relationships in the bottom-right of the matrix.

The next three steps are used to create an expected data array, containing predicted fracture intersection counts based on the null hypothesis of random fracture order.

d. For orthogonal fractures, the values *E* in the expected data array follow the formula:

Equation (1) $E_{a,b} = n_a n_b / N$

Where: n_a = total fractures measured in row *a*

n_b = total fractures measured in column *b*

N = total number of fracture intersections, the sum of all the *E* values

e. However, the angular relationship between fracture sets affects the probability of a T-intersection being detected. Fractures near 90° apart are more likely to intersect within the scan-line than fractures with lower angles of intersection (Fig. 5.7). We therefore modify the method described by Gingerich (1969), Miall (1973), and Reading (1986), to account for this. The expected probability of fracture intersection within a unit fracture length is reduced by a factor of $\sin(|\theta_a-\theta_b|)$, where $|\theta_a-\theta_b|$ is the angle between fracture sets *a* and *b* as shown in Figure 5.6b. Modified expected cell values *E'* for the table of expected frequencies are therefore calculated as follows:

Equation (2) $E'_{a,b} = n'_a n'_b \sin(|\theta_a-\theta_b|)/N'$

Where n'_a = total fractures measured in bin *a* from all scan-lines

θ_a = azimuth of the midpoint of bin *a*

θ_b = azimuth of the midpoint of bin *b*

N' = Total number of predicted intersections, or the sum of all the *E'* values

f. A further modification is needed because *N'* differs from *N*. To normalize the observed and expected tables, the expected cell values *E'* are multiplied by a constant proportion *N/N'* to produce predicted frequencies *E** that sum to the correct total number of intersections *N* where:

Equation (3) $E^*_{a,b} = N\, n'_a n'_b \sin(|\theta_a-\theta_b|)/N'^2$

The next steps are to test for randomness and to create a standardized residuals table, showing the differences between the observed and expected frequencies of fracture intersections,

g. Test for randomness using a χ2 test following the procedure of Cochran (1954). Cells in the observed and expected data tables are grouped such that the sum of the groups is >5 which is the common minimum frequency used in statistics (Cochran 1954). In this study, groups were made by summing adja-

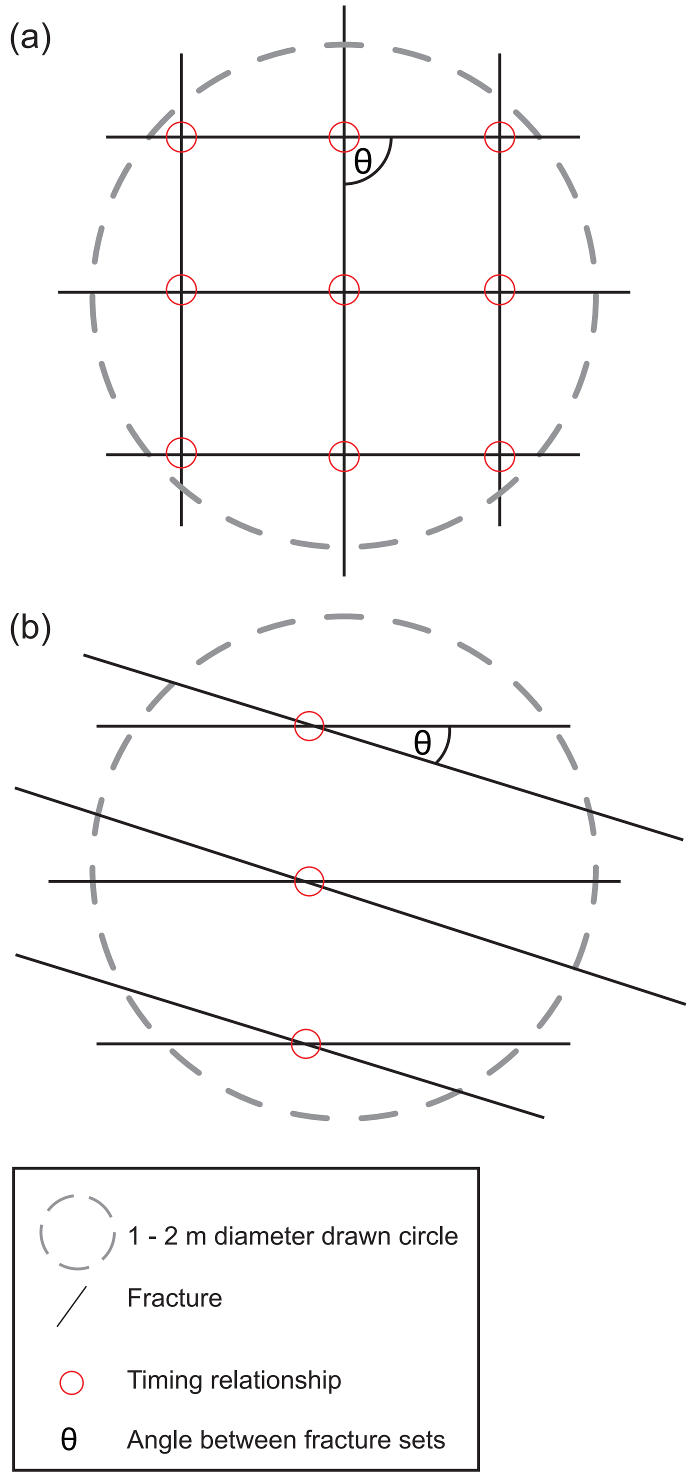

Figure 5.7. Angular relationship between fractures.

(a) Fractures with near 90° relationship intersect many times inside the circular scan-line. (b) Fracture sets with small angular relationship do not intersect inside the scan-line as often. This indicates that they are less likely to show timing relationships.

cent cells in the observed and expected tables until a value of ≥5 was reached. The degree of freedom for the χ^2 test is the total number of groups minus 1.

h. Create a table of standardized residuals in which each cell value is:

Equation (4) $R_{a,b} = [(O_{a,b} - E^*_{a,b})]/\sqrt{E^*_{a,b}}]$

Where: $R_{a,b}$ = standardized residual

$O_{a,b}$ = observed row a, column b number of intersections

$E^*_{a,b}$ = expected row a, column b number of intersections

Standardized residuals highlight intersections that occur more frequently than predicted by the null hypothesis of randomness, and show how many standard deviations above or below the expected value is the observed value.

5.7. Results

5.7.1. Joints and veins

A composite rose diagram (Fig. 5.4) displays all fractures measured from beds that dip <30°; 8 modes emerge at approximately 005°, 025°, 045°, 068°, 098°, 123°, 140°, and 163° (fractional angles are rounded to the nearest degree). Corresponding minima occur where the frequency of data points is lowest. These minima, chosen by visual inspection of the rose diagram, were used to separate observations into modal classes, corresponding to fracture sets, for analysis of fracture timing.

At locations with gently dipping strata, the most common modes are 163° and 098°. Outcrops at Horton Bluff, Cheverie, and Indian Point display gently dipping beds, and relationships between fracture sets at individual sites are easily determined. At Cheverie, the two dominant modes

(028° and 103°) are interpreted as conjugate shear fractures based on observed angular relationships. Scan-lines at Horton Bluff show modes at 040° and 128°, interpreted to be mutually orthogonal extension fractures.

Locations with steep bedding dips and abundant veins (e.g. Split Rock and Lower Selma) are interpreted to be within the allochthonous hanging wall of the Kennetcook thrust system. When displayed together on a rose diagram (no rotation to horizontal) two dominant modes at 068° and 153° emerge, with less defined modes striking 045° and 112° (Fig. 5.5). These modes are similar to those from locations with gently dipping strata (e.g. Horton Bluff and Cheverie), in the footwall of the thrust.

Fractures exposed in Kennetcook #1 and Kennetcook #2 core are dominantly open joints. Slabbed core from the Kennetcook #1 well was available from depth 4365 – 3111 ft and 107 fractures were measured. The dominant modal classes of fractures from the Kennetcook #1 core are 093° and 138° (Fig. 5.2).

5.7.2. Interpretation of fracture timing

Field observations of cross-cutting relationships (examples in Fig. 5.3f, g), and fold-fracture relationships allow first-level interpretation of fracture timing. For example, a scan-line at Cheverie in the subhorizontal Macumber Formation shows multiple generations of fractures, including closed joints (fractures with no measureable aperture width), open joints, and calcite-filled veins with blocky or fibrous fill of variable orientation (Fig. 5.8). We interpret that calcite-filled veins are better preserved at this location because the carbonate-rich host rock saturates pore water with calcium carbonate. Fracture intersections indicate that the earliest fracture sets are dominantly closed joints and fibrous veins trending ESE-WNW (100° - 120°). The second set comprises dominantly blocky calcite-filled veins trending NE-SW (055° - 070°) that dextrally offset the earlier fracture set. A third fracture set includes calcite-filled veins with red staining at the

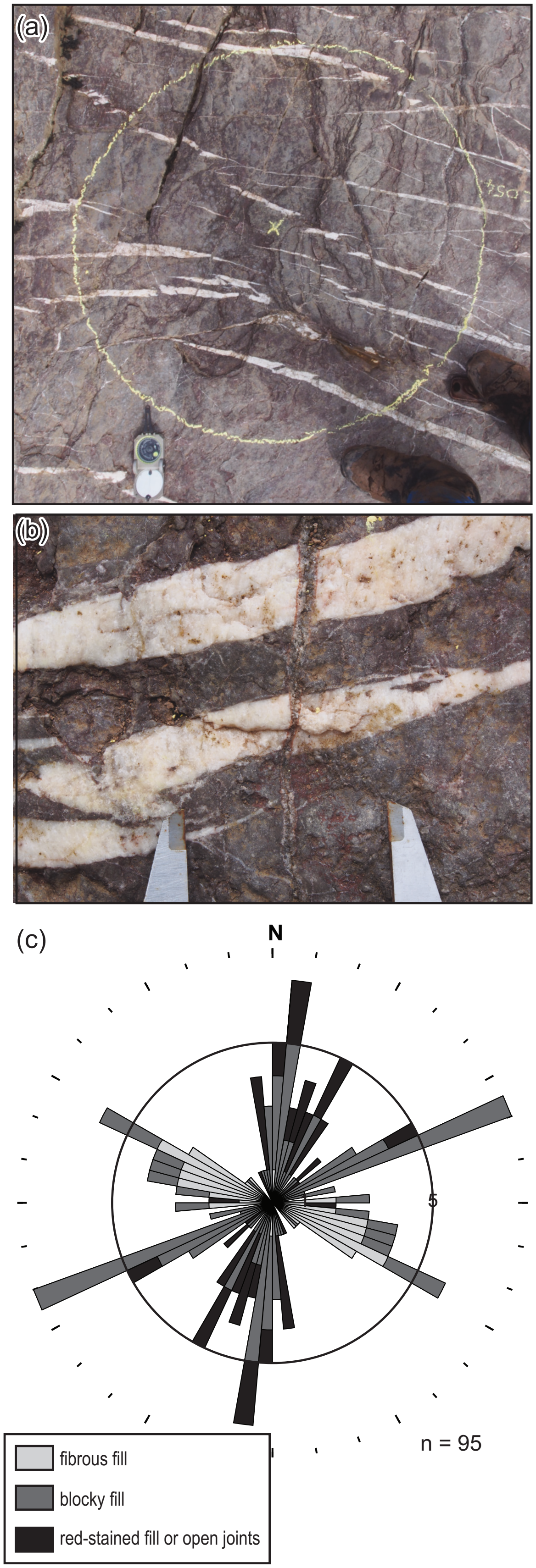

Figure 5.8. (a) Photograph of circular scan-line from the Macumber Formation at Cheverie; (b) vein showing red staining in centre line; (c) rose diagram showing three types of fractures.

Figure 5.9. Sinistral *en echelon* veins in the Macumber Formation (left) adjacent to the Pembroke Breccia (right). Blocks of Macumber Formation show veins that do not extend into the matrix of the breccia.

median line and open joints trending generally NNE-SSW (350° - 030°) that sinistrally offsets the second set.

Joints and veins were also noted in the Pembroke Breccia that immediately overlies the Macumber Formation. Clasts of Macumber Formation, within the Pembroke Breccia, are of variable orientation. Veins within these clasts are fiber-filled terminate at the edges of the clasts (Fig. 5.9), suggesting the veins formed before the formation of the Pembroke Breccia (Fig. 5.9). Open joints at this location cut across clasts and matrix trending approximately 040°. This mode is similar to the latest fracture set noted in the intact Macumber Formation (Fig. 5.8). Our interpretation is that the earlier fiber-filled veins were formed before development of the Pembroke Breccia, whereas the open joints initiated in a later stress regime. This would be consistent with the interpretation of Lavoie et al. (1995), who note local inclusion of Mesozoic material in the breccia and conclude that later evaporite solution and collapse played a role in its formation.

At locations in both the footwall and hanging wall of the Kennetcook thrust, where fractures were measured on both limbs of a fold, distributions show similar modes. Additionally, fractures are observed continually across folds without measureable deflection. These observations indicate that these fracture sets likely initiated after most of the folding history.

For fractures measured on beds dipping <30°, eight bin boundaries were chosen at minima in the composite rose diagram (Fig. 5.4) for use in Markov chain analysis. These eight bin boundaries are: 012.5°, 037.5°, 052.5°, 082.5°, 112.5°, 132.5°, 147.5°, and 177.5°. T-intersections and vein-joint interactions (Fig. 5.3f, g) were used to distinguish relative ages of fractures. Timing relationships from 35 sites, using 653 measured fractures, displaying 252 timing relationships (N) were tallied in the observed frequency table (Fig. 5.10). The expected frequency table (Fig. 5.11) used the midpoints of the bins to estimate θ ($N'=252$). A standardized residuals table is shown in Figure 5.12.

	005°	025°	045°	068°	098°	123°	140°	163°	Total
005°	0	0	2	2	2	2	2	0	11
025°	1	0	2	6	27	19	4	2	61
045°	0	1	0	3	21	13	13	3	54
068°	1	5	4	0	8	17	12	0	47
098°	1	3	3	4	0	1	5	3	20
123°	2	8	7	0	6	0	1	0	24
140°	0	3	7	2	2	2	0	0	16
163°	0	3	3	10	2	2	0	0	20
Total	5	23	28	27	68	56	37	8	252

Figure 5.10. Observed data table for Markov Chain analysis. Columns represent earlier fractures, rows represent later fractures.

	005°	025°	045°	068°	098°	123°	140°	163°
005°	0.0	0.9	1.3	2.5	2.8	2.6	0.9	0.4
025°	0.9	0.0	2.9	7.6	11.0	11.8	4.7	3.4
045°	1.3	2.9	0.0	3.3	7.1	9.0	4.0	3.5
068°	2.5	7.6	3.3	0.0	6.0	10.1	5.0	5.2
098°	2.8	11.0	7.1	6.0	0.0	5.4	3.7	4.8
123°	2.6	11.8	9.0	10.1	5.4	0.0	1.7	3.5
140°	0.9	4.7	4.0	5.0	3.7	1.7	0.0	0.9
163°	0.4	3.4	3.5	5.2	4.8	3.5	0.9	0.0
								252

Figure 5.11. Expected data table for Markov Chain analysis. Cell values calculated using Equation (3).

	005°	025°	045°	068°	098°	123°	140°	163°
005°	-	-0.9	0.6	-0.3	-0.5	-0.4	1.2	-0.7
025°	0.1	-	-0.5	-0.6	4.8	2.1	-0.3	-0.8
045°	-1.1	-1.1	-	-0.2	5.2	1.3	4.5	-0.2
068°	-0.9	-0.9	0.4	-	0.8	2.2	3.1	-2.3
098°	-1.1	-2.4	-1.5	-0.8	-	-1.9	0.7	-0.8
123°	-0.4	-1.1	-0.7	-3.2	0.3	-	-0.5	-1.9
140°	-0.9	-0.8	1.4	-1.5	-0.9	0.2	-	-0.9
163°	-0.7	-0.2	-0.2	2.1	-1.3	-0.8	-0.9	-

Figure 5.12. Standardized residuals table for Markov Chain analysis. Cell values calculated using Equation (4).

No single sequence of fracture development can explain all the observed timing relationships; contradictory timing relationships are observed between most of the possible pairs of modes. In our work, some timing relationships are over-represented (beyond their expected frequencies in a random process) suggesting that a statistical approach may reveal patterns in the fracture sequence.

A χ^2 test is applied to test the null hypothesis of randomness. χ^2 (26, *N=252*) = 124.7, $p<0.001$. With 26 degrees of freedom, a χ^2 value of 124.7 exceeds the critical value of 45.6 at $p<0.001$. The null hypothesis is rejected; the fractures are not randomly ordered in time.

Standardized residuals represent how far (in standard deviations) the observed value deviates above or below the expected value. When used in our approach, these represent fracture sets with more or fewer intersections than would be predicted in random ordering. We used the standardized residuals to compare diagonally opposed cell values to determine relative timing. If a cell value is positive and the diagonally opposed value is negative, the column mode of the pair occurred before the row mode. In making these comparisons, we noted some examples where diagonally opposite cells both contained negative standardized residuals. No significance has been attached to these values.

The results of the Markov chain analysis are shown in a flow chart in Figure 5.13. The earliest fracture group contains the 098°, 140°, and 123° modes. The 045° mode is statistically later than these three. There are two groups later than the 045° mode. One group contains the 005° mode followed by the 025° mode. The second group contains the 068° mode followed by the 163° mode.

The group containing the 098°, 123°, and 140° modes has a complex timing relationship. According to the results of the Markov chain analysis, the 140° mode is earlier than the 098° mode; the 098° mode is earlier than the 123° mode; the 123° mode is earlier than the 140° mode. This

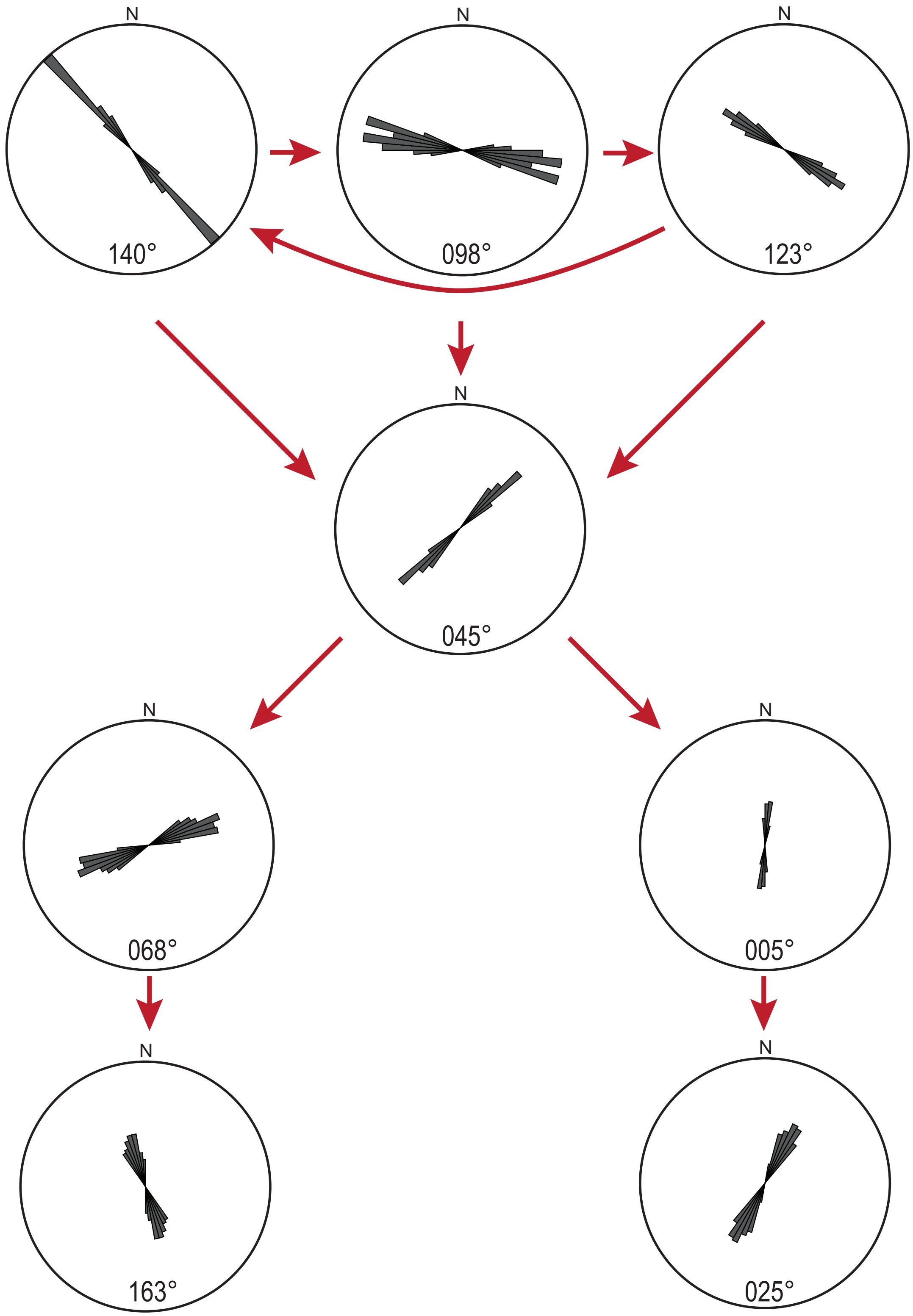

Figure 5.13. Resulting flow-chart from Markov Chain analysis. Top of the flow chart represents earliest fracture set. Arrows indicate sequence of fracture initiation.

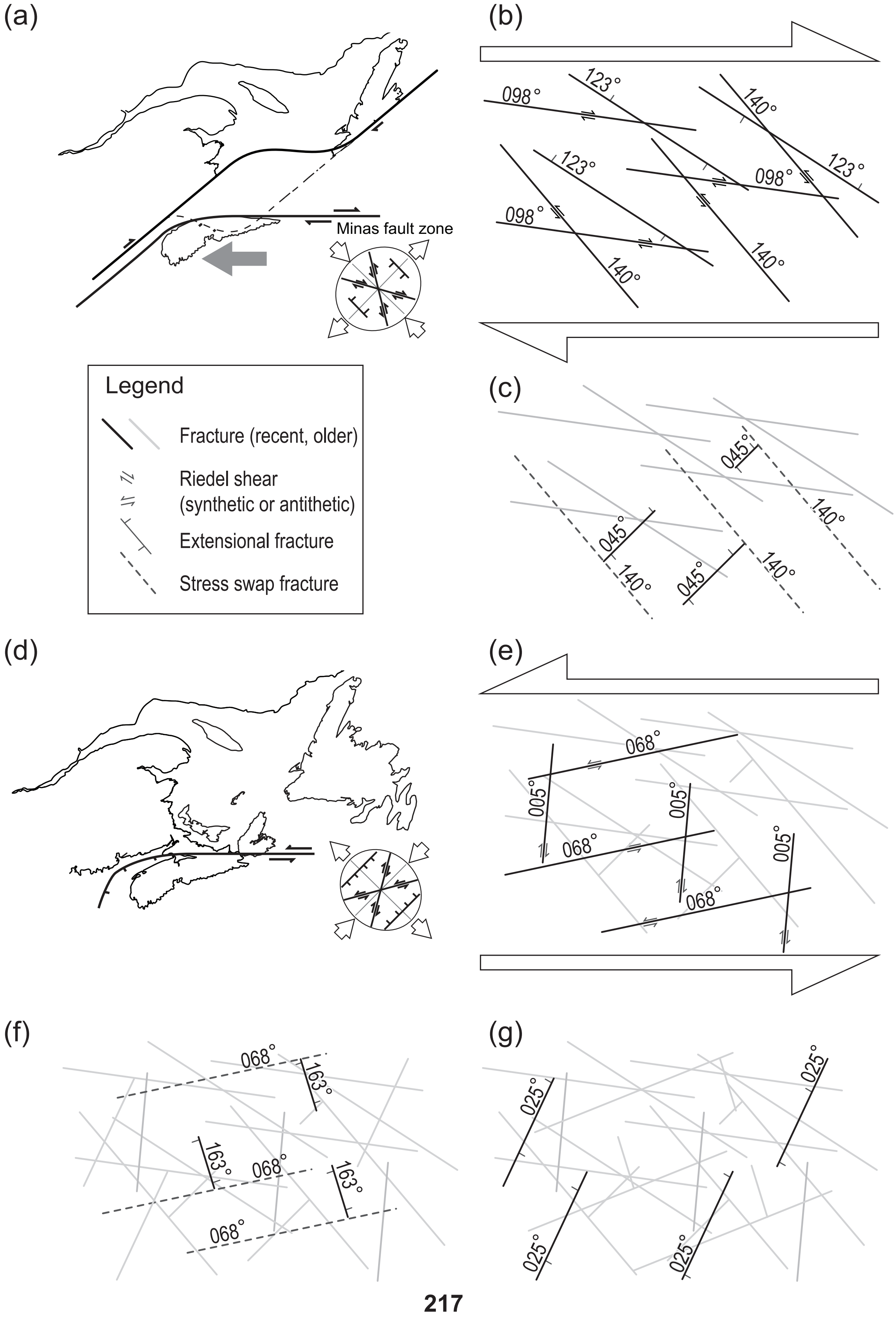
(a)
Minas fault zone
(b)
098°
123°
140°
(c)
045°
140°
Legend
Fracture (recent, older)
Riedel shear
(synthetic or antithetic)
Extensional fracture
Stress swap fracture
(d)
(e)
068°
005°
(f)
068°
163°
(g)
025°

Figure 5.14. Summary of fracture history.

(a) Carboniferous Maritimes Basin region map showing westward motion of southern Nova Scotia on the Minas Fault Zone and fracture orientations related to maximum and minimum horizontal stress, modified from Waldron et al. (2015); (b) first stage of fracture initiation related to (a); (c) second stage of fracture initiation after a stress swap; (d) Mesozoic Maritimes Basin region map showing sinistral motion on the Minas Fault Zone and fracture orientations related to minimum and maximum horizontal, modified from Waldron et al. (2015); (e) third stage of fracture initiation related to (d); (f)(g) fourth stage of fracture initiation where fracture initiation of 025° or 163° is unclear.

relationship is interpreted as the result of contemporaneous fracture initiation that rotated between these three modes.

The 005° mode and the 068° modes are both later than the 045° mode. There is no clear timing relationship between these two groups, other than in the Macumber Formation circular scan-line where fractures trending 068° are clearly cut by the 005° and 025° fractures. In comparing the row and column totals, there are few early 005° and 025° fractures, suggesting that these were amongst the most recent fractures to initiate.

5.8. Discussion

The interpreted fracture history is here related to deformation events in the Windsor-Kennetcook subbasin. However, our results show that fracture initiation was not a series of discrete 'events', but more likely occurred in overlapping episodes, resulting in a complicated series of cross-cutting and abutting fracture sets. Four main fracture groups are interpreted from the Markov chain analysis: (1) a group containing 098°, 123°, and 140° fracture sets; (2) the 045° fracture set; (3) the 005° and 025° fracture sets; (4) the 068° and 163° fracture sets.

We interpret that fractures in the first group initiated during the same time interval and that these are related to late Paleozoic dextral movement on the Minas Fault Zone (Fig. 5.14). Waldron et al. (2007) note multiple thrust faults verging SE, and normal faults, tension gashes, and boudins trending NW-SE. They interpret major NW-SE shortening and minor NE-SW extension. The 098° and 140° sets are interpreted as Riedel shears and the 123° set is the extensional fracture orientation associated with dextral strike-slip on roughly east-west strike-slip faults such as those in the Minas Fault Zone.

The 045° fractures are approximately perpendicular to the 140° set. In the Markov chain analysis, the 045° and 140° modes both have positive standardized residuals, and are commonly observed at the same sites. The 140° fracture set likely initiated first. Later in time, reactivation of the 140° set as extensional joints may have occurred, and the 045° set are interpreted to have formed as a result of temporary interchange of stress axis orientation, or stress swap, as envisaged by Caputo (1995). In this model, after a failure episode creates a fracture set, there is a drop in stress on the fracture surface as the local elastic energy is released; the normal stress on the free surface becomes equal to the fluid pressure and the shear stress becomes zero; at this drop, the intermediate (σ_2) and minimum compressive stress (σ_3) switch orientations (Hancock 1985, Caputo 1995, Bai et al. 2002). As a result of this swap in principal stresses, a second fracture set may form perpendicular to the first. After the initial stress drop, the stress may increase again, resulting in repeated fracture episodes with the same orthogonal orientations (Bons et al. 2012). In the examples we observed, both sets of fractures were approximately perpendicular to gently dipping beds suggesting that at the time of fracturing the exchanged intermediate and minimum stresses were horizontal, a configuration most likely to occur in an extensional or transtensional environment (Caputo 1995, Caputo 2005).

Two fracture groups are later than the 045° set, representing "branches" in the flow chart shown in Figure 5.13. One branch contains fractures trending 005° and 025°. The other branch contains fractures trending 068° and 163°. The 068° and 163° groups are interpreted as orthogonal fractures with an origin similar to the 140° and 045° groups, forming from a stress swap. These branches occur together, with no clear timing relationships at most locations. However at Cheverie, in the Macumber Formation (Fig. 5.8), the 005° set consistently offsets the 068° set with sinistral sense. This indicates that the 005° and 025° fracture sets were active after the 068° and 163° fracture sets. These fractures, together with those at 025° and 005° sets may be associated with sinistral reactivation of the E-W Minas Fault Zone during uplift and exhumation that occurred in the Triassic (Fig. 5.14), but preceded deposition of the Wolfville Formation (which does not display these fracture modes). The 068° and 005° modes are oriented as synthetic and antithetic Riedel shears while the 025° fracture set could be extensional fractures related to the same movement.

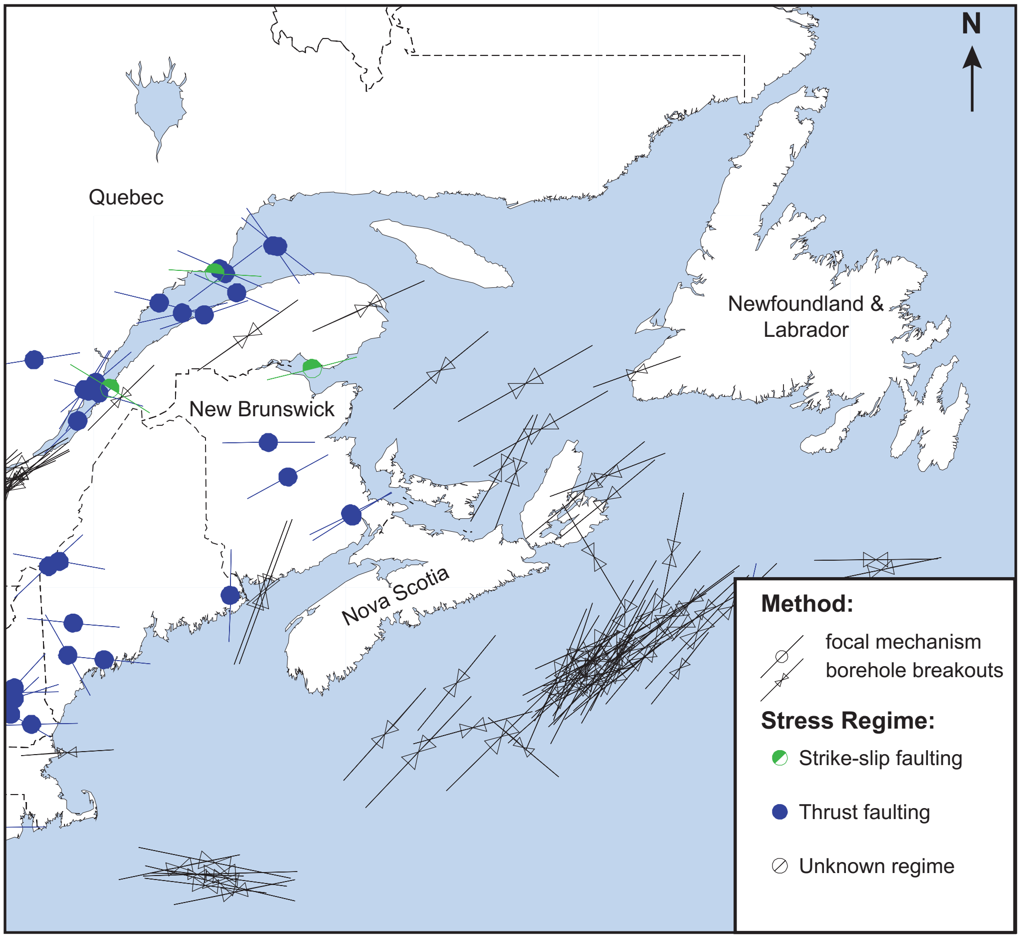

Figure 5.15. Extract from the World Stress Map (Heidbach et al. 2008), covering Atlantic Canada. Windsor-Kennetcook subbasin is in a thrust regime having a vertical minimum compressive stress.

The Fundy Group unconformably overlies the Horton Group and truncates almost all secondary structures including folds, faults, and opening-mode fractures (Waldron et al. 2007). The dominant mode of fractures present in the Wolfville Formation (110°) is not common in fracture sets present in Mississippian strata. This suggests that most of the fractures formed prior to the deposition of the Wolfville Formation during early uplift and exhumation related to rifting. The 110° fracture set observed in the Wolfville Formation does occur at Cheverie as the latest fracture set in the Macumber Formation, where some veins contain characteristic red-staining on their centre line, similar to the few veins in the Wolfville Formation. This fracture set is interpreted as the final fracture set in the Windsor-Kennetcook subbasin.

Fractures were repeatedly activated by stresses operating later in the fracture history, possibly with orientations different from those that initially formed the fractures. Olson et al. (2009) and Becker et al. (2010) reached similar conclusions, suggesting that fracture sets may remain open for millions of years and therefore do not consistently reflect single short-term events. Markov chain analysis provides a method for recognition of patterns within a complex and extended history of fracture development.

These results have implications for hydrocarbon prospectivity. Hydrocarbons in the Windsor-Kennetcook subbasin would likely be extracted by hydraulic fracturing. Bedding in the footwall of the Kennetcook thrust system is gently dipping, and fractures are dominantly vertical, perpendicular to bedding. However, in the hanging wall of the Kennetcook thrust system, bedding is moderately to steeply dipping and fractures have lower dips. Fractures likely initiated after folding and faulting of strata. Figure 5.15 shows Atlantic Canada on an enlarged excerpt of the 2008 World Stress Map. To the east and southeast of the current study area, the Nova Scotian continental margin is in a thrust regime. The maximum compressive stress is horizontal, striking NE-SW, parallel to the Scotian shelf. Under conditions of hydraulic fracturing this would likely lead to the opening of bedding-parallel fractures in gently dipping strata, which would be unlikely to drain hydrocarbons from these rocks. In areas with steeply dipping beds, mainly in the hanging wall of the Kennetcook thrust system, fractures perpendicular to bedding would be more likely to open, and would be more likely to allow movement of fluids across stratigraphic surfaces. These regions may therefore be more prospective than has been previously realized.

5.9. Conclusion

Determining a deformation history for the Windsor-Kennetcook subbasin is difficult because of the complex history of the subbasin. Parts of the deformation history can be resolved by examining fractures (joints, veins, and faults) that are present in coastal outcrops and in core. Collecting data without bias is important for fracture study, and in this case three methods (circular scan-line, vertical scan-line, and FMI Image method) were used. Data collected include fracture orientation, relative timing, aperture width, and fill; the end result is to determine timing of deformation in the subbasin. Multiple stages of fracturing are distinguished by the Markov chain analysis; 4 groups of fractures may be related to dextral strike-slip along the Minas Fault Zone in the late Paleozoic, followed by 4 groups related to sinistral reactivation of the Minas Fault Zone in the Mesozoic.

Acknowledgements

Field research was supported by a grant from Triangle Petroleum; we thank Peter Hill for his support and access to core and FMI Image logs. Parts of this work were supported by a University of Alberta Teaching Assistantship. Hayley Pothier and Maryam Dzulkefli assisted in the field. We also thank two anonymous reviewers for their constructive comments, which led to significant improvements in the paper.

5.10. References

Allard, D., Froidevaux, R. & Biver, P. 2006. Conditional simulation of multi-type non stationary markov object models respecting specified proportions. Mathematical Geology 38(8), 959-986.

Bai, T., Maerten, L., Gross, M. R. & Aydin, A. 2002. Orthogonal cross joints: Do they imply a regional stress rotation? Journal of Structural Geology 24, 77-88.

Becker, S. P., Eichhubl, P., Laubach, S. E., Reed, R. M., Lander, R. H. & Bodnar, R. J. 2010. A 48 m.Y. History of fracture opening, temperature, and fluid pressure: Cretaceous travis peak formation, east texas basin. Geological Society of America Bulletin 122(7-8), 1081-1093.

Bell, W. A. 1924. Carboniferous formations of northumberland strait, nova scotia. Geological Survey of Canada Part C, 142-180.

Bell, W. A. 1958. Possibilities for occurrence of petroleum reservoirs in nova scotia. Province of Nova Scotia Department of Mines, Halifax.

Belt, E. S. 1965. Stratigraphy and paleogeography of mabou group and related middle carboniferous facies, nova scotia, canada. Geological Society of America 76, 777-802.

Bibby, C. & Schimeld, J. 2000. Compilation of reservoir data for sandstones of the devonian-permian maritimes basin, eastern canada. Geological survey of canada, open file report 3895.

Boehner, R. C. 1996. Diamond-drill core log of nova scotia department of natural resources drillhole wbk 93-1, whitten brook, walton woods road, hants county, nova scotia. In: Open file report 96-006. Nova Scotia Department of Natural Resources.

Boehner, R. C. & Giles, P. S. 1993. Geology of the antigonish basin, antigonish county, nova scotia. 8. Department of Natural Resources.

Boehner, R. C., Moore, R. G. & Kennedy, C. M. 1999. Overview of the geology and mineral resources of the western part of the windsor (kennetcook) basin, wolfville - windsor area (nts 21h/01 and part of 21a/16), hants and kings counties, nova scotia. In: Nova scotia department of natural resources mineral resources branch report of activities - report 2000-1 (edited by MacDonald, D. R. & Mills, K. A.), 1-11.

Bons, P. D., Elburg, M. A. & Gomez-Rivas, E. 2012. A review of the formation of tectonic veins and their microstructures. Journal of Structural Geology 43, 33-62.

Brown, D. E., Wade, J. A., Fensome, R. A. & Traverse, A. 1995. The fundy basin story. Atlantic Geology 31(1), 41-41.

Calder, J. H. 1998. The carboniferous evolution of nova scotia. In: Geological society, london, special publications 143, 261-302.

Caputo, R. 1995. Evolution of orthogonal sets of coeval extension joints. Terra Nova 7(5), 479-490.

Caputo, R. 2005. Stress variability and brittle tectonic structures. Earth-Science Reviews 70(1–2), 103-127.

Ching, W.-K., Huang, X., Ng, M. K. & Siu, T.-K. 2013. Markov chains: Models, algorithms and applications second edition. International series in operations research & management science 189. Springer, New York.

Cochran, W. G. 1954. Some methods for strengthening the common $\chi 2$ tests. Biometrics 10(4), 417-451.

Davis, G. H., Reynolds, S. J. & Kluth, C. F. 2012. Structural geology of rocks and regions - 3rd. Edition. John Wiley & Sons, Inc., New York.

Dietrich, J., Hannigan, P., Kezhen, H. & Giles, P. S. 2009. Petroleum resource potential of the carboniferous maritimes basin, eastern canada. Frontiers + Innovation 2009 CSPG CSEG CWLS Convention, 1-3.

Dietrich, J., Lavoie, D., Hannigan, P., Pinet, N., Castonguay, S., Giles, P. & Hamblin, A. 2011. Geological setting and resource potential of conventional petroleum plays in paleozoic basins in eastern canada. Bulletin of Canadian Petroleum Geology 59(1), 54-84.

Ekstrom, M. P., Dahan, C. A., Chen, M. Y., Lloyd, P. M. & Rossi, D. J. 1987. Formation imaging with microelectrical scanning arrays. Log Analyst 23(3), 294-306.

Engelder, T. 1985. Loading paths to joint propagation during a tectonic cycle: An example from the appalachian plateau, u.S.A. Journal of Structural Geology 7(3/4), 459-476.

Engelder, T. & Gross, M. R. 1993. Curving cross joints and the lithospheric stress field in eastern north america. Geology 21, 817-820.

Fall, A., Eichhubl, P., Bodnar, R. J., Laubach, S. E. & Davis, J. S. 2015. Natural hydraulic fracturing of tight-gas sandstone reservoirs, piceance basin, colorado. Geological Society of America Bulletin 127(1-2), 61-75.

Gauthier, B., Bisdom, K. & Bertotti, G. 2012. Modeling 3d fracture network in carbonate nfr: Contribution from an analogue dataset, the cante perdrix quarry, calvisson, se france. AAPG.

Gibling, M. R., Culshaw, N., Rygel, M. C. & Pascucci, V. 2008. Chapter 6 the maritimes basin of atlantic canada: Basin creation and destruction in the collisional zone of pangea. In: Sedimentary basins of the world 5 (edited by Miall, A. D.). Elsevier, 211-244.

Giles, P. S. 2009. Orbital forcing and mississippian sea level change: Time series analysis of marine flooding events in the visean windsor group of eastern canada and implications for gondwana glaciation. Bulletin of Canadian Petroleum Geology 57(4), 449-471.

Gingerich, P. D. 1969. Markov analysis of cyclic alluvial sediments. Journal of Sedimentary Petrology 39(1), 330-332.

Hancock, P. L. 1985. Brittle microtectonics: Principles and practice. Journal of Structural Geology 7, 437-457.

Heidrick, T. L. & Titley, S. R. 1982. Fracture and dike patterns in laramide plutons and their structural and tectonic implicatinos: American southwest. In: Advances in geology of the porphyry copper deposits (edited by Titley, S. R.). The University of Arizona Press, Tuscon, Arizona, 73-92.

Hibbard, J. & Waldron, J. W. F. 2009. Truncation and translation of appalachian promontories: Mid-paleozoic strike-slip tectonics and basin initiation. Geology 37, 487-490.

Johnson, S. K. 1999. Structural geology of the horton and windsor groups, cheverie, nova scotia, St. Mary's University.

Keppie, J. D. 1982. The minas geofracture. In: Special paper - geological association of canada (edited by St-Julien, P. & Beland, J.). Geological Association of Canada, Toronto, 263-280.

Laubach, S. E. & Diaz-Tushman, K. 2009. Laurentian palaeostress trajectories and ephemeral fracture permeability, cambrian eriboll formation sandstones west of the moine thrust zone, nw scotland. Journal of the Geological Society of London 166(2), 349-362.

Laubach, S. E., Fall, A., Copley, L. K., Marrett, R. & Wilkins, S. J. 2016. Fracture porosity creation and persistence in a basement-involved laramide fold, upper cretaceous frontier formation, green river basin, USA. Geological Magazine 153(5-6), 887-910.

Laubach, S. E., Marrett, R. A., Olson, J. E. & Scott, A. R. 1998. Characteristics and origins of coal cleat: A review. International Journal of Coal Geology 35(1), 175-207.

Lavoie, D., Sangster, D. F., Savard, M. M. & Fallara, F. 1995. Multiple breccia events in the lower part of the carboniferous windsor group, nova scotia. Atlantic Geology 31(3), 197-207.

Lavoie, D., Sangster, D. F., Savard, M. M. & Fallara, F. 1998. Breccias in the lower part of the mississippian windsor group and their relation to zn-pb mineralization; a summary. Economic Geology 93(6), 734-745.

Leleu, S., van Lanen, X. M. T. & Hartley, A. J. 2010. Controls on the architecture of a triassic sandy fluvial system, wolfville formation, fundy basin, nova scotia, canada; implications for the interpretation and correlation of ancient fluvial successions. Journal of Sedimentary Research 80(10), 867-883.

Longman, M. W. & Koepsell, R. J. 2005. Defining and characterizing mesaverde and mancos sandstone reservoirs based on interpretation of image logs, eastern uinta basin, utah. In: Open-file report 458 Utah Department of Natural Resources, 122.

MacKay, P. A. 2011a. The analysis of fractures in petroleum reservoirs part 1. Canadian Society of Petroleum Geologists Reservoir 6, 19-24.

MacKay, P. A. 2011b. The analysis of fractures in petroleum reservoirs: Part 2. Canadian Society of Petroleum Geologists Reservoir 7, 19-29.

Martel, A. T. 2004. The horton group depositional sequence and its significance for hydrocarbon exploration. Report me 2004-002 mining matters for nova scotia 2004: Opportunities for economic development.

Martel, T. & Durling, P. 2005. The mccully gas field; production, reserves and challenges. Atlantic Geology 41(1), 71-71.

Mauldon, M. 1998. Estimating mean fracture trace length and density from observations in convex windows. Rock Mechanics and Rock Engineering 31(4), 201-216.

Miall, A. D. 1973. Markov chain analysis applied to an ancient alluvial plain succession. Sedimentology 20, 347-364.

Moore, R. G., Ferguson, S. A., Boehner, R. C. & Kennedy, C. M. 2000. Bedrock geology map of the wolfville-windsor area, nts sheet 21h/01 and part of 21a/16, hants and kings counties, nova scotia. In: Nova Scotia Department of Natural Resources Mineral Resource Branch Open File Map ME 2000-3, Version 2 scale 1: 50 000.

Murphy, J. B., Stokes, T. R., Meagher, C. & Mosher, S.-J. 1994. Geology of the eastern st. Mary's basin, central mainland nova scotia. Geological Survey of Canada Current Research 1994-D(95-102).

Murphy, J. B., Waldron, J. W. F., Kontak, D. J., Pe-Piper, G. & Piper, D. J. W. 2011. Minas fault zone: Late paleozoic history of an intra-continental orogenic transform fault in the canadian appalachians. Journal of Structural Geology 33, 312-328.

Noade, J. E. 2010. Stratigraphy of the cheverie formation type section, cheverie, hants county, nova scotia, Dalhousie University Unpublished B.Sc. thesis.

Olson, J. E., Laubach, S. E. & Lander, R. H. 2009. Natural fracture characterization in tight gas sandstones: Integrating mechanics and diagenesis. AAPG bulletin 93(11), 1535-1549.

Pollard, D. D. & Aydin, A. 1988. Progress in understanding jointing over the past century. Geological Society of America 100, 1181-1204.

Reading, H. G. 1986. Sedimentary environments and facies second edition. Blackwell Scientific Publications, Oxford.

Rohrbaugh, M. B., Dunne, W. M. & Mauldon, M. 2002. Estimating fracture trace intensity, density and mean length using circular scan lines and windows. AAPG Bulletin 86(12), 2089-2104.

Savard, M. M., Lynch, G. & Fallara, F. 1996. Burial diagenesis model for the macumber formation on cape breton island - implications for the tectonic evolution of the windsor group. Atlantic Geology 32(1), 53 - 64.

Schenk, P. E. 1967. The macumber formation of the maritime provinces, canada; a mississippian analogue to recent strand-line carbonates of the persian gulf. Journal of Sedimentary Petrology 37(2), 365-376.

Singhal, B. B. S. & Gupta, R. P. 2010. Fractures and discontinuities. In: Applied hydrogeology of fractured rocks, 347.

Snyder, M. E. & Waldron, J. W. F. 2016. Unusual soft-sediment deformation structures in the maritimes basin, canada: Possible seismic origin. Sedimentary Geology.

Tanner, L. H. & Brown, D. E. 1999. The upper triassic chedabucto formation, guysborough county, nova scotia: Depositional and tectonic context. Atlantic Geology 35, 129-138.

Utting, J. & Hamblin, A. P. 1991. Thermal maturity of the lower carboniferous horton group, nova scotia. International Journal of Coal Geology 19(1–4), 439-456.

van de Poll, H. W., Gibling, M. R. & Hyde, R. S. 1995. Upper paleozoic rocks. In: Geology of the appalachian caledonian orogen in canada and greenland (edited by Williams, H.). Geological Survey of Canada, 449-455.

Wade, J. A., Brown, D. E., Traverse, A. & Fensome, R. A. 1996. The triassic-jurassic fundy basin, eastern canada: Regional setting, stratigraphy and hydrocarbon potential. 1996.

Waldron, J. W. F., Barr, S. M., Park, A. F., White, C. E. & Hibbard, J. 2015. Late paleozoic strike-slip faults in maritime canada and their role in the reconfiguration of the northern appalachian orogen. Tectonics 34(8), 1661-1684.

Waldron, J. W. F., Roselli, C. & Johnston, S. K. 2007. Transpressional structures on a late paleozoic intracontinental transform fault, canadian appalachians. In: Tectonics of strike-slip restraining and releasing bends (edited by Cunningham, W. D., and Mann, P.). Geological Society, London, Special Publications 290, 367-385.

Waldron, J. W. F., Roselli, C., Utting, J. & Johnston, S. K. 2010. Kennetcook thrust system: Late paleozoic transpression near the southern margin of the maritimes basin, nova scotia. Canadian Journal of Earth Sciences 47, 137-159.

Waldron, J. W. F., Rygel, M. C., Gibling, M. R. & Calder, J. H. 2013. Evaporite tectonics and the late paleozoic stratigraphic development of the cumberland basin, appalachians of atlantic canada. Geological Society of America Bulletin.

Waldron, J. W. F., White, J. C., MacInnes, E. & Roselli, C. 2005. Transpression and transtension along a continental transform fault: Minas fault zone, nova scotia. Geological Association of Canada - Mineralogical Association of Canada - Canadian Society of Petroleum Geologists - Canadian Society of Soil Sciences Joint Meeting - Halifax, May 2005. Field Trip B7.

Weeks, L. G. 1948. Londonderry and bass river map-areas, colchester and hants counties, nova scotia. In: Geological survey of canada, memoir 245.

Wightman, W. G., Scott, D. B., Medioli, F. S. & Gibling, M. R. 1993. Carboniferous marsh foraminifera from coal-bearing strata at the sydney basin, nova scotia: A new tool for identifying paralic coal-forming environments. Geology 21, 631-634.

Williams, H. 1979. Appalachian orogen in canada. Canadian Journal of Earth Sciences 16, 792-807.

Wilson, P. & White, J. C. 2006. Tectonic evolution of the moncton basin, new brunswick, eastern canada; new evidence from field and sub-surface data. Bulletin of Canadian Petroleum Geology 54(4), 319-336.

Withjack, M. O., Olsen, P. E. & Schlische, R. W. 1995. Tectonic evolution of the fundy rift basin, canada: Evidence of extension and shortening during passive margin development. Tectonics 14(2), 390-405.

Withjack, M. O., Schlische, R. W. & Baum, M. S. 2009. Extensional development of the fundy rift basin, southeastern canada. Geological Journal 44(6), 631-651.

Chapter 6. Conclusions

6.1. Summary and Contributions

This research investigated deformation in the Maritimes Basin, focussing on two regions: the Windsor-Kennetcook subbasin in Nova Scotia, and the Bay St. George subbasin in Newfoundland. Four original research objectives were explored in this thesis: 1) how Horton Group soft-sediment deformation structures were formed in the Windsor-Kennetcook subbasin; 2) the development of brittle and ductile structures onshore in the Bay St. George subbasin; 3) integrating and interpreting geophysical datasets offshore in the Bay St, George subbasin; and 4) understanding the history of fracturing in the Windsor-Kennetcook subbasin. This research elucidates the sedimentological and structural history of these subbasins, which adds to overall understanding of deformation in the Maritimes Basin. In particular, this research provides a new perspective on salt movement during basin development. These research objectives are also of import to industry as both mining and petroleum potential exists in these subbasins.

6.2. Chapter 2

Soft-sediment deformation structures shed light on timing and type of deformation during formation of a sedimentary basin. The Mississippian Horton Group hosts spectacular examples of classic and unique soft-sediment structures in the Windsor-Kennetcook subbasin.

In Chapter 2 of this thesis, load structures, clastic dykes, intraformational breccia, sedimentary boudins, bulb structures, and microbasins are described in detail. These soft-sediment deformation structures were likely induced by a combination of storm wave action, paleoslope orientation, overpressure, and seismic activity.

The strong NW–SE preferential orientation of these structures is attributed to dextral strike-slip on the E–W Minas Fault Zone. Movement along the Minas Fault Zone in the area possibly induced liquidization of sediment through seismic shaking and overpressured conditions, and led to strong preferred orientation of the resulting structures.

The frequency of these structures suggests that the Windsor-Kennetcook subbasin has been tectonically active periodically since its initiation in the Late Devonian. This interpretation is consistent with descriptions of tectonic structures described in other subbasins across the Maritimes Basin (Boehner 1986, Waldron and Rygel 2005, Wilson et al. 2006, Waldron et al. 2015, Gibling et al. in press).

6.3. Chapter 3

Chapter 3 examines soft-sediment deformation, salt tectonics, faulting, and tectonic inversion in the Bay St. George subbasin in southwestern Newfoundland.

Soft-sediment deformation structures are here described from Anguille Group and the Ship Cove Formation of the Codroy Group and include soft-sediment folds, clastic dykes, bulb structures, and sedimentary boudins. Orientations of soft-sediment structures in the Bay St. George subbasin are oblique to major fold hinges in the subbasin, consistent with dextral strike-slip movement during subbasin formation. These structures are similar in timing and deformation style with the soft-sediment structures discussed in the Windsor-Kennetcook subbasin in Chapter 2 of this thesis.

The Codroy Road Formation, overlying the Ship Cove Formation, shows large dominantly ductile structures that were previously interpreted by Knight (1983) as forming at the same time as large structures such as the Flat Bay anticline, the Anguille anticline, and the Snakes Bight Fault.

These structures were interpreted in Chapter 3 as resulting from salt expulsion occurring soon after deposition.

Salt structures displace material ranging from the Codroy Road Formation of the Codroy Group, to the Searston Formation of the Barachois Group in both the northern and southern subbasin. This suggests that the subbasin was tectonically active during the entirety of its formation. Deformation was dominantly related to salt movement during and after deposition of the Codroy Road Formation. Salt was moving until after deposition of the Barachois Group.

6.4. Chapter 4

Chapter 4 is a geophysical investigation of the offshore Bay St. George subbasin. Structures imaged on seismic profiles, bathymetric maps, and aeromagnetic maps are dominated by salt structures and large faults. Internal unconformities in suprasalt strata in salt-expulsion minibasins, and our inability to trace one definite top salt reflector, suggest that Codroy Group evaporite movement began soon after deposition and continued into deposition of higher strata.

One of the most spectacular new structures identified is a tectonic wedge located in the central offshore subbasin. Novel techniques tracing minibasin trough point migration, successive flattening of horizons, and tracing of seismic reflections truncated by the roof fault of the wedge all aid in the interpretation that insertion of this tectonic wedge occurred after most salt movement.

Tectonic inversion is documented by graben-bounding faults that have reverse separation at present day, and positive flower structures separating salt structures. The timing of tectonic inversion was likely after most salt movement, during or after the final stages of tectonic wedge insertion.

6.5. Chapter 5

Fractures are often overlooked when examining outcrops, but fractures can be very useful for unravelling complicated deformation histories. Fracture initiation has been attributed to tectonic events in the Appalachian Plateau by Engelder (1985), in southern Italy by Brogi (2011), and many others. In Chapter 5 we describe fractures from coastal outcrops and well core from the Windsor-Kennetcook subbasin to link fracture orientations to tectonic events in the Maritimes Basin.

The Windsor-Kennetcook subbasin is a complexly fractured area. Multiple sets of fractures in varying orientations are visible in outcrop and in well core. Relative timing of fracturing was determined by noting cross-cutting and abutting relationships of fractures.

A new method to interpret relative timing of fracturing is described here. Cross-cutting and abutting relationships of joints, veins, and faults are compiled into binned orientations. These relative-timing relationships are used in a modified Markov chain analysis, a statistical procedure previously used in sedimentology to unravel facies relationships (Gingerich 1969, Miall 1973, Reading 1986, Ching et al. 2013). The Markov chain analysis is used to separate groups of fractures and order them from early to later in time.

Multiple stages of fracturing were distinguished by this process: four groups were related to dextral strike-slip along the Minas Fault Zone in the late Paleozoic, and four groups were related to sinistral reactivation of the Minas Fault Zone in the Mesozoic.

6.6. Future Work

For every research question answered, several more emerge. Geophysical data in the Windsor-Kennetcook subbasin and Bay St. George subbasin are old and sparse; acquiring new information is integral to solving many of the following problems:

1. Many structures on the Knight (1983) geological map of the Bay St. George subbasin are not imaged on the few seismic lines available onshore. New seismic data collection and interpretation onshore would aid in the creation of a more robust geological map of the onshore Bay St. George subbasin.

2. The previously interpreted fault running parallel to the coast just offshore (St. Georges Bay Fault of Dafoe et al. 2016) is an enigma. Acquiring seismic data that span the onshore to offshore regions would better constrain this structure. More plentiful seismic data, especially onshore to offshore seismic, would also help constrain the extent of the triangle zone in the central subbasin.

3. A tectonic wedge is poorly imaged in the northeastern subbasin around the Brow Pond Lentil in the northeastern Bay St. George subbasin. The tectonic wedge here has the same vergence as the tectonic wedge in the central offshore subbasin. It is worth investigating the occurrence of tectonic wedges in the Maritimes Basin and whether tectonic wedges are more common in strike-slip environments and/or large salt-rich basins.

4. It is as of now impossible to determine exactly when tectonic inversion took place in the subbasin. Detailed mapping in the Anguille Mountains along the Snakes Bight Fault, including attempting to find evidence of inversion (e.g. a fault breccia containing clasts of the footwall) would enable us to slim down the inversion time-range.

5. Salt welds in outcrop have been investigated in few places worldwide. Recognizing the outcrop expression of salt expulsion provides a baseline for searching out salt welds in outcrops previously interpreted as syndepositional clastic units or fault breccias. The Maritimes Basin has been inadequately recognized as a significant salt province. It is worth compiling the information on how salt welds and salt-expulsion remnants are expressed in outcrop. This would contribute in recognizing salt structures onland elsewhere in the world without the need to drill exploratory wells.

6.7. References

Boehner, R. C. 1996. Diamond-drill core log of Nova Scotia Department of Natural Resources Drillhole WBK 93-1, Whitten Brook, Walton Woods Road, Hants County, Nova Scotia. In: Open File Report 96-006. Nova Scotia Department of Natural Resources.

Brogi, A. 2011. Variation in fracture patterns in damage zones related to strike-slip faults interfering with pre-existing fractures in sandstone (Calcione area, southern Tuscany, Italy). Journal of Structural Geology 33, 644-661.

Ching, W.-K., Huang, X., Ng, M. K. & Siu, T.-K. 2013. Markov Chains: Models, Algorithms and Applications Second Edition. International Series in Operations Research & Management Science 189. Springer, New York.

Dafoe, L. T., Shaw, J., Jauer, C., Giles, P. S., Waldron, J. W. F. & Potter, D. P. 2016. New insights into the Bedrock and Quaternary Geology of St. George's Bay from a vertical integration of marine datasets, offshore western Newfoundland. Bulletin of Canadian Petroleum Geology 64(1), 1.

Engelder, T. 1985. Loading paths to joint propagation during a tectonic cycle: an example from the Appalachian Plateau, U.S.A. Journal of Structural Geology 7(3/4), 459-476.

Gibling, M. R., Culshaw, N., Pascucci, V., Waldron, J. W. F. & Rygel, M. C. in press 2018. The Maritimes Basin of Atlantic Canada: Basin Creation and Destruction during the Paleozoic Assembly of Pangea. In: Sedimentary Basins of the World (edited by Miall, A.) 5.

Gingerich, P. D. 1969. Markov analysis of cyclic alluvial sediments. Journal of Sedimentary Petrology 39(1), 330-332.

Knight, I. 1983. Geology of the Carboniferous Bay St. George subbasin, Western Newfoundland. Mineral Development Division Department of Mines and Energy, Government of Newfoundland and Labrador Memoir 1.

Miall, A. D. 1973. Markov chain analysis applied to an ancient alluvial plain succession. Sedimentology 20, 347-364.

Reading, H. G. 1986. Sedimentary Environments and Facies Second Edition. Blackwell Scientific Publications, Oxford.

Waldron, J. W. F., Barr, S. M., Park, A. F., White, C. E. & Hibbard, J. 2015. Late Paleozoic strike-slip faults in Maritime Canada and their role in the reconfiguration of the northern Appalachian orogen. Tectonics 34(8), 1661-1684.

Waldron, J. W. F. & Rygel, M. C. 2005. Role of evaporite withdrawal in the preservation of a unique coal-bearing succession: Pennsylvanian Joggins Formation, Nova Scotia. Geology 33(5), 337-340.

Wilson, P., White, J. C. & Roulston, B. V. 2006. Structural geology of the Penobsquis salt structure; late Bashkirian inversion tectonics in the Moncton Basin, New Brunswick, Eastern Canada. Canadian Journal of Earth Sciences = Revue Canadienne des Sciences de la Terre 43(4), 405-419.

Bibliography

Adams, G. C. 1991. Gypsum and anhydrite resources in Nova Scotia. In: Nova Scotia Department of Natural Resources, Mines and Energy Branches, Economic Geology Series 91-1, 15.

Albertz, M., Beaumont, C., Shimeld, J. W., Ings, S. J. & Gradmann, S. 2010. An investigation of salt tectonic structural styles in the Scotian Basin, offshore Atlantic Canada: 1. Comparison of observations with geometrically simple numerical models. Tectonics 29(4), TC4017.

Alfaro, P., Delgado, J., Estevez, A., Molina, J. M., Moretti, M. & Soria, J. M. 2002. Liquefaction and fluidization structures in Messinian storm deposites (Bajo Segura Basin, Betic Cordillera, southern Spain). International Journal of Earth Sciences 91, 505-513.

Alfaro, P., Gibert, L., Moretti, M., Garcia-Tortosa, F. J., Sanz de Galdeano, C., Galindo-Zaldivar, J. & Lopez-Garrido, A. C. 2010. The significance of giant seismites in the Plio-Pleistocene Baza palaeo-lake (S Spain). Terra Nova 22(3), 172-179.

Alfaro, P., Moretti, M. & Owen, G. 2016. Special Issue: the environmental significance of soft-sediment deformation. Sedimentary Geology 344, iii-iv.

Allard, D., Froidevaux, R. & Biver, P. 2006. Conditional simulation of multi-type non stationary markov object models respecting specified proportions. Mathematical Geology 38(8), 959-986.

Allen, J. P., Fielding, C. R., Rygel, M. C. & Gibling, M. R. 2013. Deconvolving signals of tectonic and climatic controls from continental basins: an example from the late Paleozoic Cumberland Basin, Atlantic Canada. Journal of Sedimentary Research 83(10), 847-872.

Allen, J. R. L. 1986. Earthquake magnitude-frequency, epicentral distance, and soft-sediment deformation in sedimentary basins. Sedimentary Geology 46(1_2), 67-75.

Alsop, G. I. & Marco, S. 2011. Soft-sediment deformation within seismogenic slumps of the Dead Sea Basin. Journal of Structural Geology 33, 433-457.

Bai, T., Maerten, L., Gross, M. R. & Aydin, A. 2002. Orthogonal cross joints: Do they imply a regional stress rotation? Journal of Structural Geology 24, 77-88.

Baird, D. M. & CotÇ, P. R. 1964. Lower Carboniferous sedimentary rocks in southwestern Newfoundland and their relations to similar strata in western Cape Breton Island. Canadian Institute of Mining and Metallurgy.

Barr, S. M., Brisebois, D. & Macdonald, A. S. 1985. Carboniferous volcanic rocks of the Magdalen Islands, Gulf of St. Lawrence. Canadian Journal of Earth Sciences = Revue Canadienne des Sciences de la Terre 22(11), 1679-1688.

Bastin, S. H., Quigley, M. C. & Bassett, K. 2015. Paleo-liquefaction in Christchurch, New Zealand. Geological Society of America Bulletin Pre-Issue Publication.

Becker, S. P., Eichhubl, P., Laubach, S. E., Reed, R. M., Lander, R. H. & Bodnar, R. J. 2010. A 48 m.Y. History of fracture opening, temperature, and fluid pressure: Cretaceous travis peak formation, east texas basin. Geological Society of America Bulletin 122(7-8), 1081-1093.

Bell, J. S. & Howie, R. D. 1990. Paleozoic geology--Geologie du Paleozoique The Geology of North America 2. Geological Society of America, United States, United States, 141-165.

Bell, W. A. 1924. Carboniferous formations of Northumberland Strait, Nova Scotia. Geological Survey of Canada Part C, 142-180.

Bell, W. A. 1929. Horton-Windsor District, Nova Scotia. 155. Memoir Geological Survey of Canada.

Bell, W. A. 1944. Carboniferous rocks and fossil floras of northern Nova Scotia. Canada Geological Survey Memoir 238.

Bell, W. A. 1948. Early Carboniferous Strata of St. Georges Bay Area, Newfoundland. In: Geological Survey Bulletin No. 10. Mines and Geology Branch, Department of Mines and Resources, 51.

Bell, W. A. 1958. Possibilities for occurrence of petroleum reservoirs in Nova Scotia. Province of Nova Scotia Department of Mines, Halifax.

Belt, E. S. 1964. Revision of Nova Scotia Middle Carboniferous Units. American Journal of Science 262, 653-673.

Belt, E. S. 1965. Stratigraphy and paleogeography of mabou group and related middle carboniferous facies, nova scotia, canada. Geological Society of America 76, 777-802.

Belt, E. S. 1969. Newfoundland Carboniferous Stratigraphy and its relation to the Maritimes and Ireland: Chapter 54: Late Orogenic Stratigraphy and Structure. In: Memoir 12: North Atlantic: Geology and Continental Drift (edited by Kay, M.), 734-753.

Benson, B. E., Grimm, K. A. & Clague, J. J. 1997. Tsunami Deposits beneath Tidal Marshes on Northwestern Vancouver Island, British Columbia. Quaternary Research 48(2), 192-204.

Berra, F. & Felletti, F. 2011. Syndepositional tectonics recorded by soft-sediment deformation and liquefaction structures (continental Lower Permian sediments, Southern Alps, Northern Italy): Stratigraphic significance. Sedimentary Geology 235(3_4), 249-263.

Bibby, C. & Schimeld, J. 2000. Compilation of reservoir data for sandstones of the Devonian-Permian Maritimes Basin, Eastern Canada. Geological Survey of Canada, Open File Report 3895.

Boehner, R. C. & Giles, P. S. 1993. Geology of the Antigonish Basin, Antigonish County, Nova Scotia. In: Nova Scotia Department of Natural Resources, Mines and Energy Branch, Memoir 8.

Boehner, R. C. 1986. Salt and Potash Resources in Nova Scotia. In: Nova Scotia Department of Mines and Energy Bulletin ME 005, 346 p.

Boehner, R. C. 1992. An overview of the role of evaporites in the structural development of Carboniferous basins in Nova Scotia. In: Mines and Energy Branch, Report of Activities 1991 (edited by MacDonald, D. R.) Report 92-1, 39-56.

Boehner, R. C. 1996. Diamond-drill core log of Nova Scotia Department of Natural Resources Drillhole WBK 93-1, Whitten Brook, Walton Woods Road, Hants County, Nova Scotia. In: Open File Report 96-006. Nova Scotia Department of Natural Resources.

Boehner, R. C., Adams, G. C. & Giles, P. S. 2003. Karst geology in the salt-bearing Windsor Group evaporites and controls on the origin of gypsum deposits in south-central Cape Breton Island, Nova Scotia. In: Mineral Resources Branch, Report of Activities 2002. Nova Scotia Department of Natural Resources, Report 2003-1, 9-24.

Boehner, R. C., Moore, R. G. & Kennedy, C. M. 1999. Overview of the Geology and Mineral Resources of the Western Part of the Windsor (Kennetcook) Basin, Wolfville - Windsor Area (NTS 21H/01 and part of 21A/16), Hants and Kings Counties, Nova Scotia. In: Nova Scotia Department of Natural Resources Mineral Resources Branch Report of Activities - Report 2000-1 (edited by MacDonald, D. R. & Mills, K. A.), 1-11.

Bons, P. D., Elburg, M. A. & Gomez-Rivas, E. 2012. A review of the formation of tectonic veins and their microstructures. Journal of Structural Geology 43, 33-62.

Bradley, D. C. 1982. Subsidence in Late Paleozoic basins in the Northern Appalachians. Tectonics 1(1), 107-123.

Brogi, A. 2011. Variation in fracture patterns in damage zones related to strike-slip faults interfering with pre-existing fractures in sandstone (Calcione area, southern Tuscany, Italy). Journal of Structural Geology 33, 644-661.

Brown, D. E., Wade, J. A., Fensome, R. A. & Traverse, A. 1995. The fundy basin story. Atlantic Geology 31(1), 41-41.

Burden, E. T. & Williams, S. H. 1996. Biostratigraphy and thermal maturity of strata in NHOC _ PCP St. George's A-36. Report to the Newfoundland Hunt Oil Company.

Calder, J. H. 1998. The Carboniferous evolution of Nova Scotia. In: Geological Society, London, Special Publications 143, 261-302.

Callot, J.-P., Salel, J.-F., Letouzey, J., Daniel, J.-M. & Ringenbach, J.-C. 2016. Three-dimensional evolution of salt-controlled minibasins; interactions, folding, and megaflap development. AAPG Bulletin 100(9), 1419-1442.

Caputo, R. 1995. Evolution of orthogonal sets of coeval extension joints. Terra Nova 7(5), 479-490.

Caputo, R. 2005. Stress variability and brittle tectonic structures. Earth-Science Reviews 70(1_2), 103-127.

Ching, W.-K., Huang, X., Ng, M. K. & Siu, T.-K. 2013. Markov Chains: Models, Algorithms and Applications Second Edition. International Series in Operations Research & Management Science 189. Springer, New York.

Cochran, W. G. 1954. Some methods for strengthening the common _2 tests. Biometrics 10(4), 417-451.

Collinson, J. 2005. Post-depositional sedimentary structures. In: Encyclopedia of Geology (edited by Selley, R. C., Cocks, L. R. M. & Plimer, I. R.). Elsevier, Oxford, 602-611.

Cote, P. R. 1964. Lower Carboniferous sedimentary rocks of the Horton Group in parts of Cape Breton Island, and their relation to similar strata of the Anguille Group in southwestern Newfoundland, University of Ottawa.

Craggs, S., Keighley, D., Park, A. F. & Waldron, J. W. F. 2013. Stratigraphy and salt tectonics of Missisippian-Pennsylvanian strata of the northern Cumberland Basin, Maringouin Peninsula, southeastern New Brunswick. Atlantic Geology 49, 24-24.

Craggs, S., Keighley, D., Waldron, J. W. F. & Park, A. 2015. Salt tectonics in an intracontinental transform setting: Cumberland and Sackville basins, southern New Brunswick, Canada. Basin Research, 1-18.

Dafoe, L. T., Shaw, J., Jauer, C., Giles, P. S., Waldron, J. W. F. & Potter, D. P. 2016. New insights into the Bedrock and Quaternary Geology of St. George_s Bay from a vertical integration of marine datasets, offshore western Newfoundland. Bulletin of Canadian Petroleum Geology 64(1), 1.

Dalrymple, R. W. 1979. Wave-induced liquefaction: a modern example from the Bay of Fundy. Sedimentology 26, 835-844.

Davis, G. H., Reynolds, S. J. & Kluth, C. F. 2012. Structural geology of rocks and regions - 3rd. Edition. John Wiley & Sons, Inc., New York.

Dietrich, J., Hannigan, P., Kezhen, H. & Giles, P. S. 2009. Petroleum resource potential of the Carboniferous Maritimes Basin, eastern Canada. Frontiers + Innovation 2009 CSPG CSEG CWLS Convention, 1-3.

Dietrich, J., Lavoie, D. & Hannigan, P. 2011. Geological setting and resource potential of conventional petroleum plays in Paleozoic basins in eastern Canada. Bulletin of Canadian Petroleum Geology 59(1), 54-84.

Dietrich, J., Lavoie, D. & Hannigan, P. 2011a. Geological setting and resource potential of conventional petroleum plays in Paleozoic basins in eastern Canada. Bulletin of Canadian Petroleum Geology 59(1), 54-84.

Dietrich, J., Lavoie, D., Hannigan, P., Pinet, N., Castonguay, S., Giles, P. & Hamblin, A. 2011. Geological setting and resource potential of conventional petroleum plays in paleozoic basins in eastern canada. Bulletin of Canadian Petroleum Geology 59(1), 54-84.

Dietrich, J., Lavoie, D., Hannigan, P., Pinet, N., Castonguay, S., Giles, P. & Hamblin, A. 2011b. Geological setting and resource potential of conventional petroleum plays in Paleozoic basins in eastern Canada. Bulletin of Canadian Petroleum Geology 59(1), 54-84.

Dimmel, P. 2001. Potential for Mining Salt in Western Newfoundland. Department of Mines and Energy; Government of Newfoundland and Labrador.

Dooley, T. P. & Schreurs, G. 2012. Analogue modelling of intraplate strike-slip tectonics: A review and new experimental results. Tectonophysics 574-575, 1-71.

Duffy, O. B., Fernandez, N., Hudec, M. R., Jackson, M. P. A., Burg, G., Dooley, T. P. & Jackson, C. A. L. 2017. Lateral mobility of minibasins during shortening: Insights from the SE Precaspian Basin, Kazakhstan. Journal of Structural Geology 97, 257-276.

Dumont, R. & Jones, A. 2013a. Aeromagnetic survey of offshore western Newfoundland, NTS 11-N NE, Newfoundland and Labrador--Leve aeromagnetique extracotier de l'ouest de Terre-Neuve, SNRC 11-N NE, Terre-Neuve-et-Labrador. Geological Survey of Canada : Calgary, AB, Canada, Canada.

Dumont, R. & Jones, A. 2013b. Aeromagnetic survey of offshore western Newfoundland, NTS 11-O SW, Newfoundland and Labrador--Leve aeromagnetique extracotier de l'ouest de Terre-Neuve, SNRC 11-O SW, Terre-Neuve-et-Labrador. Geological Survey of Canada : Calgary, AB, Canada, Canada.

Dumont, R. & Jones, A. 2013c. Aeromagnetic survey of offshore western Newfoundland, NTS 12-B NE, Newfoundland and Labrador--Leve aeromagnetique extracotier de l'ouest de Terre-Neuve, SNRC 12-B NE, Terre-Neuve-et-Labrador. Geological Survey of Canada : Calgary, AB, Canada, Canada.

Dumont, R. & Jones, A. 2013d. Aeromagnetic survey of offshore western Newfoundland, NTS 12-B NW, Newfoundland and Labrador--Leve aeromagnetique extracotier de l'ouest de Terre-Neuve, SNRC 12-B NW, Terre-Neuve-et-Labrador. Geological Survey of Canada : Calgary, AB, Canada, Canada.

Dumont, R. & Jones, A. 2013e. Aeromagnetic survey of offshore western Newfoundland, NTS 12-B SE, Newfoundland and Labrador--Leve aeromagnetique extracotier de l'ouest de Terre-Neuve, SNRC 12-B SE, Terre-Neuve-et-Labrador. Geological Survey of Canada : Calgary, AB, Canada, Canada.

Dumont, R. & Jones, A. 2013f. Aeromagnetic survey of offshore western Newfoundland, NTS 12-B SW, Newfoundland and Labrador--Leve aeromagnetique extracotier de l'ouest de Terre-Neuve, SNRC 12-B SW, Terre-Neuve-et-Labrador. Geological Survey of Canada : Calgary, AB, Canada, Canada.

Dumont, R. & Jones, A. 2013g. Aeromagnetic survey of offshore western Newfoundland, NTS 12-C NE, Newfoundland and Labrador--Leve aeromagnetique extracotier de l'ouest de Terre-Neuve, SNRC 12-C NE, Terre-Neuve-et-Labrador. Geological Survey of Canada : Calgary, AB, Canada, Canada.

Dumont, R. & Jones, A. 2013h. Aeromagnetic survey of offshore western Newfoundland, NTS 12-C SE, Newfoundland and Labrador--Leve aeromagnetique extracotier de l'ouest de Terre-Neuve, SNRC 12-C SE, Terre-Neuve-et-Labrador. Geological Survey of Canada : Calgary, AB, Canada, Canada.

Dumont, R. & Jones, A. 2013i. Aeromagnetic survey of offshore western Newfoundland, NTS 12-F SE, Newfoundland and Labrador--Leve aeromagnetique extracotier de l'ouest de Terre-Neuve, SNRC 12-F SE, Terre-Neuve-et-Labrador. Geological Survey of Canada : Calgary, AB, Canada, Canada.

Dumont, R. & Jones, A. 2013j. Aeromagnetic survey of offshore western Newfoundland, NTS 12-G NE, Newfoundland and Labrador--Leve aeromagnetique extracotier de l'ouest de Terre-Neuve, SNRC 12-G NE, Terre-Neuve-et-Labrador. Geological Survey of Canada : Calgary, AB, Canada, Canada.

Dumont, R. & Jones, A. 2013k. Aeromagnetic survey of offshore western Newfoundland, NTS 12-G NW, Newfoundland and Labrador--Leve aeromagnetique extracotier de l'ouest de Terre-Neuve, SNRC 12-G NW, Terre-Neuve-et-Labrador. Geological Survey of Canada : Calgary, AB, Canada, Canada.

Dumont, R. & Jones, A. 2013l. Aeromagnetic survey of offshore western Newfoundland, NTS 12-G SE and part of 12-H SW, Newfoundland and Labrador--Leve aeromagnetique extracotier de l'ouest de Terre-Neuve, SNRC 12-G SE et partie de 12-H SW, Terre-Neuve-et-Labrador. Geological Survey of Canada : Calgary, AB, Canada, Canada.

Dumont, R. & Jones, A. 2013m. Aeromagnetic survey of offshore western Newfoundland, NTS 12-H NW, Newfoundland and Labrador--Leve aeromagnetique extracotier de l'ouest de Terre-Neuve, SNRC 12-H NW, Terre-Neuve-et-Labrador. Geological Survey of Canada : Calgary, AB, Canada, Canada.

Dumont, R. & Jones, A. 2013n. Aeromagnetic survey of offshore western Newfoundland, NTS 12-I NW and part of 12-J NW, 12-O SE, 12-P SW, Newfoundland and Labrador--Leve aeromagnetique extracotier de l'ouest de Terre-Neuve, SNRC 12-I NW et partie de 12-J NW, 12-O SE, 12-P. Geological Survey of Canada : Calgary, AB, Canada, Canada.

Dumont, R. & Jones, A. 2013o. Aeromagnetic survey of offshore western Newfoundland, NTS 12-I SW, Newfoundland and Labrador--Leve aeromagnetique extracotier de l'ouest de Terre-Neuve, SNRC 12-I SW, Terre-Neuve-et-Labrador. Geological Survey of Canada : Calgary, AB, Canada, Canada.

Dumont, R. & Jones, A. 2013p. Aeromagnetic survey of offshore western Newfoundland, NTS 12-J SE, Newfoundland and Labrador--Leve aeromagnetique extracotier de l'ouest de Terre-Neuve, SNRC 12-J SE, Terre-Neuve-et-Labrador. Geological Survey of Canada : Calgary, AB, Canada, Canada.

Duranti, D. & Hurst, A. 2004. Fluidization and injection in the deep-water sandstones of the Eocene Alba Formation (UK North Sea). Sedimentology 51(3), 503-529.

Durling, P. & Marillier, F. 1993. Structural elements of the Magdalen Basin, Gulf of St. Lawrence, from seismic reflection data. Geological Survey of Canada Paper 93-1D, Canada, 147-154.

Durling, P. & Marillier, F. 1993a. Structural elements and sedimentation patterns in the Magdalen Basin. Atlantic Geology 29(1), 78-78.

Durling, P. W. & Marillier, F. J. Y. 1990. Structural trends and basement rock subdivisions in the western Gulf of St. Lawrence, northern Appalachians. 1990.

Durling, P., Harvey, P. & Howells, K. 1995. Geophysical evidence for thrust faulting in the Carboniferous Antigonish-Mabou Subbasin, Nova Scotia.

Dyson, I. A. & Marshall, T. R. 2005. Neoproterozoic salt nappe complexes and salt-withdrawal mini-basins in the Amadeus Basin. Proceedings: Central Australian Basins Symposium Special Publication 2. Northern Territory Geological Survey.

Eggleston, L. K. 2017. Deformation and kinematic history of the Sackville and Moncton Subbasins, southeastern New Brunswick, Maritimes Basin of Atlantic Canada, University of Alberta.

Eisbacher, G. H. 1970. Contemporaneous faulting and clastic intrusions in the Quirke Lake Group, Elliot Lake, Ontario. Canadian Journal of Earth Sciences 7(2), 215-225.

Ekstrom, M. P., Dahan, C. A., Chen, M. Y., Lloyd, P. M. & Rossi, D. J. 1987. Formation imaging with microelectrical scanning arrays. Log Analyst 23(3), 294-306.

Enachescu, M. E. 1992. Basement extension on the Newfoundland continental margin (Canadian east coast). Proceedings of the International Conference on Basement Tectonics 7, Vol. 1, 227-256.

Engelder, T. & Gross, M. R. 1993. Curving cross joints and the lithospheric stress field in eastern north america. Geology 21, 817-820.

Engelder, T. 1985. Loading paths to joint propagation during a tectonic cycle: an example from the Appalachian Plateau, U.S.A. Journal of Structural Geology 7(3/4), 459-476.

Ezquerro, L., Moretti, M., Liesa, C. L., Luzon, A. & Simon, J. L. 2015. Seismites from a well core of palustrine deposits as a tool for reconstructing the palaeoseismic history of a fault. Tectonophysics 655, 191-205.

Fall, A., Eichhubl, P., Bodnar, R. J., Laubach, S. E. & Davis, J. S. 2015. Natural hydraulic fracturing of tight-gas sandstone reservoirs, piceance basin, colorado. Geological Society of America Bulletin 127(1-2), 61-75.

French, B. M. & Koeberl, C. 2010. The convincing identification of terrestrial meteorite impact structures: What works, what doesn't, and why. Earth-Science Reviews 98(1_2), 123-170.

Garcia, S. F. d. M., Letouzey, J., Rudkiewicz, J.-L., Danderfer Filho, A. & Frizon de Lamotte, D. 2012. Structural modeling based on sequential restoration of gravitational salt deformation in the Santos Basin (Brazil). Marine and Petroleum Geology 35(1), 337-353.

Gatmiri, B. 1990. A simplified finite element analysis of wave-induced effective stresses and pore pressures in permeable sea beds. Geotechnique 40(1), 15-30.

Gauthier, B., Bisdom, K. & Bertotti, G. 2012. Modeling 3d fracture network in carbonate nfr: Contribution from an analogue dataset, the cante perdrix quarry, calvisson, se france. AAPG.

Ge, H., Jackson, M. P. A. & Vendeville, B. C. 1997. Kinematics and dynamics of salt tectonics driven by progradation. AAPG Bulletin 81(3), 398-423.

Gibert, L., Sanz de Galdeano, C., Alfaro, P., Scott, G. & L¢pez Garrido, A. C. 2005. Seismic-induced slump in Early Pleistocene deltaic deposits of the Baza Basin (SE Spain). Sedimentary Geology 179(3_4), 279-294.

Gibling, M. R., Culshaw, N., Pascucci, V., Waldron, J. W. F. & Rygel, M. C. in press 2018. The Maritimes Basin of Atlantic Canada: Basin Creation and Destruction during the Paleozoic Assembly of Pangea. In: Sedimentary Basins of the World (edited by Miall, A.) 5.

Gibling, M. R., Culshaw, N., Rygel, M. C. & Pascucci, V. 2008. Chapter 6 The Maritimes Basin of Atlantic Canada: Basin Creation and Destruction in the Collisional Zone of Pangea. In: Sedimentary Basins of the World 5 (edited by Miall, A. D.). Elsevier, 211-244.

Giles, K. A. & Lawton, T. F. 2002. Halokinetic Sequence Stratigraphy Adjacent to the El Papalote Diapir, Northeastern Mexico. AAPG Bulletin 86(5), 823-840.

Giles, K. A. & Rowan, M. G. 2012. Concepts in halokinetic sequence deformation and stratigraphy. Geological Society Special Publications 363, 7-31.

Giles, P. S. & Boehner, R. C. 2001. Windsor Group Stratigraphy and Structure, Open File Report ME 2003-2. Geologial Mapping for Mineral Development, South-central Cape Breton Island Targeted Geoscience Initiative (TGI). Mineral Resources Branch, Nova Scotia Department of Natural Resources.

Giles, P. S. & Utting, J. 1999. Maritimes Basin stratigraphy - Prince Edward Island and adjacent Gulf of St. Lawrence.

Giles, P. S. & Utting, J. 2001. SHELL-AMOCO Cap Rouge F-52 Gulf of St. Lawrence, eastern Canada.

Giles, P. S. 1981. Major Transgressive-Regressive Cycles in Middle to Late Visean Rocks of Nova Scotia. Mineral Resources Division Report of Activities 1981, Nova Scotia Department of Mines and Energy.

Giles, P. S. 2008. Windsor Group (Late Mississippian) stratigraphy, Magdalen Islands, Quebec; a rare eastern Canadian record of late Visean basaltic volcanism. Atlantic Geology 44, 167-185.

Giles, P. S. 2009. Orbital forcing and Mississippian sea level change: time series analysis of marine flooding events in the Visean Windsor Group of eastern Canada and implications for Gondwana glaciation. Bulletin of Canadian Petroleum Geology 57(4), 449-471.

Gingerich, P. D. 1969. Markov analysis of cyclic alluvial sediments. Journal of Sedimentary Petrology 39(1), 330-332.

Goodman, N. R. 1952. Gypsum and Anhydrite in Nova Scotia. In: Province of Nova Scotia Department of Mines Memoir No. 1, 75.

Hall, J., Langdon, G., Roberts, B., Hawkins, D., Fagan, A., Knight, I. & Kilfoil, G. 1992. Reflection seismic imaging of the Carboniferous Bay St. George subbasin, onshore western Newfoundland: a reappraisal of Paleozoic stratigraphic thickness. Bulletin of Canadian Petroleum Geology 40(4), 321-334.

Hamblin, A. P. & Rust, B. R. 1989. Tectono-sedimentary analysis of alternate-polarite half-graben basin-fill successions: Late Devonian-Early Carboniferous Horton Group, Cape Breton Island, Nova Scotia. Basin Research 2, 239-255.

Hancock, P. L. 1985. Brittle microtectonics: Principles and practice. Journal of Structural Geology 7, 437-457.

Harris, C., Murton, J. & Davies, M. C. R. 2000. Soft-sediment deformation during thawing of ice-rich frozen soils: results of scaled centrifuge modelling experiments. Sedimentology 47(3), 687-700.

Hayward, N., Dehler, S. A. & Oakey, G. N. 2001. The structure of the northeastern Gulf of St. Lawrence, Canada: new insight from geophysical data analysis. Canadian Journal of Earth Sciences 38, 1495-1516.

Hayward, N., Dehler, S. A., Grant, A. C. & Durling, P. 2014. Magnetic anomalies associated with salt tectonism, deep structure and regional tectonics in the Maritimes Basin, Atlantic Canada. Basin Research 26(2), 320-337.

Heidrick, T. L. & Titley, S. R. 1982. Fracture and dike patterns in laramide plutons and their structural and tectonic implicatinos: American southwest. In: Advances in geology of the porphyry copper deposits (edited by Titley, S. R.). The University of Arizona Press, Tuscon, Arizona, 73-92.

Hempton, M. R. & Dewey, J. F. 1983. Earthquake-induced deformational structures in young lacustrine sediments, East Anatolian Fault, southeast Turkey. Tectonophysics 98(3_4), T7-T14.

Hermanrud, C., Venstad, J. M., Cartwright, J., Rennan, L., Hermanrud, K. & Nordgard Bolas, H. M. 2013. Consequences of water level drops for soft sediment deformation and vertical fluid leakage. Mathematical Geosciences 45, 1-30.

Hesse, R. & Reading, H. G. 1978. Subaqueous clastic fissure eruptions and other examples of sedimentary transposition in the lacustrine Horton Bluff Formation (Mississippian), Nova Scotia, Canada. In: Special Publication of the International Association of Sedimentologists 2 (edited by Matter, A. & Tucker, M. E.) no. 2, 241-257.

Hibbard, J. & Waldron, J. W. F. 2009. Truncation and translation of Appalachian promontories: mid-Paleozoic strike-slip tectonics and basin initiation. Geology 37, 487-490.

Hobbs, W. H. 1907. Origin of ocean basins in the light of the new seismology. Geological Society of America Bulletin 18, 233-250.

Holzer, T. L. & Clark, M. M. 1993. Sand boils without earthquakes. Geology 21(10), 873-876.

Holzer, T. L. & Pampeyan, E. H. 1981. Earth fissures and localized differential subsidence. Water Resources Research 17(1), 223-227.

Hu, K. & Dietrich, J. 2010. Petroleum reservoir potential of upper Paleozoic sandstones in the offshore Maritimes Basin, Eastern Canada. Geological Survey of Canada : Calgary, AB, Canada, Canada.

Hudec, M. R. & Jackson, M. P. A. 2004. Regional restoration across the Kwanza Basin, Angola: Salt tectonics triggered by repeated uplift of a metastable passive margin. AAPG Bulletin 88(7), 971-990.

Hudec, M. R. & Jackson, M. P. A. 2007. Terra infirma: Understanding salt tectonics. Earth-Science Reviews 82(1_2), 1-28.

Hudec, M. R., Jackson, M. P. A. & Schultz-Ela, D. D. 2009. The paradox of minibasin subsidence into salt: Clues to the evolution of crustal basins. Geological Society of America Bulletin 121(1-2), 201-221.

Hyde, R. S., Kalkreuth, W. D. & Utting, J. 1991. Petrology, palynology, and depositional environments of coals of the Upper Carboniferous Barachois Group (Westphalian A and C), southwestern Newfoundland. Canadian Journal of Earth Sciences 28(12), 1905-1924.

Hyde, R. S., Miller, H. G., Hiscott, R. N. & Wright, J. A. 1988. Basin architecture and thermal maturation in the strike-slip Deer Lake Basin, Carboniferous of Newfoundland. Basin Research 1(2), 85-105.

Iwasaki, T. 1986. Soil liquefaction studies in Japan: state-of-the-art. Soil Dynamics and Earthquake Engineering 5(1), 2-68.

Jackson, M. P. & Hudec, M. R. 2017. Salt tectonics: Principles and practice. Cambridge University Press.

Jackson, M. P. A. & Hudec, M. R. 2005. Stratigraphic record of translation down ramps in a passive-margin salt detachment. Journal of Structural Geology 27(5), 889-911.

Jackson, M. P. A. & Talbot, C. J. 1991. A Glossary of Salt Tectonics. No. 91-4. Bureau of Economic Geology Geological Circular The University of Texas at Austin.

Jackson, M. P. A. & Vendeville, B. C. 1994. Regional extension as a geologic trigger for diapirism; with Suppl. Data 9401. Geological Society of America Bulletin 106(1), 57-73.

Jahani, S., Callot, J.-P., Letouzey, J. & Frizon de Lamotte, D. 2009. The eastern termination of the Zagros fold and thrust belt, Iran; structures, evolution, and relationships between salt plugs, folding, and faulting. Tectonics 28(6),

Javaid, K. M. 2011. Development and structure of the Kennetcook-Windsor basin, Nova Scotia, Atlantic Canada. Unpublished M.Sc. thesis, University of Alberta.

Johnson, S. K. 1999. Structural geology of the Horton and Windsor Groups, Cheverie, Nova Scotia, St. Mary's University.

Jolly, R. J. H. & Lonergan, L. 2002. Mechanisms and controls on the formation of sand intrusions. Journal of the Geological Society, London 159, 605-617.

Jutras, P., Prichonnet, G. & McCutcheon, S. 2003. Alleghanian deformation in the eastern Gaspe Peninsula of Quebec, Canada. Geological Society of America Bulletin 115(12), 1538-1551.

Kang, H.-C., Paik, I. N., Lee, H. I., Lee, J. E. & Chun, J.-C. 2010. Soft-sediment deformation structures in Cretaceous non-marine deposits of southeastern Gyeongsang Basin, Korea: occurrences and origin. Island Arc 19, 628-646.

Kawakami, F. & Asade, A. 1966. Damage to the ground and earth structures by the Niigata earthquake of June 16, 1964. Soil and Foundation 6(1), 14-30.

Keppie, J. D. 1982. The Minas Geofracture. In: Special Paper - Geological Association of Canada (edited by St-Julien, P. & Beland, J.). Geological Association of Canada, Toronto, 263-280.

Kerr, M. & Eyles, N. 1991. Storm-deposited sandstones (tempestites) and related ichnofossils of the Late Ordovician Georgian Bay Formation, southern Ontario, Canada. Canadian Journal of Earth Sciences 28, 266-282.

Kilfoil, G. J. 1988. An integrated gravity, magnetic, and seismic interpretation of the Carboniferous Bay St. George subbasin, western Newfoundland, Memorial University of Newfoundland.

Knight, I. 1983. Geology of the Carboniferous Bay St. George subbasin, Western Newfoundland. Mineral Development Division Department of Mines and Energy, Government of Newfoundland and Labrador Memoir 1.

Kontak, D. J., Ansdell, K. & Douglas, A. 2000. Zn-Pb mineralization associated with a mafic dyke at Cheverie, Hants County, Nova Scotia: implications for Carboniferous metallogeny. Atlantic Geology 36, 7-26.

Koyi, H. 1998. The shaping of salt diapirs. Journal of Structural Geology 20(4), 321-338.

Koyi, H. A., Ghasemi, A., Hessami, K. & Dietl, C. 2008. The mechanical relationship between strike-slip faults and salt diapirs in the Zagros fold-thrust belt. Journal of the Geological Society of London 165(6), 1031-1044.

Krull, E. S. & Reta Ilack, G. J. 1995. Clastic dikes as evidence for discontinuous permafrost paleoclimate in Permian coal measures, Allan Hills Antarctica. Geological Society of America Abstracts with Programs 27, A265.

Langdon, G. S. & Hall, J. 1994. Devonian-Carboniferous tectonics and basin deformation in the Cabot Strait area, Eastern Canada. AAPG Bulletin 78(11), 1748-1774.

Laubach, S. E. & Diaz-Tushman, K. 2009. Laurentian palaeostress trajectories and ephemeral fracture permeability, cambrian eriboll formation sandstones west of the moine thrust zone, nw scotland. Journal of the Geological Society of London 166(2), 349-362.

Laubach, S. E., Fall, A., Copley, L. K., Marrett, R. & Wilkins, S. J. 2016. Fracture porosity creation and persistence in a basement-involved laramide fold, upper cretaceous frontier formation, green river basin, USA. Geological Magazine 153(5-6), 887-910.

Laubach, S. E., Marrett, R. A., Olson, J. E. & Scott, A. R. 1998. Characteristics and origins of coal cleat: A review. International Journal of Coal Geology 35(1), 175-207.

Laubach, S. E., Schultz-Ela, D. D. & Tyler, R. 2000. Differential compaction of interbedded sandstone and coal. In: Forced folds and fractures (edited by Cosgrove, J. W.) 169. Geological Society of London, London, 51-60.

Lavoie, D., Sangster, D. F., Savard, M. M. & Fallara, F. 1995. Multiple breccia events in the lower part of the carboniferous windsor group, nova scotia. Atlantic Geology 31(3), 197-207.

Lavoie, D., Sangster, D. F., Savard, M. M. & Fallara, F. 1998. Breccias in the lower part of the Mississippian Windsor Group and their relation to Zn-Pb mineralization; a summary. Economic Geology 93(6), 734-745.

Leleu, S., van Lanen, X. M. T. & Hartley, A. J. 2010. Controls on the architecture of a triassic sandy fluvial system, wolfville formation, fundy basin, nova scotia, canada; implications for the interpretation and correlation of ancient fluvial successions. Journal of Sedimentary Research 80(10), 867-883.

Long, D. G. F. 2004. The tectonostatigraphic evolution of the Huronian basement and the subsequent basin fill: geological constraints on impact models of the Sudbury event. Precambrian Research 129(3_4), 203-223.

Longman, M. W. & Koepsell, R. J. 2005. Defining and characterizing mesaverde and mancos sandstone reservoirs based on interpretation of image logs, eastern uinta basin, utah. In: Open-file report 458 Utah Department of Natural Resources, 122.

Lowe, D. R. 1975. Water escape structures in coarse-grained sediments. Sedimentology 22(2), 157.

Lynch, G., Keller, J. V. A. & Giles, P. S. 1998. Influence of the Ainslie Detachment on the stratigraphy of the Maritimes Basin and mineralization in the Windsor Group of northern Nova Scotia. Economic Geology 93, 703-718.

MacKay, P. A. 2011a. The analysis of fractures in petroleum reservoirs part 1. Canadian Society of Petroleum Geologists Reservoir 6, 19-24.

MacKay, P. A. 2011b. The analysis of fractures in petroleum reservoirs: Part 2. Canadian Society of Petroleum Geologists Reservoir 7, 19-29.

Maltman, A. J. & Bolton, A. 2003. How sediments become mobilized. In: Subsurface Sediment Mobilizations (edited by Van Rensbergen, P., Hillis, R. R., Maltman, A. J. & Morley, C. K.). Geological Society, London. Special Publication 216, 9-20.

Maltman, A. J. 1994. Introduction and overview. In: The Geological Deformation of Sediments (edited by Maltman, A. J.). Chapman and Hall, London, 1-35.

Martel, A. T. & Gibling, M. R. 1991. Wave-dominated lacustrine facies and tectonically controlled cyclicity in the Lower Carboniferous Horton Bluff Formation, Nova Scotia, Canada. In: Lacustrine Facies Analysis (edited by Anadon, P., Cabrera, L. & Kelts, K.). Blackwell Publising Ltd., Halifax, 223-243.

Martel, A. T. & Gibling, M. R. 1993. Clastic dykes of the Devono-Carboniferous Horton Bluff Formation, Nova Scotia: storm-related structures in shallow lakes. Sedimentary Geology 87, 103-119.

Martel, A. T. & Gibling, M. R. 1996. Stratigraphy and tectonic history of the Upper Devonian to Lower Carboniferous Horton Bluff Formation, Nova Scotia. Atlantic Geology 32, 13-38.

Martel, A. T. 2004. The Horton Group Depositional Sequence and its Significance for Hydrocarbon Exploration. Report ME 2004-002 Mining Matters for Nova Scotia 2004: Opportunities for Economic Development.

Martel, A. T., McGregor, D. C. & Utting, J. 1993. Stratigraphic significance of Upper Devonian and Lower Carboniferous miospores from the type area of the Horton Group, Nova Scotia. Canadian Journal of Earth Sciences 30(5), 1091-1098.

Martel, T. & Durling, P. 2005. The McCully gas field; production, reserves and challenges. Atlantic Geology 41(1), 71-71.

Mauldon, M. 1998. Estimating mean fracture trace length and density from observations in convex windows. Rock Mechanics and Rock Engineering 31(4), 201-216.

McBride, B. C., Weimer, P. & Rowan, M. G. 1998. The effect of allochthonous salt on the petroleum systems of northern Green Canyon and Ewing Bank (offshore Louisiana), northern Gulf of Mexico. AAPG Bulletin 82(5B), 1083-1112.

McCutcheon, S. R. & Robinson, P. T. 1987. Geological constraints on the genesis of the Maritimes Basin, Atlantic Canada. In: Sedimentary Basins and Basin-Forming Mechanisms (edited by Beaumont, C. & Tankard, A. J.) 5. Atlantic Geoscience Society Special Publications, Halifax, 287-297.

McGregor, D. C. & McCutcheon, S. R. 1988. Implications of spore evidence for Late Devonian age of the Piskahegan Group, southwestern New Brunswick. Canadian Journal of Earth Sciences 25(9), 1349-1364.

Miall, A. D. 1973. Markov chain analysis applied to an ancient alluvial plain succession. Sedimentology 20, 347-364.

Miller, H. G., Kilfoil, G. & Peavy, S. T. 1990. An integrated geophysical interpretation of the Carboniferous Bay St. George Subbasin, Western Newfoundland. Bulletin of Canadian Petroleum Geology 38(3), 320-331.

Molina, J. M., Alfaro, P., Moretti, M. & Soria, J. M. 1998. Soft-sediment deformation structures induced by cyclic stress of storm waves in tempestites (Miocene, Guadalquivir Basin, Spain). Terra Nova 10(3), 145-150.

Moore, R. G., Ferguson, S. A., Boehner, R. C. & Kennedy, C. M. 2000. Bedrock geology map of the Wolfville-Windsor area, NTS Sheet 21H/01 and part of 21A/16, Hants and Kings Counties, Nova Scotia. In: Nova Scotia Department of Natural Resources Mineral Resource Branch Open File Map ME 2000-3, Version 2 scale 1: 50 000.

Moretti, M. & Sabato, L. 2007. Recognition of trigger mechanisms for soft-sediment deformation in the Pleistocene lacustrine deposits of the Sant_Arcangelo Basin (Southern Italy): Seismic shock vs. overloading. Sedimentary Geology 196(1_4), 31-45.

Moretti, M., Alfaro, P., Caselles, O. & Canas, J. A. 1999. Modelling seismites with a digital shaking table. Tectonophysics 304(4), 369-383.

Murphy, J. B. & Keppie, J. D. 2005. The Acadian Orogeny in the Northern Appalachians. International Geology Review 47(7), 663-687.

Murphy, J. B. & Rice, R. J. 1998. Stratigraphy and depositional environment of the Horton Group in the St. Marys Basin, central mainland Nova Scotia. Atlantic Geology 34, 1-25.

Murphy, J. B., Stokes, T. R., Meagher, C. & Mosher, S.-J. 1994. Geology of the eastern st. Mary's basin, central mainland nova scotia. Geological Survey of Canada Current Research 1994-D(95-102).

Murphy, J. B., Waldron, J. W. F., Kontak, D. J., Pe-Piper, G. & Piper, D. J. W. 2011. Minas Fault Zone: Late Paleozoic history of an intra-continental orogenic transform fault in the Canadian Appalachians. Journal of Structural Geology 33, 312-328.

Murray, R. C. 1964. Origin and diagenesis of gypsum and anhydrite. Journal of Sedimentary Petrology 34(3), 512-523.

Nikolaeva, S. B. 2009. Seismites in Late Pleistocene and Holocene deposits of the northwestern Kola region (northern Baltic Shield). Russian Geology and Geophysics 50, 644-650.

Noade, J. E. 2010. Stratigraphy of the Cheverie Formation type section, Cheverie, Hants County, Nova Scotia, Dalhousie University Unpublished B.Sc. thesis.

Obermeier, S. F. 1996. Use of liquefaction-induced features for paleoseismic analysis _ An overview of how seismic liquefaction features can be distinguished from other features and how their regional distribution and properties of source sediment can be used to infer the location and strength of Holocene paleo-earthquakes. Engineering Geology 44(1_4), 1-76.

Obermeier, S. F. 2009. Chapter 7 Using Liquefaction-Induced and Other Soft-Sediment Features for Paleoseismic Analysis. In: International Geophysics 95 (edited by James, P. M.) Volume 95. Academic Press, 497-564.

Obermeier, S. F., Jacobson, R. B., Smoot, J. P., Weems, R. E., Gohn, G. S., Monroe, J. E. & Powars, D. S. 1990. Earthquake-induced liquefaction features in the coastal setting of South Carolina and in the fluvial setting of the New Madrid seismic zone. U. S. Geological Survey professional paper: 1504. U. S. Geological Survey, Washington.

Olson, J. E., Laubach, S. E. & Lander, R. H. 2009. Natural fracture characterization in tight gas sandstones: Integrating mechanics and diagenesis. AAPG bulletin 93(11), 1535-1549.

Opdyke, N. D., Giles, P. S. & Utting, J. 2012. Magnetic stratigraphy and palynostratigraphy of the Mississippian - Pennsylvanian boundary interval in eastern North America and the stratigraphic position of the beginning of the Kiamen. American Geophysical Union Fall Meeting 2012, GP13B-1124.

Osborne, M. J. & Swarbrick, R. E. 1997. Mechanisms for generating overpressure in sedimentary basins: a reevaluation. AAPG Bulletin 81(6), 1023-1041.

Owen, G. & Moretti, M. 2011. Identifying triggers for liquefaction-induced soft-sediment deformation in sands. Sedimentary Geology 235, 141-147.

Owen, G. 1987. Deformation processes in unconsolidated sands. In: Defomration of sediments and sedimentary rocks (edited by Jones, M. E. & Preston, R. F.) 29. Geological Society, London, Special Publications 29, 11-24.

Owen, G. 2003. Load structures: gravity-driven sediment mobilization in the shallow subsurface. Geological Society, London, Special Publications 216(1), 21-34.

Palmer, S. E., Waldron, J. W. F. & Skilliter, D. M. 2002. Post-Taconian shortening, inversion and strike slip in the Stephenville area, western Newfoundland. Canadian Journal of Earth Sciences 39, 1393-1410.

Park, A. F., Keighley, D. G., St. Peter, C. & Wilson, P. 2010. Overstep and imbrication along a sidewall ramp and its relationship to a hydrocarbon play in Tournasian rocks of the Moncton Basin; the Peck Creek section, Albert Mines area, southeastern New Brunswick. Bulletin of Canadian Petroleum Geology 58(3), 268-282.

Parnell, J. & Kelly, J. 2003. Remobilization of sand from consolidated sandstones: evidence from mixed bitumen-sand intrusions. In: Subsurface Sediment Mobilization (edited by Van Rensbergen, P., Hillis, R. R., Maltman, A. J. & Morley, C. K.) 216. Geological Society, London. Special Publication 216, 503-513.

Peavy, S. T. 1985. A gravity and magnetic interpretation of the Bay St. George Carboniferous subbasin in western Newfoundland, Memorial University of Newfoundland Master of Science Thesis.

Peel, F. J. 2014. How do salt withdrawal minibasins form? Insights from forward modelling, and implications for hydrocarbon migration. Tectonophysics 630, 222-235.

Pinet, N., Dietrich, J., Duchesne, M. J., Hinds, S. J. & Brake, V. 2018. Low-angle faulting in strike-slip dominated settings: Seismic evidence from the Maritimes Basin, Canada. Tectonophysics 738-739, 33-40.

Plint, A. G. 1985. Possible earthquake-induced soft-sediment faulting and remobilization in Pennsylvanian alluvial strata, southern New Brunswick, Canada. Canadian Journal of Earth Sciences 22, 907-912.

Pollard, D. D. & Aydin, A. 1988. Progress in understanding jointing over the past century. Geological Society of America 100, 1181-1204.

Ramsay, J. G. & Huber, M. I. 1987. The techniques of modern structural geology Volume 2: folds and fractures. Academic Press Orlando.

Reading, H. G. 1986. Sedimentary Environments and Facies Second Edition. Blackwell Scientific Publications, Oxford.

Rehill, T. A., Gibling, M. R. & Williamson, M. A. 1995. Stratigraphy of the Central Maritimes Basin, eastern Canada: non-marine sequence stratigraphy. In: Current Research 1995-E. Geological Survey of Canada, 221-231.

Rhoden, H. N. 1998. Preliminary evaluation of Fischells Brook rock-salt deposit in western Newfoundland, a mining project to supply the Atlantic-coast road de-icing market., St. John's Newfoundland.

Rodriguez-Pascua, M. A., Calvo, J. P., De Vicente, G. & Gomez-Gras, D. 2000. Soft-sediment deformation structures interpreted as seismites in lacustrine sediments of the Prebetic Zone, SE Spain, and their potential use as indicators of earthquake magnitudes during the Late Miocene. Sedimentary Geology 135(1-4), 117-135.

Rohrbaugh, M. B., Dunne, W. M. & Mauldon, M. 2002. Estimating fracture trace intensity, density and mean length using circular scan lines and windows. AAPG Bulletin 86(12), 2089-2104.

Roliff, W. A. 1962. The Maritimes Carboniferous Basin of Eastern Canada. Proceedings of the Geological Association of Canada 14, 21-41.

Roselli, C. 2003. Transpression and overthrusting in the Minas basin, Nova Scotia. Unpublished M.Sc. thesis, University of Alberta.

Rossetti, D. D. F. 1999. Soft-sediment deformation structures in late Albian to Cenomanian deposits, SΔo Lu°s Basin, northern Brazil: evidence for palaeoseismicity. Sedimentology 46(6), 1065-1081.

Rowan, M. G., Lawton, T. F. & Giles, K. A. 2012. Anatomy of an exposed vertical salt weld and flanking strata, La Popa Basin, Mexico. Geological Society, London, Special Publications 363(1), 33-57.

Savard, M. M., Lynch, G. & Fallara, F. 1996. Burial diagenesis model for the macumber formation on cape breton island - implications for the tectonic evolution of the windsor group. Atlantic Geology 32(1), 53 - 64.

Schenk, P. E. 1967. The Macumber Formation of the Maritime Provinces, Canada; a Mississippian analogue to Recent strand-line carbonates of the Persian Gulf. Journal of Sedimentary Petrology 37(2), 365-376.

Scott, B. & Price, S. 1988. Earthquake-induced structures in young sediments. Tectonophysics 147, 165-170.

Shaw, J., Courtney, R. C. & Currie, J. R. 1997. Marine geology of St. George's Bay, Newfoundland, as interpreted from multibeam bathymetry and back-scatter data. Geo-Marine Letters 17(3), 188-194.

Sibson, R. H. 2003. Brittle-failure controls on maximum sustainable overpressure in different tectonic regimes. AAPG Bulletin 87(6), 901-908.

Sims, J. D. 1975. Determining earthquake recurrence intervals from deformational structures in young lacustrine sediments. Tectonophysics 29(1_4), 141-152.

Singhal, B. B. S. & Gupta, R. P. 2010. Fractures and discontinuities. In: Applied hydrogeology of fractured rocks, 347.

Snyder, M. E. & Waldron, J. W. F. 2016. Unusual soft-sediment deformation structures in the Maritimes Basin, Canada; possible seismic origin. Sedimentary Geology 344, 145-159.

Snyder, M. E. & Waldron, J. W. F. 2018. Fracture overprinting history using Markov chain analysis; Windsor-Kennetcook Subbasin, Maritimes Basin, Canada. Journal of Structural Geology 108, 80-93.

Solomon, S. M. 1987. Sedimentology and fossil-fuel potential of the Upper Carboniferous Barachois Group, western Newfoundland.

Spathopoulos, F. 1996. An insight on salt tectonics in the Angola Basin, South Atlantic. Geological Society, London, Special Publications 100(1), 153.

St. Peter, C. 1993. Maritimes Basin evolution: key geologic and seismic evidence from the Moncton subbasin of New Brunswick. Atlantic Geology 29, 233-270.

St. Peter, C. J. & Johnson, S. C. 2009. Palynological Data for Late Devonian_Carboniferous Strata of the Maritimes Basin of Southeastern New Brunswick (NTS 21 H/9, 10, 14, 15, 16 and 21 I/01, 02). Minerals, Policy and Planning Division, Open File

Stockmal, G. S., Slingsby, A. & Waldron, J. W. F. 1998. Deformation styles at the Appalachian structural front, western Newfoundland: implications of new industry seismic reflection data. Canadian Journal of Earth Sciences 35(11), 1288-1306.

Taki, H. E. & Pratt, B. R. 2012. Syndepositional tectonic activity in an epicontinental basin revealed by deformation of subaqueous carbonate laminites and evaporites: seismites in Red River strata (Upper Ordovician) of southern Saskatchewan, Canada. Bulletin of Canadian Petroleum Geology 60(1), 37-58.

Tanner, L. H. & Brown, D. E. 1999. The upper triassic chedabucto formation, guysborough county, nova scotia: Depositional and tectonic context. Atlantic Geology 35, 129-138.

Thomas, A. K. & Waldron, J. W. F. 2017. Faults in the late Paleozoic Antigonish sub-basin, Nova Scotia, reinterpreted as potential salt welds. In: Program with Abstracts - Geological Association of Canada; Mineralogical Association of Canada: Joint Annual Meeting 40, Kingston, Ontario, 376.

Thomas, W. A. 1977. Evolution of the Appalachain-Ouachita salients and recesses from reentrants and promontories in the continental margin. American Journal of Science 277, 1233-1278.

Thomas, W. A. 1991. The Appalachian Ouachita rifted margin of southeastern North America. Geological Societry of America Bulletin 103, 415-431.

Trusheim, F. 1960. Mechanism of salt migration in northern Germany. AAPG Bulletin 44(9), 1519-1540.

Utting, J. & Giles, P. S. 2004. Biostratigraphical implications of new palynological data from the MIssissippian of Newfoundland and Nova Scotia, Canada. In: Memoirs of the Association of Australasian Palaeontologists 29, 115-160.

Utting, J. & Giles, P. S. 2008. Palynostratigraphy and lithostratigraphy of Carboniferous Upper Codroy Group and Barachois Group, southwestern Newfoundland. Canadian Journal of Earth Sciences 45(1), 45-67.

Utting, J. & Hamblin, A. P. 1991. Thermal maturity of the lower carboniferous Horton group, Nova Scotia. International Journal of Coal Geology 19(1_4), 439-456.

Utting, J., Keppie, J. D. & Giles, P. S. 1989. Palynology and stratigraphy of the Lower Carboniferous Horton Group, Nova Scotia. In: Contributions to Canadian Paleontology 396. Geological Survey of Canada Bulletin, 117-143.

van de Poll, H. W., Gibling, M. R. & Hyde, R. S. 1995. Upper Paleozoic Rocks. In: Geology of the Appalachian Caledonian Orogen in Canada and Greenland (edited by Williams, H.). Geological Survey of Canada, 449-455.

van Loon, A. J. & Mazumder, R. 2011. Can once lithified rocks later undergo soft-sediment deformation. Sedimentary Geology 238, 101-105.

van Rensbergen, P., Hillis, R. R., Maltman, A. J. & Morley, C. K. 2003. Subsurface sediment mobilization: introduction. In: Geological Society of London, Special Publication 216 (edited by van Rensbergen, P., Hillis, R. R., Maltman, A. J. & Morley, C. K.) 216, 1-8.

Wade, J. A., Brown, D. E., Traverse, A. & Fensome, R. A. 1996. The triassic-jurassic fundy basin, eastern canada: Regional setting, stratigraphy and hydrocarbon potential. 1996.

Wagner III, B. H. & Jackson, M. P. A. 2011. Viscous flow during salt welding. Tectonophysics 510, 309-326.

Waldron, J. W. & van Staal, C. R. 2001. Taconian orogeny and the accretion of the Dashwoods block: A peri-Laurentian microcontinent in the Iapetus Ocean. Geology 29(9), 811-814.

Waldron, J. W. F. & Gagnon, J.-F. 2011. Recognizing soft-sediment structures in deformed rocks of orogens. Journal of Structural Geology 33, 271-279.

Waldron, J. W. F. & Rygel, M. C. 2005. Role of evaporite withdrawal in the preservation of a unique coal-bearing succession: Pennsylvanian Joggins Formation, Nova Scotia. Geology 33(5), 337-340.

Waldron, J. W. F. 2004. Anatomy and evolution of a pull-apart basin, Stellarton, Nova Scotia. Geological Society of America Bulletin 116, 109-207.

Waldron, J. W. F. 2004. Anatomy and evolution of a pull-apart basin, Stellarton, Nova Scotia. Geological Society of America Bulletin 116(1-2), 109-127.

Waldron, J. W. F. 2005. Extensional fault arrays in strike-slip and transtension. Journal of Structural Geology 27, 23-34.

Waldron, J. W. F., Anderson, S. D., Cawood, P. A., Goodwin, L. B., Hall, J., Jamieson, R. A., Palmer, S. E., Stockmal, G. S. & Williams, P. F. 1998. Evolution of the Appalachian Laurentian margin: lithoprobe results in western Newfoundland. Canadian Journal of Earth Sciences 35, 1271-1287.

Waldron, J. W. F., Barr, S. M., Park, A. F., White, C. E. & Hibbard, J. 2015. Late Paleozoic strike-slip faults in Maritime Canada and their role in the reconfiguration of the northern Appalachian orogen. Tectonics 34(8), 1661-1684.

Waldron, J. W. F., Giles, P. S. & Thomas, A. K. 2017. Correlation chart for Late Devonian to Permian stratified rocks of the Maritimes Basin, Atlantic Canada.

Waldron, J. W. F., Roselli, C. & Johnston, S. K. 2007. Transpressional structures on a Late Paleozoic intracontinental transform fault, Canadian Appalachians. In: Tectonics of Strike-Slip Restraining and Releasing Bends (edited by Cunningham, W. D., and Mann, P.). Geological Society, London, Special Publications 290, 367-385.

Waldron, J. W. F., Roselli, C., Utting, J. & Johnston, S. K. 2010. Kennetcook thrust system: late Paleozoic transpression near the southern margin of the Maritimes Basin, Nova Scotia. Canadian Journal of Earth Sciences 47, 137-159.

Waldron, J. W. F., Rygel, M. C., Gibling, M. R. & Calder, J. H. 2013. Evaporite tectonics and the late Paleozoic stratigraphic development of the Cumberland Basin, Appalachians of Atlantic Canada. Geological Society of America Bulletin 125(5-6), 945-960.

Waldron, J. W. F., Schofield, D. I., Murphy, J. B. & Thomas, C. W. 2014. How was the Iapetus Ocean infected with subduction? Geology 42, 1095-1098.

Waldron, J. W. F., White, J. C., MacInnes, E. & Roselli, C. 2005. Transpression and transtension along a continental transform fault: Minas Fault Zone, Nova Scotia. Geological Association of Canada - Mineralogical Association of Canada - Canadian Society of Petroleum Geologists - Canadian Society of Soil Sciences Joint Meeting - Halifax, May 2005. Field Trip B7.

Wallace, K. & Eyles, N. 2015. Seismites within Ordovician_Silurian carbonates and clastics of Southern Ontario, Canada and implications for intraplate seismicity. Sedimentary Geology 316(0), 80-95.

Weeks, L. G. 1948. Londonderry and bass river map-areas, colchester and hants counties, nova scotia. In: Geological survey of canada, memoir 245.

Weimer, P., Bouroullec, R., van den Berg, A. A., Lapinski, T. G., Roesink, J. G. & Adson, J. 2017. Structural setting and evolution of the Mensa and Thunder Horse intraslope basins, northern deep-water Gulf of Mexico: A case study. AAPG Bulletin 101(7), 1145-1172.

White, S. E. 2018. Evolution of the Western Newfoundland Appalachian Orogen and its Foreland Basin, University of Alberta.

Wightman, W. G., Scott, D. B., Medioli, F. S. & Gibling, M. R. 1993. Carboniferous marsh foraminifera from coal-bearing strata at the Sydney basin, Nova Scotia: A new tool for identifying paralic coal-forming environments. Geology 21, 631-634.

Williams, H. 1979. Appalachian Orogen in Canada. Canadian Journal of Earth Sciences 16, 792-807.

Williams, H. 1985. Geology, Stephenville Map Area, Newfoundland (edited by Geological Survey of Canada, M. A.).

Williams, P. F., Goodwin, L. B. & Lafrance, B. 1995. Brittle faulting in the Canadian Appalachians and the interpretation of reflection seismic data. Journal of Structural Geology 17, 215-232.

Wilson, P. & White, J. C. 2006. Tectonic evolution of the Moncton Basin, New Brunswick, Eastern Canada; new evidence from field and sub-surface data. Bulletin of Canadian Petroleum Geology 54(4), 319-336.

Wilson, P., White, J. C. & Roulston, B. V. 2006. Structural geology of the Penobsquis salt structure; late Bashkirian inversion tectonics in the Moncton Basin, New Brunswick, Eastern Canada. Canadian Journal of Earth Sciences = Revue Canadienne des Sciences de la Terre 43(4), 405-419.

Wilson, P., White, J. C. & Roulston, B. V. 2006. Structural geology of the Penobsquis salt structure: late Bashkirian inversion tectonics in the Moncton Basin, New Brunswick, eastern Canada. Canadian Journal of Earth Sciences 43, 405-419.

Withjack, M. O., Olsen, P. E. & Schlische, R. W. 1995. Tectonic evolution of the fundy rift basin, canada: Evidence of extension and shortening during passive margin development. Tectonics 14(2), 390-405.

Withjack, M. O., Schlische, R. W. & Baum, M. S. 2009. Extensional development of the fundy rift basin, southeastern canada. Geological Journal 44(6), 631-651.